TECHNIQUES OF CHANNEL ESTIMATION

FOR HF RADIO LINKS

by

R. HARUN, BSc., MSc

A Doctoral Thesis
Submitted in Partial Fulfilment of the Requirements
for the Award of the PhD Degree
of the Loughborough University of Technology

August 1984

Supervisor: Professor A P Clark
Department of Electronic and Electrical Engineering

LIST OF CONTENTS

426

ABSTRACT

The thesis is concerned with the estimation of the sampled impulse-response of time-varying voiceband channels, and in particular with the proposed synchronous serial transmission of 16-level quadrature amplitude modulated digital data signals at 9600 bit/s over HF radio links. With such a system, the optimum detector at the receiver is a maximum likelihood detector implemented, for example, using the Viterbi algorithm. In this case, the detector requires knowledge of the sampled impulse-response of the channel. Channel estimators can also be used for estimating the response of any time-varying linear bandpass channel and need not be restricted in use only with a maximum likelihood detector. They may be employed in any such application where a time-varying channel must be tracked to ensure the correct operation of the detector.

The thesis includes a description of the ionospheric propagation medium, with particular emphasis on the nature of the impairments that are likely to be encountered by the data signal. An appropriate model of the HF channel is simulated for subsequent use in testing the channel estimators. A summary is also given of the more important forms of channel estimators that are used for time-invariant or slowly time-varying channels.

The characteristics of the HF radio medium may vary rapidly with time, so an estimator based on the Kalman filter is investigated in order to exploit the fast tracking capability of the filter.

It is shown that inadequate modelling of the channel by the Kalman filter results in suboptimum performance (in the minimum mean square error sense) of the estimator, however, this can be improved by including a suitable predictor. The performance of the Kalman filter estimator, with and without the predictor, is then compared with the corresponding estimator which uses a feedforward transversal filter.

The recently developed HF channel estimator based on the feedforward transversal-filter estimator is also investigated, but it is tested here over the simulated HF radio links with three independent Rayleigh fading sky waves, which represent typical poor conditions over actual links. Various degrees of prediction are also studied and based on the results, a change in the degree of prediction from that previously proposed is suggested as a better arrangement for use with the estimator when there are three sky waves. Finally, it is shown that a considerable reduction in the equipment complexity can be achieved by exploiting a self-correcting property of the estimator that has been discovered.

ACKNOWLEDGEMENTS

The author would like to express his gratitude to his supervisor, Professor A P Clark, for his considerable help and guidance.

The financial support of the Government of Malaysia and the Malaysian Telecommunications Department, is gratefully acknowledged.

The author would also like to thank his wife, Zareena, and his son, Johari, for their patience and encouragement during the project, and Janet Smith for her excellent typing.

GLOSSARY OF SYMBOLS AND TERMS

$a(t)$	Impulse response of a filter
$A(f)$	Frequency response of a filter
$\|A(f)\|$	Absolute value of $A(f)$
c	Step size of feedforward transversal-filter estimator
e_i	Error in the estimated value of r_i
$E[\cdot]$	Expectation operator
$g+1$	Number of samples in the sampled impulse-response of linear baseband channel
j	When not used as a subscript, $j = \sqrt{-1}$
K_i	Kalman gain vector
m^2	Number of possible levels of complex-valued data-symbol s_i
n	Delay in estimation (in sampling intervals)
$n(t)$	White Gaussian noise with zero mean and two-sided power spectral density of $\frac{1}{2}N_o$
N	Number of sky waves
$\frac{1}{2}N_o$	Power spectral density of $n(t)$
$P_{i,i-1}$	A priori error covariance matrix (Kalman filter)
$P_{i,i}$	A posteriori error covariance matrix (Kalman filter)
$q_h(t)$	Statistically independent random processes
$\{q_{h,i}\}$	Sequences obtained by sampling $q_h(t)$
Q_i	Covariance matrix of V_i
$\mathfrak{Re}[\cdot]$	Real part of a complex number
$r(t)$	Received signal
$\{r_i\}$	Sequence of received signal samples
s_i	Data symbol

superscript *	Complex conjugate
superscript T	Matrix transpose
superscript (*T)	Complex conjugate transpose
T	Sampling interval
$\frac{1}{T}$	Signal-element rate (bauds)
V_i	Vector whose components are statistically independent random variables
$w(t)$	Gaussian random process with zero mean
$y(t)$	Impulse response of linear baseband channel
Y_i	Sampled impulse-response of linear baseband channel at time $t=iT$
Y_i'	Estimate of Y_i at time $t=iT$
$Y_{i+n,i}'$	Prediction of Y_{i+n}, at time $t=iT$, obtained from the $\{Y_h'\}$ for $h = i, i-1, \ldots$
θ	Small positive quantity
ξ	Mean-square error in the estimate (prediction) of Y_i
ξ_i	Square of the error in the estimate (prediction) of Y_i
σ^2	Variance of $w(t)$ or $\{w_i\}$
ψ	Signal-to-noise ratio ($= 10 \log_{10} \frac{1}{\sigma^2}$)

1. INTRODUCTION

1.1 BACKGROUND

For many years, the radio wave spectrum has been utilized for various communication purposes. At the lower end of the spectrum, the very low frequency (VLF) band (3-30 kHz) is used principally for long-range navigation and submarine communication. Further up the spectrum, we find the high frequency (HF) band (3-30 MHz) which is used for military communication, fixed service operation, point-to-point communication and international broadcasting[64,101,105]. New technologies have also opened up frequencies well above the HF band for telecommunication purposes. With the use of satellites for beyond line-of-sight applications, HF radio, which is plagued by multipath fading, may have been thought to be losing out and becoming less important. However, this has not happened. The HF spectrum remains fully occupied with the variety of uses because HF radio offers economical and/or secure communication when compared with the alternative systems, e.g. satellite, cable or line-of-sight terrestrial microwave systems[106,107].

HF radio relies on the ionosphere for wave propagation. The dependence on the ionosphere results in many problems of which the HF system designer must take full account. A radio wave incident onto the ionosphere is refracted back to Earth often by two or more different ionised layers, which means that it can travel to the receiver via several distinct paths. This is known as multipath

propagation. The lengths of these paths are slightly different so that the time taken by the signal traversing each path is not exactly the same. The relative delay in transmission, i.e. the interval between the arrival of the first and the last sky waves, is typically a few milliseconds. In addition, the signal on each path is subjected to random fluctuations both in amplitude and phase resulting in the frequency-selective fading of the resultant radio wave. Fade rates are usually in the region of 10 to 50 fades per minute[65]. Despite these and other forms of distortion[63,65,66,68], the HF radio link permits reliable communication (90% path reliability) for distances up to 6400 km[73].

Due to the highly dispersive nature of the HF radio medium, the transmission of digital data has been confined in the past to very low data rates (typically 50-75 bit/s)[109]. The simplest of these systems is the on-off-keying (OOK) morse system, where a continuous wave carrier is manually interrupted according to the morse symbol. At these rates, the signal-element duration with serial transmission greatly exceeds the multipath spread, so that the signal is subjected to flat fading. With the appropriate signal design and detection process, the interchannel and intersymbol interference effects can now be reduced to negligible levels. At higher data rates, the signal-element duration is smaller, so that the multipath spread can be several sampling intervals long, the performance of the system is now degraded by intersymbol interference[2,65,106]. This is the condition caused by the spreading in time of individual signal-elements by the HF radio link resulting in the overlapping of

adjacent signal-elements. The presence of unwanted components originating from the neighbouring signal-elements means that the system is less tolerant to noise and may be subject to the incorrect detection of the received signal even in a noiseless environment[2].

Until recently, the preferred method of transmitting digital data at medium to high-speeds (> 1200 bit/s)[110,111] has been to employ a number of low speed channels in parallel so as to avoid intersymbol interference. The parallel modem may, for example, employ 16 sub-channels with quaternary differential phase-shift-keying (DPSK) modulation to achieve a speed typically around 2400 bit/s[111]. An alternative approach is to use serial transmission and employing some form of adaptive signal processing at the receiver. Comparisons of the two transmission techniques at a speed of 2400 bit/s[96,110,112] have suggested that the serial modem may offer a better overall performance. With the increase in the processing speed of digital hardware and also improvements in signal processing techniques, the serial modems are now challenging the dominance of parallel modems for high speed applications.

In the detection of serially transmitted digital data, the detector may adopt one of several strategies which are broadly classified into two groups[2]. In the first group, the detector employs a device known as an equalizer to remove intersymbol interference which has been identified as the main cause of poor system performance. Each equalized signal-element is free from interference from the neighbouring signal-elements and can be detected as it arrives. The second group of detection processes

uses maximum likelihood sequence estimation (MLSE) algorithms known as maximum likelihood detectors[2,19,24]. These algorithms are basically decoding procedures for obtaining the most likely transmitted data sequence. Unlike the equalizer, the MLSE makes no attempt to remove intersymbol interference so that the whole of the received signal energy is used in the detection of the data symbols. When the data signal is received in the presence of additive white Gaussian noise, the MLSE is the optimum detection process in the sense that it minimizes the probability of error in the detection of the entire received sequence[19]. In many cases, its performance is as good as if intersymbol interference were absent.

The basic requirement for the maximum likelihood detector is that the sampled impulse-response of the channel is known[2,19-21,27]. This may be achieved by using a channel estimator which estimates the sampled impulse-response of the channel from the received signal. Many estimator designs have been described in the literature, (17,21,26,27,48,52-58,62) that are simple to implement and provide accurate estimates of the channel, provided only that the sampled impulse-response of the channel does not vary too rapidly with time. However, when there is rapid variation in the channel characteristics, as in the case of an HF radio link, a more sophisticated technique (16,33,37,50,89,95-97) is required, the estimation process being performed adaptively such that the detector is held correctly adjusted at all times for the channel. The need for a channel estimator is not confined to the MLSE alone. For instance, a particular type of equalizer employing the discrete Kalman filter

also requires a channel estimator in order to adapt to a time-varying channel[33].

1.2 OUTLINE OF THE INVESTIGATION

A recent development of an HF channel estimator[95,97] that exploits some of the available prior knowledge of the basic structure of the HF radio channel has shown that a reasonably accurate estimate of the sampled impulse-response may be obtained using a relatively simple structure. Consequently, the main objectives of this investigation are to study various aspects of the performance of this estimator and also another estimator known as the Kalman filter. The former of the two is an estimator based on the feed-forward transversal-filter estimator[26,27] which has been developed to include a predictor[44,89] so as to give an acceptable performance when used on HF channels. The Kalman filter is studied because it is recognized, under certain conditions, as the best linear estimator and it gives the fastest possible rate of convergence[114,116]. The latter property is essential if the estimator is to track the rapid variations that can occur in the characteristics of an HF channel. Thus, the Kalman filter seems to be very suitable for use on HF channels and it is potentially a better estimator if it can be developed along similar lines as the feedforward transversal-filter estimator.

Before describing the estimators, a brief description is given in Section 2 of a general model of a data-transmission system. This is followed by a description of a data-transmission system which

employs combined amplitude and phase modulation known as Quadrature Amplitude Modulation (QAM). This type of modulation is frequently used for high-speed data transmission[9,10,13-17,22,23]. Also described in Section 2 is the theory and a possible method of implementation of a detection process known as the Maximum Likelihood Sequence Estimation (MLSE) which, under the appropriate conditions, is considered as the optimum detection process.

The basic requirement of a detector employing the MLSE is that the sampled impulse-response of the channel must be known. In most cases, the correct (exact) value of the sampled impulse-response at any time is not obtainable, but an estimate of this may be found by means of a channel estimator which derives the estimate from the received signal. In Section 3, some of the more important channel estimators for use on time-invariant or slowly time-varying channels are described. Two of these estimators form the basis of the HF channel estimators to be described in Sections 6 and 7.

Section 4 is solely concerned with the HF radio channels. Here, a description is given of the physical composition of the ionosphere and also of the mechanism of radio wave propagation through this medium. Various types of signal impairment are also identified. Using this information, the HF channel is modelled and simulated on a computer for subsequent use in the testing of the estimators.

In Section 5, brief descriptions of the recently developed HF channel estimators are given. In particular, the first estimator is the feedforward transversal-filter estimator described in Section 3 with a predictor incorporated into it. The second estimator is actually the previous estimator but now the knowledge of the basic structure of the HF channel is used which consequently gives an improved performance.

It is well known that the Kalman filter possesses far superior tracking capability than any other linear estimator, when used under the condition for which it has been designed. Therefore, in Section 6, the development of the Kalman filter as an HF channel estimator is studied. Various modifications subsequently made to the original Kalman algorithm are also described. These involve the inclusion of the least-squares fading-memory predictor for use when updating the estimate of the channel and also various schemes to account for errors in modelling the HF channel. The performances of the Kalman estimator are compared with the corresponding estimator which uses a feedforward transversal-filter estimator. Results of computer simulation tests are presented and analysed.

Section 7 considers the improved channel estimator which is only briefly mentioned in Section 5. The estimator is, here, tested over a model of an HF channel (Section 4) with three independent Rayleigh fading sky waves which represent a typical poor channel condition over actual HF links. Various degrees of prediction are also described. Finally, results of computer simulation tests are given and analysed.

2. DATA-TRANSMISSION SYSTEM

2.1 GENERAL MODEL OF A DATA-TRANSMISSION SYSTEM

In general, there are two forms of transmission for digital data. The system where the signal-elements are transmitted as a sequential stream and whose frequency spectrum occupies the whole of the available bandwidth is known as a serial system. A parallel system is one in which two or more sequential streams of signal-elements are sent simultaneously, and the spectrum of an individual data stream occupies only part of the available bandwidth[1].

Most often in a serial system the signal-elements are transmitted at a steady rate of a given number of elements per seconds (bauds), the receiver being held in time synchronism with the received signal. Such a system is known as a synchronous serial system and, in applications where a relatively high transmission rate is required over a given channel, it is the most commonly used system[2]. Therefore, the synchronous serial system will be assumed throughout the thesis. A model of the data-transmission system is shown in Figure 2.1.1.

In practice, the signal at the input to the transmitter filter would be in the form of a rectangular or rounded waveform. Each signal-element has the same duration of T seconds and is transmitted immediately after the preceding element, so that the signal-element rate is $\frac{1}{T}$ bauds[2]. However, in order to simplify the theoretical analysis of the system, it is now assumed that the input signal is

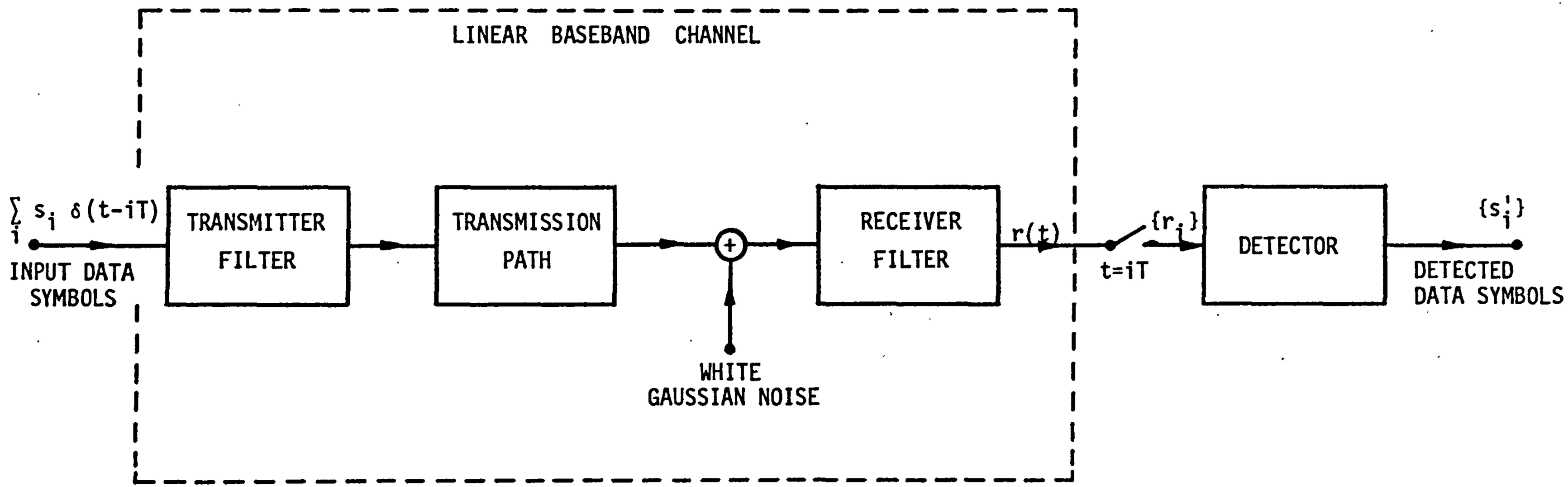

FIGURE 2.1.1: GENERAL MODEL OF A DATA-TRANSMISSION SYSTEM

a sequence of regularly spaced impulses, the i^{th} of which occurs at time t = iT seconds. This form of representation of the signal-elements does not affect in any way the operation of the system other than an appropriate change in the transmitter filter. The input sequence can be represented in the form

$$\sum_i s_i \, \delta(t-iT)$$

where $\delta(t-iT)$ is a unit impulse at time t=iT seconds. The value, or area, of each impulse, $s_i \, \delta(t-iT)$, is therefore, given by the corresponding data-symbol s_i. It is assumed that s_i may have one of m possible values. The $\{s_i\}$ are statistically independent and equally likely to have any of the m possible values. Where this condition is not satisfied, it can normally be achieved by 'scrambling' the transmitted sequence of data symbols and appropriately 'descrambling' the corresponding detected data symbols at the receiver[2].

The transmitter filter is used to shape the frequency spectrum of the transmitted signal to match the available bandwidth of the transmission path. This minimizes the signal power lost in transmission and so maximizes the signal-to-noise power ratio at the receiver input for a given transmitted signal power[1].

The transmission path could be either a lowpass or a bandpass channel. In the latter case, the transmission path is assumed to include a linear modulator at the transmitter and a linear demodulator at the receiver. An example of such a system is an arrangement using vestigial sideband suppressed carrier (VSSC) amplitude modulation (AM)

at the transmitter and coherent demodulation at the receiver. A low-level pilot carrier is, in fact, inserted into the transmitted signal to enable the reference carrier of the coherent demodulator to be synchronized to the received signal. In such a system, where the instantaneous frequency of the reference carrier is held constant at the average instantaneous frequency of the received signal carrier (assuming that the latter does not drift steadily with time), the bandpass channel together with the modulator at the transmitter and the demodulator at the receiver appear as a linear baseband channel, with the same fading characteristics as those of the original bandpass channel[2]. The theoretical analysis of the resultant system, therefore, reduces to that of a simple linear baseband system.

The bandpass channel could be a telephone circuit or a high frequency (HF) radio link. These are the two main types of voice-frequency channels and the nominal bandwidth of these channels is 300-3000 Hz[1].

In practice, the data-transmission system is expected to operate on different channels which may have considerably different characteristics. Over the switched telephone network, the characteristics of a particular circuit may not vary significantly with time. However, a new circuit, obtained by dialling a new connection, usually has different characteristics from the previous circuit[1]. Therefore, the characteristics of the channel are usually not known prior to a transmission. Also, the channel may itself vary considerably (but usually slowly) with time, such as over point-to-point HF radio links. The receiver must then track the channel variation to ensure correct operation. In both cases, the sampled impulse-response of the channel

must be estimated at the receiver from the received signal. Where the channel characteristics do not vary significantly with time, this may be carried out at the start of a transmission[2-4], and where the channel characteristics vary with time, this must be carried out continuously using the received data signal.

The model assumes that the only noise introduced by the system is additive white Gaussian noise. The other types of additive and multiplicative noise have been neglected. It has been shown that the relative tolerances of different data-transmission systems to additive white Gaussian noise is a good measure of their relative overall tolerances to most practical types of additive noise[2]. The Gaussian noise has zero mean and a two-sided power spectral density of $\frac{1}{2}N_0$, and is added to the data signal at the output of the transmission path.

The receiver filter removes the noise components outside a frequency band approximately corresponding to the bandwidth of the received signal, without excessively bandlimiting the signal itself. It is assumed that the receiver filter is such that the sample values of the noise function w(t) at the output of the receiver filter, taken at intervals of T seconds by the sampler are statistically independent Gaussian random variables with zero mean and fixed variance, the precise conditions to be satisfied by the receiver filter here being considered in detail elsewhere[1]. It has been shown that if the amplitude response $|B(f)|$ of the receiver filter in Figure 2.1.1 is in a constant ratio b to the amplitude response $|A(f)|$ of the transmitter filter, over all values of frequency f, and the transmission

path introduces no attenuation, delay or distortion, then the signal-to-noise power ratio at the detector input is maximized[1].

The transmission path together with the transmitter and receiver filters are assumed here to form a linear baseband channel with impulse response y(t). Depending on the type of the transmission path, the impulse response, y(t), may or may not vary significantly with time. At transmission rates of up to 2400 bit/s over the switched telephone network, it is often reasonable to assume that the impulse response of the channel is unlikely to vary significantly over the duration of one transmission[2], and so it is safe to assume that y(t) is time-invariant. At higher transmission rates over the switched telephone network, and also usually the case over the HF radio links, y(t) may vary significantly with time[2]. However, in order not to make the description of the model of the data-transmission system unduly complicated, it is here assumed that the impulse response of the channel is time-invariant, at least over the period involved in processing any one received signal element at the receiver. For practical purposes, the impulse response of the baseband channel is also assumed to be of finite duration.

The received signal at the output of the baseband channel in Figure 2.1.1 is

$$r(t) = \sum_i s_i \, y(t-iT) + w(t) \qquad (2.1.1)$$

where w(t) is the noise component in r(t). The power spectral density of w(t) is[1]

$$\tfrac{1}{2}N_o \, |B(f)|^2$$

where $|B(f)|$ is the amplitude response of the receiver filter. It is assumed here that

$$B(f) = \begin{cases} T^{\frac{1}{2}} & , \quad -\frac{1}{2T} < f < \frac{1}{2T} \\ 0 & , \quad \text{elsewhere} \end{cases} \qquad (2.1.2)$$

The autocorrelation function of w(t) is given by[1],

$$R_w(\tau') = \tfrac{1}{2}N_o \int_{-\frac{1}{2T}}^{\frac{1}{2T}} |B(f)|^2 \exp(j2\pi f\tau')df \qquad (2.1.3)$$

and for the assumed B(f), equation 2.1.3 becomes,

$$R_w(\tau') = \tfrac{1}{2}N_o \frac{\sin \pi \frac{\tau'}{T}}{\pi \frac{\tau'}{T}} \qquad (2.1.4)$$

The received signal r(t) is sampled once per signal-element at the time instants {iT}, where i takes on all positive integer values. It is assumed that the delay in transmission, other than that involved in the time dispersion of the transmitted signal, is here neglected, so that $y(hT) = 0$ for $h < 0$ and $h > g$. Therefore, the sampled value of the received signal at the output of the baseband channel, at time $t=iT$, is,

$$r_i = \sum_{h=0}^{g} s_{i-h} \, y_h + w_i \qquad (2.1.5)$$

where $y_h = y(hT)$ for h = 0,1, ..., g is the sampled impulse-response of the baseband channel. Let Y represent the (g+1)-component column vector given by the sampled impulse-response, so that

$$Y = [y_0\ y_1\ \ldots\ y_g]^T \qquad (2.1.6)$$

where the superscript T denotes transposition.

The $\{w_i\}$ in equation 2.1.5 are samples of w(t) at the time instants {iT}. They are Gaussian random variables with zero mean and variance given by,

$$\sigma_w^2 = R_w(0) = \tfrac{1}{2}N_0 \qquad (2.1.7)$$

Furthermore, from equation 2.1.4,

$$R_w(iT) = \tfrac{1}{2}N_0 \frac{\sin \pi i}{\pi i}$$

$$= 0 \text{ for any nonzero integer } i \qquad (2.1.8)$$

The noise samples have zero mean and since the separation between any two noise samples w_i and w_ℓ is a multiple of T seconds, from equation 2.1.8, they are uncorrelated and therefore statistically independent Gaussian random variables[1]. The statistical independence of the noise samples $\{w_i\}$ can be obtained using other more practical forms of the transfer function of the receiver filter. One such example is the square root of a raised cosine transfer function[1].

The detector in Figure 2.1.1 operates on the received samples $\{r_i\}$ to produce the sequence of detected data symbols $\{s'_i\}$. With correct detection, the $\{s'_i\}$ are identical to the transmitted data symbols $\{s_i\}$. However, in practice, it is not possible to recover the transmitted data sequence with certainty due to the randomness of w(t). The best that can be done is to take $\{s'_i\}$ as the detected data sequence which has the least probability of error.

2.2 THE TRANSMISSION OF DIGITAL DATA USING QUADRATURE AMPLITUDE MODULATION (QAM)

The information to be transmitted over a voice-frequency channel is originally in the form of a baseband signal. The baseband signal cannot itself be transmitted satisfactorily over this type of channel because a significant fraction of the signal power will usually be lost in transmission. Also, the received signal will normally be so severely distorted as to make satisfactory detection impossible. A good number of the voice-frequency channels introduce a small frequency-offset into the transmitted signal. Where this occurs, the whole of the spectrum of the baseband data signal is shifted by a few Hz so as to make it impossible to detect the transmitted data signal correctly, unless the frequency shift is determined exactly and suitably corrected for at the receiver[2]. A much simpler approach is to use the original baseband signal to modulate a sinusoidal carrier. The frequency of the carrier is such that the spectrum of the transmitted data signal is placed in the centre of the available frequency band[1,5,6].

A sinusoidal waveform has just three features which distinguish it from other sinusoids - phase, frequency and amplitude[7]. Therefore, the phase, frequency, amplitude or a combination of these is varied in accordance with the information to be transmitted. There are various digital modulation formats, such as phase shift keying (PSK), frequency shift keying (FSK), amplitude shift keying (ASK), and a hybrid combination of ASK and PSK which is commonly known as quadrature amplitude modulation (QAM). Among the various possible modulation formats, QAM is frequently used for high-speed data transmission, e.g. 4800 bit/s and above[2,8-15].

A QAM signal is the sum of two double-sideband suppressed carrier AM signals whose carriers are of the same frequency but in phase quadrature (i.e. at phase angle of 90^{o}). The two AM signals are in element synchronism. Clearly, a QAM system requires two modulators at the transmitter and two coherent demodulators at the receiver, which inevitably complicates the system. However, there are several important advantages of using QAM and some of these are summarized as follows[2,5,8,16,17].

1. It is a linear modulation method which greatly simplifies the implementation of the detector.
2. Efficient bandwidth utilization.
3. By using a suitable detection process, no particular phase relationship need be maintained between the reference carriers used for the demodulation of the two double-sideband AM signals and the suppressed carriers of the two AM signals themselves, just as long as the rate of change of the relative phase angles remains fairly small.

4. Ability to track phase jitter unaided by any auxiliary transmitted pilot tone.

5. High immunity to Gaussian noise.

It is due to these and also other advantages[2,5,8,16,17] that a QAM system is used in the investigation.

The two double-sideband suppressed carrier AM signals which constitute a QAM signal are transmitted in phase quadrature. With appropriate interconnection, the transmission path together with the two modulators at the transmitter and the two coherent demodulators at the receiver then appears as two linear baseband channels[2]. If one of the baseband channels is considered as carrying a 'real' signal and the other as carrying an 'imaginary' signal, the two baseband channels can be considered as a single baseband channel carrying a 'complex' signal. The theoretical analysis of the resultant system therefore reduces to that of a linear baseband channel.

The model of a data-transmission system using QAM is shown in Figure 2.2.1. The information to be transmitted is carried by two streams of data-symbols $\{s_{r,i}\}$ and $\{s_{q,i}\}$. The $\{s_{r,i}\}$ and $\{s_{q,i}\}$ are statistically independent and equally likely to have any of m possible values, so that there are m^2 possible combinations of any two data-symbols $(s_{r,i}, s_{q,i})$. The two data streams are fed separately to two transmitter filters such that the resulting QAM signal is limited to the available bandwidth of the transmission path. It is assumed that the amplitude response $|A(f)|$ of the transmitter filter has a cosine shape (square root of a raised cosine shape) as shown in Figure 2.2.2.

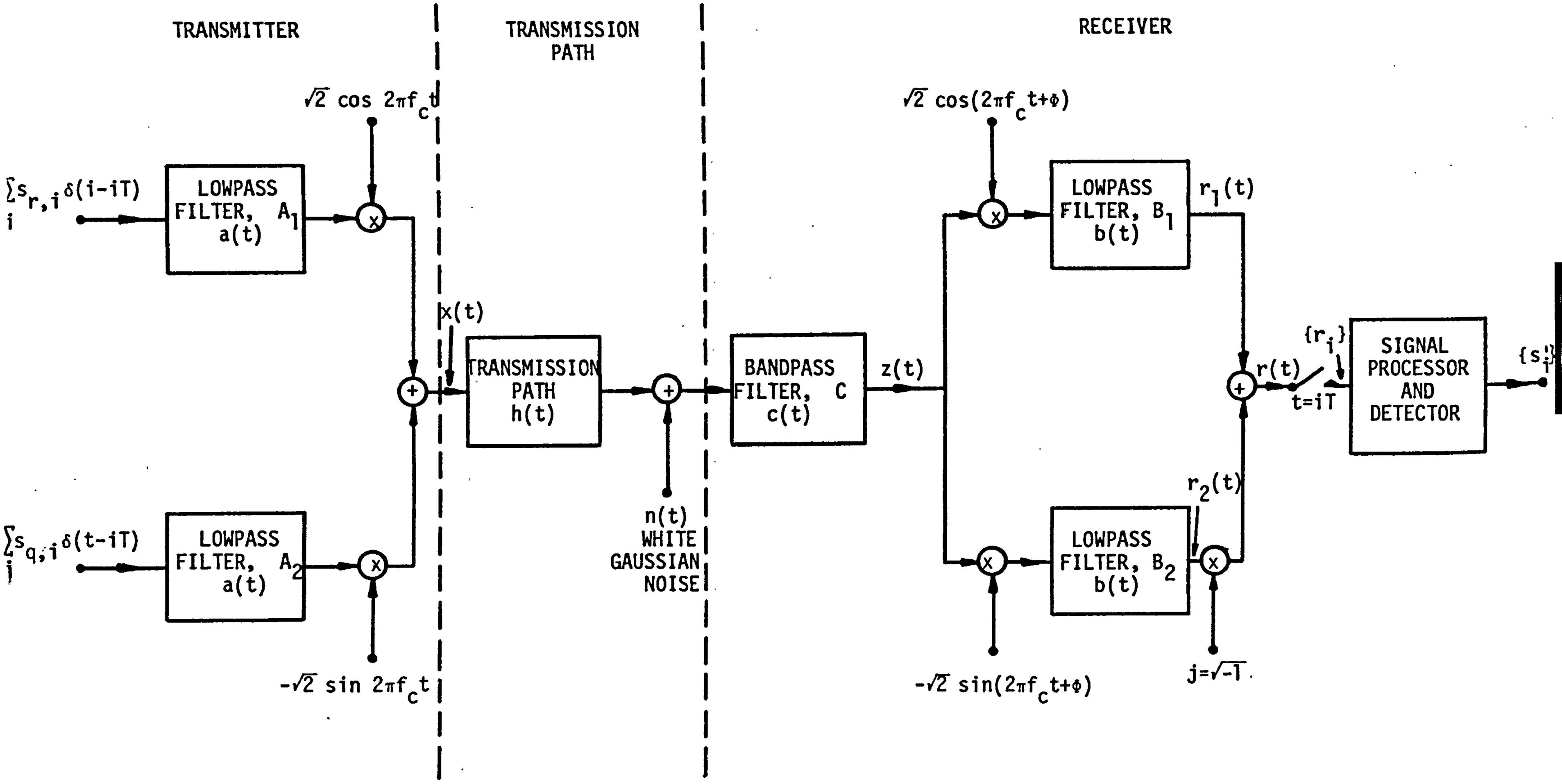

FIGURE 2.2.1: MODEL OF A DATA-TRANSMISSION SYSTEM USING QAM

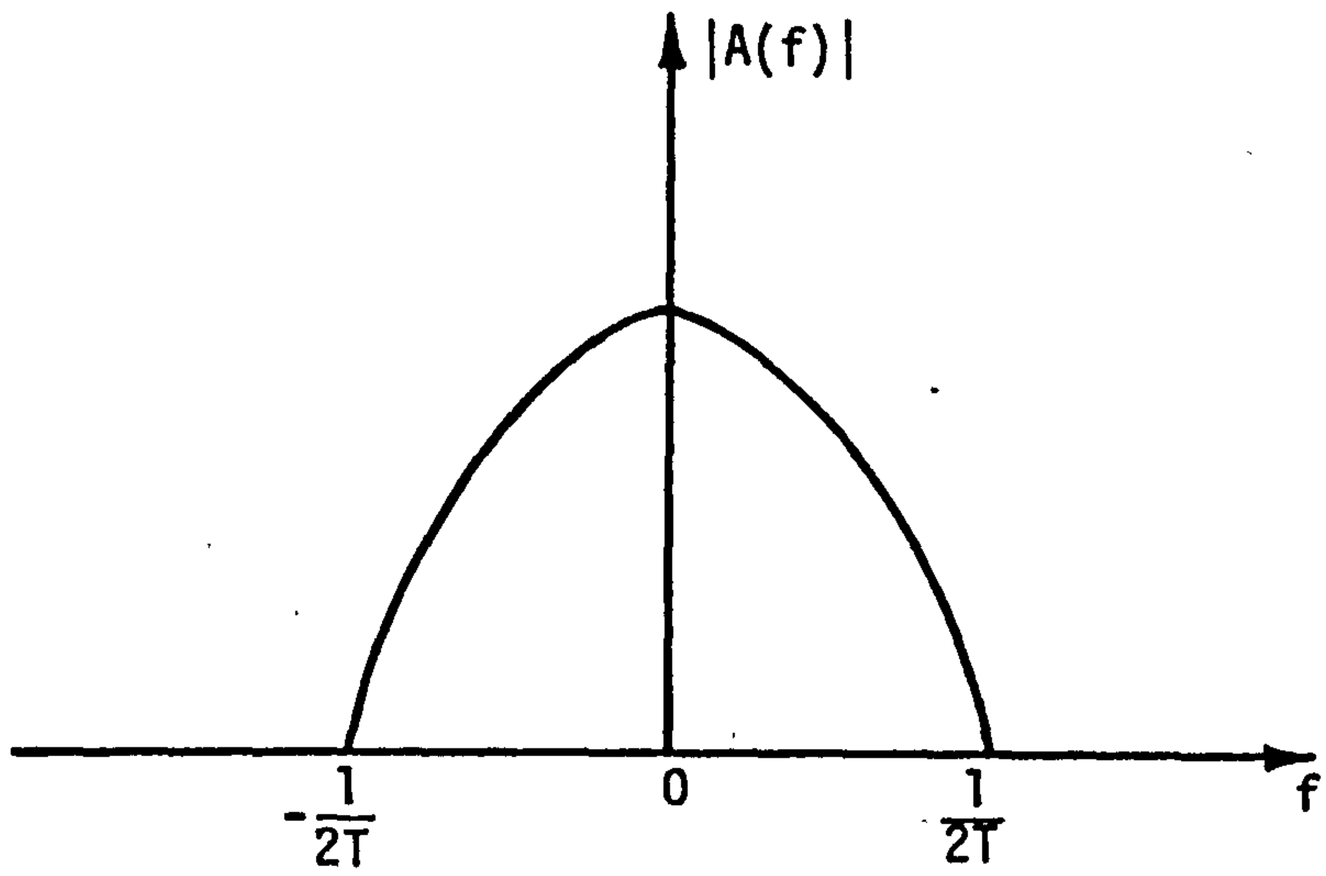

FIGURE 2.2.2: AMPLITUDE RESPONSE OF LOWPASS FILTER A

One of the filtered data streams amplitude modulates a cosine carrier, and the other amplitude modulates a sine carrier. The two carriers have the same frequency, f_c, but are in phase quadrature. The signals at the output of the linear modulators are added together to form the QAM signal, x(t). The carrier frequency is chosen so that the amplitude spectrum of the QAM signal fits into the frequency characteristics of the transmission path without appreciable loss in the transmitted signal energy.

The QAM signal at the input to the transmission path is given by,

$$x(t) = \sqrt{2}\left[\sum_i s_{r,i}\, a(t-iT) \cos 2\pi f_c t - \sum_i s_{q,i}\, a(t-iT) \sin 2\pi f_c t\right] \qquad (2.2.1)$$

where $s_{r,i}$ and $s_{q,i}$ are the i^{th} input data symbols and a(t-iT) is the impulse response of the transmitter filter delayed by iT seconds. If we define s_i as a complex data symbol, i.e.

$$s_i = s_{r,i} + js_{q,i} \qquad (2.2.2)$$

where $j = \sqrt{-1}$, then it is easily shown that equation 2.2.1 may be written as,

$$x(t) = \sqrt{2}\, Re\left[\sum_i s_i\, a(t-iT) \exp(j2\pi f_c t)\right] \qquad (2.2.3)$$

or equivalently,

$$x(t) = \frac{1}{\sqrt{2}} \left[\sum_i \left(s_i \exp(j2\pi f_c t) + s_i^* \exp(-j2\pi f_c t)\right) a(t-iT)\right] \tag{2.2.4}$$

where $(s_i^* \exp(-j2\pi f_c t))$ is the complex conjugate of $(s_i \exp(j2\pi f_c t))$.

The only additive noise assumed here is a stationary white Gaussian noise with zero mean and two-sided power spectral density of $\frac{1}{2} N_o$. The noise is added at the output of the transmission path.

At the receiver, the bandpass filter suppresses the out-of-band noise and all signals that are outside the frequency range of interest. Furthermore, the demodulator is assumed to know the nominal value of the carrier frequency. However, a small difference in frequency and phase may exist between the transmitter and receiver carrier frequencies. The resulting phase error, Φ, is modelled as a system where the transmitter and receiver carrier frequencies are exact but the phase of the local oscillator in the receiver is in error. The signal at the output of the receiver filter is then coherently demodulated by two reference carriers of the same frequency but in phase quadrature.

The signal at the input to the coherent demodulator is given by,

$$z(t) = (x(t)*h(t)*c(t)) + (n(t)*c(t)) \tag{2.2.5}$$

where * denotes convolution. $h(t)$ and $c(t)$ are the impulse responses of the transmission path and the bandpass filter C, respectively.

n(t) is the additive white Gaussian noise. The signals at the output of the cosine and sine demodulator are, respectively,

$$r_1(t) = \sqrt{2}\, z(t) \cos (2\pi f_c t + \Phi) * b(t) \qquad (2.2.6)$$

and $$r_2(t) = -\sqrt{2}\, z(t) \sin (2\pi f_c t + \Phi) * b(t) \qquad (2.2.7)$$

Combining $r_1(t)$ and $r_2(t)$ to form the complex output signal

$$r(t) = r_1(t) + j\, r_2(t) \qquad (2.2.8)$$

From equations 2.2.6, 2.2.7 and 2.2.8,

$$r(t) = \sqrt{2}\, (z(t)\, e^{-j(2\pi f_c t + \Phi)}) * b(t) \qquad (2.2.9)$$

and from equations 2.2.4, 2.2.5 and 2.2.9,

$$r(t) = \{[[\sum_i (s_i e^{j2\pi f_c t} + s_i^* e^{-j2\pi f_c t})\, a(t-iT)] * h(t) * c(t)]\, x$$

$$x\, e^{-j(2\pi f_c t + \Phi)}\} * b(t) + \sqrt{2}[[n(t) * c(t)] e^{-j(2\pi f_c t + \Phi)}] * b(t)$$

(2.2.10)

Using the property that[16],

$$(f_1(t) * f_2(t))e^{-j2\pi f_c t} = (f_1(t)e^{-j2\pi f_c t}) * (f_2(t)e^{-j2\pi f_c t}) \qquad (2.2.11)$$

which results by the direct application of the convolution integral, equation 2.2.10 becomes,

$$r(t) = \sum_i s_i \{a(t-iT) * [(h(t) * c(t))e^{-j2\pi f_c t}]\} e^{-j\Phi} * b(t) +$$

$$+ \sum_i s_i^* \{e^{-j4\pi f_c t} a(t-iT) * [(h(t) * c(t))e^{-j2\pi f_c t}]\}e^{-j\Phi} * b(t) +$$

$$+ \sqrt{2}\,[(n(t) * c(t))\, e^{-j(2\pi f_c t + \Phi)}] * b(t) \qquad (2.2.12)$$

Hence, r(t) is made up of three terms, the second of which reduces to zero since the spectrum of $(e^{-j4\pi f_c t} a(t-iT))$ lies outside the frequency band of the receiver lowpass filters. Therefore, equation 2.2.12 can be simplified to,

$$r(t) = \sum_i s_i\, y(t-iT) + w(t) \qquad (2.2.13)$$

where,

$$y(t) = \{a(t) * [(h(t) * c(t))e^{-j2\pi f_c t}]\}e^{-j\Phi} * b(t) \qquad (2.2.14)$$

is the overall system impulse response, and,

$$w(t) = \sqrt{2}[(n(t) * c(t))e^{-j2\pi f_c t}] * b(t) \qquad (2.2.15)$$

is the noise component in the received signal r(t).

At first sight, y(t) as given by equation 2.2.14 does not appear to be a baseband waveform because of the carrier component, $e^{-j2\pi f_c t}$. However, the waveform which results from the convolution of h(t) and c(t) is a bandpass waveform, i.e. the resulting spectrum is centred about the carrier frequency, f_c. Thus, by multiplying this with $e^{-j2\pi f_c t}$, together with the bandlimiting action of the lowpass filters a(t) and b(t), the bandpass waveform is transformed into a lowpass waveform, i.e. the whole spectrum is now shifted back by $-f_c$. Therefore, the overall impulse response given by equation 2.2.14 represents the impulse response of a baseband system which may be used to represent the QAM system shown in Figure 2.2.1. The baseband equivalent of the QAM system is shown in Figure 2.2.3.

In practice, the amplitude and phase/frequency characteristics of a channel are asymmetric and therefore y(t) is complex-valued. Also, y(t) usually persists over several sampling intervals. The first effect causes crosstalk interference between the real and imaginary data streams and the second effect causes intersymbol interference.

From equation 2.2.13, the sample value of r(t) at time t=kT is,

$$r_k = \sum_i s_i\, y((k-i)T) + w(kT) \qquad (2.2.15)$$

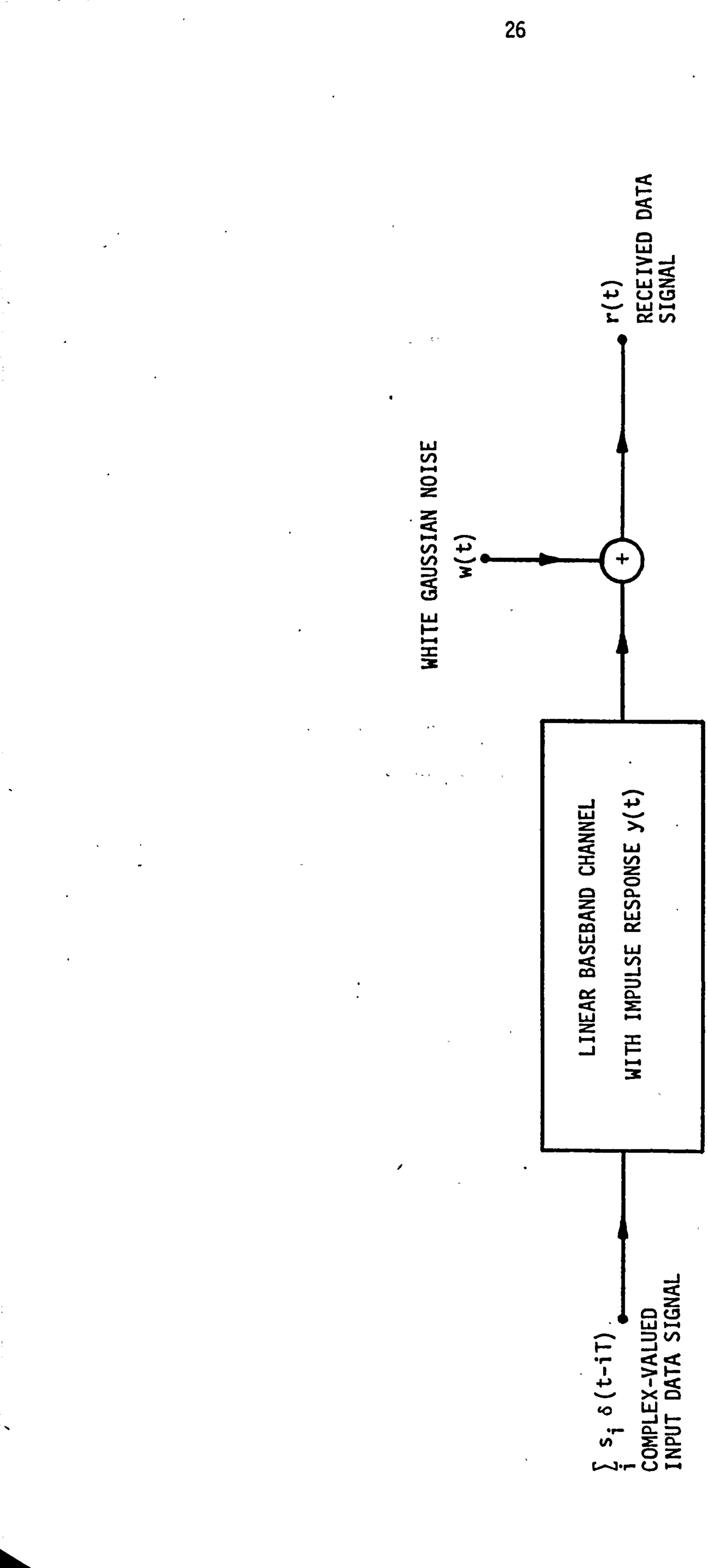

FIGURE 2.2.3: BASEBAND EQUIVALENT OF A QAM DATA-TRANSMISSION SYSTEM

or,

$$r_k = \sum_i s_i \, y_{k-i} + w_k \qquad (2.2.16)$$

However, y(t) is assumed to be of finite duration, so that $y_h = 0$ for $h < 0$ and $h > g$, consequently,

$$r_k = \sum_{h=0}^{g} s_{k-h} \, y_h + w_k \qquad (2.2.17)$$

2.3 MAXIMUM LIKELIHOOD SEQUENCE ESTIMATION (MLSE)

2.3.1 Basic Theory

The function of the detector in Figure 2.1.1 is to operate on the received data sequence $\{r_i\}$ to produce the detected data sequence $\{s'_i\}$, which is identical to the transmitted data sequence $\{s_i\}$ if the detection is correct. There are various techniques available that can be employed in the detection of digital data signals in the presence of intersymbol interference and they may be classified into two separate groups[2]. In the first of these, an equalizer is employed to correct the distortion introduced by the channel so that the intersymbol interference is reduced and the received signal is restored into a copy of the transmitted signal. Therefore, the equalizer acts as an inverse of the channel, so that the channel in cascade with the equalizer introduces no signal distortion and thus each signal-element is detected as it arrives by comparing the corresponding sample value with the appropriate threshold level. In the second group of detection processes, the decision process

itself is modified to take into account the signal distortion introduced by the channel. Often, no attempt is made to remove or even reduce the signal distortion prior to the actual decision process.

In practice, a detection process is chosen so that it gives the best compromise between performance and equipment complexity[2]. For the two criteria to be satisfied, the adopted system may or may not be optimum according to the two main definitions[2,18] of what is the optimum detection process. In the first definition, the optimum detection process minimizes the probability of error in the detection of an individual received signal-element and hence minimizes the average error rate in the detected data-symbol values. The detector, here, evaluates the a posteriori probability of each of the possible values of a received data symbol, given the whole of the received signal, and then accepts the data-symbol value having the largest a posteriori probability as the detected value. This is a process of maximum a posteriori estimation (MAP). The second type of optimum detection process is known as maximum likelihood sequence estimation (MLSE). Here, the probability of error in the detection of the whole message (entire sequence) is minimized. The detector evaluates the a posteriori probability of each possible received message and accepts as the detected message the sequence having the highest a posteriori probability as being correct.

It is inherent in either detection process (MAP or MLSE) that there is a certain delay before a decision is made, since the detector has to wait for the arrival of the complete message. With a long

message, the detection process is also far too complex to be implemented. In practice, the received sequence is divided into relatively small overlapping groups, so that in the detection of the whole message, many detection processes are involved, in fact, one per received data symbol[2]. At high signal-to-noise ratios and with additive white Gaussian noise, the MLSE, in addition to minimizing the probability of error in the detection of the whole message, also, for practical purposes, minimizes the average error rate in the detected data symbols[2]. Since the MLSE is appreciably less complex to implement than the other[19], it is considered as the optimum detection process. The MLSE will now be considered in detail.

Consider again the data-transmission system in Figure 2.1.1, the sample value of the received signal at the output of the baseband channel, at time t=iT seconds, is given by equation 2.1.5,

$$r_i = \sum_{h=0}^{g} s_{i-h}\, y_h + w_i \qquad (2.3.1)$$

In practice, the sampled impulse-response of the baseband channel is assumed to be of finite duration, so that $y_h = 0$ for $h < 0$ and $h > g$, therefore, the discrete-time model of the data-transmission system that is equivalent to that in Figure 2.1.1 has only g+1 taps and this is shown in Figure 2.3.1[19-21]. In this model, $\{r_i\}$ is the received signal samples, $\{s_i\}$ is the input data symbols and $\{y_h\}$ is the sampled impulse-response of the channel. The convolution of the $\{s_i\}$ and $\{y_h\}$ gives the signal components $\{r_i\}$. $\{w_i\}$ is the

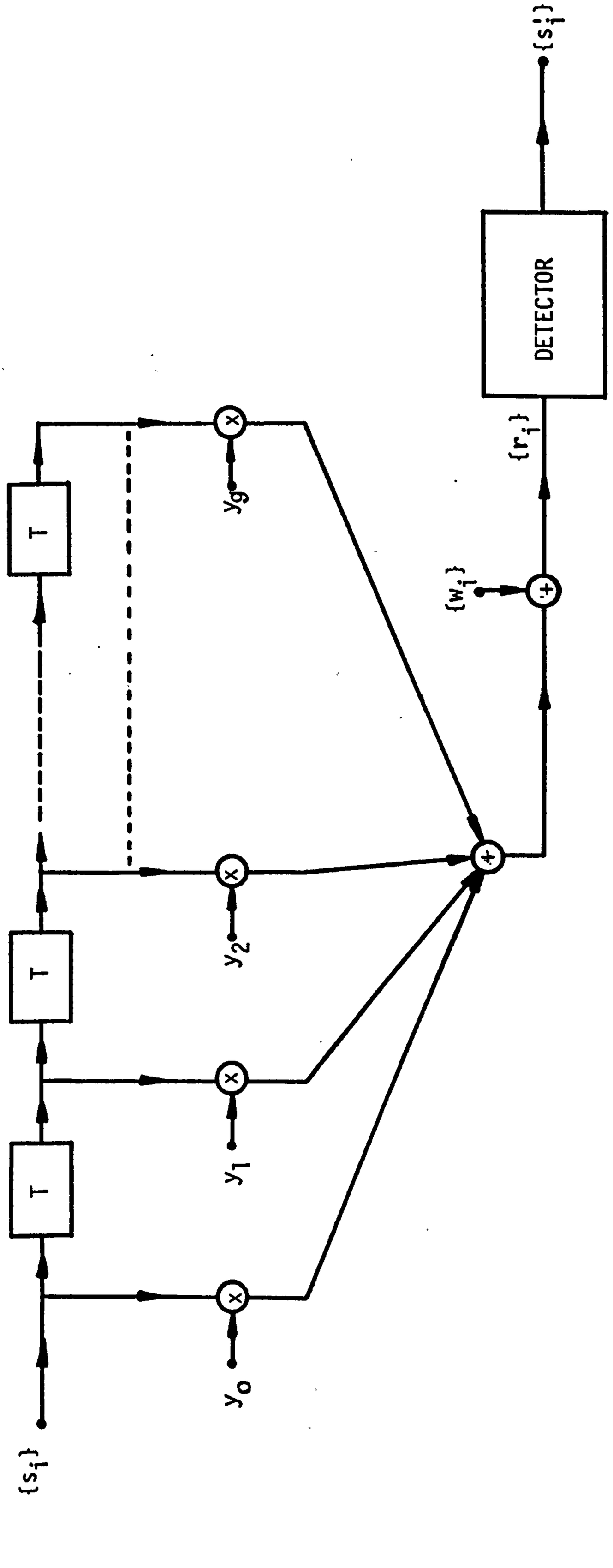

FIGURE 2.3.1: DISCRETE-TIME MODEL OF DATA-TRANSMISSION SYSTEM

white Gaussian noise samples with zero mean and variance σ^2. Let Y be the (g+1)-component column vector which represents the tap gains of the feedforward transversal filter in Figure 2.3.1,

$$Y = [y_0\ y_1\ \cdots\ y_g]^T \tag{2.3.2}$$

where the superscript T denotes transposition. Let S_N and W_N be the N-component column vectors representing the entire transmitted sequence and the noise sequence, respectively. Then,

$$S_N = [s_1\ s_2\ \cdots\ s_N]^T \tag{2.3.3}$$

where the $\{s_i\}$ are statistically independent and equally likely to have any one of m possible values, and

$$W_N = [w_1\ w_2\ \cdots\ w_N]^T \tag{2.3.4}$$

Let R_N be the corresponding N-component column vector of the received signals,

$$R_N = [r_1\ r_2\ \cdots\ r_N]^T \tag{2.3.5}$$

where the $\{r_i\}$ are related to the $\{s_i\}$, $\{y_h\}$ and $\{w_i\}$ according to equation 2.3.1. Also, let X_N, Z_N and U_N be the N-component column vectors given respectively by the following equations,

$$X_N = [x_1\ x_2\ \ldots\ x_N]^T \tag{2.3.6}$$

$$Z_N = [z_1\ z_2\ \ldots\ z_N]^T \tag{2.3.7}$$

and
$$U_N = [u_1\ u_2\ \ldots\ u_N]^T \tag{2.3.8}$$

where x_i has one of m possible values of s_i,

$$z_i = \sum_{h=0}^{g} x_{i-h}\, y_h \tag{2.3.9}$$

and u_i is the possible value of w_i satisfying,

$$r_i = z_i + u_i \tag{2.3.10}$$

The received message contains N data symbols and clearly there are m^N equally likely vectors $\{X_N\}$. The detector has prior knowledge of both Y and the possible values of s_i. It is required to make an estimate of S_N from the set of vectors $\{X_N\}$, given the received vector R_N. One of these vectors for which $p(X_N|R_N)$ is maximum is the maximum-likelihood estimate of S_N. $p(X_N|R_N)$ is the conditional probability density of X_N given R_N.

However, from Bayes' theorem[2],

$$p(X_N|R_N) = \frac{p(X_N)}{p(R_N)}\ p(R_N|X_N) \tag{2.3.11}$$

where $p(\cdot)$ indicates the probability density function of $(\cdot)$. Since $p(R_N)$ does not depend on X_N, and $p(X_N)$ is a constant for all the m^N equally likely vectors $\{X_N\}$, the value of X_N that maximizes $p(X_N|R_N)$ also maximizes $p(R_N|X_N)$ and vice versa. Thus, the vector X_N can also be chosen to maximize $p(R_N|X_N)$.

The components $\{w_i\}$ in the noise sequence of equation 2.3.4 are statistically independent Gaussian random variables with zero mean and variance σ^2. However, the following analysis can also be applied to other statistically independent random variables[2]. The Gaussian distribution is used here as it is the type of noise assumed in all models of the data-transmission system. Since the receiver is assumed to have prior knowledge of the vector Y and the possible values of s_i, it can be seen from equation 2.3.9 that z_i is determined by the given $\{x_i\}$. From equation 2.3.10, it is a standard result that for the given value of r_i and z_i, r_i is also a sample value of a Gaussian random variable with mean z_i and variance σ^2, the N $\{r_i\}$ being sample values of statistically independent Gaussian random variables. Therefore, given the $\{x_i\}$, the probability density function of any received sample r_j is given by,

$$p(r_j|x_1, x_2, \ldots, x_N) = \frac{1}{\sqrt{2\pi\sigma^2}} \exp[-\frac{(r_j - z_j)^2}{2\sigma^2}] \quad (2.3.12)$$

It is also a standard result that[2], for a sequence of statistically independent random variables $\{r_i\}$, the probability density function of the sequence of N $\{r_i\}$, given the sequence of N $\{x_i\}$, satisfies the following equation,

$$p(r_1, r_2, \ldots, r_N | x_1, x_2, \ldots, x_N) = p(r_1, r_2, \ldots, r_N | X_N)$$

$$= \prod_{j=1}^{N} p(r_j | X_N) \qquad (2.3.13)$$

where $p(r_j | X_N)$ is the conditional probability density of r_j when X_N is given.

Now, the quantity to be minimized is $p(R_N | X_N)$, which can also be written as,

$$p(R_N | X_N) = p(r_1, r_2, \ldots, r_N | X_N) \qquad (2.3.14)$$

Using equations 2.3.12 and 2.3.13, equation 2.3.14 becomes,

$$p(R_N | X_N) = \prod_{j=1}^{N} \frac{1}{\sqrt{2\pi\sigma^2}} \exp\left[-\frac{(r_j - z_j)^2}{2\sigma^2}\right]$$

$$= \frac{1}{(2\pi\sigma^2)^{N/2}} \exp\left[-\frac{1}{2\sigma^2} \sum_{j=1}^{N} (r_j - z_j)^2\right]$$

$$= \frac{1}{(2\pi\sigma^2)^{N/2}} \exp\left[-\frac{1}{2\sigma^2} |R_N - Z_N|^2\right] \qquad (2.3.15)$$

where $|R_N - Z_N|$ is the Euclidean distance between R_N and Z_N. It is clear, from equation 2.3.15, that $p(R_N | X_N)$ is maximum when the distance between R_N and Z_N is a minimum. Now, from equation 2.3.10,

$$R_N - Z_N = U_N \tag{2.3.16}$$

thus,

$$p(R_N|X_N) = \frac{1}{(2\pi\sigma^2)^{N/2}} \exp[-\frac{1}{2\sigma^2} |U_N|^2] \tag{2.3.17}$$

Hence, the maximum-likelihood vector X_N is its possible value such that

$$|U_N|^2 = u_1^2 + u_2^2 + \ldots + u_N^2 \tag{2.3.18}$$

is minimized. The quantity $|U_N|^2$ is also known as the cost function for the sequence of N $\{x_i\}$. For an m-level signal and a given vector R_N, the cost function can take on m^N possible values corresponding to the different possible sequences $\{X_N\}$. Therefore, one possible method of finding the maximum-likelihood sequence X_N is for the detector to evaluate the m^N possible values of the cost function and the maximum-likelihood sequence is that which corresponds to the smallest cost function.

The above derivation holds for real signals and is readily generalized to complex signals, where now the real and imaginary parts of the $\{u_i\}$ are statistically independent Gaussian random variables with zero mean and variance σ^2, and

$$|U_N|^2 = |u_1|^2 + |u_2|^2 + \ldots + |u_N|^2 \tag{2.3.19}$$

where $|u_i|$ is the modulus (absolute value) of u_i. $|R_N - Z_N|$ is now the unitary distance between R_N and Z_N, and again the maximum-likelihood sequence X_N is that for which $|U_N|^2$ is minimum[2,10,16].

2.3.2 Implementation of the MLSE Using the Viterbi Algorithm

As mentioned in the last section, the direct implementation of the MLSE involves the computation of m^N cost functions. This is obviously impractical when the number of data symbols which constitute a message is several thousands long. The detector now has to consider an almost infinite number of possible sequences and the associated costs. However, a computationally efficient algorithm, known as the Viterbi algorithm, exists and can produce the maximum-likelihood sequence recursively. The algorithm will now be described to show how the MLSE can be implemented. The description of the algorithm is really an extension from the previous section.

Let S_k, R_k and W_k be the k-component column vectors whose i^{th} components are s_i, r_i and w_i, respectively, for $i = 1, 2, \ldots, k$ and $k < N$. Also, let X_k, Z_k and U_k be the k-component column vectors whose i^{th} components are x_i, z_i and u_i, respectively, for $i = 1, 2, \ldots k$, where x_i has one of the m possible values of s_i,

$$z_i = \sum_{h=0}^{g} x_{i-h}\, y_h \qquad (2.3.20)$$

and u_i is the possible value of w_i satisfying,

$$r_i = z_i + u_i \tag{2.3.21}$$

The maximum-likelihood vector X_k is its possible value such that,

$$|U_k|^2 = |u_1|^2 + |u_2|^2 + \ldots + |u_k|^2 \tag{2.3.22}$$

is minimized.

In the Viterbi algorithm detector, instead of the simultaneous processing of all the m^N possible vectors $\{X_N\}$, the receiver holds in store the last n components $\{x_i\}$ of each of the m^g different vectors $\{X_k\}$, where the vectors have all possible combinations of their last g components $\{x_i\}$. Let the set of n-component vectors be $\{Q_k\}$, where,

$$Q_k = [x_{k-n+1}\ x_{k-n+2} \cdots x_k]^T \tag{2.3.23}$$

Each vector Q_k is here the maximum-likelihood vector subject to the constraint that its last g components have the given values. One of these vectors is the true maximum-likelihood vector. Thus, following the receipt of r_k, each of the stored vectors $\{Q_k\}$ corresponding to the different possible combinations of values of

$$[x_{k-n+1}\ x_{k-n+2} \cdots x_k]^T$$

is a possible realization of the transmitted data sequence

$$[s_{k-n+1}\ s_{k-n+2}\ \cdots\ s_k]^T$$

Associated with each stored vector Q_k is stored the cost $|U_k|^2$, where $|U_k|^2$ is evaluated using equations 2.3.20-2.3.22. The lower the cost, the more likely is the vector to be correct. The data-symbol s_{k-n+1} is detected as the value of x_{k-n+1} in the true maximum-likelihood vector Q_k which is the one of the vectors having the smallest cost. In this case, the delay in detecting a data symbol has been fixed to n-1 sampling intervals, and n should be made as large as possible, preferably no less than 3g, in order to achieve the best available tolerance to noise[21-23].

On receipt of the sample r_{k+1}, each stored vector $\{Q_k\}$ is 'expanded' to give m vectors $\{Q_{k+1}\}$, where the $\{Q_{k+1}\}$ are the possible combinations of

$$[x_{k-n+2}\ x_{k-n+3}\ \cdots\ x_{k+1}]^T$$

The values of x_{k-n+2}, x_{k-n+3}, ..., x_k are as in the original sequence, and x_{k+1} takes on its m possible values. The number of possible vectors has increased to m^{g+1} and the cost associated with each vector is evaluated according to,

$$|U_{k+1}|^2 = |U_k|^2 + (r_{k+1} - \sum_{h=0}^{g} x_{k-h+1}\ y_h)^2 \qquad (2.3.24)$$

where $|U_k|^2$ is the cost of the vector Q_k from which Q_{k+1} originated. From the m^{g+1} vectors $\{Q_{k+1}\}$ are then selected the m^g vectors having

the m^g different possible combinations of the values of

$$[x_{k-g+2}\ x_{k-g+3} \cdots x_{k+1}]^T$$

together with the lowest costs. The remaining vectors are discarded. The true maximum-likelihood vector Q_{k+1} is the one of the set of m^g surviving vectors $\{Q_{k+1}\}$ having the smallest cost. The process continues in this way.

It can be seen that the detection process involves m^{g+1} squaring operations per received data symbol together with the storage of m^g n-component vectors $\{Q_k\}$ and m^g values of $\{|U_k|^2\}$. Clearly, when $g >> 1$, the number of operations per received data symbol is excessive and also a large amount of storage is required. Therefore, various techniques have been developed to reduce the number of computations and stored values and yet maintained near optimum performance[2,22-25]. However, these developments will not be dealt into since they are not essential to the subject matter of this investigation.

The Viterbi algorithm is optimum for maximum-likelihood estimation of the entire transmitted sequence, if an unbounded delay in detection is allowed, and is also effectively optimum in the same sense for reasonable finite delays[19]. The algorithm is not designed to minimize the symbol-error probability P(e), but at high signal-to-noise ratios, the detector that minimizes P(e) cannot improve substantially on the performance of this detector[19]. It is shown in Ref. 19 that, when the noise components $\{w_i\}$ are zero mean and

variance σ^2 Gaussian random variables, the upper and lower bounds for P(e) are given by,

$$K_\ell \, Q[\frac{d_{min}}{2\sigma}] \leq P(e) \leq K_u \, Q[\frac{d_{min}}{2\sigma}] \qquad (2.3.25)$$

where $Q[\cdot]$ is the probability of error function and is given by,

$$Q[x] \triangleq \frac{1}{\sqrt{2\pi}} \int_x^\infty \exp\left(-\frac{y^2}{2}\right) dy \qquad (2.3.26)$$

d_{min} is the minimum distance between any pair of the m^N possible vectors $\{Z_N\}$, (equation 2.3.7). K_u is a constant independent of σ^2 and K_ℓ is another constant typically within an order of magnitude of K_u. Therefore, equation 2.3.25 can be used to assess the performance of the maximum-likelihood estimator.

3. CHANNEL ESTIMATORS FOR TIME-INVARIANT OR SLOWLY TIME-VARYING CHANNELS

3.1 INTRODUCTION

In the above discussion on the MLSE, it is assumed that the detector knows the vector Y, the sampled impulse-response of the channel. In fact, the knowledge of Y is required so that the possible signal vectors $\{Z_N\}$, given by equations 2.3.7 and 2.3.9, can be calculated before evaluating the cost functions and hence selecting the maximum-likelihood sequence. Since the characteristics of the channel are usually unknown prior to a transmission and also possibly vary with time, some form of algorithm or device is needed to provide the detector with an accurate knowledge of the sampled impulse-response of the channel.

Over telephone circuits, the channel characteristics only vary very slowly with time, however by dialling another connection, the new path may have considerably different characteristics[2]. In this case, the sampled impulse-response may be estimated continuously or if the transmission time is relatively short, it is estimated at the start of transmission and the values are held fixed for the duration of the transmission. When data is transmitted over an HF radio link, it is necessary to estimate the sampled impulse-response continuously, so that the detector is held correctly adjusted for the channel[2]. Also, in high speed data-transmission systems (>2400 bit/s), the channel characteristics may vary significantly with time even over telephone circuits[2] and so the sampled impulse-

response must be estimated continuously at the receiver from the received data signal.

In the following sections, several algorithms that can be used to estimate the sampled impulse-response of a channel will be examined. Our attention is here restricted only to noisy linear channels which are time invariant or else vary slowly with time. The identification of nonlinear channels is beyond the scope of this thesis. However, as an example, the interested reader is referred to Ref. 25 which describes some techniques for estimating the sampled impulse-response of time-invariant, dispersive nonlinear systems with noisy outputs. We first begin in Section 3.2 with an outline of various assumptions concerning the data-transmission system, some of these are necessary in order to simplify the descriptions of the estimators. In Section 3.3, an estimate of the channel is derived using the least mean-squared error criterion. This is the most commonly used estimation criterion. Sections 3.4-3.7 describe the channel estimators.

3.2 BASIC ASSUMPTIONS

Since we are only interested in the estimation of the sampled impulse-response of the channel, the model of the data-transmission system of Figure 2.2.1 is simplified to that in Figure 3.2.1. Here, for convenience, the detector is omitted, so that any delay in the detection of a data symbol, which is the inherent property of, for example, the maximum likelihood detectors, is neglected. Thus, the data-symbol s_i is detected upon the arrival of the received signal r_i.

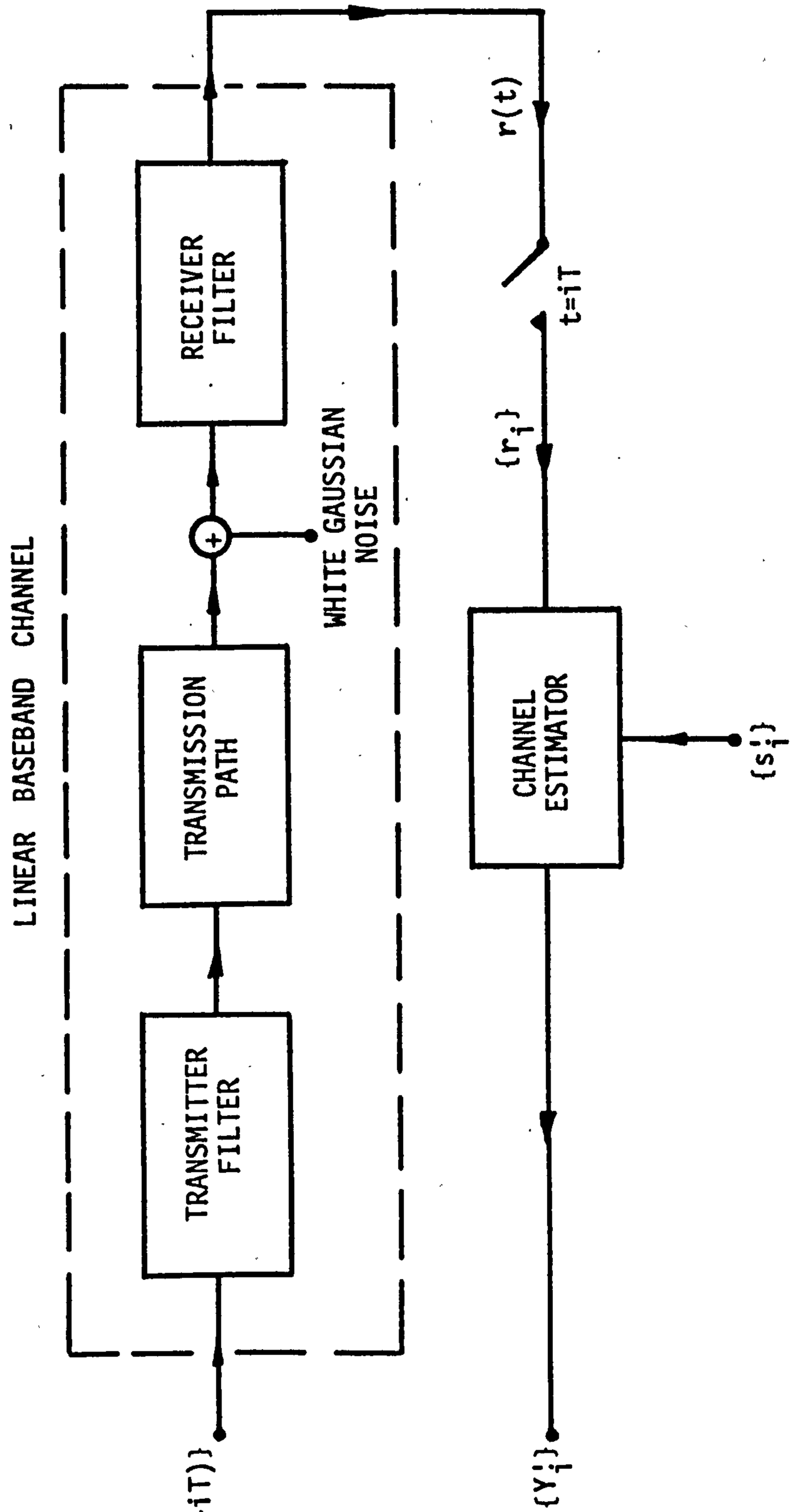

FIGURE 3.2.1: MODEL OF CHANNEL AND ESTIMATOR

The estimator uses both of these signals for the estimation of the sampled impulse-response.

The signal at the input to the baseband channel is a sequence of regularly spaced impulses $\{s_i\ \delta(t-iT)\}$, where the $\{s_i\}$ are assumed to be statistically independent and equally likely to have any of m possible values. It is assumed that transmission starts at time t = T seconds. The linear baseband channel is assumed to have an impulse response y(t) with an effective duration of less than (g+1)T seconds, where g is a given positive integer. The only noise introduced by the channel is stationary white Gaussian noise which is added to the data signal at the output of the transmission path such that the noise waveform w(t) at the output of the receiver filter is a band-limited Gaussian noise. At the output of the baseband channel, the received signal r(t) is sampled once per received signal-element, at the time instants {iT}, giving the received samples $\{r_i\}$, where,

$$r_i = \sum_{h=0}^{g} s_{i-h}\, y_h + w_i \qquad (3.2.1)$$

In the foregoing equation, $r_i = r(iT)$, $y_h = h(hT)$ and $w_i = w(iT)$. For simplicity, it is assumed that the $\{s_i\}$, $\{y_h\}$, $\{w_i\}$ and hence $\{r_i\}$ have only real values. The delay in transmission is neglected so that $y_i = 0$ for $i<0$ and $i>g$. Let Y represent the (g+1)-component column vector of the sampled impulse-response of the channel,

$$Y = [y_0\ y_1\ \ldots\ y_g]^T \qquad (3.2.2)$$

where the superscript T denotes transposition, and Y is time invariant. The noise samples $\{w_i\}$ have zero mean and a fixed variance of σ^2. It is assumed that the $\{w_i\}$ are statistically independent of the $\{s_i\}$. Since it is assumed that there is no delay in the detection of a data symbol, s_i is detected immediately after the reception of r_i. The detected value of s_i is designated s_i'. Normally, the error rates for data communication are less than 10^{-4}[33], and with so few errors in the $\{s_i'\}$ it is reasonable to assume that the $\{s_i\}$ are all correctly detected. Thus, $s_i' = s_i$ for all $\{i\}$. The signals r_i and s_i' are fed to the channel estimator to give an estimate Y_i' of Y at time t=iT, where,

$$Y_i' = [y_{i,o}' \; y_{i,1}' \; \cdots \; y_{i,g}']^T \qquad (3.2.3)$$

The estimate Y_i' is used by the detector for the detection of the next data symbol.

Obviously, in the above description the channel estimator is assumed to be recursive. However, some of the estimators to be examined are nonrecursive. In this case, the estimator waits for the arrival of all $\{r_i\}$, resulting from the transmission of a fairly short data sequence, before estimating the sampled impulse-response of the channel.

3.3 LEAST-SQUARES ESTIMATION

The sample value of the received signal taken at time t=kT is given by,

$$r_k = \sum_{h=0}^{g} s_{k-h}\, y_h + w_k \qquad (3.3.1)$$

where $\{y_h\}$, h = 0,1,...,g are the g+1 unknown parameters. $\{y_h\}$ are the sampled impulse-response of the channel and these are to be estimated in some manner. $\{w_k\}$ are statistically independent Gaussian random variables with zero mean and variance σ^2. Also, the $\{w_k\}$ are statistically independent of the $\{s_k\}$. w_k is the noise component in r_k.

Let us assume that at time t=iT, i samples $\{r_k\}$ have been received and the corresponding i data symbols have been detected. If Y_i' (equation 3.2.3) is an estimate of Y based on the i received samples $r_1, r_2, \ldots, r_i$ then the estimate of the k^{th} received signal r_k is given by,

$$r_k' = \sum_{h=0}^{g} s_{k-h}\, y'_{i,h} \qquad k = 1,2,\ldots,i \qquad (3.3.2)$$

bearing in mind that the $\{s_i\}$ are assumed to be correctly detected, and $y'_{i,h}$ is in general a better estimate of y_h than is $y_{k,h}$ for k<i. The error in the estimate of r_k is,

$$e_k = r_k - \sum_{h=0}^{g} s_{k-h}\, y'_{i,h} \quad k = 1,2,..,i \qquad (3.3.3)$$

The sum of the squares of the errors in the estimates of the $\{r_k\}$ using equation 3.3.2 up to time t=iT is given by,

$$M_i = \sum_{k=1}^{i} (r_k - \sum_{h=0}^{g} s_{k-h} y'_{i,h})^2 \qquad (3.3.4)$$

The sequence of values $\{y'_{i,h}\}$ that minimizes M_i is the least-squares estimate of Y. Differentiating M_i with respect to each of the $\{y'_{i,h}\}$ gives,

$$\frac{\partial M_i}{\partial y'_{i,j}} = 2 \sum_{k=1}^{i} (r_k - \sum_{h=0}^{g} s_{k-h}\, y'_{i,h})\, s_{k-j} \quad j = 0,1,\ldots,g \qquad (3.3.5)$$

Defining the cross-correlation vector and the autocorrelation matrix, respectively, as,

$$b_j = \sum_{k=1}^{i} r_k\, s_{k-j} \qquad j = 0,1,\ldots,g \qquad (3.3.6)$$

and

$$q_{h,j} = \sum_{k=1}^{i} s_{k-h}\, s_{k-j} \qquad \begin{matrix} h = 0,1,\ldots,g \\ j = 0,1,\ldots,g \end{matrix} \qquad (3.3.7)$$

The sequence of values $\{y'_{i,h}\}$ that minimizes M_i can be found by setting to zero the partial derivatives of M_i w.r.t. $\{y'_{i,h}\}$, that is,

$$2 \sum_{k=1}^{i} (r_k - \sum_{h=0}^{g} s_{k-h}\, y'_{i,h})\, s_{k-j} = 0 \qquad j = 0,1,\ldots,g$$

or
$$\sum_{h=0}^{g} y'_{i,h} \sum_{k=1}^{i} s_{k-h}\, s_{k-j} = \sum_{k=1}^{i} r_k\, s_{k-j} \qquad j = 0,1,\ldots,g$$

or
$$\sum_{h=0}^{g} y'_{i,h}\, q_{h,j} = b_j \qquad j = 0,1,\ldots,g \qquad (3.3.8)$$

Let

$$B_i = [b_o\ b_1\ \ldots\ b_g]^T \qquad (3.3.9)$$

and

$$C_i = \begin{bmatrix} s_1 & s_2 & \cdot & \cdot & \cdot & s_i \\ s_o & s_1 & \cdot & \cdot & \cdot & s_{i-1} \\ \cdot & \cdot & & & & \cdot \\ \cdot & \cdot & & & & \cdot \\ \cdot & \cdot & & & & \cdot \\ s_{1-g} & s_{2-g} & \cdot & \cdot & & s_{i-g} \end{bmatrix} \qquad (3.3.10)$$

then, the set of equations 3.3.8 may be written in matrix form as,

$$C_i C_i^T\, Y'_i = B_i \qquad (3.3.11)$$

If $C_i C_i^T$ is nonsingular, then it has an inverse, so that the solution for Y'_i is given by,

$$Y_i' = A_i B_i \tag{3.3.12}$$

where,

$$A_i = (C_i C_i^T)^{-1} \tag{3.3.13}$$

Furthermore, if S_k is a (g+1)-component column vector of the detected data symbols and defined as,

$$S_k = [s_k' \quad s_{k-1}' \quad \cdot \quad \cdot \quad \cdot \quad s_{k-g}']^T$$

$$= [s_k \quad s_{k-1} \quad \cdot \quad \cdot \quad \cdot \quad s_{k-g}]^T \tag{3.3.14}$$

then, it is easily shown that,

$$C_i C_i^T = \sum_{k=1}^{i} S_k S_k^T \tag{3.3.15}$$

and

$$B_i = \sum_{k=1}^{i} r_k S_k \tag{3.3.16}$$

Therefore, the least-squares solution can also be written as,

$$Y_i' = [\sum_{k=1}^{i} S_k S_k^T]^{-1} \sum_{k=1}^{i} r_k S_k \tag{3.3.17}$$

For sufficiently large values of i, equation 3.3.17 can be replaced by[28],

$$E[S_k S_k^T]Y_i' = E[r_k S_k] \tag{3.3.18}$$

where E is the expectation operator. Expanding the foregoing equation, we have,

$$\begin{bmatrix} E[s_k\ s_k] & E[s_k\ s_{k-1}] & \cdots & E[s_k\ s_{k-g}] \\ E[s_{k-1}s_k] & E[s_{k-1}s_{k-1}] & \cdots & E[s_{k-1}s_{k-g}] \\ \vdots & \vdots & & \vdots \\ E[s_{k-g}s_k] & E[s_{k-g}s_{k-1}] & \cdots & E[s_{k-g}s_{k-g}] \end{bmatrix} \begin{bmatrix} y_{i,o}' \\ y_{i,1}' \\ \vdots \\ y_{i,g}' \end{bmatrix} = \begin{bmatrix} E[r_k s_k] \\ E[r_k s_{k-1}] \\ \vdots \\ E[r_k s_{k-g}] \end{bmatrix} \tag{3.3.19}$$

Since the $\{s_i\}$ are uncorrelated and also statistically independent of the $\{w_i\}$, equation 3.3.19 reduces to

$$\begin{bmatrix} E[s_k s_k] & & & 0 \\ & E[s_{k-1}s_{k-1}] & & \\ & & \ddots & \\ 0 & & & E[s_{k-g}s_{k-g}] \end{bmatrix} \begin{bmatrix} y_{i,o}' \\ y_{i,1}' \\ \vdots \\ y_{i,g}' \end{bmatrix} = \begin{bmatrix} y_o E[s_k s_k] \\ y_1 E[s_{k-1}s_{k-1}] \\ \vdots \\ y_g E[s_{k-g}s_{k-g}] \end{bmatrix} \tag{3.3.20}$$

The inverse of the nonsingular diagonal matrix on the left-hand side of equation 3.3.20 is simply

$$\begin{bmatrix} (E[s_k s_k])^{-1} & & & 0 \\ & (E[s_{k-1} s_{k-1}])^{-1} & & \\ & & \ddots & \\ 0 & & & (E[s_{k-g} s_{k-g}])^{-1} \end{bmatrix}$$

Premultiplying equation 3.3.20 by this inverse, results in,

$$Y_i' = Y \tag{3.3.21}$$

Hence, when i is large and the statistical properties of the $\{s_k\}$ and $\{w_k\}$ are met, the estimate Y_i' converges exactly to the actual value of Y. Otherwise, by noting that $S_k^T Y_i' = Y_i'^T S_k$ and $B_i = A_i^{-1} Y_i'$ (equation 3.3.12), the minimum value of M_i is,

$$M_{i(min)} = \sum_{k=1}^{i} (r_k - Y_i'^T S_k)^2$$

$$= \sum_{k=1}^{i} (r_k^2 - 2r_k Y_i'^T S_k + Y_i'^T S_k S_k^T Y_i')$$

$$= \sum_{k=1}^{i} r_k^2 - 2Y_i'^T \sum_{k=1}^{i} r_k S_k + Y_i'^T (\sum_{k=1}^{i} S_k S_k^T) Y_i'$$

$$= \sum_{k=1}^{i} r_k^2 - 2Y_i'^T B_i + Y_i'^T A_i^{-1} Y_i'$$

$$= \sum_{k=1}^{i} r_k^2 - 2Y_i'^T A_i^{-1} Y_i' + Y_i'^T A_i^{-1} Y_i'$$

$$= \sum_{k=1}^{i} r_k^2 - Y_i'^T A_i^{-1} Y_i' \qquad (3.3.22)$$

3.4 RECURSIVE LEAST-SQUARES ESTIMATOR

Although the estimate Y_i' as given by equation 3.3.12 is optimum in the sense that the least-squares criterion function is minimized, it is nonrecursive and difficult to implement in practice. The first difficulty is that all the components of the (g+1)xi matrix C_i must be known beforehand. Secondly, the matrix $C_i C_i^T$ has to be inverted every time which will involve a large amount of processing time when g and i are large. Therefore, a recursive form of the solution given by equation 3.3.12 is desirable where the new estimate Y_i' at time t=iT is derived from past estimates.

The nonrecursive least-squares estimate of Y is

$$Y_i' = A_i B_i \qquad (3.4.1)$$

where

$$A_i = \left(\sum_{k=1}^{i} S_k S_k^T \right)^{-1} \qquad (3.4.2)$$

and

$$B_i = \sum_{k=1}^{i} r_k S_k \qquad (3.4.3)$$

Using equations 3.4.2 and 3.4.3, A_i and B_i can be related to their previous values A_{i-1} and B_{i-1}, respectively, by the following equations,

$$A_i^{-1} = A_{i-1}^{-1} + S_i S_i^T \tag{3.4.4}$$

and

$$B_i = B_{i-1} + r_i S_i \tag{3.4.5}$$

Let us consider equation 3.4.4. Premultiplying it by A_i and post-multiplying by A_{i-1} gives,

$$A_{i-1} = A_i + A_i S_i S_i^T A_{i-1} \tag{3.4.6}$$

Postmultiplying by S_i,

$$A_{i-1}S_i = A_i S_i + A_i S_i S_i^T A_{i-1} S_i$$

$$= A_i S_i \, (1 + S_i^T A_{i-1} S_i) \tag{3.4.7}$$

Postmultiplying by $(1 + S_i^T A_{i-1} S_i)^{-1} S_i^T A_{i-1}$,

$$A_{i-1}S_i(1 + S_i^T A_{i-1} S_i)^{-1} S_i^T A_{i-1} = A_i S_i S_i^T A_{i-1} \tag{3.4.8}$$

Substituting the value of $A_i S_i S_i^T A_{i-1}$ from equation 3.4.6 into the foregoing equation, we have

$$A_{i-1}S_i\ (1 + S_i^T A_{i-1}S_i)^{-1}S_i^T A_{i-1} = A_{i-1} - A_i$$

or

$$A_i = A_{i-1} - A_{i-1}S_i(1 + S_i^T A_{i-1}S_i)^{-1}S_i^T A_{i-1}$$

$$= A_{i-1} - K_i S_i^T A_{i-1} \qquad (3.4.9)$$

where,

$$K_i = A_{i-1}S_i\ (1 + S_i^T A_{i-1}S_i)^{-1} \qquad (3.4.10)$$

Finally, using equations 3.4.5, 3.4.9 and 3.4.10, equation 3.4.1 becomes,

$$Y_i' = (A_{i-1} - K_i S_i^T A_{i-1})(B_{i-1} + r_i S_i)$$

$$= A_{i-1}B_{i-1} + r_i A_{i-1}S_i - K_i S_i^T A_{i-1}B_{i-1} -$$

$$- r_i K_i S_i^T A_{i-1}S_i$$

$$= A_{i-1}B_{i-1} + r_i K_i\ (1 + S_i^T A_{i-1}S_i) -$$

$$- K_i S_i^T A_{i-1}B_{i-1} - r_i K_i S_i^T A_{i-1}S_i$$

$$= A_{i-1}B_{i-1} + K_i(r_i - S_i^T A_{i-1}B_{i-1})$$

$$= Y_{i-1}' + K_i\ (r_i - S_i^T Y_{i-1}') \qquad (3.4.11)$$

Therefore, equations 3.4.9, 3.4.10 and 3.4.11 constitute a recursive form of the least-squares solution and these are regrouped in the order in which they are executed as follows.

$$K_i = A_{i-1}S_i \left(1 + S_i^T A_{i-1} S_i\right)^{-1} \qquad (3.4.12a)$$

$$A_i = A_{i-1} - K_i S_i^T A_{i-1} \qquad (3.4.12b)$$

$$Y_i' = Y_{i-1}' + K_i \left(r_i - S_i^T Y_{i-1}'\right) \qquad (3.4.12c)$$

Notice here that no matrix inversion is required. The term $(1 + S_i^T A_{i-1} S_i)$ in equation 3.4.12a is simply a scalar quantity. To start the estimator, values of A_o and Y_o' are required. As an example, Y_o' may be set to a null vector and A_o is set to a diagonal matrix with large diagonal elements[32].

In deriving the above algorithms, no mention was made of the statistical properties of the noise components $\{w_i\}$. To improve the estimator, we can include this information in the algorithms and this is done as follows.

The least-squares estimate Y_i' given by equation 3.3.12 can be shown[40] to be an unbiased estimate, that is,

$$E[Y_i'] = Y \qquad (3.4.13)$$

Also, if we define the error covariance matrix P_i as,

$$P_i = E[(Y_i' - Y)(Y_i' - Y)^T] \qquad (3.4.14)$$

then it can easily be shown that, under the conditions assumed here[40],

$$P_i = \sigma^2 A_i \qquad (3.4.15)$$

where σ^2 is the variance of the $\{w_i\}$. Therefore, using the relationship in equation 3.4.15, the recursive algorithms of equations 3.4.12a-3.4.12c are transformed into a new set of algorithms as given below,

$$K_i = P_{i-1}S_i(\sigma^2 + S_i^T P_{i-1} S_i)^{-1} \qquad (3.4.16a)$$

$$P_i = P_{i-1} - K_i S_i^T P_{i-1} \qquad (3.4.16b)$$

$$Y_i' = Y_{i-1}' + K_i(r_i - S_i^T Y_{i-1}') \qquad (3.4.16c)$$

Clearly, the inclusion of the statistical properties of the $\{w_i\}$ has improved the estimator. In addition to providing the least-squares estimates Y_i', we are now able to get an indication of the accuracy of these estimates through the error covariance matrix P_i. The initial values required here are those of P_o and Y_o'. Since P_i is an error covariance matrix, P_o may be chosen to reflect the degree of confidence in the initial estimate Y_o'. Usually, little is known of Y at the start of the estimation process, so the most useful value for Y_o' is the null vector, and P_o is set to be a diagonal matrix with large diagonal elements[32].

The nonrecursive least-squares solution (equation 3.3.12) and both algorithms 3.4.12(a)-(c) and 3.4.16(a)-(c) assume implicitly that Y is reasonably time-invariant over the interval $T<t<iT$. When this is not the case or if there is an uncertainty on this point, both recursive algorithms can be reformulated to include the knowledge of the variation of Y.

Let us assume that the variation of Y is described by a first-order recursive process driven by zero mean white noise process, that is,

$$Y_i = \Phi_{i,i-1} Y_{i-1} + V_{i-1} \tag{3.4.17}$$

where $\Phi_{i,i-1}$ is the $(g+1)x(g+1)$ transition matrix and V_{i-1} is the $(g+1)$-component column vector of random variables representing the fluctuations in Y_i. The received sample r_i which contains the information on Y_i is given by,

$$r_i = S_i^T Y_i + w_i \tag{3.4.18}$$

where S_i is defined in equation 3.3.14 and w_i is the noise component in r_i. $\{w_i\}$ and $\{V_i\}$ have the following statistics.

$$\left.\begin{aligned} E[w_i] &= 0 \\ E[V_i] &= 0 \\ E[w_i^2] &= \sigma^2 \\ E[V_i V_j^T] &= Q_i \delta_{ij} \\ E[w_i V_j^T] &= 0 \qquad \text{for all } i,j \end{aligned}\right\} \quad (3.4.19)$$

where Q_i is the covariance matrix of V_i, and $\delta_{i,j}$ is the Kronecker delta which is defined as

$$\delta_{ij} = \begin{cases} 0 & i \neq j \\ 1 & i = J \end{cases} \quad (3.4.20)$$

at time t=iT and just prior to the receipt of r_i, the knowledge of the variation in Y (equation 3.4.17) can be used to make an a priori prediction $Y'_{i,i-1}$ or Y_i. From equation 3.4.17, since $E[V_i] = 0$, we have,

$$E[Y_i] = \Phi_{i,i-1} Y_{i-1} \quad (3.4.21)$$

so that, the best prediction of Y_i just before the arrival of the next received sample r_i is

$$Y'_{i,i-1} = \Phi_{i,i-1} Y'_{i-1} \quad (3.4.22)$$

and the covariance of the error in this prediction is given by,

$$P_{i,i-1} = E[(Y'_{i,i-1} - Y_i)(Y'_{i,i-1} - Y_i)^T] \tag{3.4.23}$$

$$= E[(\Phi_{i,i-1}Y'_{i-1} - \Phi_{i,i-1}Y_{i-1} - V_{i-1})(\Phi_{i,i-1}Y'_{i-1} - \Phi_{i,i-1}Y_{i-1} - V_{i-1})^T]$$

$$= E[(\Phi_{i,i-1}(Y'_{i-1} - Y_{i-1}) - V_{i-1})(\Phi_{i,i-1}(Y'_{i-1} - Y_{i-1}) - V_{i-1})^T]$$

$$= E[\Phi_{i,i-1}(Y'_{i-1} - Y_{i-1})(Y'_{i-1} - Y_{i-1})^T\Phi^T_{i,i-1}] -$$

$$- E[\Phi_{i,i-1}(Y'_{i-1} - Y_{i-1})V^T_{i-1}] -$$

$$- E[V_{i-1}(\Phi_{i,i-1}(Y'_{i-1} - Y_{i-1}))^T] +$$

$$+ E[V_{i-1}V^T_{i-1}] \tag{3.4.24}$$

But, from equation 3.4.17, V_{i-1} only affects Y_i, so that

$$E[\Phi_{i,i-1}(Y'_{i-1} - Y_{i-1})V^T_{i-1}] = 0$$

$$E[V_{i-1}(\Phi_{i,i-1}(Y'_{i-1} - Y_{i-1}))^T] = 0$$

and equation 3.4.24 reduces to,

$$P_{i,i-1} = \Phi_{i,i-1}P_{i-1}\Phi^T_{i,i-1} + Q_{i-1} \tag{3.4.25}$$

where P_{i-1} is the error covariance matrix of the previous estimate Y'_{i-1} and is defined by equation 3.4.14. Therefore, using equations 3.4.22 and 3.4.25 as the a priori information, the algorithms giving the mean-square estimate is as follows.

$$Y'_{i,i-1} = \Phi_{i,i-1} Y'_{i-1} \tag{3.4.26a}$$

$$P_{i,i-1} = \Phi_{i,i-1} P_{i-1} \Phi^T_{i,i-1} + Q_{i-1} \tag{3.4.26b}$$

$$K_i = P_{i,i-1} S_i \, (\sigma^2 + S_i^T P_{i,i-1} S_i)^{-1} \tag{3.4.26c}$$

$$P_i = P_{i,i-1} - K_i S_i^T P_{i,i-1} \tag{3.4.26d}$$

$$Y'_i = Y'_{i,i-1} + K_i \, (r_i - S_i^T Y'_{i,i-1}) \tag{3.4.26e}$$

The algorithms 3.4.26(a)-(e) are normally known as the Kalman filter estimator. In order to use the above algorithms, Φ and Q as well as P_o, Y'_o and σ^2 must be specified. In some cases, it is difficult to specify the model of the channel as in equation 3.4.17. However, Φ may be set to the identity matrix and V may be used to cover any error in the modelling of the channel and also any random fluctuations of the channel. A potential weakness of this estimation process is clearly the error that may be introduced into the estimate of Y by the assumptions that are made about a channel whose behaviour is not accurately known. The more prior knowledge that is used about a channel, the greater is the error that is likely to be caused in the estimate by any inaccuracies in the channel model. As before, Y'_o is set to

the null vector and P_o is set to a diagonal matrix with large diagonal elements. The optimum value of σ^2 can be determined by trial and error. Clearly, when Q is set to the null matrix, the algorithms 3.4.26(a)-(e) are identical to algorithms 3.4.16(a)-(c) where the channel is time-invariant.

Now, for the case when $\Phi = I$, where I is the identity matrix, the algorithms 3.4.26(a)-(e) simplify to,

$$P_{i,i-1} = P_{i-1} + Q_{i-1} \tag{3.4.27a}$$

$$K_i = P_{i,i-1}S_i \left(\sigma^2 + S_i^T P_{i,i-1} S_i\right)^{-1} \tag{3.4.27b}$$

$$P_i = P_{i,i-1} - K_i S_i^T P_{i,i-1} \tag{3.4.27c}$$

$$Y_i' = Y_{i-1}' + K_i \left(r_i - S_i^T Y_{i-1}'\right) \tag{3.4.27d}$$

Under the assumed conditions, all four estimators (algorithms 3.4.12(a)-(c), 3.4.16(a)-(c), 3.4.26(a)-(e) and 3.4.27(a)-(d) yield the optimal estimate (in the minimum mean-square error sense) of the channel.

As a measure of complexity, the number of multiplications per received sample using algorithms 3.4.27(a)-(d) is $3(g+1)^2 + 3(g+1)$. By comparison, the nonrecursive solution which involves matrix inversion (equation 3.4.1) requires of the order of $(g+1)^3$ multiplications. When g is large, even the algorithms 3.4.27(a)-(d) involve a considerable amount of computation per received sample,

and so various other estimators have been designed but may not perform so well.

3.5 FEEDFORWARD TRANSVERSAL-FILTER ESTIMATOR

The estimator has been developed by Magee and Proakis[27]. Its structure is identical to that of the linear feedback transversal equalizer[2,116]. The estimator has g+1 taps which is equal to the number of components in the sampled impulse-response of the channel and these tap gains are adjusted in such a way as to minimise the mean-square error between the actual received sample r_i and its estimate r_i' at the output of the estimator. Under ideal conditions, the resulting values of the tap gains are the components of the sampled impulse-response of the equivalent discrete-time channel model (Figure 2.3.1)[27].

The feedforward transversal-filter estimator operates as follows. Each box labelled T in Figure 3.5.1 is a store that holds the corresponding detected data-symbols $\{s_{i-h}'\}$. Each time the stores are triggered, the stored values are shifted one place to the right. At time t=iT, the estimator is fed with the received sample r_i and the detected data-symbol s_i'. If Y_{i-1}' is the previous stored estimate of Y, then an estimate r_i' of r_i at the output of the estimator is given by,

$$r_i' = \sum_{h=0}^{q} s_{i-h}' y_{i-1,h}' \qquad (3.5.1)$$

The error in this estimate which is

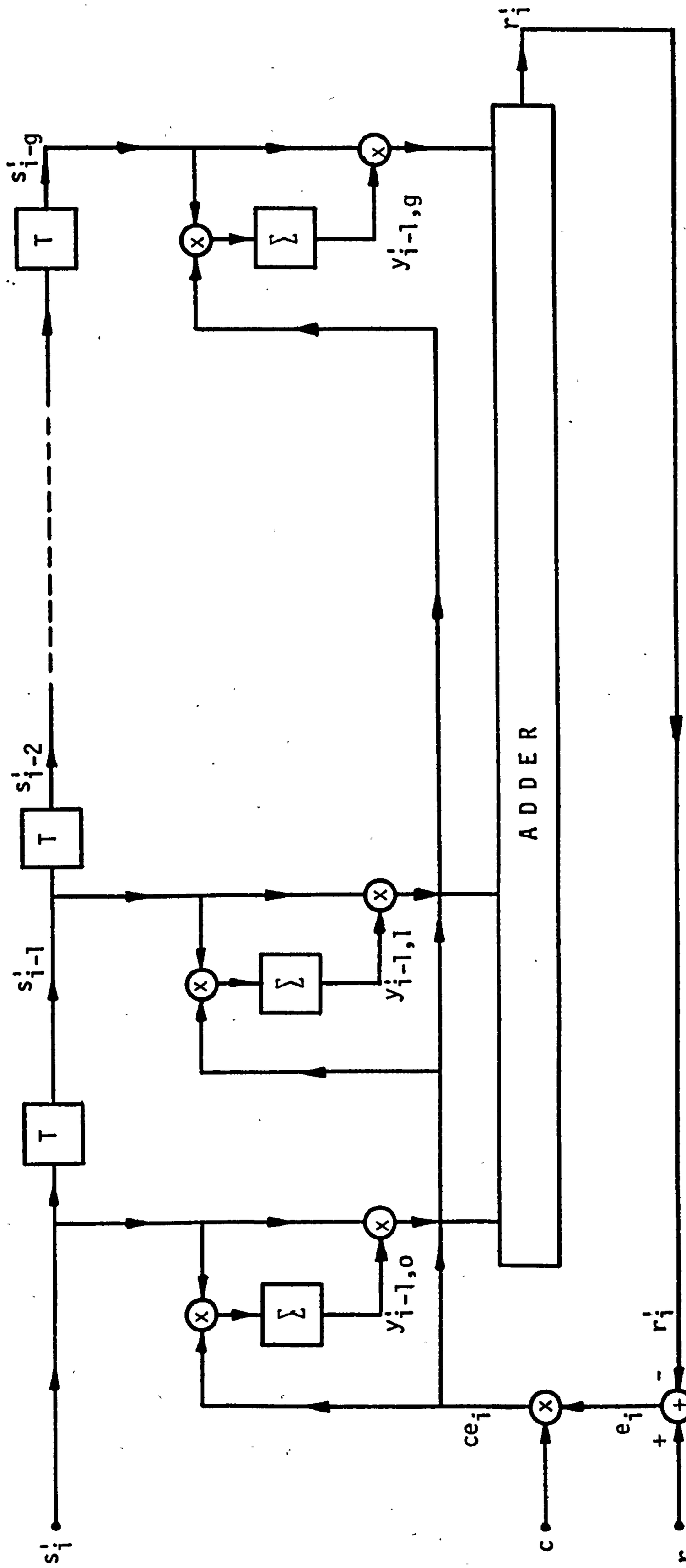
r_i'
s_{i-g}'
T
Σ
$y_{i-1,g}'$
ADDER
s_{i-2}'
T
s_{i-1}'
T
Σ
$y_{i-1,1}'$
T
Σ
$y_{i-1,o}'$
s_i'
ce_i
c
e_i
r_i'
r_i
FEEDFORWARD TRANSVERSAL-FILTER ESTIMATOR

FIGURE 3.5.1:

$$e_i = r_i - r'_i \qquad (3.5.2)$$

is then scaled by a small positive quantity c resulting in the signal ce_i. Each signal s'_{i-h} for h = 0, 1,...,g is multiplied by ce_i and the products are added to the corresponding components of the previous estimate Y'_{i-1}, giving the new stored estimate Y'_i, where the $(i+1)^{th}$ component of Y'_i is given by,

$$y'_{i,h} = y'_{i-1,h} + ce_i s'_{i-h} \qquad (3.5.3)$$

Equation 3.5.3 is usually known as the stochastic gradient algorithm and it can be shown[17] that it is the steepest descent algorithm for adjusting the tap gains of the estimator. When it is properly optimized in the absence of noise, the values of the tap gains are the values of the sampled impulse-response of the channel (see Section 3.3).

The factor c in equation 3.5.3 is usually known as the step size of the estimator and it need not necessarily be a constant. It is desirable to make c as small as possible so that the additive noise will have a small effect on Y'_i. However, this results in the estimator having a slower rate of response to changes in Y[26]. It can be seen that the number of multiplications involved in generating Y'_i is equal to (2g+3).

Clearly, the feedforward transversal-filter estimator can be implemented easily and it is also able to track slow variations in the channel response[21]. However, it is well known that when the input samples $\{s_i\}$ are highly correlated, the convergence of the

estimate to the optimum value is slow[37]. When the channel variation is rapid, such as that obtainable over some HF links, the Kalman filter estimator might be expected to be better at coping with these variations.

3.6 FEEDBACK ESTIMATOR

The feedback estimator was developed by Clark et al[26]. A brief description of its operation will now be given.

The estimator obtains for each received sample r_{i+g} a 'raw' estimate $\hat{Y}_i$ of Y which is then used to update the stored estimate Y'_{i-1}. When $Y'_{i-1} \simeq Y$ and there is negligible noise, $\hat{Y}_i \simeq Y$. Let Z_i be the (g+1)x(g+1) matrix defined as,

$$Z_i = \begin{bmatrix} s_i & s_{i-1} & s_{i-2} & \cdots & s_{i-g} \\ s_{i+1} & s_i & s_{i-1} & \cdots & s_{i-g+1} \\ s_{i+2} & s_{i+1} & s_i & \cdots & s_{i-g+2} \\ \vdots & \vdots & \vdots & & \vdots \\ s_{i+g} & s_{i+g-1} & s_{i+g-2} & \cdots & s_i \end{bmatrix} \qquad (3.6.1)$$

and let D_i, E_i and F_i be the (g+1)x(g+1) matrices, all derived from Z_i, and are defined as follows,

$$D_i \text{ (diagonal matrix)} = \begin{bmatrix} s_i & & & 0 \\ & s_i & & \\ & & \cdot & \\ & & & \cdot \\ 0 & & & s_i \end{bmatrix} \qquad (3.6.2)$$

$$E_i \text{ (upper triangular matrix)} = \begin{bmatrix} 0 & s_{i-1} & s_{i-2} & \cdots & s_{i-g} \\ 0 & 0 & s_{i-1} & \cdots & s_{i-g+1} \\ 0 & 0 & 0 & \cdots & s_{i-g+2} \\ \cdot & \cdot & \cdot & & \cdot \\ \cdot & \cdot & \cdot & & \cdot \\ \cdot & \cdot & \cdot & & \cdot \\ 0 & 0 & 0 & \cdots & 0 \end{bmatrix} \qquad (3.6.3)$$

$$F_i \text{ (lower triangular matrix)} = \begin{bmatrix} 0 & 0 & 0 & \cdots & 0 \\ s_{i+1} & 0 & 0 & \cdots & 0 \\ s_{i+2} & s_{i+1} & 0 & \cdots & 0 \\ \cdot & \cdot & \cdot & & \cdot \\ \cdot & \cdot & \cdot & & \cdot \\ \cdot & \cdot & \cdot & & \cdot \\ s_{i+g} & s_{i+g-1} & s_{i+g-2} & \cdots & 0 \end{bmatrix} \qquad (3.6.4)$$

Clearly,

$$Z_i = D_i + E_i + F_i \qquad (3.6.5)$$

and D_i is nonsingular, so long as $s_i \neq 0$. Let us define,

$$R_i = [r_i \; r_{i+1} \; \cdot \; \cdot \; \cdot \; r_{i+g}]^T \tag{3.6.6}$$

and

$$W_i = [w_i \; w_{i+1} \; \cdot \; \cdot \; \cdot \; w_{i+g}]^T \tag{3.6.7}$$

When Y is time invariant over the time interval $iT \leq t \leq (i+g)T$, the received samples r_i to r_{i+g} are given in matrix form by,

$$R_i = (D_i + E_i + F_i)Y + W_i \tag{3.6.8}$$

The estimator starts operation by making an estimate L_i of $(E_i + F_i)Y$. In forming L_i, the estimator uses one or more of the previous estimates of Y and also its knowledge of E_i and F_i derived from the $\{s_i'\}$ which are assumed to be correct. Subtracting L_i from R_i gives,

$$N_i = R_i - L_i$$

$$= D_iY + (E_i + F_i)Y - L_i + W_i \tag{3.6.9}$$

Premultiplying the foregoing equation by D_i^{-1} gives,

$$\hat{Y}_i = D_i^{-1}N_i$$

$$= Y + D_i^{-1}((E_i + F_i)Y - L_i) + D_i^{-1}W_i \tag{3.6.10}$$

The inversion of a diagonal matrix D_i is, of course, trivial. D_i^{-1} is also a diagonal matrix with each element along the main diagonal equal to the reciprocal of the corresponding diagonal element of the original matrix D_i.

When $L_i \simeq (E_i + F_i)Y$, equation 3.6.10 reduces to,

$$\hat{Y}_i \simeq Y + D_i^{-1}W_i \qquad (3.6.11)$$

$\hat{Y}_i$ is then used to update the previous estimate Y'_{i-1} to give the new estimate,

$$\begin{aligned} Y'_i &= c\hat{Y}_i + (1 - c)Y'_{i-1} \\ &= Y'_{i-1} + c(\hat{Y}_i - Y'_{i-1}) \qquad (3.6.12) \end{aligned}$$

The role of the parameter c is similar to the step size of the transversal-filter estimator. Usually, $c << 1$ but need not necessarily be a constant. Notice here that Y_i is determined after the reception of r_{i+g} and not r_i as in the previous estimators. The change simplifies the terminology.

The raw estimate $\hat{Y}_i$ can be formed using various methods. Clark et al[26] presented two of these which were named Feedback Estimators 1 and 2. However, we will not go into these estimators, it is sufficient here to indicate only the complexity of each estimator when forming the estimate Y'_i. For the Feedback Estimator 1, the number of multiplications are $\frac{1}{2}(g+1)(g+2)+2g+1$ and the Feedback Estimator 2 requires $4g+2$ multiplications.

3.7 FAST CHANNEL ESTIMATORS

As the name suggests, these estimators yield the optimum estimate of the channel at the fastest possible rate. They usually require some special inputs and are ideal for use during the training period at the start of a transmission.

3.7.1 Recursive Channel Estimator Using a Pseudorandom Binary Sequence (PRBS)

The estimator is developed by Luvison et al[52,53] and it operates as follows. The input training sequence is a pseudorandom binary sequence (PRBS)[60,61] of length $N = 2^n - 1$, where n is the number of cells in the shift register that is used to generate the sequence. The PRBS is cyclic with a period of N and it has a two-level autocorrelation function which approximates to that of a truly random sequence.

Let S_i (equation 3.3.14) be a (g+1)-component column vector consisting of the transmitted data-symbols {±1}. Associated with each S_i is the received signal r_i (equation 3.3.1). The algorithms for estimating the sampled impulse-response of the channel are,

$$\hat{S}_i = S_i - S_{i-1} + \alpha_i \hat{S}_{i-1} \qquad (3.7.1a)$$

$$\hat{r}_i = r_i - r_{i-1} + \alpha_i \hat{r}_{i-1} \qquad (3.7.1b)$$

$$Y'_i = Y'_{i-1} + (N+1)^{-1} \alpha_{i+1} \hat{r}_i \hat{S}_i \qquad (3.7.1c)$$

where $\alpha_i = (N - i + 3)(N - i + 2)^{-1}$ (3.7.1d)

and $i = 1,2,\ldots,N$. All the initial values are simply set to zero. The vectors $\{S_i\}$ are formed as follows. Let $\{d_i\}$ be the components of the PRBS, where

$$d_{N+i} = d_i \qquad i = 1,2,\ldots \tag{3.7.2}$$

then the $\{s_i\}$ in equation 3.3.14 are given by,

$$s_i = d_{g+i} \qquad \text{for } i = 0,1,2,\ldots \text{ and } i = -1,-2,\ldots \tag{3.7.3}$$

so that the vectors $\{S_i\}$ are given by,

$$[S_1\ S_2\ \cdots\ S_{N-g}S_{N-g+1}S_{N-g+2}\ \cdots\ S_N]$$

$$= \begin{bmatrix} d_{g+1} & d_{g+2} & \cdots & d_N & d_1 & d_2 & \cdots & d_g \\ d_g & d_{g+1} & \cdots & d_{N-1} & d_N & d_1 & & d_{g-1} \\ d_{g-1} & d_g & \cdots & d_{N-2} & d_{N-1} & d_N & & d_{g-2} \\ \vdots & \vdots & & \vdots & \vdots & \vdots & & \vdots \\ d_1 & d_2 & \cdots & d_{N-g} & d_{N-g+1} & d_{N-g+2} & \cdots & d_N \end{bmatrix} \tag{3.7.4}$$

3.7.2 Channel Estimator Using the Fast Hadamard Transform

The estimator is developed by Justesen[55] and it is based on the correlation method[56]. The sampled impulse-response is obtained by correlating the output and input sequences. The input training sequence is the maximum length shift register sequence (or PRBS) of period $N = 2^n - 1$, and all 0's and 1's produced by the shift register are replaced by 1's and -1's, respectively. If the values of the sampled impulse-response $\{y_h\}$ are zero for h>g, then the PRBS is chosen such that its length N is equal to g+1, or if a sequence of that length is unavailable, the next longer sequence is chosen. In the latter case, the number of components in the sampled impulse-response is extended to N by adding the required number of zeroes at the end of the response. The number of components in the sampled impulse-response, for convenience, is still given by g+1.

Associated with each vector S_i (equation 3.3.14) of the input signal is the received signal r_i (equation 3.3.1). In the absence of noise, r_i is given by,

$$r_i = \sum_{h=0}^{g} s_{i-h} y_h \qquad (3.7.5)$$

The periodic autocorrelation function of the pseudorandom sequence is given by[60],

$$b_k = \frac{1}{g+1} \sum_{i=1}^{g+1} s_i s_{i+k} = \begin{cases} 1 & k = 0 \pmod{g+1} \\ -\frac{1}{g+1} & k \neq 0 \pmod{g+1} \end{cases} \qquad (3.7.6)$$

A measure of the cross-correlation between the input and output sequences, for a shift of k places, where k = 0,1,...,g, is given by,

$$c_k = \sum_{i=1}^{g+1} r_{i+k} s_i$$

$$= \sum_{i=1}^{g+1} \sum_{h=0}^{g} s_{i+k-h} y_h s_i \qquad (3.7.7)$$

$$= \sum_{h=0}^{g} y_h \sum_{i=1}^{g+1} s_{i+k-h} s_i \qquad (3.7.8)$$

Notice that the actual value of the cross-correlation between the $\{r_i\}$ and the $\{s_i\}$ is (g+1) times c_k. Using equation 3.7.6, equation 3.7.8 becomes,

$$c_k = (g+1)y_k - \sum_{\substack{h=0 \\ h \neq k}}^{g} y_h \qquad (3.7.9)$$

Summing the $\{r_i\}$ for i = 1,2,...,g+1 and using equation 3.7.5 we have,

$$\sum_{i=1}^{g+1} r_i = \sum_{i=1}^{g+1} \sum_{h=0}^{g} y_h s_{i-h}$$

$$= \sum_{h=0}^{g} y_h \sum_{i=1}^{g+1} s_{i-h}$$

$$= - \sum_{h=0}^{g} y_h$$

$$= - y_k - \sum_{\substack{h=0 \\ h \neq k}}^{g} y_h \qquad (3.7.10)$$

The above derivation uses the fact that, for the PRBS,

$$\sum_{i=1}^{g+1} s_i = -1 \qquad (3.7.11)$$

Subtracting equation 3.7.10 from equation 3.7.9, gives

$$y_k = (g+2)^{-1} \left(c_k - \sum_{i=1}^{g+1} r_i\right) \qquad (3.7.12)$$

The unknown quantities in equation 3.7.12 are the $\{c_k\}$. The novelty of Justesen's estimator is in the way the $\{c_k\}$ are calculated, which is performed as follows. Expanding equation 3.7.7 we have,

$$\begin{aligned}
c_0 &= s_1 r_1 + s_2 r_2 + \ldots + s_{g+1} r_{g+1} \\
c_1 &= s_1 r_2 + s_2 r_3 + \ldots + s_{g+1} r_{g+1+1} \\
&\vdots \\
c_g &= s_1 r_{g+1} + s_2 r_{g+1+1} + \ldots + s_{g+1} r_{g+1+g}
\end{aligned} \qquad (3.7.13)$$

However, $r_{g+1+i} = r_i$ for $i = 1,2,\ldots$ as the input sequence is periodic with period equal to g+1. Therefore equation 3.7.13 becomes

$$
\begin{aligned}
c_0 &= s_1 r_1 + s_2 r_2 + \cdots + s_{g+1} r_{g+1} \\
c_1 &= s_1 r_2 + s_2 r_3 + \cdots + s_{g+1} r_1 \\
&\vdots \\
c_g &= s_1 r_{g+1} + s_2 r_1 + \cdots + s_{g+1} r_g
\end{aligned}
\qquad (3.7.14)
$$

Rearranging and writing equation 3.7.14 in matrix form,

$$
\begin{bmatrix} c_0 \\ c_1 \\ \vdots \\ c_g \end{bmatrix} = \begin{bmatrix} s_1 & s_2 & \cdots & s_{g+1} \\ s_{g+1} & s_1 & \cdots & s_g \\ \vdots & \vdots & & \\ s_2 & s_3 & \cdots & s_1 \end{bmatrix} \begin{bmatrix} r_1 \\ r_2 \\ \vdots \\ r_{g+1} \end{bmatrix} \qquad (3.7.15)
$$

The matrix in equation 3.7.15 is now increased in size by adding a row and a column of 1's to give a (g+2)x(g+2) matrix. The rows and columns of the resultant matrix are rearranged such that the matrix is converted to the Hadamard matrix, that is

$$
H_n = \begin{bmatrix} H_{n-1} & H_{n-1} \\ H_{n-1} & -H_{n-1} \end{bmatrix} \qquad (3.7.16)
$$

where, for example

$$H_1 = \begin{bmatrix} 1 & 1 \\ 1 & -1 \end{bmatrix} \qquad (3.7.17)$$

and

$$H_2 = \begin{bmatrix} H_1 & H_1 \\ H_1 & -H_1 \end{bmatrix} = \begin{bmatrix} 1 & 1 & 1 & 1 \\ 1 & -1 & 1 & -1 \\ 1 & 1 & -1 & -1 \\ 1 & -1 & -1 & 1 \end{bmatrix} \qquad (3.7.18)$$

The reordering of the rows and columns is taken as the permutation that takes the binary n-vectors listed in the order in which they appear in the linear feedback shift register into the sequence of integers in binary positional notation[55]. When the matrix is in the Hadamard form, application of the fast Hadamard transform, which involves only additions and subtractions, yields the $\{c_k\}$. The channel coefficients are then obtained using equation 3.7.12.

3.7.3 Channel Estimator Using the Fast Fourier Transform

The estimator, which was developed by Butcher and Cook[57], uses the fast Fourier transform (FFT) to calculate the sampled impulse-response of the channel. It operates as follows.

By definition, the $(k+1)^{th}$ component of the discrete Fourier transform (DFT) of any sequence of N sample values $\{x_i\}$ is[2,59]

$$x_k^{\dagger} = \sum_{i=0}^{N-1} x_i \exp(-j \frac{2\pi ki}{N}) \qquad k = 0,1,\ldots,N-1 \qquad (3.7.19)$$

and the inverse discrete Fourier transform (IDFT) is given by,

$$x_i = \sum_{k=0}^{N-1} x_k^{\dagger} \exp(+j \frac{2\pi ki}{N}) \qquad i = 0,1,\ldots,N-1 \qquad (3.7.20)$$

where $j = \sqrt{-1}$. Let us assume that the channel whose sampled impulse-response we wish to identify has g+1 components $\{y_h\}$ where $h = 0,1,\ldots,g$. Through this channel, a sequence of only m+1 data symbols is transmitted, so that $s_i = 0$ for $i<0$ and $i>m$. The corresponding received signal sequence is given by the convolution of the $\{s_i\}$ and $\{y_h\}$ (equation 3.3.1). Alternatively, if

$$S_N^{\dagger} = [s_0^{\dagger}\ s_1^{\dagger}\ .\ .\ .\ .\ .\ s_{N-1}^{\dagger}]^T \qquad (3.7.21)$$

and

$$Y_N^{\dagger} = [y_0^{\dagger}\ y_1^{\dagger}\ .\ .\ .\ .\ .\ y_{N-1}^{\dagger}]^T \qquad (3.7.22)$$

are the N-point DFT's of the input sequence and the sampled impulse-response of the channel, respectively, then the $(k+1)^{th}$ component of the N-point DFT of the received signal sequence $\{r_i\}$, in the absence of noise, is given by,

$$r_k^{\dagger} = s_k^{\dagger} y_k^{\dagger} \qquad (3.7.23)$$

that is, the convolution of the $\{s_i\}$ and the $\{y_h\}$ in the time domain is replaced by a simple multiplication in the frequency domain. The inverse DFT (IDFT) of $r_0^{\dagger}, r_1^{\dagger}, \ldots, r_{N-1}^{\dagger}$ gives the $\{r_i\}$. Clearly, because of the periodic nature of equations 3.7.19 and 3.7.20, the results of the convolution are also periodic. In order to avoid the result of the convolution over one period being interfered

by the neighbours, N is chosen according to the relationship

$$N \geq (m+1) + (g+1) - 1 \qquad (3.7.24)$$

In addition, N is selected as a power of 2 so as to obtain maximum efficiency when computing the DFT's using the algorithms known as the FFT[59]. From equation 3.7.23, the $(k+1)^{th}$ component of the DFT of the sampled impulse-response is

$$y_k^{\dagger} = r_k^{\dagger}/s_k^{\dagger} \qquad (3.7.25)$$

that is, each component of the DFT of the received signal sequence is simply divided by the corresponding component of the input signal sequence. For a channel which is time invariant at least over N sampling intervals and in the absence of additive noise, equation 3.7.25 gives the exact values of the sampled impulse-response. When additive noise is present in the $\{r_i\}$, the estimates $\{y_n'\}$ are chosen to minimize the function

$$M_k = \sum_{k=0}^{N-1} \left| \frac{z_k^{\dagger}}{s_k^{\dagger}} - (y_k')^{\dagger} \right|^2 \qquad (3.7.26)$$

where $z_k^{\dagger}$ and $(y_k')^{\dagger}$ are the $(k+1)^{th}$ components of the DFT of the corrupted received signal sequence and the DFT of the estimate of the sampled impulse-response, respectively. The minimization of equation 3.7.26 yields[57],

$$y'_h = \frac{1}{N} \sum_{k=0}^{N-1} \frac{z'_k}{s'_k} \exp\left(j \frac{2\pi kh}{N}\right) \qquad h = 0,1,\ldots,g \qquad (3.7.27)$$

Evaluation of the $\{y_h\}$ using equation 3.7.25 requires three applications of the transform. For $N = 2^n$, the FFT requires $Nn/2$ complex multiplications.

4. THE HF RADIO LINK

Before attempting to develop any HF channel estimator, it is essential that the ionospheric propagation medium is well understood. Thus, we begin in Section 4.1 with a lengthy discussion on the physical composition of the ionosphere. This is followed in Section 4.2 with an outline of the mechanism of radio wave propagation through the ionosphere. In Section 4.3, various forms of signal impairments that are encountered by the radio signal are identified. A model of the HF channel is then considered and it is simulated on a digital computer (Section 4.4), the simulated channel being used later in the testing of the estimators. Finally, a discussion is presented on the transmission of digital data using QAM over the model of the HF radio link (Section 4.5).

4.1 THE IONOSPHERE

The ionosphere is a region about 50 km above the surface of the Earth[66,69]. It is composed mainly of molecules and atoms of oxygen and nitrogen. These molecules are progressively replaced by their respective atoms as the height increases[68]. In addition, as the result of electrical discharges, some oxygen and nitrogen atoms combine to produce a small proportion of nitric oxide. It is generally believed that the Sun's radiation and, to a lesser extent, cosmic rays cause these molecules and atoms to be converted into ions and free electrons[63,67,68]. Also, a significant amount of

ionization is caused by meteors travelling through this atmosphere[68].

The degree of ionization is not constant throughout the height of the ionosphere. There are regions where the ionization is more intense[66,67]. As an example, Figure 4.1.1 which is taken from Ref. 69, shows a typical electron density profile for summer noon and midnight at middle latitudes. Generally, the ionosphere is divided into three regions, D, E and F regions. Each region consists of one or more layers. The different regions of the ionosphere have been determined using vertical and oblique soundings, and also using rockets and satellites[63,68].

The height of each region varies from day to night and with the seasons, and is in fact changing continuously[67]. The part of the ionosphere between 50 and 90 km is known as the D-region. Here, the electron concentration is low (10^8 - 10^9 electrons/m^3). The critical frequency or plasma frequency, defined as the highest carrier frequency of a vertically-incident ray which can be reflected by the layer[69], is given by[68],

$$f_o = \frac{1}{2\pi} \left(\frac{N \varepsilon^2}{m \varepsilon_o}\right)^{\frac{1}{2}}$$

$$\simeq 9N^{\frac{1}{2}} \qquad (4.1.1)$$

where N is the number of electrons per m^3,

ε is the negative charge of an electron = -1.6×10^{-19} C,

ε_o is the permittivity of free space = $\frac{1}{36\pi} \times 10^{-9}$ F/m,

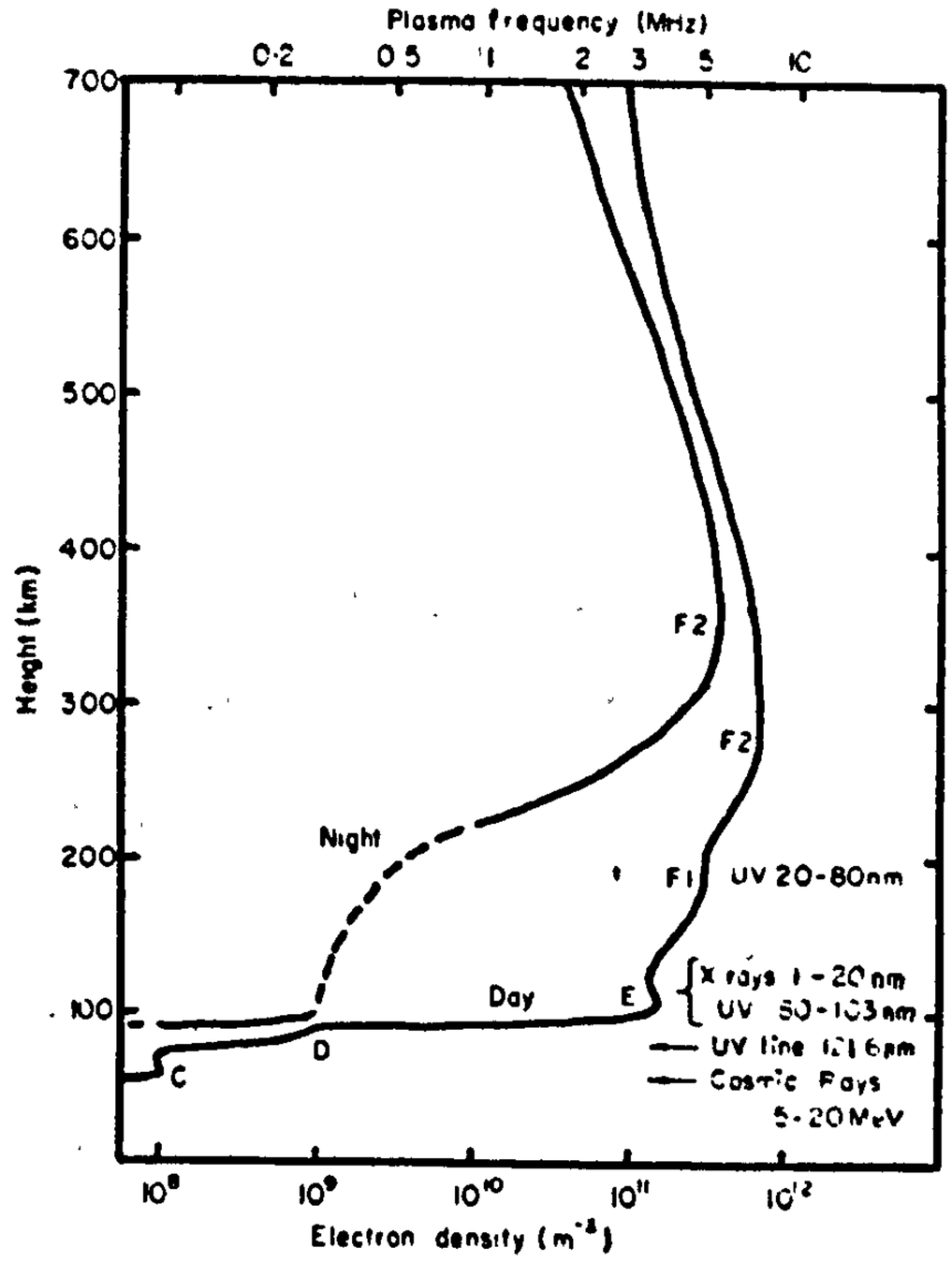

FIGURE 4.1.1: ELECTRON DENSITY PROFILE

and m is the mass of an electron = 9×10^{-31} kg.

The critical frequency is dependent on the ionization level and therefore is low for the D-region (100-700 kHz). The molecular concentration is high (of the order of 10^{20} molecules/m^3) and the collision frequency between electrons and molecules is high (5×10^5 - 5×10^6 per m^3/s). Thus, for HF radio waves, the D-region acts principally as an attenuator. The D-region is a daytime phenomena. At night, in the absence of solar radiation, very little ionization takes place, being limited to that due to meteors. The ions now combine with the electrons and the D-region virtually disappears. The attenuation is therefore not present so that propagation over long distances is possible but the background interference has increased.

The E-region spans the altitude 90 to 150 km[68,69]. The maximum ionization is found at around 120 km[68] and at this height the electron density is of the order of 10^{11} electrons/m^3 and the corresponding critical frequency is around 4 MHz. At night, a certain amount of ionization still persists due to imperfect ion recombination and ionization due to meteors and so the critical frequency drops by an order of magnitude from its daytime value. The critical frequency can be calculated approximately using the equation[63],

$$f_0E = 0.9\ [(180 + 1.44R)\ \cos\ \chi]^{0.25} \qquad (4.1.2)$$

where R is the sunspot number and χ is the solar zenith angle. The value of f_oE obtained from equation 4.1.2 is usually very close (within 0.2 MHz) to the observed value and is independent of the time of day or year[63]. The number of collisions between electrons and molecules is rather large (5×10^3 - 2×10^4 per m^3/s) so that there is still a significant amount of absorption but not as much as in the D-region[68]. The E-region can support propagation for distances up to around 2000 km.

Occasionally, within the E-region, patches of much denser ionized clouds appear and these are capable of reflecting high frequencies. These clouds are known as sporadic E-layers[63,68] because of their unpredictable occurrence. The sporadic E-layer is obviously responsible for creating interference because signals are being reflected into areas which they are not intended for.

The F-region of the ionosphere extends upwards from about 150 km. The lower part behaves differently from the upper part and so it has been divided into two layers, F_1 and F_2. The F_1-layer is observed only during the day at a height of about 200 km. Absorption in this layer is small and the critical frequency for any time of day and for any season can be approximated by[63],

$$f_oF_1 = (4.3 + 0.01R) \cos^{0.2} \chi \qquad (4.1.3)$$

The F_1-layer is not generally used for long-distance communication[66].

The F_2-layer is the part of the ionosphere above 250 km and contains the highest concentration of electrons, typically around 10^{12} electrons/m^3 at the altitude of 300 km. The critical frequency is between 5 to 10 MHz at middle latitude. The F_2-layer is the most useful part of the ionosphere for HF radio communication. It is the most reliable reflecting media during both day and night. Due to its considerable height, the F_2-layer can support propagation for a distance of 4000km or more, even using single-hop transmission. However, it has the most complex behaviour. For instance, unlike the D, E and F_1 layers, the critical frequency is not directly related to the solar zenith angle. Its value is higher at noon in winter than the corresponding time in summer and usually the maximum value occurs not at noon but slightly later (1500 or 1600 hours)[68]. During nighttime and sometimes during the day, especially in winter, the F_1-layer merges with the F_2-layer resulting in a single F-layer around the altitude of 300 km[66,69]. The critical frequency drops to around 3 to 5 MHz (see Figure 4.1.1).

4.2 IONOSPHERIC RADIO PROPAGATION

The ionosphere affects the propagation of all waves up to a frequency of about 50 MHz. Frequencies lower than approximately 30 MHz are propagated by refraction and frequencies between 30 and 50 MHz are propagated by scattering[68]. The HF radio waves are refracted back to the Earth because the refractive index, n, of the layer changes continuously with its height. This is due to the dependence of n on the electron density of the ionized medium. The

refractive index of the medium is given by[63,68],

$$\eta = (1 - \frac{N \varepsilon^2}{m \varepsilon_o \omega^2})^{\frac{1}{2}} \qquad (4.2.1)$$

where ω is the angular frequency of the radio wave and all other symbols are as defined previously in Section 4.1. Since the electron density increases with the height of the layer (see Figure 4.1.1), the refractive index decreases continuously for a given value of ω. Therefore, at a certain height of the layer where the electron density is sufficiently large to reduce the value of η such that

$$\eta = \sin \theta_i \qquad (4.2.2)$$

the wave will be refracted back to Earth. θ_i is the angle of incidence of the wave measured from the normal. From equations 4.2.1 and 4.2.2, we have

$$\sin \theta_i = (1 - \frac{N \varepsilon^2}{m \varepsilon_o \omega^2})^{\frac{1}{2}} \qquad (4.2.3)$$

With normal incidence, $\theta_i = 0$, we obtain from equation 4.2.3,

$$\omega = (\frac{N_{max} \varepsilon^2}{m \varepsilon_o})^{\frac{1}{2}} \qquad (4.2.4)$$

where N_{max} is the electron density at the maximum height.

Hence, by writing $\omega = 2\pi f_o$, the critical frequency is given by,

$$f_o = \frac{1}{2\pi} \left(\frac{N_{max}\, \varepsilon^2}{m\, \varepsilon_o}\right)^{\frac{1}{2}} \qquad (4.2.5)$$

which is the highest frequency that can be reflected from the layer using vertical incidence. The frequency f_o is the critical frequency mentioned previously in Section 4.1. Clearly, by using other values of θ_i (i.e. oblique incidence) a given layer can reflect higher frequencies. Using equations 4.2.3 and 4.2.5, the frequencies can be calculated using

$$f = f_o \sec \theta_i \qquad (4.2.6)$$

So far, the terms refraction and reflection have sometimes been used interchangeably to describe the process by which the radio wave is returned to the Earth. This is supported by a theorem by Breit and Tuve[63,68] which shows that the refraction process at some height B is equivalent to a mirror-like reflection at height A. In Figure 4.2.1 where a plane Earth and a plane ionosphere is assumed, B is known as the real height, and A is the so-called virtual height, so that TBR is the actual ray path and TAR is the virtual ray path. The height B is always lower than A. Also, waves of any angle of incidence which have the same real refraction height can be shown[68] to have the same virtual reflection height. Furthermore, Martyn's theorem[63] shows that the virtual height of reflection for an obliquely incident wave is the same as the equivalent vertical wave.

Therefore, the actual ray path can be replaced by a virtual ray which travels in a medium with refractive index of 1 and reflected by a plane at the virtual height. Thus, the geometry of the ray path becomes very simple. For practical purposes, the principal reflecting layers are the E and F_2 layers, and so in Figure 4.2.2 some of the possible ray paths are illustrated.

Now, consider a tramsission over a distance d (see Figure 4.2.1). Since the wave experiences the equivalent of a mirror-like reflection at height A, by simple geometry, the angle TAP is equal to the angle of incidence θ_i. Thus, θ_i is related to the virtual height h' by

$$\tan \theta_i = \frac{\frac{d}{2}}{h'}$$

$$= \frac{d}{2h'} \qquad (4.2.7)$$

So that, from equation 4.2.6, we have

$$f = f_o \sec \theta_i = f_o \left[1 + \left(\frac{d}{2h'}\right)^2\right]^{\frac{1}{2}} \qquad (4.2.8)$$

The solution for f is usually found graphically.

Figure 4.2.3[63] shows a plot of a family of curves that give h' as a function of f_o for a distance of 2000 km. These graphs are superimposed on a curve obtained using echo sounding (i.e. the ionogram). The three sections of this curve correspond to reflections from the E, F_1 and F_2 layers. Consider as an example, the wave with a carrier

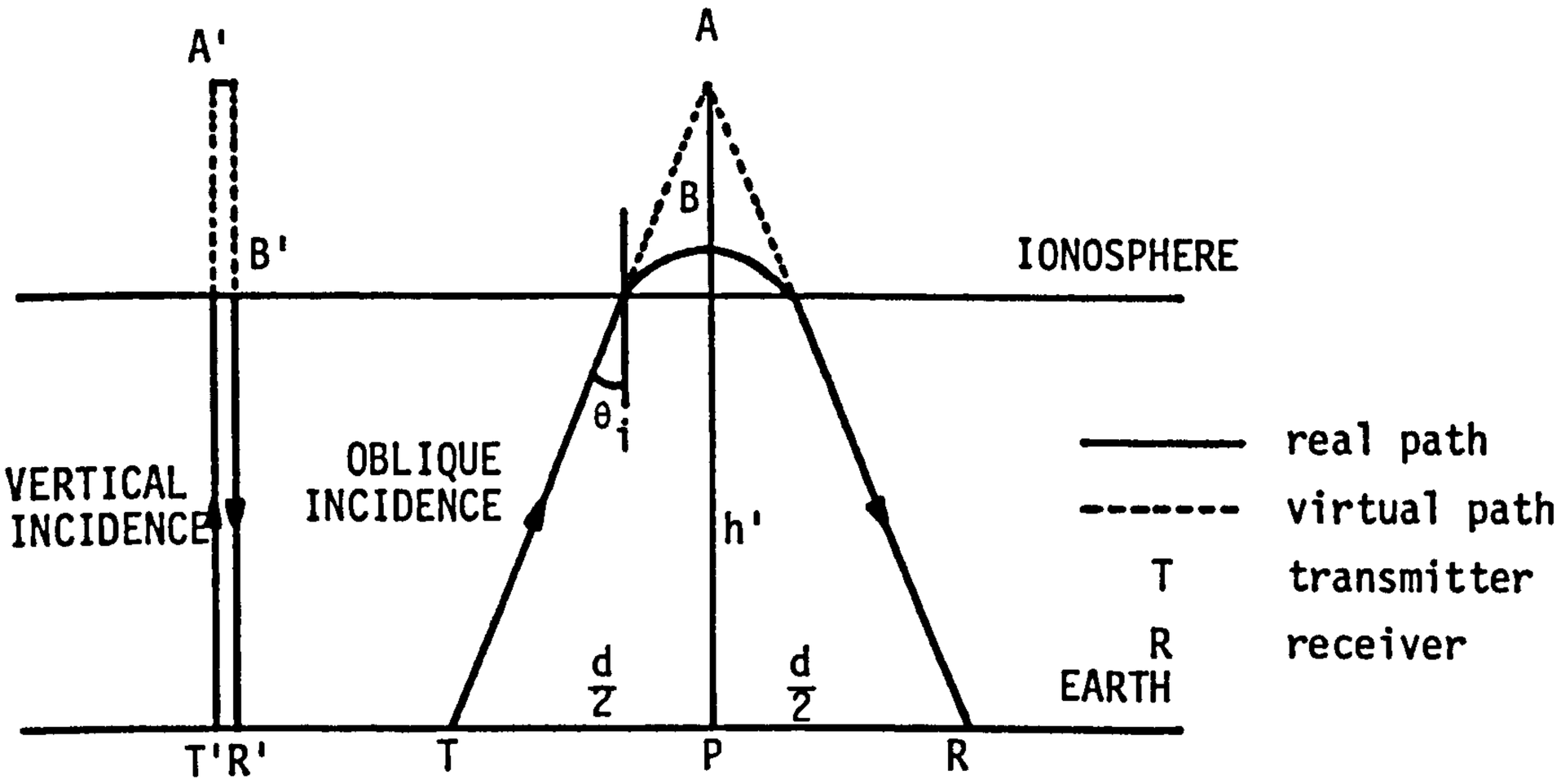

FIGURE 4.2.1: RELATION BETWEEN THE REAL HEIGHT AND VIRTUAL HEIGHT

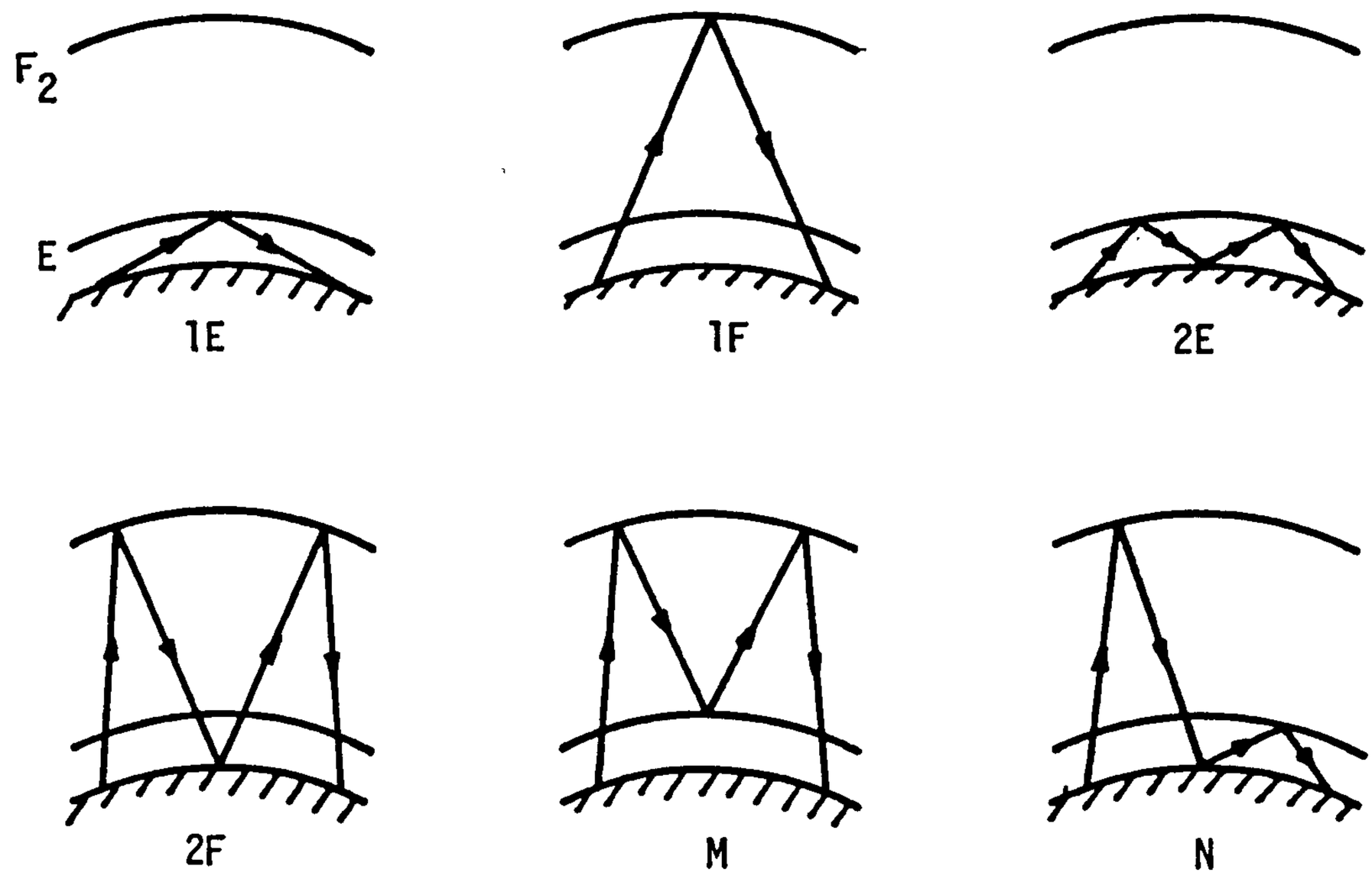

FIGURE 4.2.2: EXAMPLES OF DIFFERENT MODES OF PROPAGATION

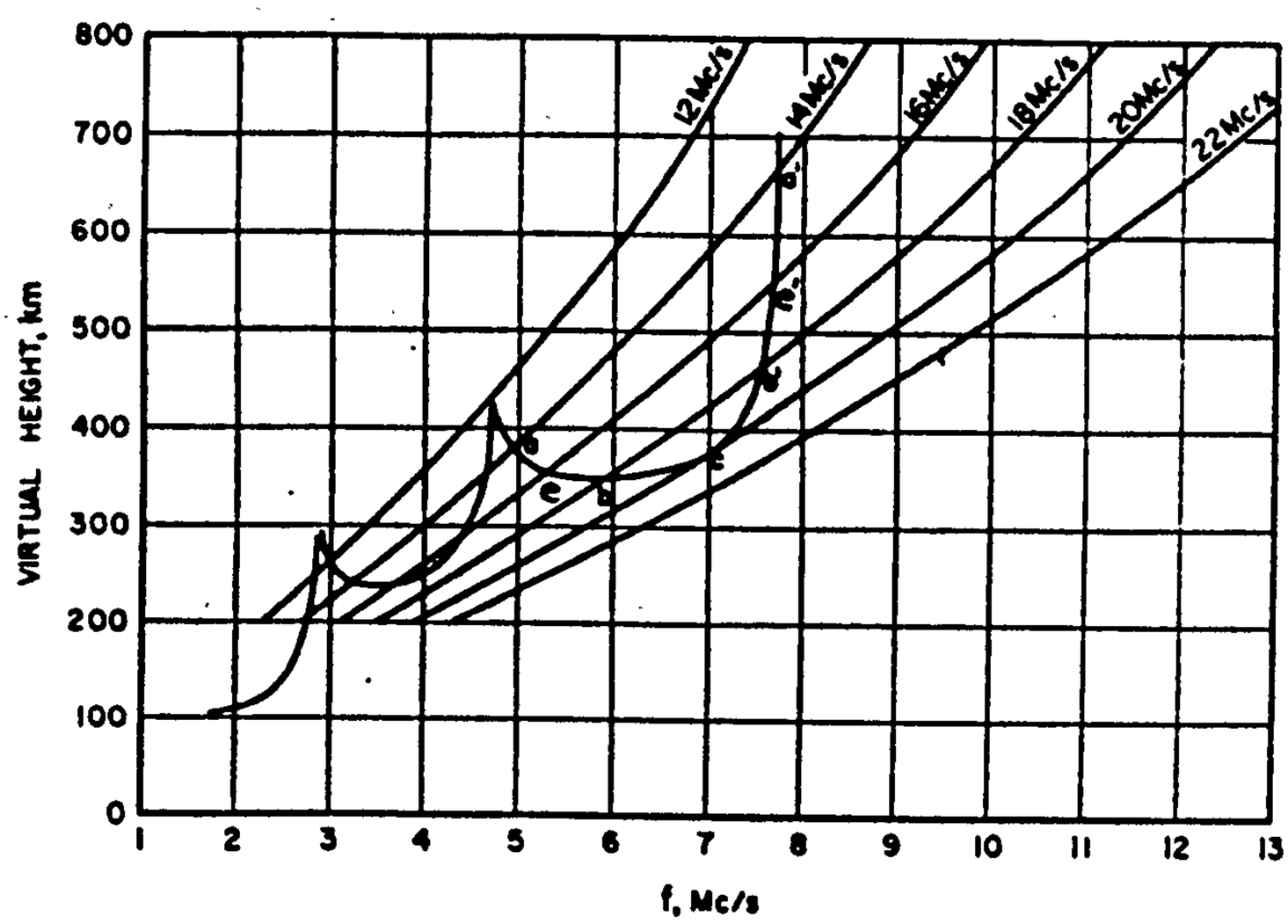

FIGURE 4.2.3: FAMILY OF TRANSMISSION CURVES FOR A FIXED DISTANCE OF 2000 km SUPERIMPOSED ON IONOGRAMS

frequency of 14 MHz propagating over the distance of 2000 km. The ray can travel by several paths. Two of these paths could be reflected from the F_2-layer at heights corresponding to the intersections at a and a'. The ray which is reflected from the lower virtual height is called the low-angle ray and that reflected from the higher virtual height is known as the high-angle ray. The 14 MHz ray is also reflected at two heights from the F_1-layer and only one reflection from the E-layer. These ray paths are shown in Figure 4.2.4. Now, as the carrier frequency increases, the points of intersection (ee' and bb') get closer and finally the 20 MHz curve becomes a tangent at the point c to the h' versus f_o curve and so the low- and high-angle rays merge together. This frequency is known as the maximum usable frequency (MUF). Above the MUF, no frequencies are reflected. Therefore, when the carrier frequency is lower than the MUF, reflections from a single layer produce two ray paths.

In the preceding discussion, the curvature of the Earth and also of the ionosphere have been neglected. However, it can be shown (63,68) that these effects can be taken into account by introducing corrective terms. Furthermore, the effects of the Earth magnetic field has been shown[(63,68)] to split an incident wave on entering the ionized medium into two circularly polarized waves, the ordinary and the extra-ordinary waves. The effect is known as magneto-ionic splitting. The two rays travel along different paths but they can sometimes recombine on leaving the ionized medium, to give an elliptically polarized wave[(68)]. Under extreme conditions only one of the two rays is reflected.

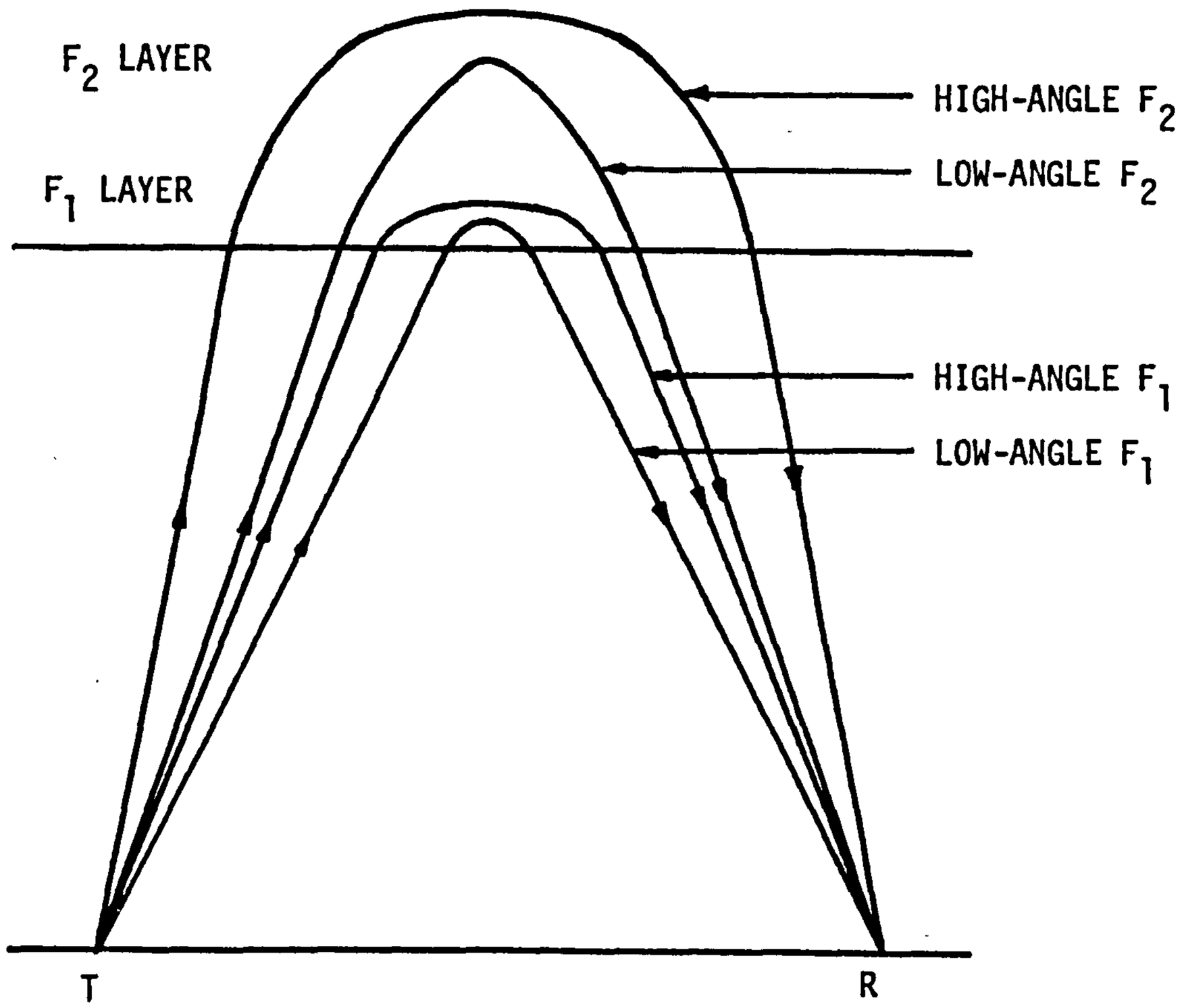

FIGURE 4.2.4: RAY PATHS CORRESPONDING TO INTERSECTIONS OF TRANSMISSION CURVES AND IONOGRAMS

4.3 TYPES OF DISTORTION ON HF CHANNELS

When a data signal is transmitted through a channel, it is bound to suffer some form of distortion. Over an HF channel, the random fluctuations of the ionosphere contribute more severe forms of distortion and these will be discussed in the next few subsections.

4.3.1 Multipath Propagation and Time Dispersion

We have seen in the previous section that the transmitted radio wave may be propagated to the receiver along one or more different paths of unequal lengths, that is, by multipath propagation. Many of these propagation paths or modes are possible, especially for long-distance propagation; however, the number of 'effective' modes are small. Clearly, the time taken by the signals traversing these paths are different, so that when a short pulse of RF energy is transmitted, the received signal will have a profile such as that in Figure 4.3.1.

In Figure 4.3.1, the time between the reception of the first and the last pulses is known as the time spread or time dispersion of the received signal. It is caused by the difference in the group delays between the different modes. When the reciprocal of the signalling rate is comparable with the relative multipath delay, the signals received over the different modes overlap each other giving rise to intersymbol interference. Figure 4.3.2 shows the variation in the maximum relative time delay with path length[63]. It can be seen that for a 2500 km path, the maximum time dispersion is about 3 ms and for a 1000 km path, the value is about 5 ms.

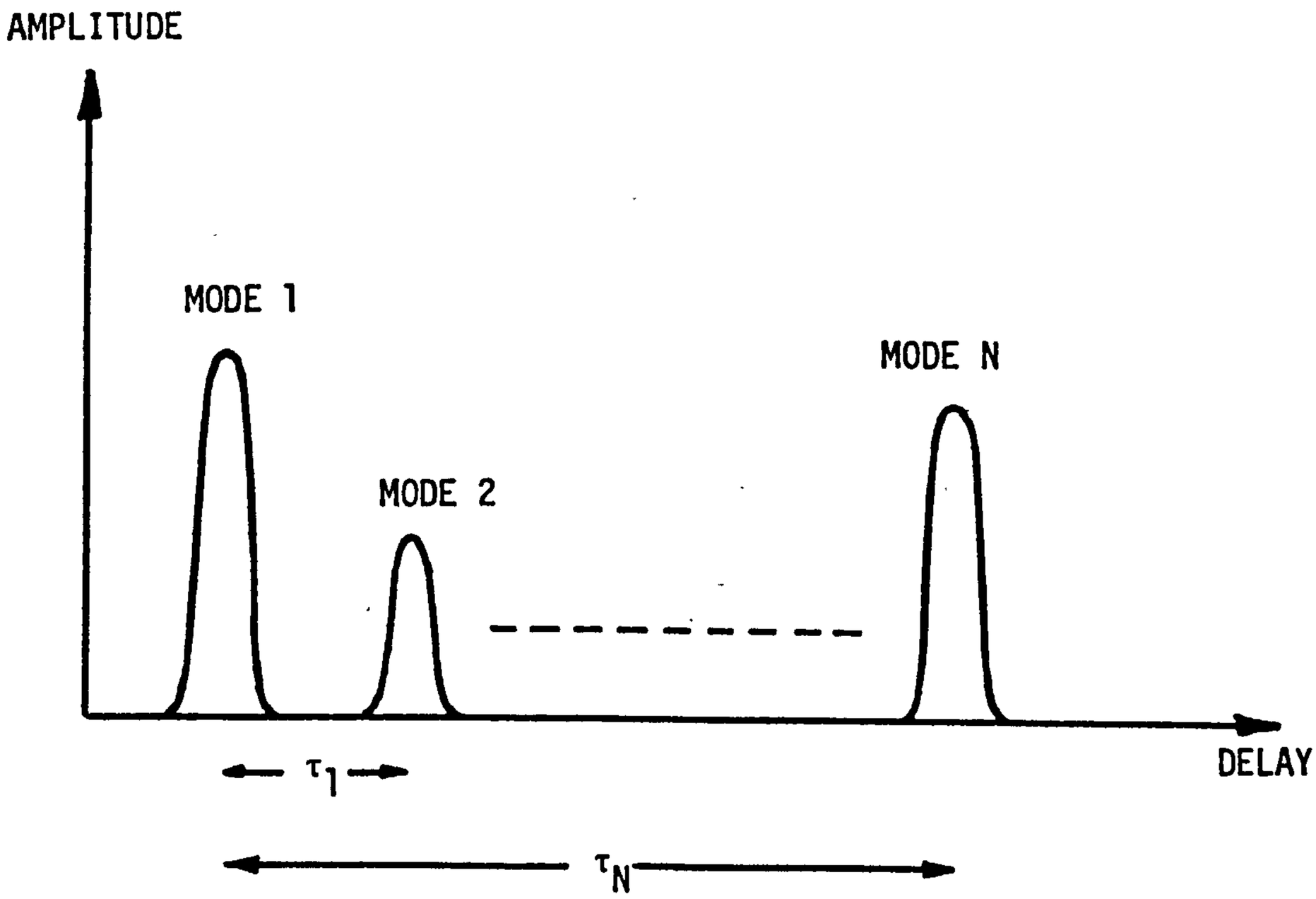

FIGURE 4.3.1: TYPICAL RESPONSE OF MULTIPATH CHANNEL

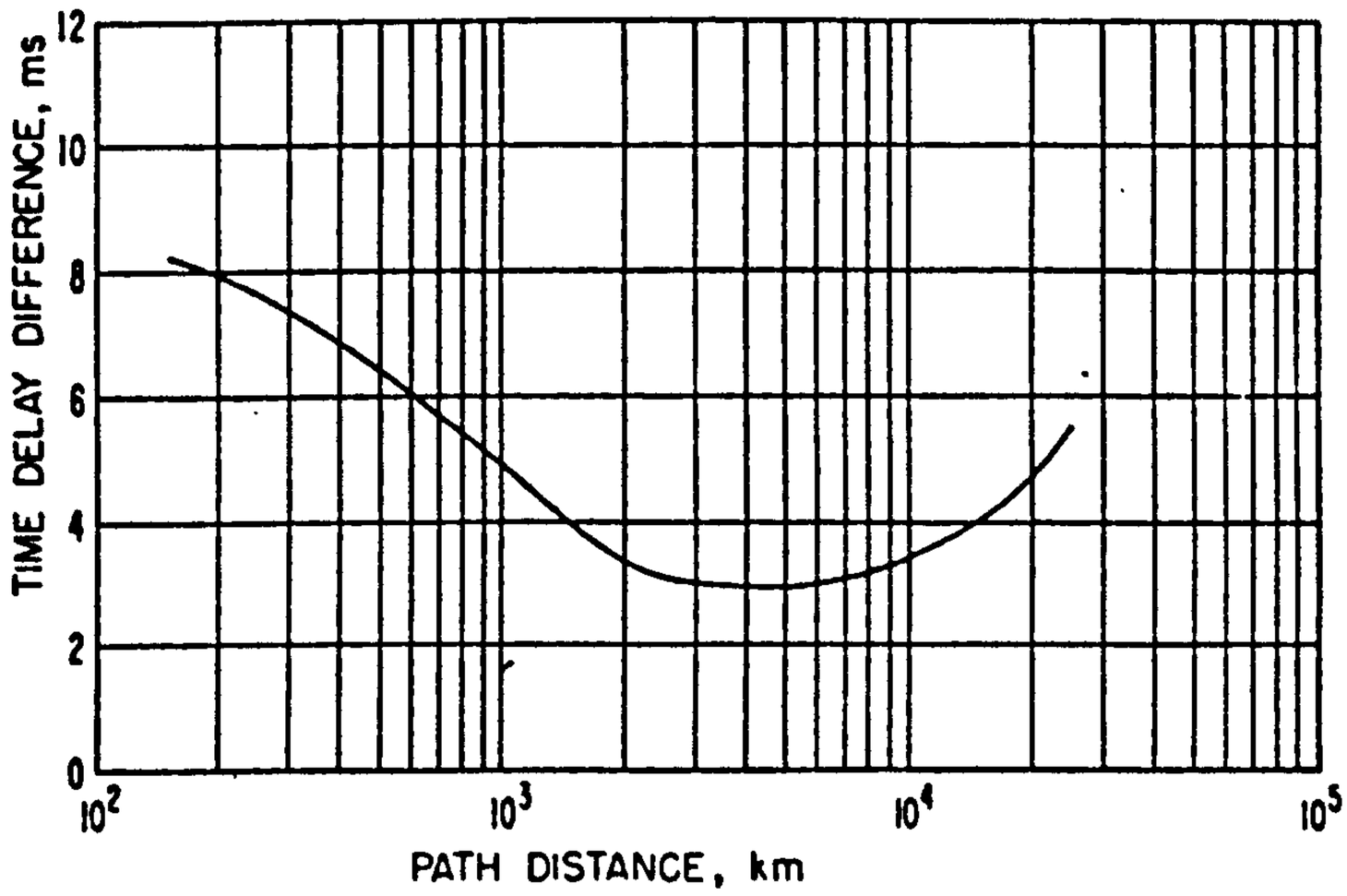

FIGURE 4.3.2: MAXIMUM EXPECTED MULTIPATH SPREAD

4.3.2 Fading

Fading is another form of distortion experienced over HF channels. Generally fading may be classified under one or more of the following headings,[63,65,67]

1. Interference fading
2. Polarization fading
3. Absorption fading
4. Skip fading.

We have seen in Section 4.2 that the received signal may consist of high- and low-angle rays, each having ordinary and extraordinary components. In addition, there may be other sets of signals corresponding to rays propagating over different modes. The relative phases of these rays vary randomly because of the continuous variation in the path lengths as a result of the movement of ionospheric irregularities[63]. Since the received signal is a vector sum of all these signals, interference fading occurs. Clearly, when all the individual components are in phase, the resultant amplitude of the received signal is a maximum. The amplitude distribution of the received signal approximates to a Rayleigh distribution[63,65-68] when the various components are of about the same amplitude and the relative phases are varying randomly. When a specular (steady amplitude) component is present, due to a ground wave, for example, the distribution becomes Ricean[63]. However, for a continuous wave and also for trains of pulses, the amplitude distribution is usually close to Rayleigh[63].

Interference fading is usually frequency selective because it depends on the wavelength of the interfering signals[63]. For this type of fading, the fading period varies from a fraction of a second to several seconds[63].

Polarization fading occurs because of the continuous change in the polarization of the individual signal reflected from the ionosphere[67]. This is due to the effect of the Earth's magnetic field on the ionosphere during the reflection process. The fading period also varies from a fraction of a second to several seconds[63].

Absorption fading is caused by the variation with time of ionospheric absorption[63] and is usually greatest at sunrise and sunset[65]. The fading period is here of the order of an hour or longer.

Skip fading is caused by the continuous variation over short periods of time of the MUF for a given path. When the MUF decreases temporarily below that for the particular path and the frequency in use, the skip distance[63] (the distance for which a given frequency is also the maximum frequency) lengthens, so that the receiver is brought within the skip zone and therefore no signal is received. Skip fading is generally non-periodic and can be avoided by working well below the MUF[63,65].

To give some idea of the depths of fading and also the fading rates, Figure 4.3.3 is included. This is taken from Ref. 65, and gives the average fading rates and depths for a typical HF channel at middle latitudes. It can be seen that the very deep fades occur infrequently and, for most of the time, lie between 5 and 10 dB, the latter

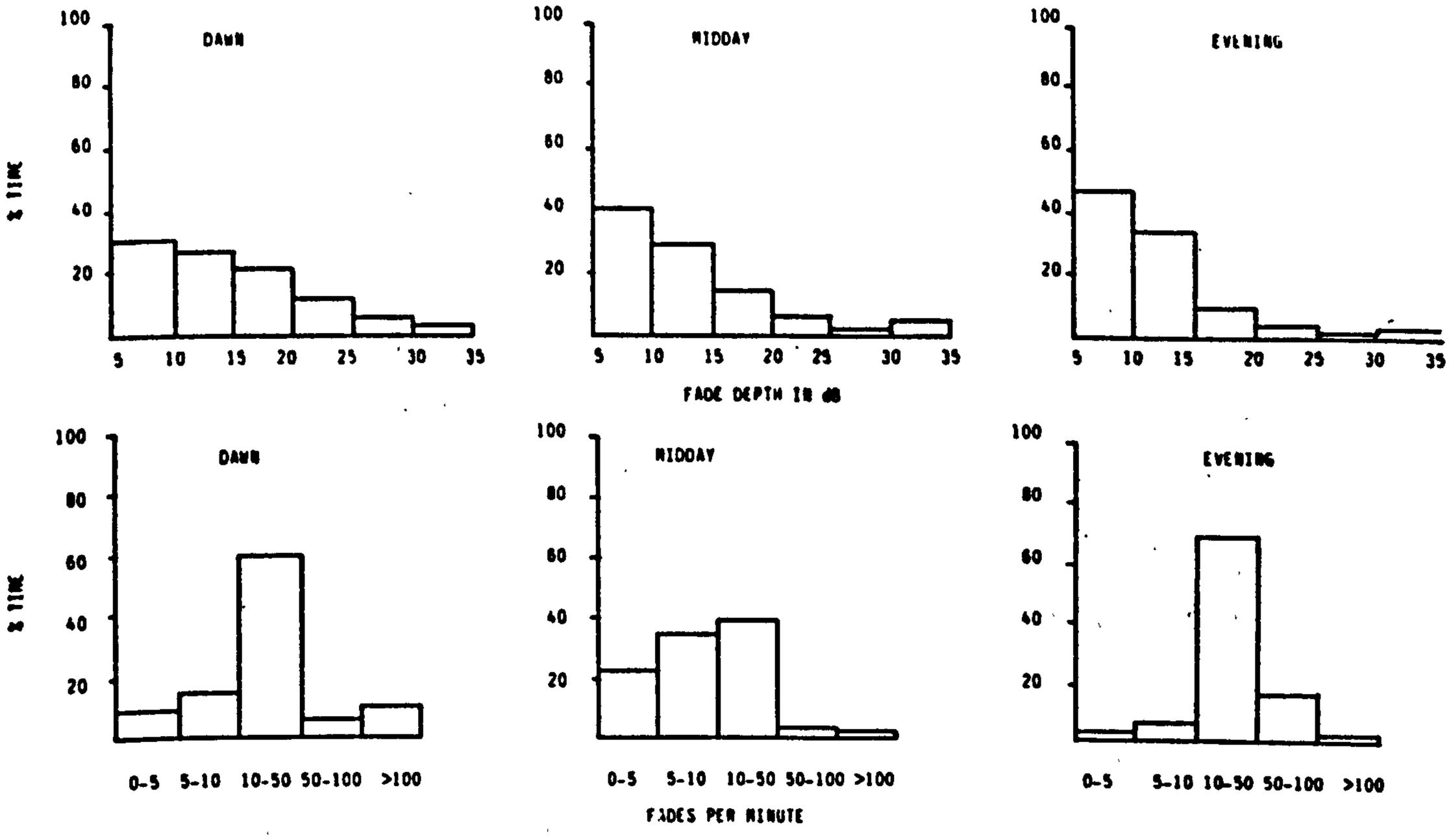

FIGURE 4.3.3: TYPICAL FADE RATES AND DEPTHS

occurring most frequently in the evening. Also, it is shown in Figure 4.3.3 that the fading rates of 10 to 50 fades per minute are the most common, especially at dawn and in the evening, whereas at midday, they are distributed rather evenly between 0 to 50 fades per minute.

4.3.3 Frequency Dispersion

The variation of path length due to the movement of the ionospheric reflecting layers which, for example, can reach 50 km/hour for the F_2-layer, and also the time variation of the electron density and hence the refractive index along the propagation path cause the received signal to be shifted in frequency[2,65,72,73]. The frequency (Doppler) shifts are relatively small at night. Also, the shifts are considerably greater for propagation involving the F-layer than the E-layer. Typical values are in the range 0.01 to 1 Hz[65]. However, greater frequency shifts are possible when the ionosphere is disturbed. For instance, shifts of 5-10 Hz[65] may be encountered when the conditions which give rise to spread F[63] occurs. Values of up to 50 Hz have also been observed during strong solar flares, but this is very rare[65].

The frequency shift on one propagation path is different from that on another path. This causes the frequency spreading of the received signal[2,65]. Under normal conditions, during the so-called 'quiet' days, typical values of the frequency shift are 0.02 Hz for E modes and 0.15 Hz for F modes[65].

4.3.4 Delay Distortion

Group delay is defined as the rate of change of phase with frequency[73] and thus for a signal reflected from the ionosphere the group delay is not constant across the signal bandwidth. This results in the distortion of the received signal known as delay distortion. In Figure 4.3.4[65], the variation in group delay with frequency is shown for a 430 km path and a 1365 km path, obtained by oblique soundings. From these graphs, it is clear that the E-layer causes very small dispersion; typical value of the rate of change of group delay with frequency is 5×10^{-6} μs/Hz[65]. The F-layer, however, can give more rapid changes of group delay with frequency, particularly near its MUF.

4.4 MODEL AND SIMULATION OF AN HF CHANNEL

Practical evaluation of HF digital communication systems may be carried out either by testing the equipment over actual HF channels or by testing it by computer simulation with an appropriate model of the channel. The first method may be costly to implement as any change required for the adjustments and/or improvements of the equipment could well involve alterations to the hardware. Also, when several systems are to be compared, they have to be tested simultaneously because the same propagation and channel conditions are difficult to obtain at different times due to the random variation in time and frequency of the HF channel. To avoid such problems, laboratory measurements using a valid model of the HF channel offer a considerable reduction in cost

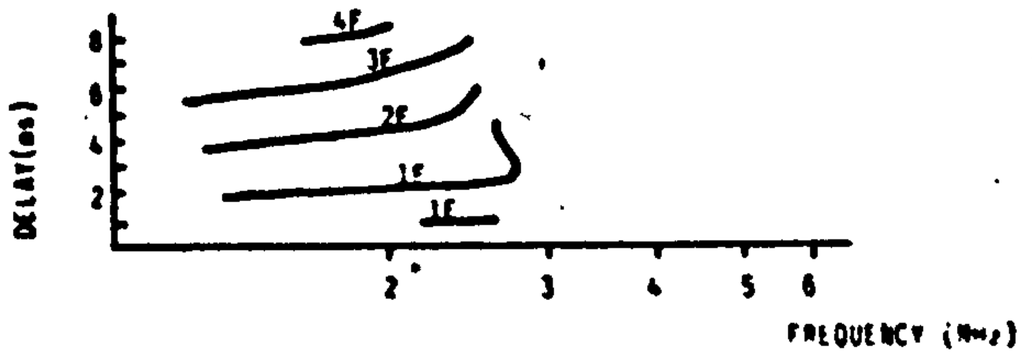

(a) 430 km path

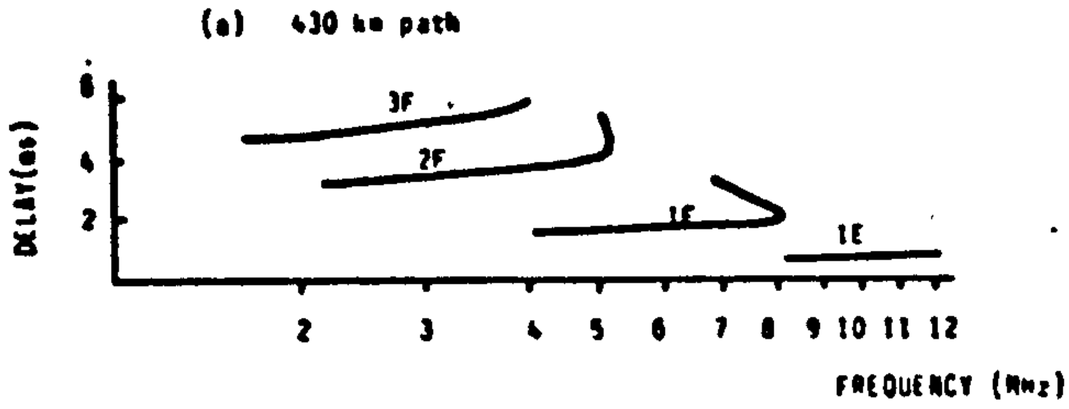

(b) 1365 km path

FIGURE 4.3.4: IONOGRAMS SHOWING DISPERSION CHARACTERISTICS

because in the testing and certainly in the initial study of the system, the simulator is usually in the form of software, so that any alteration required will merely involve changes to the computer simulation program.

HF channel simulators, whether in hardware or software form, are versatile, in that a variety of channel conditions can simply be produced. If desired, these can be repeated any number of times with consistent results. Also, the type and amount of distortion can be controlled so that any particular weakness of the system can be identified and studied in isolation.

In addition to the above techniques, one can also carry out theoretical analyses of the performance of the system. Here, a valid model of the channel is also required. However, because many factors are involved complete analyses are usually laborious and often difficult. Therefore, computer testing of the system over the channel simulator is usually preferred.

Although ionospheric channels are nonstationary in both frequency and time, most narrowband channels (say, 10 kHz) can be represented by a given model at least for short time durations (say, 10 minutes)[76]. Thus, the HF channel can be adequately studied by computer simulation. Many simulator designs have been described in the literature[76-88]; most of these are based on the tapped delay-line model which has been proposed by Watterson, et al in Ref. 76. This model has been adopted unanimously by the International Radio Consultative Committee (CCIR) of the International Telecommunication Union (ITU). This investigation

also uses the tapped delay-line model as shown in Figure 4.4.1, but operating here on a complex-valued baseband signal.

The input signal is fed to an ideal delay line and is delivered at several taps, one for each ionospheric propagation path. Rayleigh fading is then imposed on the delayed signals by multiplying each signal by a suitable tap gain function $Q_h(t)$. The resulting delayed and modulated signals from the different taps are added to form an output of the tapped delay line. The received signal is the sum of the output of the tapped delay line and an additive noise term $V_N(t)$ which represents the noise and/or interference on HF channels. Although various types of noise, such as atmospheric, man-made and thermal, are present on HF channels, it is a common practice to represent these by white Gaussian noise[78,87,88].

Now, if we consider only one propagation path, the Rayleigh fading introduced by the sky wave is modelled as in Figure 4.4.2[89], where $q_1(t)$ and $q_2(t)$ are two random processes which must have the following properties[78]:

1. Each random process must be Gaussian with zero mean and the same variance.

2. The random processes $q_1(t)$ and $q_2(t)$ must be statistically independent.

3. The power spectrum of each random process must be Gaussian in shape and with the same rms frequency, f_{rms}.

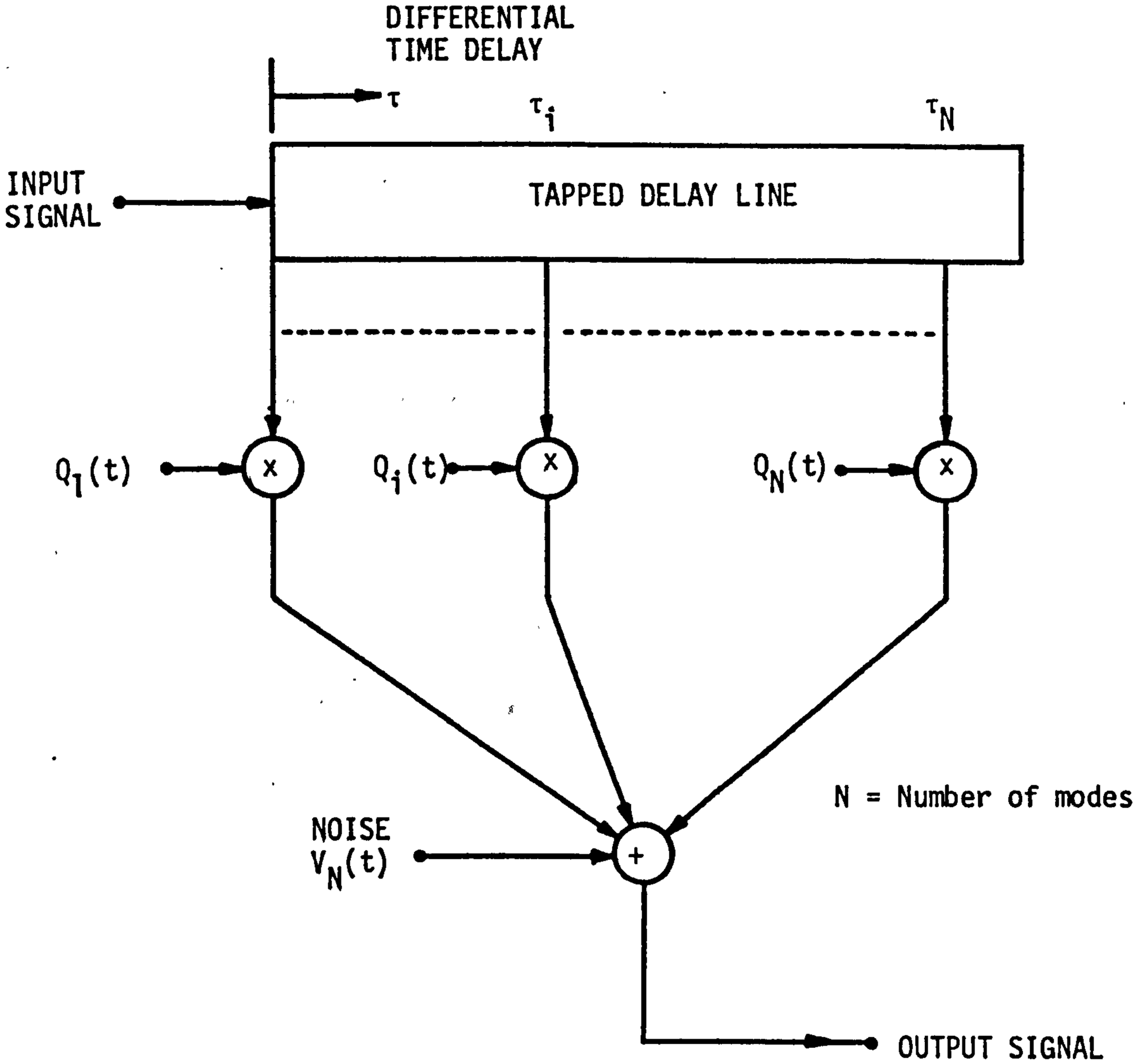

FIGURE 4.4.1: GENERAL MODEL OF AN HF CHANNEL

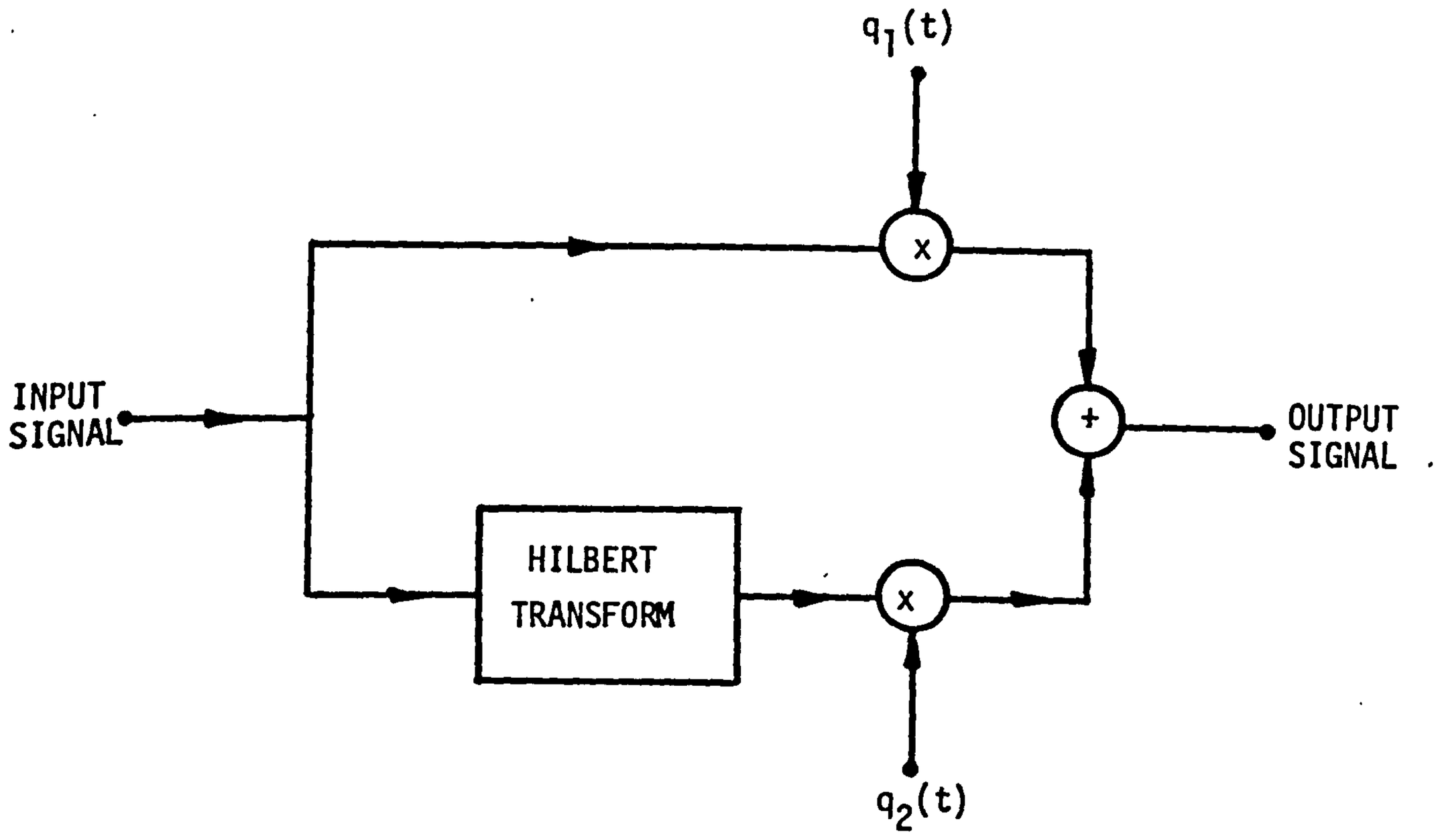

FIGURE 4.2.2: RAYLEIGH FADING INTRODUCED BY A SKY WAVE

The power spectra of $q_1(t)$ and $q_2(t)$ are given by,

$$|Q_1(f)|^2 = |Q_2(f)|^2 = \exp\left(-\frac{f^2}{2f_{rms}^2}\right) \qquad (4.4.1)$$

and are shown in Figure 4.4.3. The frequency (Doppler) spread, f_{sp}, introduced by $q_1(t)$ and $q_2(t)$ into an unmodulated carrier is defined[78] as the width of the power spectrum and this is given by,

$$f_{sp} = 2f_{rms} \qquad (4.4.2)$$

The rms frequency is related to the fading rate, f_e, which is defined[78] (for a single carrier) as the average number of downward crossings per second of the envelope through the median value, according to the equation[78],

$$f_{rms} = \frac{f_e}{1.475} \qquad (4.4.3)$$

From equations 4.4.2 and 4.4.3, f_{sp} is related to f_e by,

$$f_{sp} = 1.356\ f_e \qquad (4.4.4)$$

so, for example, a 1 Hz frequency spread is equivalent to a fading rate of 44 fades/min.

The random process $q_1(t)$ is generated by filtering a zero mean white Gaussian noise waveform $v_1(t)$ as shown in Figure 4.4.4. $q_2(t)$ is similarly generated but using a different Gaussian noise waveform

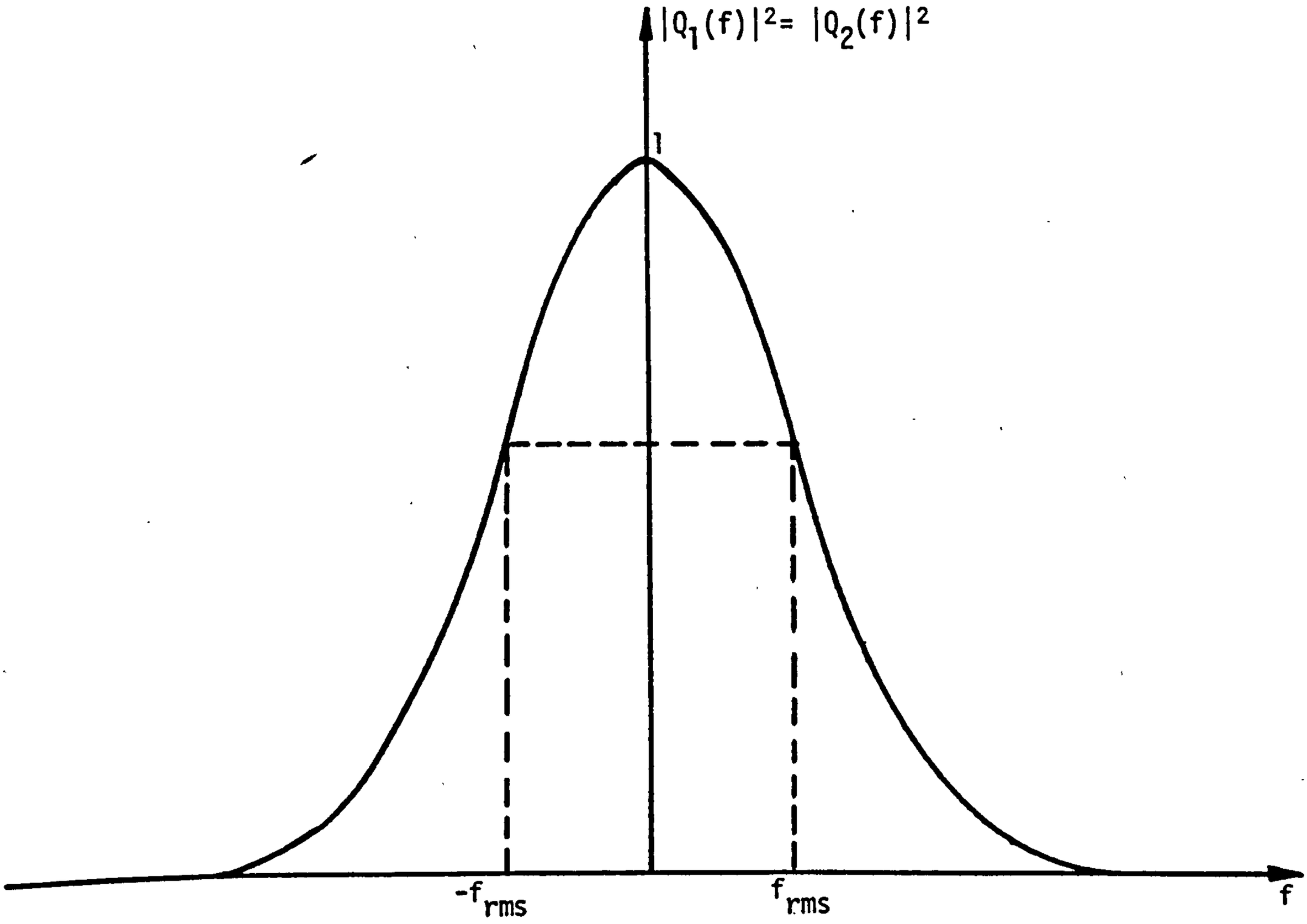

FIGURE 4.4.3: POWER SPECTRUM OF $q_1(t)$ AND $q_2(t)$

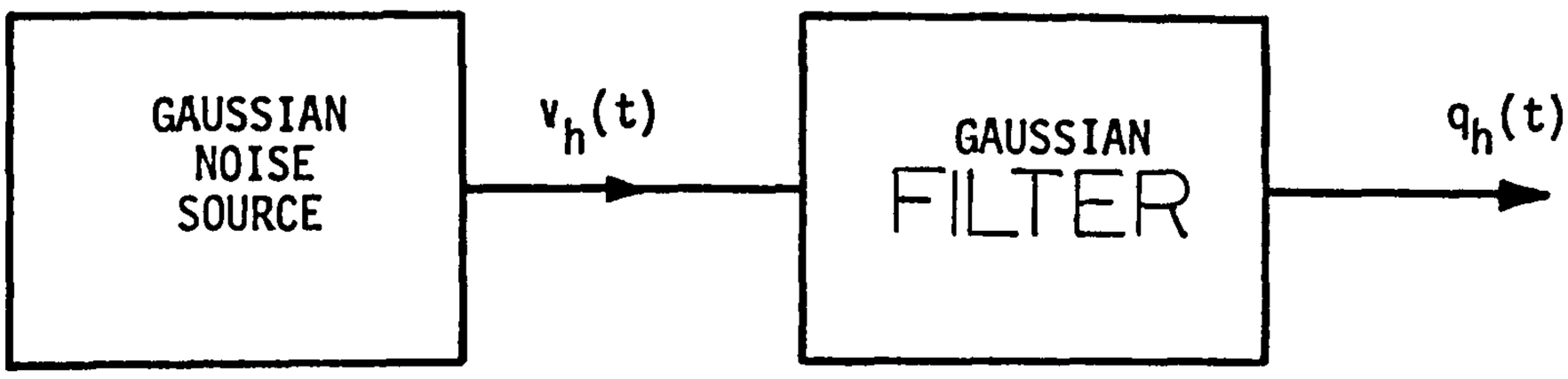

FIGURE 4.4.4: METHOD OF GENERATING $q_h(t)$

$v_2(t)$, which is independent of $v_1(t)$. The frequency response of the linear filter is also Gaussian, so that it matches the required power spectra of $q_1(t)$ and $q_2(t)$. The square of the absolute value of the transfer function of each filter is given by equation 4.4.1. Consequently, the frequency response of the filter is given by,

$$F(f) = \exp\left(-\frac{f^2}{4\, f_{rms}^2}\right) \tag{4.4.5}$$

From equation 4.4.5, the 3-dB cutoff frequency of the filter is,

$$f_c = 1.17741\ f_{rms} \tag{4.4.6}$$

Using equation 4.4.2, an alternative expression for f_c is,

$$f_c = 0.588705\ f_{sp} \tag{4.4.7}$$

It is well known[92] that as the order of a Bessel filter is increased, the frequency and impulse responses of the filter tend towards Gaussian. Therefore, two Bessel filters are used to filter the Gaussian noise process $v_1(t)$ and $v_2(t)$. The s-plane transfer function of the Bessel filter is[92],

$$H(s) = \frac{d_o}{\sum_{k=0}^{L} d_k s^k} \tag{4.4.8}$$

where L is the order of the filter and

$$d_k = \frac{(2L-k)!}{2^{L-k}\, k!\, (L-k)!} \qquad (4.4.9)$$

As a practical choice, L has been chosen to be 5, so that equation 4.4.8 becomes,

$$H(s) = \frac{945}{s^5 + 15s^4 + 105s^3 + 420s^2 + 945s + 945} \qquad (4.4.10)$$

Factorizing the denominator in equation 4.4.10, yields,

$$H(s) = \frac{945}{\prod_{i=0}^{5} (s-p_i)} \qquad (4.4.11)$$

where the $\{p_i\}$ are known as the poles of H(s) and are given by[90],

$$\left.\begin{aligned} p_1 &= -3.64674 + j0 \\ p_2, p_3 &= -3.35196 \pm j1.74266 \\ p_4, p_5 &= -2.32467 \pm j3.57102 \end{aligned}\right\} \qquad (4.4.12)$$

Thus, the frequency response of the fifth order Bessel filter is given by equation 4.4.11 by substituting s by $j\Omega$, i.e.

$$H(j\Omega) = \frac{945}{\prod_{i=1}^{5} (j\Omega-p_i)} \qquad (4.4.13)$$

where Ω is the angular frequency, $j = \sqrt{-1}$ and the poles $\{p_i\}$ are given by equation 4.4.12. The 3-dB cutoff angular frequency is[16],

$$\Omega_c = 2.4274 \text{ rad/s} \tag{4.4.14}$$

Since three channels with different frequency spreads are required to be simulated, the cutoff frequency of the Bessel filter must be changeable to correspond to the different frequency spreads. This is achieved by first introducing a new angular frequency variable ω, such that

$$\omega = c_o \Omega \tag{4.4.15}$$

where

$$c_o = \frac{\omega_c}{\Omega_c} = \frac{2\pi f_c}{\Omega_c} \tag{4.4.16}$$

where f_c is the desired cutoff frequency. From equations 4.4.14 and 4.4.16,

$$c_o = 2.58844\ f_c \tag{4.4.17}$$

Using equation 4.4.17 to replace Ω in equation 4.4.13, we have,

$$H(j\omega) = \frac{945}{\prod_{i=1}^{5} \left(j \frac{\omega}{c_o} - p_i\right)}$$

or

$$H(j\omega) = \frac{945\ c_o^{\,5}}{\prod_{i=1}^{5} (j\omega - p_i')} \qquad (4.4.18)$$

and substituting the value of c_o from equation 4.4.17, gives,

$$H(j\omega) = \frac{109805.05\ f_c^{\,5}}{\prod_{i=1}^{5} (j\omega - p_i')} = \frac{d_o}{\prod_{i=1}^{5} (j\omega - p_i')} \qquad (4.4.19)$$

where the $\{p_i'\}$ are the poles of the Bessel filter and are given by,

$$p_i' = c_o p_i$$

or

$$p_i' = 2.58844\ f_c p_i \quad \text{for } i = 1,2,..,5 \qquad (4.4.20)$$

Substituting $j\omega = s$, equation 4.4.19 becomes,

$$H(s) = \frac{d_o}{\prod_{i=1}^{5} (s - p_i')} \qquad (4.4.21)$$

The three different values of the frequency spreads are ½, 1 and 2 Hz. Using equation 4.4.7, the corresponding cutoff frequencies of the Bessel filter are 0.2943, 0.5887 and 1.1774 Hz, respectively. Thus, all the parameters of the Bessel filter have been specified and they are summarized in Table 4.4.1.

Frequency spread, f_{sp}(Hz)		½	1	2
Cutoff frequency, f_c(Hz)		0.2943	0.5887	1.1774
Constant, d_o		242.42	7764.124	248451.98
Filter poles in the s-plane	p_1'	-2.7785+j0	-5.5570+j0	-11.1140+j0
	p_2' ,p_3'	-2.5540±j1.3277	-5.1078±j2.6555	-10.2156±j5.3110
	p_4' ,p_5'	-1.7712±j2.7208	-3.5424±j5.4400	-7.0848±j10.8830

TABLE 4.4.1: FIFTH ORDER ANALOG BESSEL FILTER FOR DIFFERENT FREQUENCY SPREADS

The Bessel filters derived above are all in analog form. Since they are to be simulated on a digital computer, a digital form of the filters is required. Various methods, such as impulse invariance, bilinear and matched z transformations[92] may be applied to digitize the analog transfer function (equation 4.4.21). Here, the impulse invariance technique is chosen so that the impulse response of the resulting digital filter is a sampled version of the impulse response of the analog filter[92]. Using this technique, the poles $\{p_i'\}$ in the s-plane are transformed to poles at $\{e^{p_i' T}\}$ in the z-plane[92], where T is the sampling period. Thus, the transfer function given by equation 4.4.21 becomes,

$$H(z) = \frac{K}{\prod_{i=1}^{5} (1 - e^{p_i' T} z^{-1})} \qquad (4.4.22)$$

or

$$H(z) = \frac{K}{\prod_{i=1}^{5} (1 - P_i z^{-1})} \qquad (4.4.23)$$

where the $\{P_i\}$ are the poles of the filters in the z-plane and K is a constant whose role will be explained later.

From Nyquist theorem, for the accurate representation of the $q_h(t)$, they must be sampled at least at twice the highest frequency contained in them. However, $q_h(t)$ have Gaussian spectra, and so contain all frequencies, but from Table 4.4.1, it can be seen that the 3-dB bandwidths of the analog filters are at most about 2.4 Hz, which implies that the frequency components at a filter output, above 25 Hz, are negligible, so that a sampling rate of 50 samples/s should be adequate. For reasons connected with the processing of the transmitted data signal, the actual sampling rate used is 4800 samples/s. Unfortunately, at this rate the filter poles are very close to the unit circle in the z-plane, and to obtain the desired filter characteristics, these poles must be specified with very high degree of accuracy. Therefore, as a solution, the required sampling rate is achieved by sampling at a lower rate and obtaining the remaining samples by linear interpolation. Here, the sampling frequency is 50 Hz, so that T = 20 ms. This value is chosen as a compromise between the requirements for the Nyquist sampling criterion and the need to limit the degree of interpolation used. The values of K and the poles $\{P_i\}$ of the equivalent digital filter aregiven in Table 4.4.2[16].

Frequency spread, f_{sp}(Hz)		½	1	2
Constant, K^{-1}		325623.4	16121.6	893.06
Filter poles in the z-plane	P_1	0.9460+j0	0.8950+j0	0.8010+j0
	P_2,P_3	0.9500±j0.0252	0.9018±j0.0479	0.8109±j0.0863
	P_4,P_5	0.9638±j0.0524	0.9262±j0.1010	0.8477±j0.1872

TABLE 4.4.2: FIFTH ORDER DIGITAL BESSEL FILTER FOR DIFFERENT FREQUENCY SPREADS

The digital filter is implemented as shown in Figure 4.4.5. It is a cascade of two 2-pole sections and one 1-pole section. Each 2-pole section has complex conjugate poles and the 1-pole section has a real pole. The filter coefficients $\{c_i\}$ are given by[16,97],

$$\left.\begin{aligned} c_1 &= -P_1 \\ c_2 &= -(P_2 + P_3) \\ c_3 &= P_2P_3 \\ c_4 &= -(P_4 + P_5) \\ c_5 &= P_4P_5 \end{aligned}\right\} \qquad (4.4.24)$$

The input to the filter, $\{v_{h,i}\}$ is a sequence of statistically independent Gaussian random variables with zero mean and a fixed variance. In the computer simulation, the $\{v_{h,i}\}$ are obtained by calling the Gaussian random number generator subroutine GØ5DDF(0,1) from the NAG Library[94].

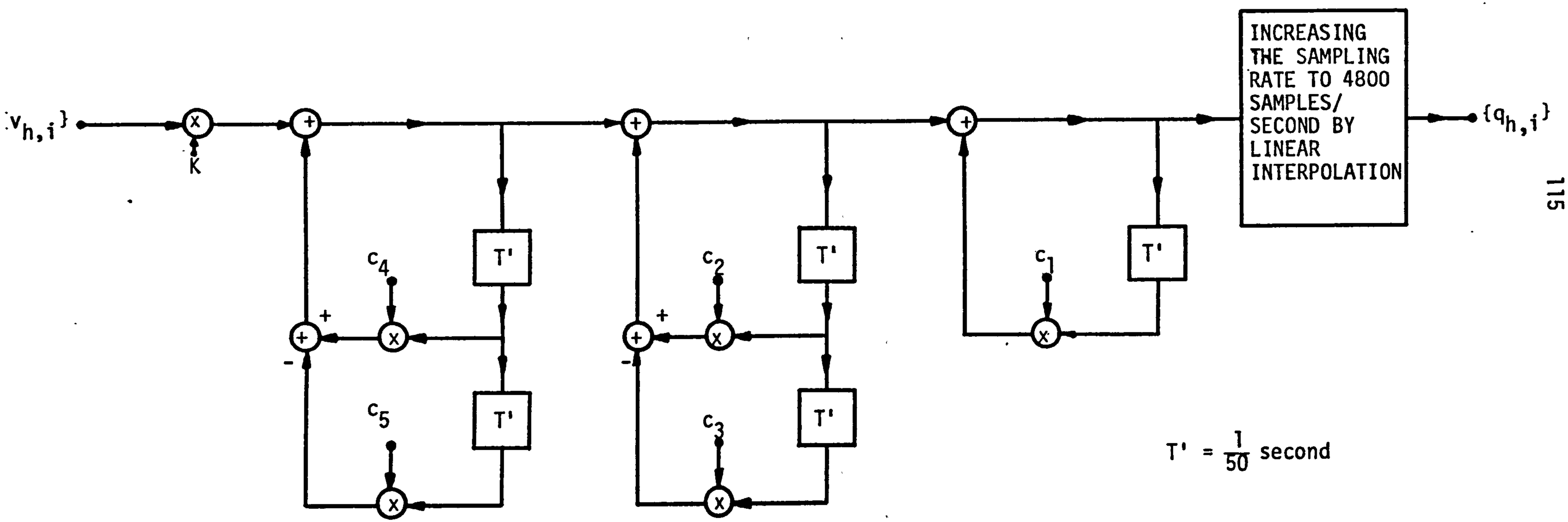

FIGURE 4.4.5: REALIZATION OF FIFTH ORDER DIGITAL BESSEL FILTER

We have seen earlier (Figure 4.4.2) that two signals $q_1(t)$ and $q_2(t)$ are required for the fading of a sky wave. For the second sky wave, another two signals $q_3(t)$ and $q_4(t)$ are required; and so on. These signals are generated by the method described above but using different input Gaussian noise waveforms $\{v_h(t)\}$. The variances of the $\{q_{h,i}\}$ are equal and the actual values depend on the number of sky waves present. For example, if there are two sky waves, the number of signals $q_h(t)$ required is 4 and the variance of each $\{q_{h,i}\}$ is $\frac{1}{4}$. When there are three sky waves, 6 of the signals $q_h(t)$ are required, the variance of each $\{q_{h,i}\}$ becomes 1/6. Thus, by having the variance of each $\{q_{h,i}\}$ equal to the reciprocal of the number of $q_h(t)$ required, the total variance of the $\{q_{h,i}\}$ equals 1. The reason for this will become clear later. The value of the gain K at the input of the filter (Figure 4.4.5) is adjusted such that the $\{q_{h,i}\}$ have the required variance. In Table 4.4.2, the values of K for the three filters ensure that each of the $\{q_{h,i}\}$ has variance of $\frac{1}{4}$. Finally, a complete model of the HF radio link with N sky waves is given in Figure 4.4.6.

4.5 DATA TRANSMISSION OVER A MODEL OF AN HF CHANNEL USING QAM

In Section 2.2, a general description is given of a model of a data-transmission system using QAM. Here, we will consider the transmission of the QAM signals over a model of an HF radio channel that has been described in the previous section.

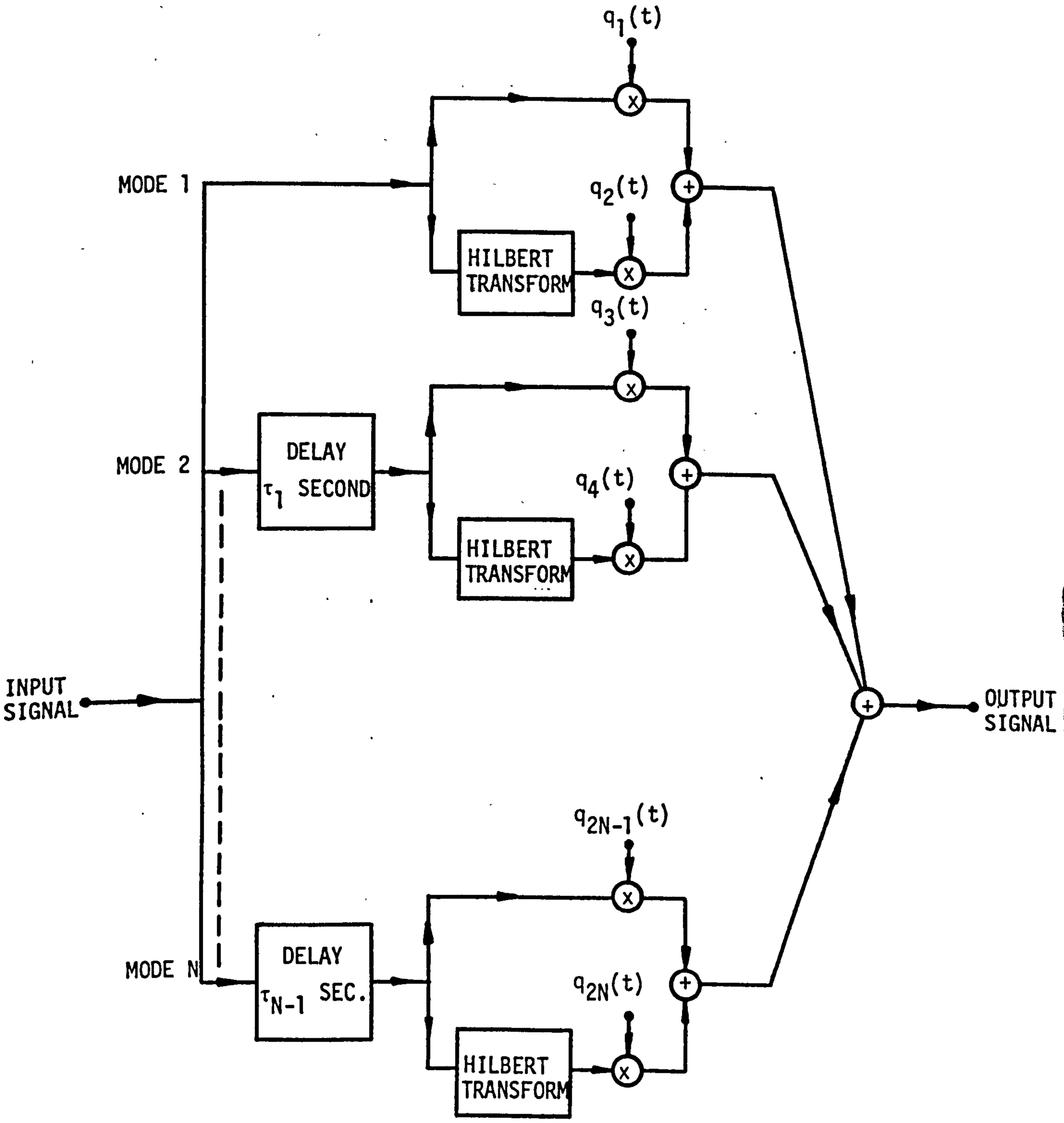

FIGURE 4.4.6: MODEL OF HF RADIO LINK

In order to simplify the description of the system, it is assumed that the HF channel has only two independent Rayleigh fading sky waves. The relative delay in transmission between the sky waves is τ seconds. Figure 4.5.1 shows the model of the data-transmission system which employs the HF radio channel as the transmission medium.

The signal at the input to the system is a sequence of signal elements $\sum_i s_i\ \delta(t-iT)$, where s_i is a complex-valued data signal and may have one of a finite number of possible values, and T is the signalling interval. The function of the filter A' is to shape the spectrum of the input signal so that it matches the available bandwidth of the HF channel. The transmitted signal is then modulated using QAM with a carrier frequency of f_c. The frequency response of the filter A' is assumed such that

$$\left[\begin{array}{ll} A'(f) = 0 & \text{for } f < -f_c + kf_{sp} \\ & \text{and } f > f_c - kf_{sp} \end{array}\right] \qquad (4.5.1)$$

where f_{sp} is the maximum expected value of the frequency spread that is introduced into the data signal by the HF channel, and k is an integer. The QAM signal $x_2(t)$ that is fed to the radio-transmitter filter is the real part of the complex signal $x_1(t)$ (see Section 2.2) at the output of the modulator. The radio-transmitter filter G uses single sideband suppressed carrier amplitude modulation to shift the spectrum of the modulated signal from the voice channel to the HF band, without of course changing the bandwidth of the signal. The resulting signal x(t) is transmitted via the two sky waves

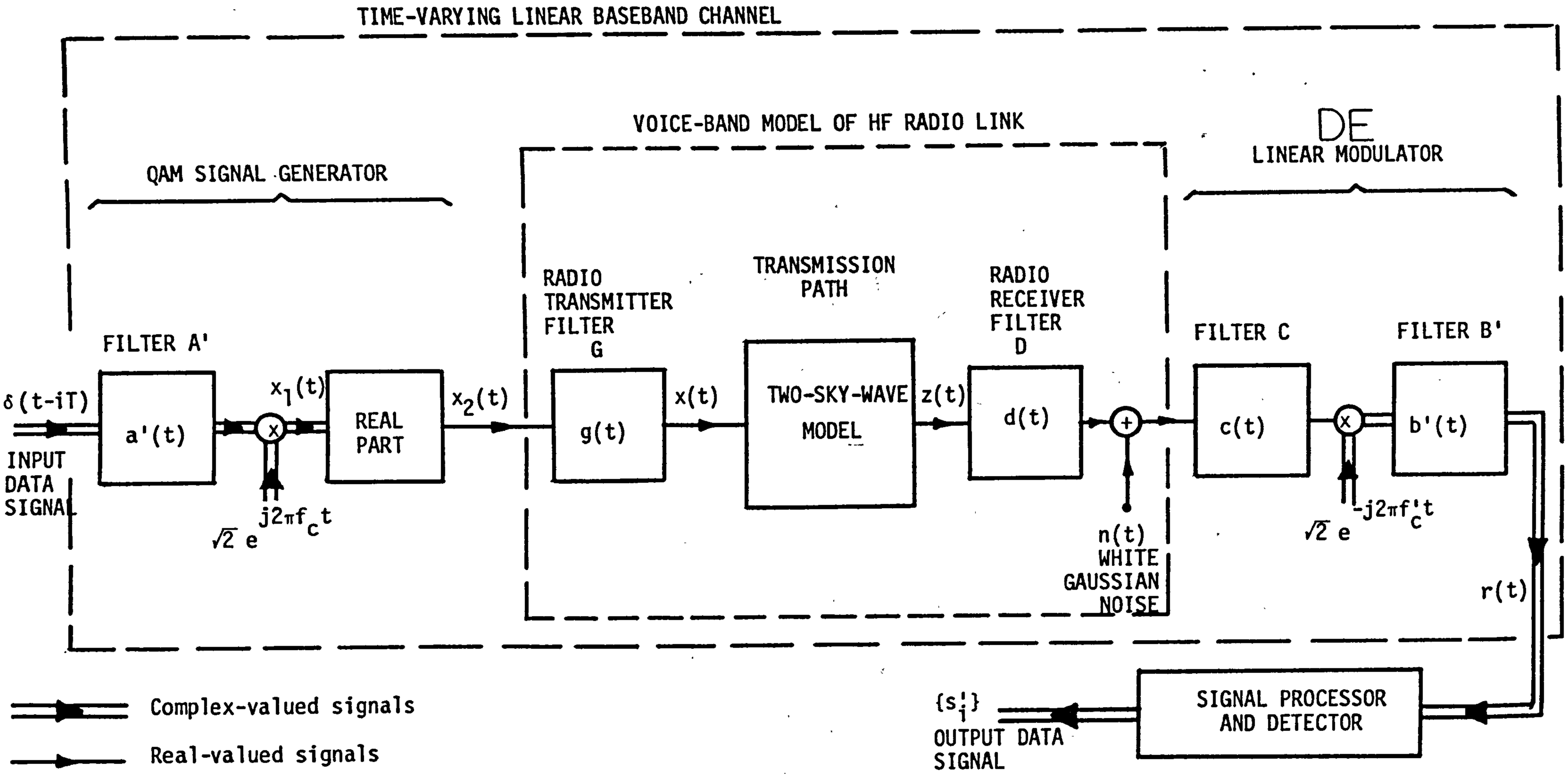

FIGURE 4.5.1: MODEL OF THE QAM DATA-TRANSMISSION SYSTEM OVER AN HF RADIO LINK

and is subjected to Rayleigh fading. The radio-receiver filter D shifts the spectrum of the signal z(t) at the output of the transmission path back to voice-band. It is assumed that the only form of noise present is a white Gaussian noise n(t) which is added to the signal $z(t)$[89,95]. The additive white Gaussian noise has zero mean and two-sided power spectral density of $\frac{1}{2}N_o$. The bandpass filter C removes the noise frequencies outside the bandwidth of the data signal without unduly distorting it. The noisy, distorted and Rayleigh-faded QAM signal is then coherently demodulated by multiplying it by complex-valued reference signal $\sqrt{2}\, e^{-j2\pi f_c' t}$ and low-pass filtered by the filter B' so that the high frequency components of the signal are removed. It is assumed that the reference carrier f_c' is equal to the average instantaneous carrier frequency of the received signal, thus eliminating any constant or near-constant frequency offset in the received QAM signal. Thus,

$$f_c' = f_c \tag{4.5.2}$$

The frequency response of the receiver filter B' is such that

$$\left[B'(f) = 0 \qquad \text{for } |f| > f_c\right] \tag{4.5.3}$$

The signal x(t) at the output of the radio-transmitter filter G is,

$$x(t) = \mathrm{Re}\left[\sqrt{2} \sum_i s_i\, a'(t-iT) e^{j2\pi f_c t}\right] * g(t) \tag{4.5.4}$$

where * denotes convolution, and a'(t) and g(t) are the impulse responses of the filters A' and G, respectively. The foregoing equation can also be written as[16],

$$x(t) = \frac{1}{\sqrt{2}} \left[\sum_i s_i \, a(t-iT)e^{j2\pi f_c t} + s_i^* \, a^*(t-iT)e^{-j2\pi f_c t}\right] \tag{4.5.5}$$

where s_i^* and $a^*(t-iT)$ are the complex conjugates of s_i and $a(t-iT)$, respectively, and

$$a(t-iT) = a'(t-iT)*(g(t)e^{-j2\pi f_c t}) \tag{4.5.6}$$

Equation 4.5.6 shows the overall filtering carried out at the transmitter side of the system, where the filtering is considered as operating entirely on the baseband signal. Thus a(t) is the impulse response of the resultant equivalent baseband filter at the transmitter. Now, let $\hat{x}(t)$ represents the Hilbert transform of x(t), then,

$$\hat{x}(t) = x(t)*f(t) \tag{4.5.7}$$

where f(t) is a function such that its Fourier transform $\Gamma(f)$ is given by,

$$\Gamma(f) = \begin{cases} j & f < 0 \\ 0 & f = 0 \\ -j & f > 0 \end{cases} \tag{4.5.8}$$

Subsituting for x(t) from equation 4.5.5 in equation 4.5.7, we have,

$$\hat{x}(t) = \frac{1}{\sqrt{2}} \{\sum s_i [a(t-iT)e^{j2\pi f_c t}] * f(t) +$$

$$+ s_i^* [a^*(t-iT)e^{-j2\pi f_c t}] * f(t)\} \qquad (4.5.9)$$

which may be written as[16],

$$\hat{x}(t) = \frac{1}{\sqrt{2}} \{\sum s_i [a(t-iT) * f(t)e^{-j2\pi f_c t}] e^{j2\pi f_c t} +$$

$$+ s_i^* [a^*(t-iT) * f(t)e^{j2\pi f_c t}] e^{-j2\pi f_c t} \qquad (4.5.10)$$

From equation 4.5.6, it can be seen that A(f), the frequency response of a(t), is bandlimited to that of A'(f) (equation 4.5.1). The Fourier transform of $f(t)e^{-j2\pi f_c t}$ is $\Gamma(f+f_c)$ which is the spectrum of $\Gamma(f)$ shifted down in frequency by f_c. Consequently, $\Gamma(f+f_c)$ has the value -j over the frequency range $-f_c < f < f_c$. The Fourier transform of $f(t)e^{j2\pi f_c t}$ is $\Gamma(f-f_c)$ which is the spectrum of $\Gamma(f)$ shifted up in frequency by f_c. Therefore, $\Gamma(f-f_c)$ is equal to j for $-f_c < f < f_c$. By taking the Fourier transform of $\hat{x}(t)$, and replacing $\Gamma(f+f_c)$ and $\Gamma(f-f_c)$ by their values obtained above, and then taking the inverse Fourier transform, equation 4.5.10 becomes,

$$\hat{x}(t) = \frac{1}{\sqrt{2}} [\sum -js_i a(t-iT)e^{j2\pi f_c t} + js_i^* a^*(t-iT)e^{-j2\pi f_c t}] \qquad (4.5.11)$$

The signal at the output of the model of the HF radio channel is given by,

$$z(t) = x(t)q_1(t) + \hat{x}(t)q_2(t) + x(t-\tau)q_3(t) + \hat{x}(t-\tau)q_4(t) \qquad (4.5.12)$$

From equation 4.5.5 and 4.5.11, we have

$$\begin{aligned} z(t) = \frac{1}{\sqrt{2}} \{ & \sum s_i a(t-iT)\ [q_1(t) - jq_2(t)]\ e^{j2\pi f_c t} + \\ & + s_i^*\ a^*(t-iT)\ [q_1(t) + jq_2(t)]\ e^{-j2\pi f_c t} + \\ & + s_i a(t-\tau-iT)\ [q_3(t) - j\ q_4(t)] e^{j2\pi f_c (t-\tau)} + \\ & + s_i^*\ a^*(t-\tau-iT)\ [q_3(t) + jq_4(t)]\ e^{-j2\pi f_c (t-\tau)} \end{aligned} \qquad (4.5.13)$$

If we let

$$\begin{aligned} h_i(t-iT) = & a(t-iT)\ [q_1(t) - jq_2(t)] + \\ & + a(t-\tau-iT)\ [q_3(t) - jq_4(t)]\ e^{-j2\pi f_c \tau} \end{aligned} \qquad (4.5.14)$$

then, equation 4.5.13 can be rewritten as,

$$z(t) = \frac{1}{\sqrt{2}} [\sum s_i h_i(t-iT) e^{j2\pi f_c t} + s_i^*\ h_i^*(t-iT) e^{-j2\pi f_c t}] \qquad (4.5.15)$$

The delay τ is assumed to be a constant. Therefore, the factor $e^{-j2\pi f_c \tau}$ in equation 4.5.14 is a complex-valued scalar with absolute value of 1, and since $q_3(t)$ and $q_4(t)$ are statistically independent with zero mean, it has no effect on the statistical properties of $\{[q_3(t) - jq_4(t)]\, e^{-j2\pi f_c \tau}\}$ nor does it affect the power spectrum of this signal. Thus, we may rewrite equation 4.5.14 as,

$$h_i(t-iT) = a(t-iT)\,[q_1(t) - jq_2(t)] + a(t-\tau-iT)\,[q_3(t) - jq_4(t)] \qquad (4.5.16)$$

The signal at the output of the linear demodulator is now,

$$r(t) = \sqrt{2}\,\{[z(t)*d(t)*c(t)]\, e^{-j2\pi f_c t}\}*b'(t) + \sqrt{2}\,\{n(t)*c(t)]\, e^{-j2\pi f_c t}\}*b'(t) \qquad (4.5.17)$$

where d(t), c(t) and b'(t) are the impulse responses of the filters D, C and B', respectively. It is assumed in equation 4.5.17 that $f_c' = f_c$. If we let

$$b(t) = \{[d(t)*c(t)]\, e^{-j2\pi f_c t}\}*b'(t) \qquad (4.5.18)$$

and

$$w(t) = \sqrt{2}\,\{[n(t)*c(t)]e^{-j2\pi f_c t}\}*b'(t) \qquad (4.5.19)$$

then equation 4.5.17 may be written as,

$$r(t) = \sqrt{2}\ [z(t)e^{-j2\pi f_c t}]*b(t) + w(t) \qquad (4.5.20)$$

b(t) represents the overall filtering at the receiver end of the system when considered as operating on the demodulated baseband signal, and w(t) is the Gaussian noise component in r(t). Clearly, both b(t) and w(t) are baseband waveforms. Substituting for z(t) from equation 4.5.15 into equation 4.5.20, we have

$$r(t) = \sum[s_i h_i(t-iT) + s_i^* h_i^*(t-iT)e^{-j4\pi f_c t}]*b(t)+w(t) \qquad (4.5.21)$$

It may be shown[16] that the Fourier transform of $s_i^* h_i^*(t-iT)e^{-j4\pi f_c t}$ is outside the passband of the lowpass filter whose impulse response is b(t), and so equation 4.5.21 reduces to,

$$r(t) = \sum s_i h_i(t-iT)*b(t) + w(t) \qquad (4.5.22)$$

Let

$$y_i(t-iT) = h_i(t-iT)*b(t) \qquad (4.5.23)$$

then equation 4.5.22 becomes,

$$r(t) = \sum s_i \underbrace{y_i(t-iT)} + w(t) \qquad (4.5.24)$$

The impulse response $y_i(t-iT)$ in equation 4.5.23 may also be written as,

$$y_i(t-iT) = \{a(t-iT)\,[q_1(t) - jq_2(t)] + a(t-\tau-iT)\,[q_3(t) - jq_4(t)]\} * b(t) \qquad (4.5.25)$$

where $h_i(t-iT)$ has been replaced by its value from equation 4.5.16. $y_i(t-iT)$ is the impulse response of the linear baseband channel in Figure 4.5.1 which is obviously time-varying.

Equation 4.5.24 represents the baseband model of the QAM system over the HF radio link and this is shown in Figure 4.5.2. In this model, the impulse response a(t) (equation 4.5.6) represents the overall filtering at the transmitter side of the data-transmission system, and b(t) (equation 4.5.18) is the overall filtering at the receiver side of the system, each impulse response being, of course, a baseband waveform. The characteristics of these filters (or, in fact, the characteristics of their combinations) are given in Figures 4.5.3-4.5.5, where the filters are, for convenience, shown as the equivalent bandpass filter operating on the voiceband signal, since this enables them to be compared with the corresponding radio filter (Figure 4.5.5). The noise waveform w(t) (equation 4.5.19) is a complex-valued Gaussian random process with autocorrelation which may be shown to be[16],

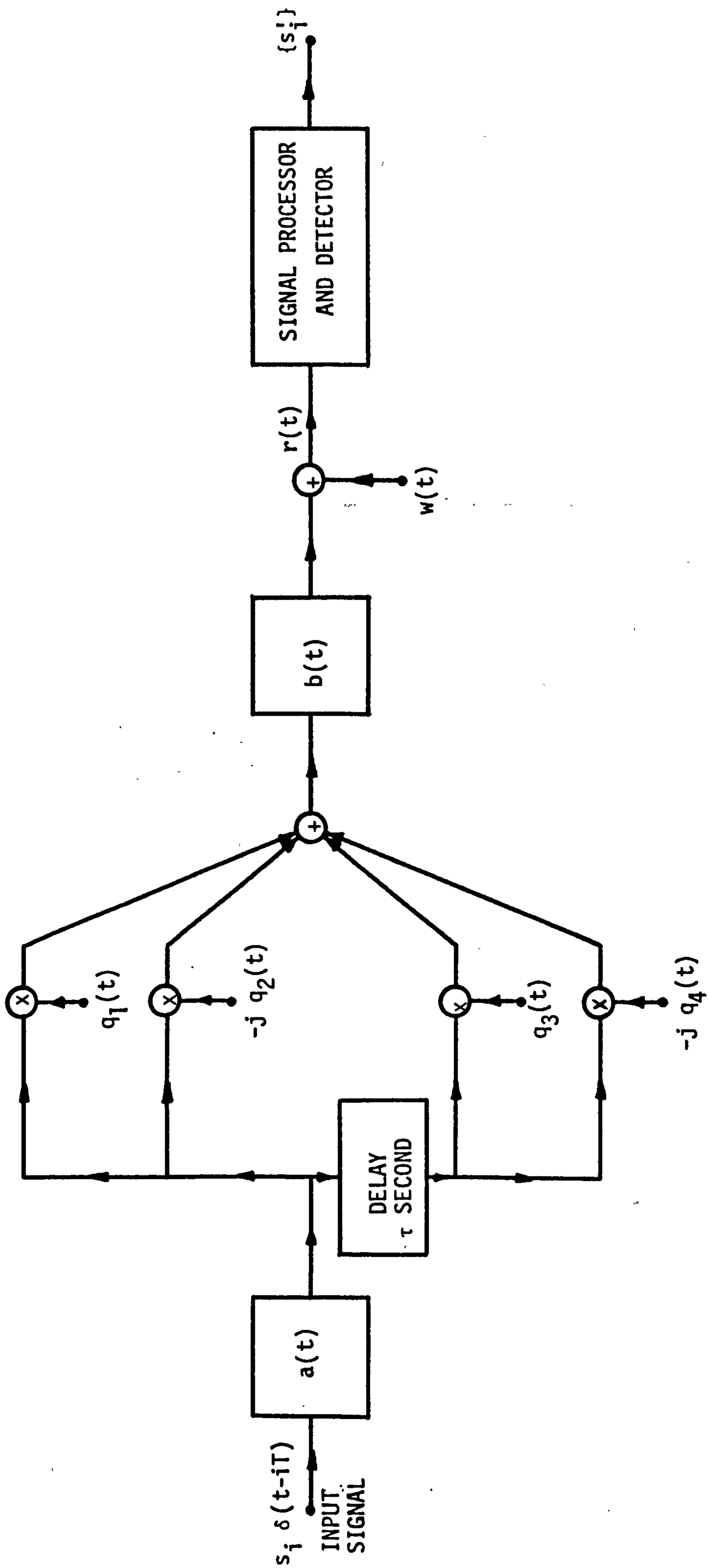

FIGURE 4.5.2: BASBEBAND MODEL OF THE QAM SYSTEM OVER THE HF RADIO LINK

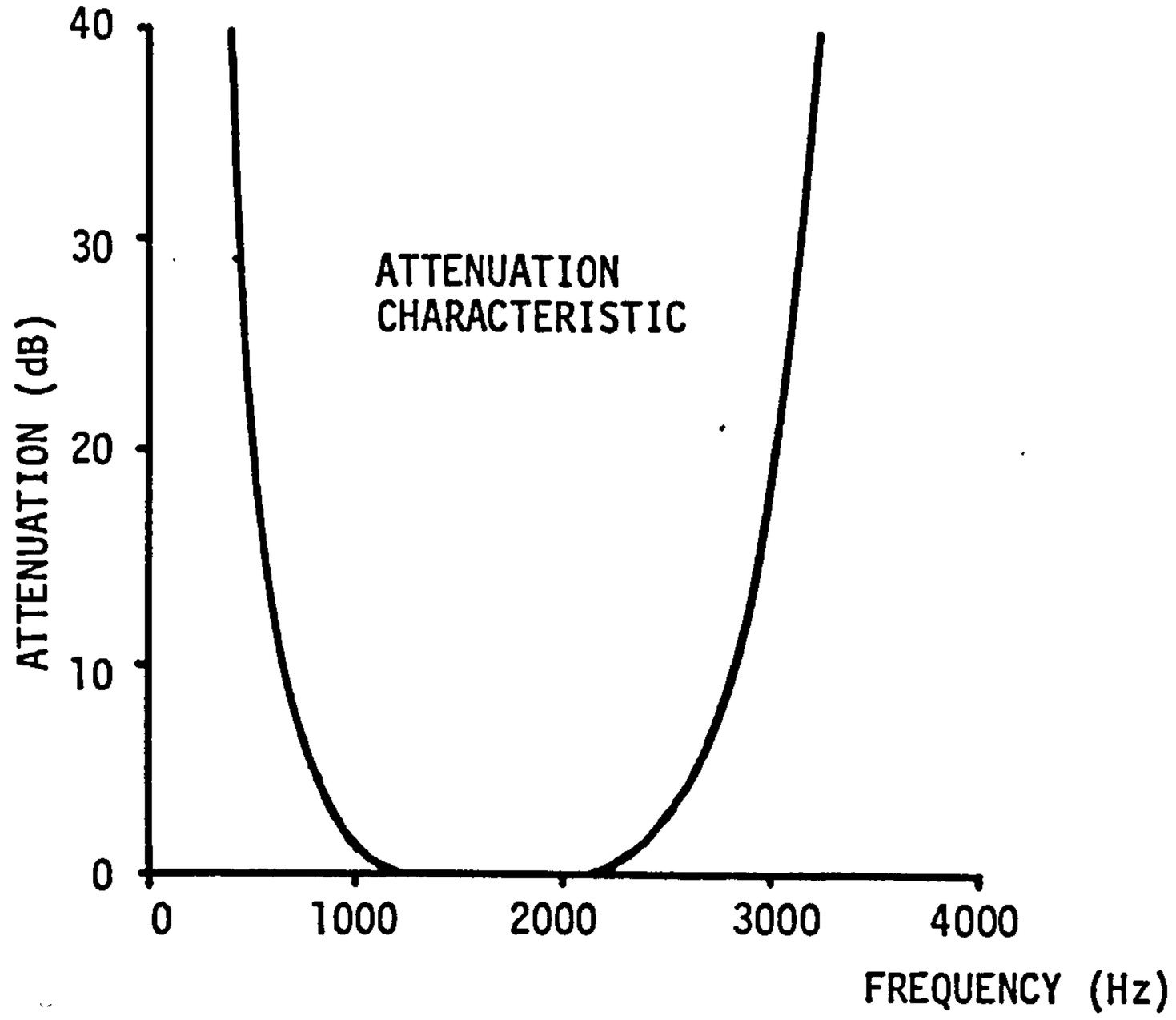

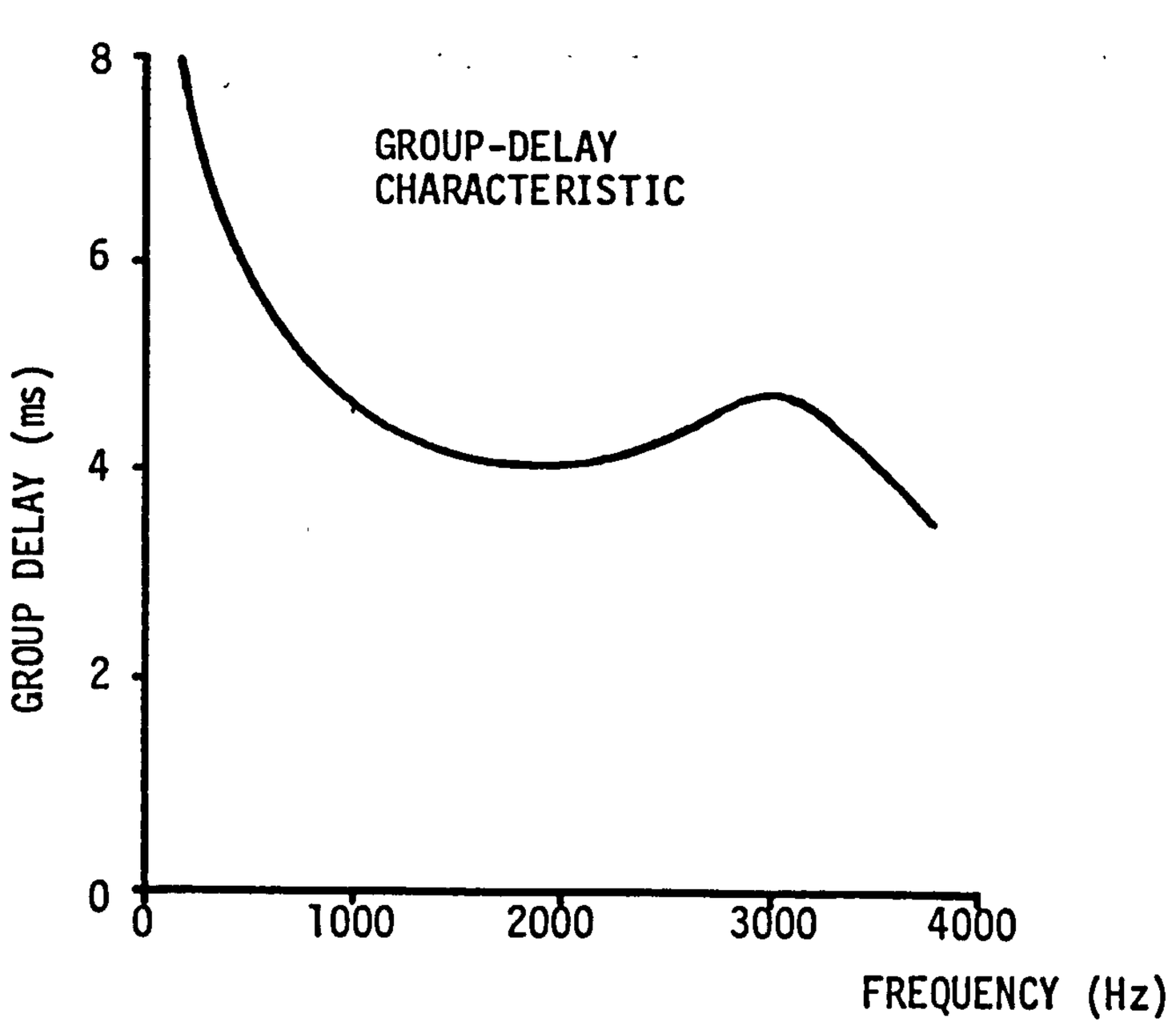

FIGURE 4.5.3: CHARACTERISTICS OF THE TRANSMITTER AND RECEIVER FILTERS IN CASCADE WITH RADIO FILTERS

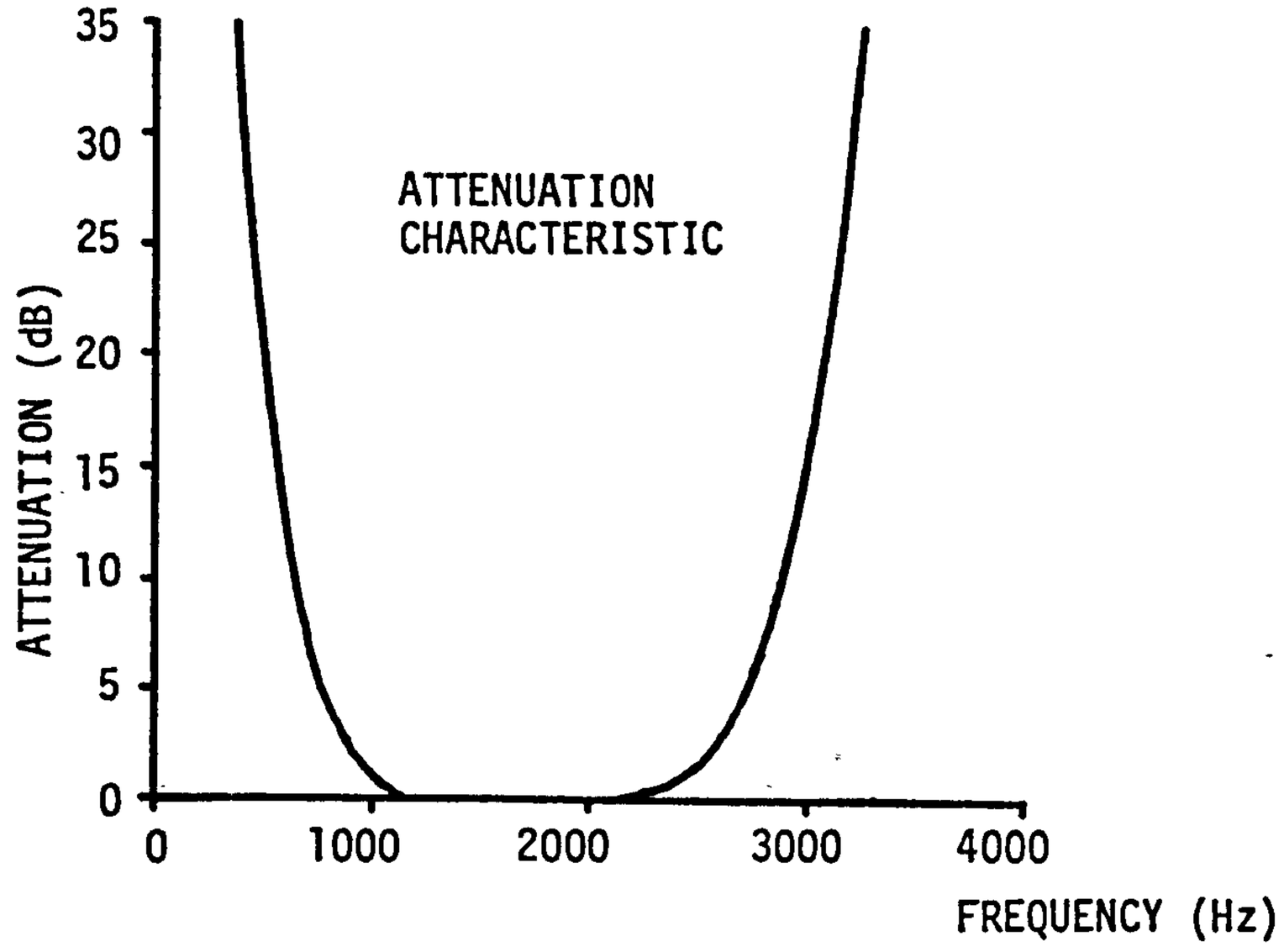

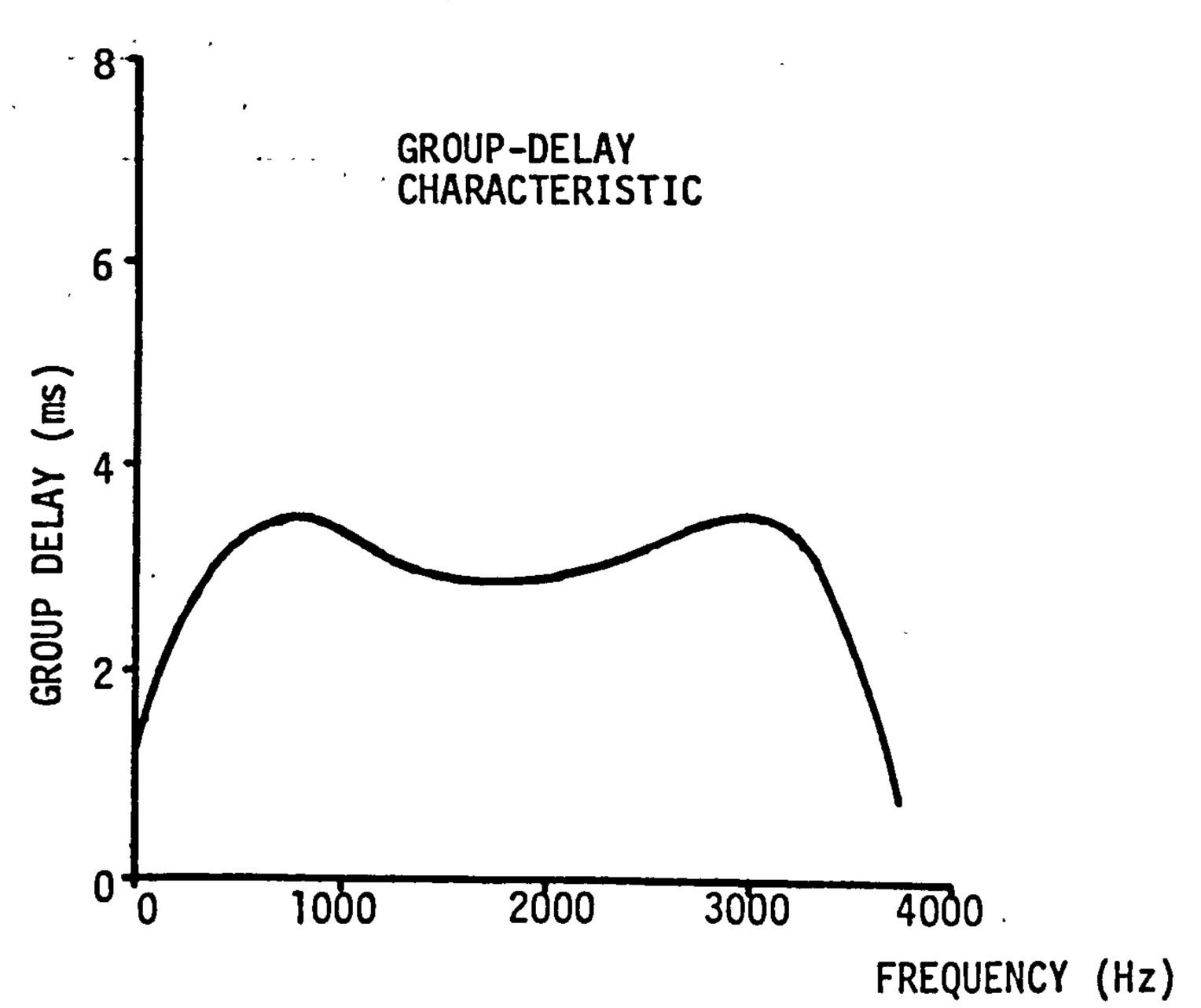

FIGURE 4.5.4: CHARACTERISTICS OF THE TRANSMITTER AND RECEIVER FILTERS IN CASCADE

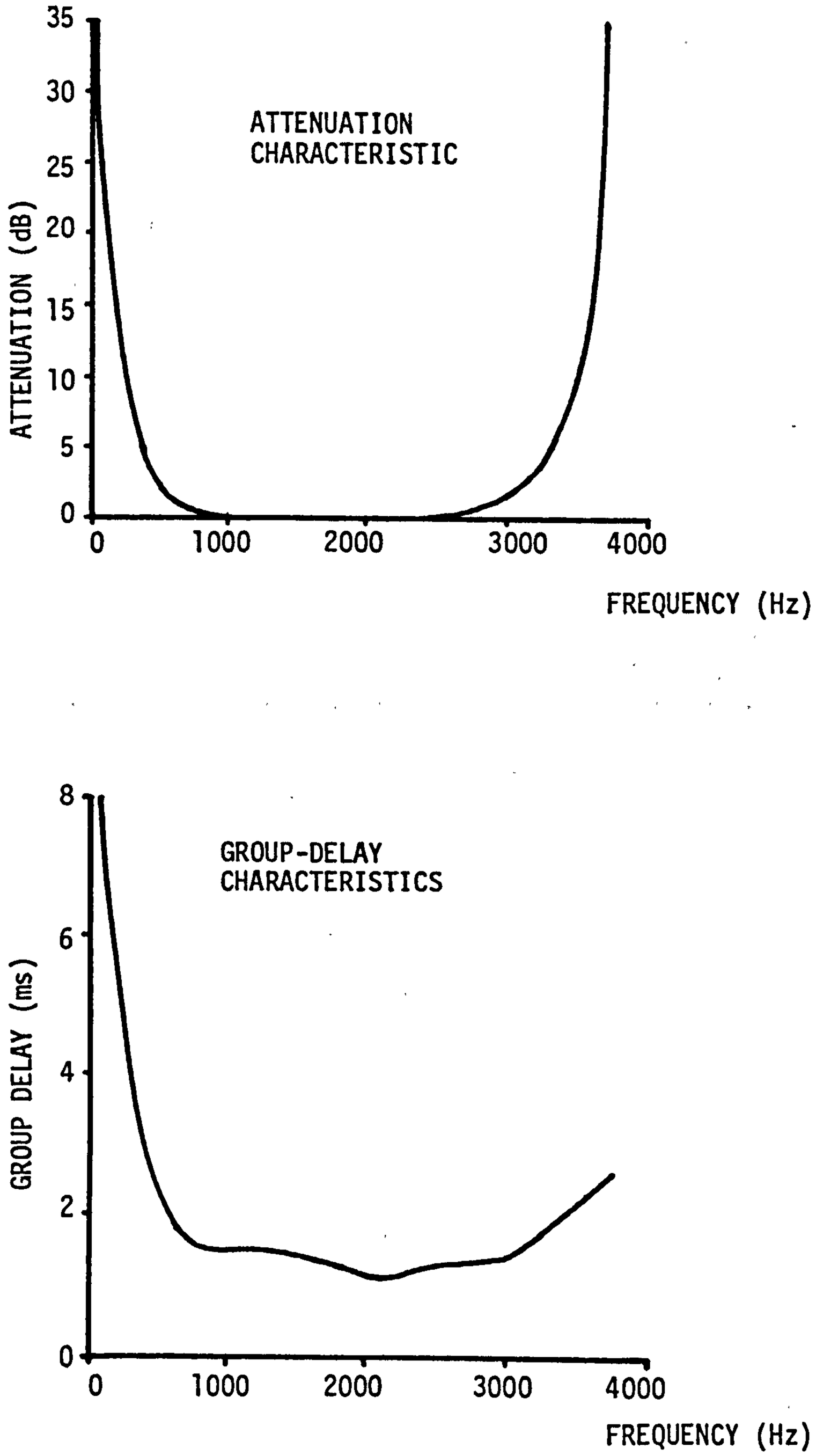

FIGURE 4.5.5: CHARACTERISTICS OF THE CLANSMAN VRC 321 RADIO FILTERS

$$R_w(\tau') = N_o \int_{-f_c}^{f_c} |C(f+f_c)|^2 |B'(f)|^2 \, e^{j2\pi f\tau'} \, df \qquad (4.5.26)$$

It has been shown[16] that when $R_w(\tau')$ is real, the real and imaginary part of w(t) are uncorrelated, and this is achieved when C(f) is symmetric about f_c. The variance of w(t) is, of course, given by,

$$R_w(0) = N_o \int_{-f_c}^{f_c} |C(f+f_c)|^2 |B'(f)|^2 df \qquad (4.5.27)$$

The average transmitted energy per signal-element at the output of the transmitter filter in Figure 4.5.2 is given by,

$$E_t = E\left[\int_{-\infty}^{\infty} |s_i a(t-iT)|^2 \, dt\right] \qquad (4.5.28)$$

where E[·] is the expected value of [·]. If we denote

$$\overline{s_i^2} = E[|s_i|^2] \qquad (4.5.29)$$

then using Parseval's theorem[101], equation 4.5.28 becomes,

$$E_t = \overline{s_i^2} \int_{-\infty}^{\infty} |A(f)|^2 \, df \qquad (4.5.30)$$

The average energy per signal-element at the input of the receiver filter in Figure 4.5.2 is given by,

$$E_r = E[\int_{-\infty}^{\infty} |s_i\{a(t-iT)(q_1(t) - jq_2(t)) +$$

$$+ a(t-\tau-iT)\ (q_3(t) - jq_4(t))\}|^2\ dt$$

$$= \overline{s_i^2}\ (\overline{q_1^2(t)} + \overline{q_2^2(t)} + \overline{q_3^2(t)} + \overline{q_4^2(t)}) \int_{-\infty}^{\infty} |A(f)|^2 df$$

(4.5.31)

where $\overline{q_1^2(t)}$, $\overline{q_2^2(t)}$, $\overline{q_3^2(t)}$ and $\overline{q_4^2(t)}$ are the variances of $q_1(t)$, $q_2(t)$, $q_3(t)$ and $q_4(t)$, respectively. Clearly, when these four variances are equal and their sums equal 1, the energy E_r is the same as E_t. This means that the sky waves do not introduce, on average, any gain or attenuation into the transmitted data signal, which greatly simplifies the calculation of the signal-to-noise ratio in the computer simulation tests.

5. HF CHANNEL ESTIMATORS

5.1 INTRODUCTION

In a study on channel estimators, Clark et al[26] have suggested that where the channel varies in a particularly unpredictable manner or where the receiver has only a limited knowledge of the correct model of the channel, a linear feedforward transversal-filter estimator (Section 3.5) is likely to form the basis of the most cost-effective estimator (see Section 3). However, with the feedforward transversal-filter estimator, the present estimate of the channel is simply derived from the immediate past estimate (equation 3.5.3). Clearly, when the characteristics of the channel vary rapidly, which is possible on HF radio links, a considerable advantage may be gained by first making a prediction of the sampled impulse-response, and then using the prediction in the estimation process[89]. The resulting arrangement has been shown to give an acceptable performance when used in a synchronous serial HF radio data-transmission system which transmits 4-level QAM signal at 2400 bit/s[89,96,97]. Unfortunately, at a data rate of 9600 bit/s, the number of components in the sampled impulse-response is almost doubled and the estimator no longer works satisfactorily[95]. However, by incorporating some prior knowledge of the basic structure of the channel, an acceptable estimate of the channel response is now possible[95]. This arrangement is known as the improved channel estimator.

In Section 5.2, various arrangements of prediction for the possible use with the feedforward transversal-filter estimator are described. In the following section (Section 5.3), a brief outline of the improved channel estimator is given. Finally, the performances of the estimators are summarized in Section 5.4.

5.2 FEEDFORWARD TRANSVERSAL-FILTER ESTIMATOR AS AN HF CHANNEL ESTIMATOR

The method of steepest descent (gradient algorithm) used to obtain an estimate of Y_i is given in Section 3.5 by equation 3.5.3. The quantities involved in equation 3.5.3 are all real, whereas here, the input and output signals as well as the channel response are complex-valued quantities, and so equation 3.5.3 is modified to[89], (in vector form),

$$Y_i' = Y_{i-1}' + c\, e_i\, S_i^* \qquad (5.2.1)$$

where, as usual, c is a small positive quantity which influences the rate of convergence of the estimator; e_i is the error in the estimate of the i^{th} received signal r_i, so that

$$e_i = r_i - \sum_{h=0}^{g} s_{i-h}'\, y_{i-1,h}' \qquad (5.2.2)$$

and S_i^* is a (g+1)-component vector given by,

$$S_i^* = [(s_i')^*\ (s_{i-1}')^* \ldots (s_{i-g}')^*]^T \qquad (5.2.3)$$

When a prediction of Y_i is available, the estimator uses this instead of Y'_{i-1} to give the estimate Y'_i in equation 5.2.1. Thus, at time t=(i-1)T, a prediction is made of Y_i and the prediction is designated $Y'_{i,i-1}$. The estimator uses $Y'_{i,i-1}$ to form the new estimate r'_i of r_i, so that

$$r'_i = \sum_{h=0}^{g} s'_{i-h}\, y'_{i,i-1,h} \qquad (5.2.4)$$

The estimate Y'_i of Y_i is now given by,

$$Y'_i = Y'_{i,i-1} + c\, e_i\, S^*_i \qquad (5.2.5)$$

where e_i is no longer given by equation 5.2.2, but becomes,

$$e_i = r_i - \sum_{h=0}^{g} s'_{i-h}\, y'_{i,i-1,h} \qquad (5.2.6)$$

where $y'_{i,i-1,h}$ is the $(h+1)^{th}$ component of $Y'_{i,i-1}$. (The detailed implementation of equation 5.2.5 is given in Section 6.4.)

The HF channel estimator is designed for use with a maximum-likelihood detector (Section 2.3). Inherent with this type of detector is a delay of n-1 sampling intervals before the detection of a data symbol, such that s_i is detected after the reception of r_{i+n-1}. Thus, the received samples r_i, r_{i+1}, ..., r_{i+n-1} must be stored in a shift register and fed at the appropriate time to the channel estimator for the generation of the corresponding error signals e_i, e_{i+1}, ..., e_{i+n-1}. Therefore, at time t=(i+n-1)T, the inputs to the

channel estimator are s_i' and r_i to give Y_i' at the output. The estimate Y_i' is then used by the detector on the receipt of r_{i+n} for the detection of s_{i+1}. Thus, the effective delay in estimation is n sampling intervals. Ideally, the detector must use the estimate Y_{i+n}' of Y_{i+n} in the detection of s_{i+1}. This is the case when n is large or when there are rapid variations in the channel impulse-response. However, Y_{i+n}' is not available yet, which means that it has to be predicted. The n-step prediction $Y_{i+n,i}'$ is derived from the estimates Y_i' , Y_{i-1}', ... Various methods of forming the predictions $Y_{i+1,i}'$ and $Y_{i+n,i}'$ have been studied in Ref. 89 and these will be reviewed next.

To summarize, we have seen that when there is a delay in detection of n-1 sampling intervals, the delay in estimation is n sampling intervals. Also, on the receipt of r_{i+n} and after Y_i' has been formed, two predictions $Y_{i+1,i}'$ of Y_{i+1} and $Y_{i+n,i}'$ of Y_{i+n} are required. The first of these is for use in the estimator for the evaluation of the next estimate Y_{i+1}' of Y_{i+1}. The second prediction $Y_{i+n,i}'$ is used by the detector in place of Y_i' for the detection of s_{i+1}.

5.2.1 Fixed-Memory Prediction[89]

At any time t=iT, the m+2 most recent estimates of the sampled impulse-response of the channel are

$$Y_i' , Y_{i-1}', \ldots, Y_{i-m-1}'$$

and based on some or all of these estimates, the predictor makes two predictions $Y'_{i+1,i}$ of Y_{i+1} and $Y'_{i+n,i}$ of Y_{i+n}, where n is the delay in estimation. The fixed-memory predictor assumes that these estimates are reasonably accurate and that they meet a certain condition. For example, when $Y'_{i-h} - Y'_{i-h-1}$ is a constant for $h = 0,1,\ldots, m-1$, then it is likely that

$$Y'_{i+1} - Y'_i = Y'_i - Y'_{i-1} \tag{5.2.7}$$

which gives,

$$Y'_{i+1} = Y'_i + (Y'_i - Y'_{i-1}) \tag{5.2.8}$$

Clearly, good predictions of Y_{i+1} and Y_{i+n} from the estimates $Y'_i, Y'_{i-1}, \ldots, Y'_{i-m}$ are now given by,

$$Y'_{i+1,i} = Y'_i + \Delta_{1,i} \tag{5.2.9}$$

and

$$Y'_{i+n,i} = Y'_i + n\,\Delta_{1,i} \tag{5.2.10}$$

where

$$\Delta_{1,i} = \frac{1}{m}(Y'_i - Y'_{i-m}) \tag{5.2.11}$$

Equations 5.2.9 and 5.2.10 represent arrangements of degree-1 fixed-memory prediction.

If, however, $((Y'_{i-h} - Y'_{i-h-1}) - (Y'_{i-h-1} - Y'_{i-h-2}))$ is a constant for $h = 0, 1, \ldots, m-1$, then it is likely that

$$(Y'_{i+1} - Y'_i) - (Y'_i - Y'_{i-1}) = (Y'_i - Y'_{i-1}) - (Y'_{i-1} - Y'_{i-2}) \tag{5.2.12}$$

which gives,

$$Y'_{i+1} = Y'_i + (Y'_i - Y'_{i-1}) + ((Y'_i - Y'_{i-1}) - (Y'_{i-1} - Y'_{i-2})) \tag{5.2.13}$$

Then, good predictions of Y_{i+1} and Y_{i+n} from the estimates Y'_i , Y'_{i-1}, ..., Y'_{i-m-1} can be shown to be given by[89],

$$Y'_{i+1,i} = Y'_i + \Delta_{1,i} + a\Delta_{2,i}$$

$$= Y'_i + (a+1)\,\Delta_{1,i} - a\Delta_{1,i-1} \tag{5.2.14}$$

and $$Y'_{i+n,i} = Y'_i + n\Delta_{1,i} + n\,(a + \tfrac{1}{2}(n-1))\Delta_{2,i}$$

$$= Y'_i + n(a+1 + \tfrac{1}{2}(n-1))\,\Delta_{1,i} - n(a + \tfrac{1}{2}(n-1))\Delta_{1,i-1} \tag{5.2.15}$$

where a is given by[97],

$$a = \tfrac{1}{2}(m+1) \tag{5.2.16}$$

and $$\Delta_{2,i} = \frac{1}{m}((Y'_i - Y'_{i-1}) - (Y'_{i-m} - Y'_{i-m-1})) \tag{5.2.17}$$

Equations 5.2.14 and 5.2.15 represent arrangements of degree-2 fixed-memory prediction.

On the other hand, if Y'_i , Y'_{i-1}, ... are all approximately equal, a good prediction of Y_{i+1} and Y_{i+n} from these estimates are simply given by,

$$Y'_{i+1,i} = Y'_i \tag{5.2.18}$$

and

$$Y'_{i+n,i} = Y'_i \tag{5.2.19}$$

respectively. Equations 5.2.18 and 5.2.19 represent arrangements of degree-0 fixed-memory prediction, and as such represent the absence of any prediction.

5.2.2 Simple Fading-Memory Prediction[89]

With simple degree-2 fixed-memory prediction, only the m+2 estimates Y'_i , Y'_{i-1}, ..., Y'_{i-m-1} are used in forming the predictions $Y'_{i+1,i}$ and $Y'_{i+n,i}$, the rest being totally ignored. Each of these estimates is given equal emphasis or weight. However, in practice, the reliability of an estimate for use in the prediction process is likely to decrease with its age, and so a better prediction scheme is one where no estimates are totally ignored but the older estimates are progressively given less weight.

The arrangements for degree-1 simple fading-memory prediction is given by[89],

$$Y'_{i+1,i} = Y'_i + \Delta_{1,i} \tag{5.2.20}$$

and $$Y'_{i+n,i} = Y'_i + n\,\Delta_{1,i} \qquad (5.2.21)$$

and for degree-2 prediction, they are given by[89],

$$Y'_{i+1,i} = Y'_i + \Delta_{1,i} + \frac{1}{b}\Delta_{2,i} \qquad (5.2.22)$$

and $$Y'_{i+n,i} = Y'_i + n\Delta_{1,i} + n(\frac{1}{b} + \frac{1}{2}(n-1)\Delta_{2,i} \qquad (5.2.23)$$

where b is a small positive real constant, and $\Delta_{1,i}$ and $\Delta_{2,i}$ are now given by[89],

$$\Delta_{1,i} = (1-b)\Delta_{1,i-1} + b(Y'_i - Y'_{i-1})$$

$$= \Delta_{1,i-1} + b(Y'_i - Y'_{i-1} - \Delta_{1,i-1}) \qquad (5.2.24)$$

and $$\Delta_{2,i} = (1-b)\Delta_{2,i-1} + b(Y'_i - 2Y'_{i-1} + Y'_{i-2})$$

$$= \Delta_{2,i-1} + b(Y'_i - 2Y'_{i-1} + Y'_{i-2} - \Delta_{2,i-1}) \qquad (5.2.25)$$

from which it can be shown that[89],

$$\Delta_{2,i} = \Delta_{1,i} - \Delta_{1,i-1} \qquad (5.2.26)$$

The initial values of the various quantities in equations 5.2.24 and 5.2.25 are assumed to be,

$$Y'_0 = Y'_{-1} = Y'_{-2} \simeq Y_0 \qquad (5.2.27)$$

and

$$\Delta_{1,0} = \Delta_{1,-1} = 0 \qquad (5.2.28)$$

The parameter b determines the number of estimates Y'_i , Y'_{i-1},... which are used in the prediction process. A small value of b means that more estimates are effectively involved in forming a prediction.

5.2.3 Least-Squares Fading-Memory Prediction[89]

Here, a set of g+1 polynomials of given degree (0, 1 or 2) are determined, and each gives the weighted least-squares fit to the components in the corresponding location in the vectors Y'_i , Y'_{i-1}, ... The predictions $Y'_{i+1,i}$ and $Y'_{i+n,i}$ are the values of the polynomials at times t = (i+1)T and t = (i+n)T, respectively. The arrangements of degree-0, 1 and 2 least-squares fading-memory predictions are given by,

Degree-0:

$$Y'_{i+1,i} = Y'_{i,i-1} + (1-\theta)E_i \qquad (5.2.29)$$

$$Y'_{i+n,i} = Y'_{i+1,i} \qquad (5.2.30)$$

Degree-1:

$$(Y'_{i+1,i})' = (Y'_{i,i-1})' + (1-\theta)^2 E_i \qquad (5.2.31)$$

$$Y'_{i+1,i} = Y'_{i,i-1} + (Y'_{i+1,i})' + (1-\theta^2)E_i \qquad (5.2.32)$$

$$Y'_{i+n,i} = Y'_{i+1,i} + (n-1)(Y'_{i+1,i})' \qquad (5.2.33)$$

Degree-2:

$$(Y'_{i+1,i})'' = (Y'_{i,i-1})'' + \frac{1}{2}(1-\theta)^3 E_i \qquad (5.2.34)$$

$$(Y'_{i+1,i})' = (Y'_{i,i-1})' + 2(Y'_{i+1,i})'' + \frac{3}{2}(1-\theta)^2(1+\theta)E_i \qquad (5.2.35)$$

$$Y'_{i+1,i} = Y'_{i,i-1} + (Y'_{i+1,i})' - (Y'_{i+1,i})'' + (1-\theta^3)E_i \qquad (5.2.36)$$

$$Y'_{i+n,i} = Y'_{i+1,i} + (n-1)(Y'_{i+1,i})' + (n-1)^2(Y'_{i+1,i})'' \qquad (5.2.37)$$

where E_i is given by,

$$E_i = Y'_i - Y'_{i,i-1} \qquad (5.2.38)$$

The quantities $(Y'_{i+1,i})'$ and $(Y'_{i+1,i})''$ are, respectively, functions of the first and second differentials of $Y'_{i+1,i}$ with respect to time. Since they appear essentially as dummy variables in the algorithm, their only function being to assist in determining the required prediction, it is not necessary to consider them in further detail. The initial values of the various quantities in the above arrangements are,

$$Y'_{1,0} = Y'_0 \simeq Y_0 \qquad (5.2.39)$$

$$(Y'_{1,0})' = 0 \qquad (5.2.40)$$

$$(Y'_{l,o})'' = 0 \qquad (5.2.41)$$

The parameter θ is a real constant in the range 0 to 1. By increasing the value of θ towards 1, the weight factor that is used when fitting the polynomials decreases more slowly with age and so more estimates are effectively involved in the prediction process.

5.3 IMPROVED CHANNEL ESTIMATOR

This estimator is the subject of the whole of Section 7 and so it is sufficient here to outline it briefly.

The improved channel estimator is basically a feedforward transversal-filter estimator which employs the least-squares fading-memory prediction. The latter has been shown to be the most effective arrangement of prediction[89]. However, the predictor is greatly reduced in complexity because, instead of involving a separate prediction process for each of the g+1 components of Y_i, only some two or three prediction processes are employed. The simplification is possible because the estimator assumes that the basic structure of the HF channel is of a certain form. Specifically, it assumes that the sampled impulse-response of a two-sky-wave channel is represented by,

$$Y_i = \lambda_i L + \mu_i M \qquad (5.3.1)$$

where L and M are fixed (g+1)-component vectors, and λ_i and μ_i are the time-variable scalar quantities. The vectors L and M span a two-dimensional subspace of the (g+1)-component unitary vector space that contains Y_i. If L and M can be determined, the estimation of Y_i simplifies to only the estimation of the two random variables λ and μ. However, L and M are difficult to determine and instead, the estimator determines (estimates) two orthonormal vectors A and B which also span the subspace, such that Y_i is also given by,

$$Y_i = a_i A + b_i B \tag{5.3.2}$$

The estimation of A and B is implemented adaptively according to an algorithm very similar to the well known gradient algorithm. Therefore, the predictions that are involved in the formation of $Y'_{i+1,i}$ and $Y'_{i+n,i}$ are merely the predictions of the scalar variables a_i and b_i (see Section 7).

5.4 PERFORMANCE OF ESTIMATORS

The results of computer simulation tests on the above estimators have been presented by Clark and McVerry in Refs. 89 and 95. Here, we will summarize only their main conclusions.

At a high signal-to-noise ratio of 60 dB, the estimator in Section 5.2 with the best performance is that which employs degree-2 least-squares fading-memory prediction. However, over the range of signal-to-noise ratios from 10 to 30 dB, the three degree-1 predictors

are the best, with the degree-1 fixed-memory predictor marginally better than the other two, and these are closely followed by the degree-2 least-squares fading-memory predictor. The degree-1 fixed-memory predictor requires a smaller number of computations per cycle than the other two degree-1 predictors. However, it has the disadvantage of requiring a substantial amount of storage to hold the $\{Y_i'\}$, because the optimum value of m is typically around 100. Therefore, the most promising of the predictors appears to be the degree-1 least-squares fading-memory predictor. In Ref. 95, it is shown that the performance of the feedforward transversal-filter estimator using degree-1 least-squares fading-memory prediction is improved considerably with the help of additional information on the basic structure of the HF channel. This is described in Section 7.

6. HF CHANNEL ESTIMATORS BASED ON THE KALMAN FILTER

6.1 INTRODUCTION

The radio frequency band in the region of 3 to 30 MHz is traditionally known as the high-frequency (HF) band[66]. At these frequencies, propagation of the radio signal is achieved by ionospheric reflection (refraction) from one or more layers of the ionosphere[63-73]. Ionospheric radio propagation is characterised by fading and multipath propagation, that is, the radio signal is normally received via several different paths, and the signal on each path is subjected to random fluctuations both in amplitude and phase, which results in the frequency selective fading of the received signal. The random variations are caused by the continuously changing physical characteristics of the ionosphere, which means that the impulse response of the HF channel is time-varying.

The fading and dispersive nature of the HF channel has meant that high-speed data transmission over this medium, comparable to that which can be achieved over the telephone network, remains impossible. However, a speed of 2400 bit/s has been achieved satisfactorily with both serial and parallel modems[96,110,111]. Comparative tests of the two systems[96,110] have suggested that, under most conditions, the performance of the serial modem is likely to be better than that of the parallel modem. The serial modem may employ QAM as the signal modulation format and a detector of the maximum-likelihood type[96]. The difficulty with the design of such a system

is in the extraction of the sampled impulse-response of the channel, a knowledge of which is required by the maximum-likelihood detector in the detection of the data signal.

A comparison of several channel estimators[26], for the application involving a constant or a completely random channel, has suggested that the feedforward transversal-filter estimator is likely to be the most cost-effective estimator. A major drawback with this estimator is however its slow rate of convergence. On the other hand, the least-squares (Kalman) estimator has far superior convergence, especially when the estimator has no prior knowledge of the channel. In fact, when the Kalman estimator is correctly optimized, it has the best possible performance[26,114]. With the feedforward estimator, it has been shown that the inclusion of a suitable predictor improves its performance considerably[89,96]. The prediction of the sampled impulse-response is here derived from past estimates of the channel[89]. The estimator, in turn, uses the appropriate prediction of the channel when forming the required updated estimate.

Unfortunately, the Kalman estimator has a major disadvantage which is the excessive number of operations required when there are many components in the sampled impulse-response of the channel. It is possible to reduce these by using the 'fast' Kalman algorithm[128]. The improvements obtained by using a predictor with the feedforward estimator suggest that it may also be possible to achieve similar results by making the corresponding modifications to the Kalman estimator. In order to assess the cost effectiveness of the modified

Kalman estimator, its performance will have to be compared with the corresponding feedforward estimator which is still the simpler arrangement of the two.

The latest modification to the feedforward estimator is the arrangement known as the improved channel estimator[95]. This is an arrangement which consists of the feedforward estimator and a predictor, and utilizes a knowledge of the basic structure of the HF channel, giving a considerable improvement in performance over the arrangement which has no such knowledge. The Kalman filter, with its well known superior convergence and tracking capabilities, is potentially a better estimator if it can be modified in a similar manner to the feedforward estimator.

In this section, both the feedforward estimator (Section 6.4) and the Kalman estimator (Section 6.3) are described. An arrangement of prediction which is of the least-squares fading-memory type, is described next in Section 6.5. In Section 6.6, the performances of the conventional Kalman estimator and various modifications are presented, and these are then compared with the corresponding versions of the feedforward estimator. The estimators are tested on a model of an HF radio link with two Rayleigh fading sky waves, the model being part of a simulated data-transmission system which uses a 16-level QAM signal transmitted at a rate of 9600 bit/s.

6.2 BASIC ASSUMPTIONS

The model of the data-transmission system that is used in the tests is shown in Figure 6.2.1. It is a synchronous serial system involving a model of an HF radio link as the transmission path. The transmission of QAM signals over a model of such a system has been described in Section 4.5.

The input data signal is assumed to be a sequence of data symbols $\{s_i\}$ which are statistically independent and equally likely to have any one of their 16 possible values. The i^{th} data symbol is here given by,

$$s_i = s_{r,i} + js_{q,i} \qquad (6.2.1)$$

where $j = \sqrt{-1}$, $s_{r,i} = \pm 1$ or ± 3, and $s_{q,i} = \pm 1$ or ± 3. The baseband signal generator and linear modulator converts the $\{s_i\}$ into a stream of 16-level QAM signal-elements with an 1800 Hz carrier and an element rate of 2400 bauds. Each signal-element is, in fact, the sum of two quaternary double-sideband suppressed carrier amplitude modulated elements with their carriers in phase quadrature, the values of the 'in-phase' and 'quadrature' components being determined, respectively, by the real and imaginary parts of the corresponding data-symbol s_i (equation 6.2.1). The average transmitted energy per bit of information is arranged to be unity.

The HF radio link uses linear modulation to shift the spectrum of the input data signal from the voice band to the HF band, the bandwidth

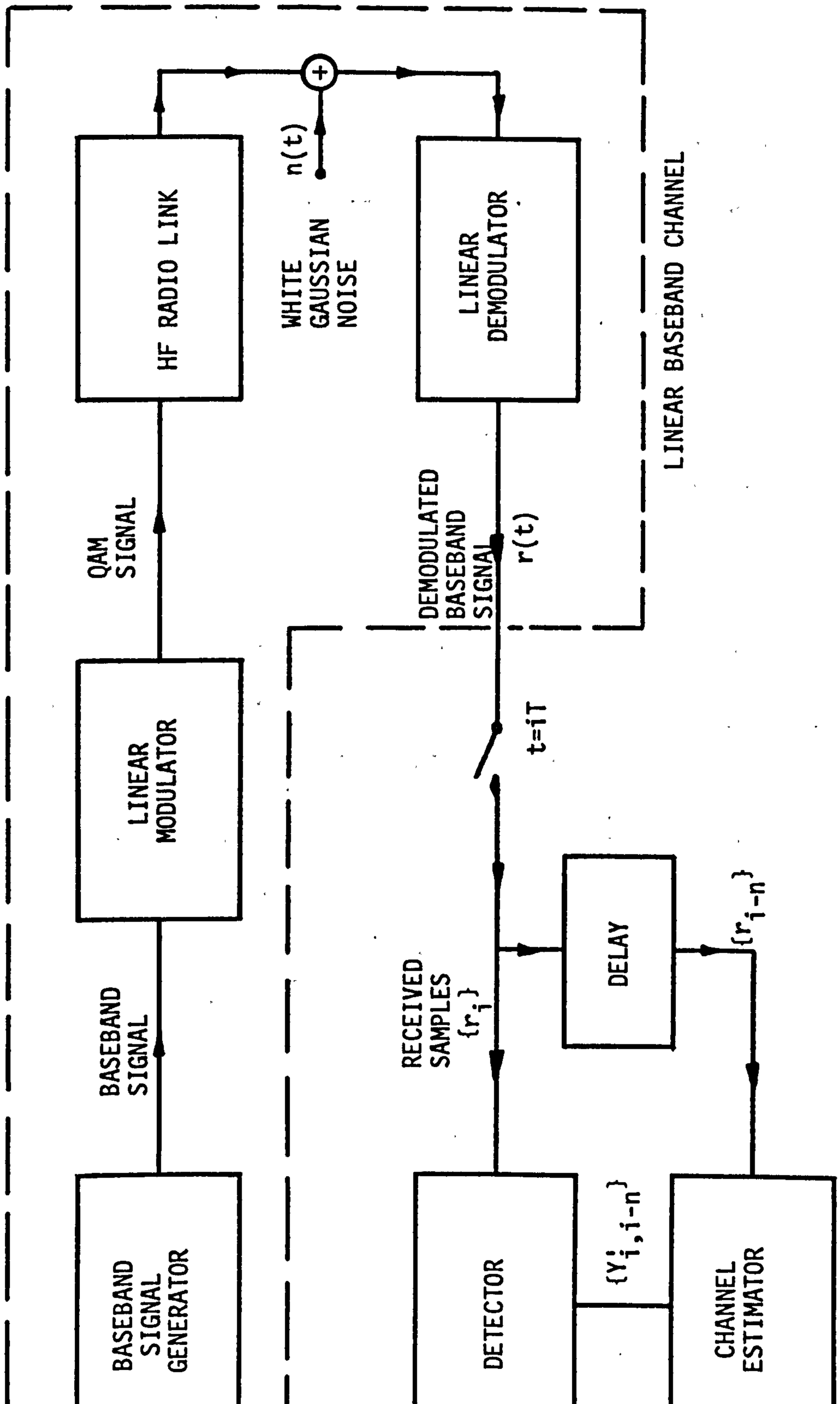

FIGURE 6.2.1: MODEL OF DATA-TRANSMISSION SYSTEM

of the signal being some 2400 Hz. The resulting HF radio signal is transmitted via two independent Rayleigh fading sky waves (Figure 4.4.6). The waveforms $q_h(t)$ for h = 1,2,3 or 4 (Figure 4.4.6) are real-valued narrow-band Gaussian noise waveforms whose spectral shaping is approximately Gaussian (Section 4.4). They are statistically independent with zero mean, the same variance and the same root-mean-square bandwidth of $\frac{1}{2}$ Hz. Therefore, the signal received over each sky wave has the same mean-square value and the same frequency spread of 1 Hz. The relative delay in transmission between the two sky waves is 2 ms. At the radio receiving equipment, the spectrum of the received signal is shifted back to the voice-band by a process of linear coherent demodulation.

The various types of additive noise that are normally introduced by an HF radio channel are neglected. It is assumed that the only noise is stationary white Gaussian noise with zero mean and a two-sided power spectral density of $\frac{1}{2}N_0$. The noise is added to the data signal at the output of the HF radio link.

The linear demodulator in the model of the system uses linear coherent demodulation to recover the complex-valued baseband modulating waveform from the received QAM signal . It includes at its input a bandpass filter which removes as much as possible the noise outside the frequency band of the data signal without excessively distorting it. The two reference carriers used for demodulation are adaptively adjusted so that they are of the same average instantaneous frequency as the carrier of the received signal, thus eliminating any constant frequency offset in the received signal. The phases of the

reference carriers are not kept to any given relationship with the phase of the received signal, so that the whole of the time-varying distortion introduced by the HF radio link appears in the demodulated waveform. The values of the demodulated signals from the 'in-phase' and 'quadrature' channels are, respectively, taken as the real and imaginary values of the demodulated baseband signal r(t).

The signal r(t) is sampled, once per received signal-element, to give the sequence of complex-valued samples $\{r_i\}$, the i^{th} of which is given by,

$$r_i = \sum_{h=0}^{g} s_{i-h}\, y_{i,h} + w_i \qquad (6.2.2)$$

For practical purposes, it is assumed that $y_{i,h} = 0$ for $h<0$ and $h>g$, so that the sampled impulse-response of the linear baseband channel in Figure 6.2.1, at time $t=iT$, is given by the $(g+1)$-component column vector

$$Y_i = [y_{i,o}\ y_{i,1} \cdots y_{i,g}]^T \qquad (6.2.3)$$

Y_i is obtained by sampling the impulse responses $\{y_i(t-iT)\}$ where $y_i(t-iT)$ is given by equation 4.5.25 as,

$$y_i(t-iT) = \{a(t-iT)[q_1(t) - jq_2(t)] + a(t-\tau-iT)\,[q_3(t) - jq_4(t)]\} * b(t) \qquad (6.2.4)$$

at a rate of 2400 samples/second ($T = \frac{1}{2400}$ seconds). It is important to observe from equation 6.2.2 that Y_i is not here given by the successive samples of the impulse response, but rather by the g+1 components of successive impulse responses that are coincident at time t=iT. This definition of the sampled impulse-response is used for two reasons. Firstly, it is the definition of the sampled impulse-response employed by a maximum likelihood detector, and secondly, over practical time-varying channels, the delay in transmission of the first nonzero component of the sampled impulse-response of the channel is not necessarily known or well defined, leading to possible confusion as to the precise meaning of the sampled impulse-response at time t=iT. The adopted definition, on the other hand, gives a precise and unique definition of the sampled impulse-response, since it requires no knowledge of the delay in transmission.

In order to avoid any aliasing that is likely to occur when any of the $q_h(t)$ is changing rapidly, the convolution as indicated by equation 6.2.4 is carried out at a sampling rate of 4800 samples/second, which is well above the Nyquist rate for the transmitter and receiver filters (see Figures 4.5.3 and 4.5.4). Therefore, each of the sequences $\{q_{h,i}\}$ for h = 1, 2, 3 or 4 is, in fact, given by the values of the corresponding waveform $q_h(t)$ sampled at 4800 samples/second. The multipath propagation delay τ is expressed as a whole number of sampling periods ρ plus a sampling phase $\rho'(< \frac{T}{2})$, i.e.

$$\tau = \rho\frac{T}{2} + \rho' \qquad (6.2.5)$$

For example, with a delay of 2 ms, the relevant values are

$$\left.\begin{aligned} \rho &= 9 \\ \rho' &= 0.6/4800 \end{aligned}\right\} \qquad (6.2.6)$$

The time delay introduced in transmission over each sky wave is taken to be fixed over the duration of the data signal and the timing waveform at the receiver that determines the sampling instants {iT} is taken to have a constant phase relationship with the received stream of signal elements.

The detector in Figure 6.2.1 is a near-maximum-likelihood detector which operates directly on the received samples $\{r_i\}$ without using any adaptive linear prefilter[1]. The delay in detection is n-1 sampling intervals, so that the detected data-symbol s'_{i+1} is determined following the reception of r_{i+n}, at time t=(i+n)T. However, we are concerned with the operation of the channel estimator and not the detector, so that it is assumed that $s'_i = s_i$ for all {i}, even at low signal-to-noise ratios. The performance of the channel estimator is only seriously affected by errors in the $\{s'_i\}$ at the higher error rates[95].

From equation 6.2.2, it is evident that the updated estimate Y'_i of Y_i can only be determined when r_i and s'_i are available at the inputs of the channel estimator. Since the delay in detection is n-1 sampling intervals, s'_i is fed to the channel estimator after a delay of n sampling intervals and so the sequence of received

samples $\{r_i\}$ that is also fed to the channel estimator must be delayed by n sampling intervals.

In practice, Y_i may be more conveniently estimated after the detection of s_i and before the receipt of r_{i+n}, rather than immediately after the receipt of r_{i+n} and before the detection of s_{i+1}. For the sake of clarity, we will assume the latter arrangement in the analysis. Since the sampled impulse-response of the linear baseband channel is time-varying, the error in using Y_i' in the detection of s_{i+1} may be excessive. Ideally, the detector uses Y_{i+n}' in the detection of s_{i+1}, but since this estimate is not available, the estimator forms a prediction $Y_{i+n,i}'$ of Y_{i+n} from the estimates Y_i', Y_{i-1}', ... Various techniques of forming the prediction have been discussed previously in Section 5. In this section, we will use the degree-1 least-squares fading-memory predictor which is described in Section 6.5.

6.3 DERIVATION OF KALMAN FILTER ESTIMATOR

Since the appearance of the classical paper by Kalman[29], the discrete Kalman filter has been derived in many ways[34,44,51,114]. The original derivation by Kalman uses the concept of orthogonal projections[114] which we will now follow.

Consider a time-varying channel which is described by the linear vector difference equation,

$$Y_{i+1} = \Phi_{i+1,i}\, Y_i + \Gamma_i V_i \qquad (6.3.1)$$

where,

$$Y_i = [y_{i,o}\ y_{i,1} \cdots y_{i,g}]^T \qquad (6.3.2)$$

is the sampled impulse-response of the linear baseband channel (Figure 6.2.1) at time t=iT,

$\Phi_{i+1,i}$ is the (g+1)x(g+1) transition matrix,

Γ_i is the (g+1)x(g+1) weight matrix,

$$V_i = [v_{i,o}\ v_{i,1} \cdots v_{i,g}]^T \qquad (6.3.3)$$

whose components are statistically independent random variables.

The measurement model is given by the linear algebraic equation,

$$r_i = \sum_{h=0}^{g} s_{i-h} y_{i,h} + w_i \qquad (6.3.4)$$

or

$$r_i = S_i^T Y_i + w_i \qquad (6.3.5)$$

or

$$r_i = Y_i^T S_i + w_i \qquad (6.3.6)$$

where,

$$S_i = [s_i\ s_{i-1} \cdots s_{i-g}]^T \qquad (6.3.7)$$

is a sequence of input data symbols,

w_i is a Gaussian random variable which represents the noise component in r_i.

All quantities in equations 6.3.1-6.3.7 are complex-valued. The superscript T used in the above description denotes transposition. It is assumed that the random variables in equations 6.3.1 and 6.3.6 have the following statistical properties,

$$
\left.
\begin{aligned}
E[V_i] &= 0 \\
E[w_i] &= 0 \\
E[V_i V_j^{*T}] &= Q_i \delta_{ij} \\
E[w_i w_j^{*}] &= \sigma^2 \\
E[V_i w_j^{*}] &= 0, \text{ for all } i,j
\end{aligned}
\right\} \qquad (6.3.8)
$$

where,

E is the expectation operator, so that $E[\cdot]$ is the expected value of $[\cdot]$,

$\delta_{i,j}$ is the Kronecker delta, such that,

$$
\delta_{i,j} = \begin{cases} 1 & i = j \\ 0 & i \neq j \end{cases} \qquad (6.3.9)
$$

* indicates the complex conjugate.

Equation 6.3.8 merely states that the random variable w_i has zero mean and variance σ^2. Also, the mean of V_i is a zero vector and its covariance matrix is Q_i. In addition, w_i and the components of V_i, which are $\{v_{i,h}\}$, are uncorrelated.

Based on the sequence of received samples,

$$
R_i = [r_1 \; r_2 \; \cdots \; r_i]^T \qquad (6.3.10)
$$

we wish to determine the optimum linear minimum-error-variance unbiased estimate of Y_i which will be denoted as $Y'_{i,i}$, or simply Y'_i. The error in this estimate is given by,

$$X_i = Y_i - Y'_i \tag{6.3.11}$$

Since the estimate is required to be unbiased, the estimation error X_i has zero mean and so $E[Y'_i] = E[Y_i]$[114]. Of the many possible linear unbiased estimators, we select here the one which gives the minimum error variance. The linear minimum variance estimate of Y_i given the vector R_i is then the conditional expectation of Y_i, given R_i[114,115,122], that is,

$$Y'_i = \hat{E}[Y_i|R_i] \tag{6.3.12}$$

The symbol $\hat{E}$ has been used instead of E because, in the general case, the linear minimum variance estimator is not the true conditional mean[114,115]. $\hat{E}[Y_i|R_i]$ will become $E[Y_i|R_i]$ if Y, V and w all have Gaussian distributions, but this is not necessary in the derivation, so that the resulting estimator may not be the best but only the best linear estimator[114].

Although we ultimately require the estimate Y'_i which is equal to $\hat{E}[Y_i|R_i]$, we shall first derive the 1-step prediction $Y'_{i+1,i}$ and later use it to find Y'_i. The 1-step prediction $Y'_{i+1,i}$ is defined as,

$$Y'_{i+1,i} = \hat{E}[Y_{i+1}|R_i] \tag{6.3.13}$$

and is the prediction of Y_{i+1} using data which are available up to time t=iT. Let us assume that, at time t=iT, $Y'_{i,i-1}$, which is the prediction of Y_i based on data up to time t=(i-1)T, is known. Using the newly arrived information r_i and $Y'_{i,i-1}$, we are required to compute $Y'_{i+1,i}$. In general, r_i is not statistically orthogonal to the components of R_{i-1}, but it is easily shown that the so-called 'innovation' process[51,114],

$$e_{i,i-1} = r_i - Y'^{T}_{i,i-1} S_i \tag{6.3.14}$$

is orthogonal to R_{i-1}[28,51,114,115], which means that

$$E[e_{i,i-1} R^{*T}_{i-1}] = 0 \tag{6.3.15}$$

Now, using equation 6.3.14, we may rewrite equation 6.3.13 as,

$$Y'_{i+1,i} = \hat{E}[Y_{i+1}|R_{i-1},r_i]$$

$$= \hat{E}[Y_{i+1}|R_{i-1},e_{i,i-1}] \tag{6.3.16}$$

since $r_i - e_{i,i-1}$ is contained in R_{i-1} and thus adds no 'new information' to the representation of $Y'_{i+1,i}$. $e_{i,i-1}$ is orthogonal to R_{i-1} (equation 6.3.15), and so we may use the linearity property of the minimum variance estimator and the orthogonal projection lemma[114] to rewrite equation 6.3.16 as,

$$Y'_{i+1,i} = \hat{E}[Y_{i+1}|R_{i-1}] + \hat{E}[Y_{i+1}|e_{i,i-1}] \qquad (6.3.17)$$

or

$$Y'_{i+1,i} = Y'_{i+1,i-1} + \hat{E}[Y_{i+1}|e_{i,i-1}] \qquad (6.3.18)$$

because $\hat{E}[Y_{i+1}|R_{i-1}]$ is, by definition, equal to $Y'_{i+1,i-1}$.

Thus, the predictor has taken the familiar predictor-corrector form. Equation 6.3.18 shows that the prediction $Y'_{i+1,i}$ is obtained by predicting Y_{i+1} using the received samples up to time t=(i-1)T, and then correcting the prediction with the new information $e_{i,i-1}$ in the current sample.

Let us examine the two terms on the right-hand side of equation 6.3.17. Substituting the value of Y_{i+1} from equation 6.3.1 into the first term gives,

$$\hat{E}[Y_{i+1}|R_{i-1}] = \hat{E}[(\Phi_{i+1,i}Y_i + \Gamma_i V_i)|R_{i-1}]$$

$$= \Phi_{i+1,i}\,\hat{E}[Y_i|R_{i-1}] + \Gamma_i\hat{E}[V_i|R_{i-1}] \qquad (6.3.19)$$

By definition,

$$\hat{E}[Y_i|R_{i-1}] = Y'_{i,i-1} \qquad (6.3.20)$$

Thus, equation 6.3.19 becomes,

$$\hat{E}[Y_{i+1}|R_{i-1}] = \Phi_{i+1,i}\, Y'_{i,i-1} + \Gamma_i \hat{E}[V_i|R_{i-1}] \qquad (6.3.21)$$

Now, it follows from equations 6.3.1 and 6.3.6 that R_{i-1} is dependent on V_j only for $j<i-1$, so that the expected value of V_i, given R_{i-1} is simply given by $E[V_i]$ which is a zero vector (equation 6.3.8). Therefore, equation 6.3.21 reduces to,

$$\hat{E}[Y_{i+1}|R_{i-1}] = \Phi_{i+1,i}\, Y'_{i,i-1} \qquad (6.3.22)$$

Next, we consider the term $\hat{E}[Y_{i+1}|e_{i,i-1}]$ on the right-hand side of equation 6.3.17. We quote here without proof the results obtained by Sage and Melsa[114] which show that, with the appropriate modifications for complex signals, the orthogonal projection theorem may be used to write $\hat{E}[Y_{i+1}|e_{i,i-1}]$ as,

$$\hat{E}[Y_{i+1}|e_{i,i-1}] = E[Y_{i+1}e^*_{i,i-1}]\{E[e_{i,i-1}e^*_{i,i-1}]\}^{-1}\, e_{i,i-1} \qquad (6.3.23)$$

Substituting the value of Y_{i+1} from equation 6.3.1 into the term $E[Y_{i+1}e^*_{i,i-1}]$ on the right-hand side of equation 6.3.23,

$$E[Y_{i+1}e^*_{i,i-1}] = E[(\Phi_{i+1,i}Y_i + \Gamma_i V_i)e^*_{i,i-1}] \qquad (6.3.24)$$

But, with r_i given by equation 6.3.6, $e_{i,i-1}$ in equation 6.3.14 may be written as,

$$e_{i,i-1} = Y_i^T S_i + w_i - Y_{i,i-1}'^T S_i$$

$$= (Y_i^T - Y_{i,i-1}'^T)S_i + w_i \qquad (6.3.25)$$

If we denote the error in the 1-step prediction of Y_i as,

$$X_{i,i-1} = Y_i - Y_{i,i-1}' \qquad (6.3.26)$$

then, equation 6.3.25 reduces to,

$$e_{i,i-1} = X_{i,i-1}^T S_i + w_i \qquad (6.3.27)$$

Substituting for $e_{i,i-1}$ in equation 6.3.24, we have

$$E[Y_{i+1}e_{i,i-1}^*] = E[(\Phi_{i+1,i}Y_i + \Gamma_i V_i)(X_{i,i-1}^{*T}S_i^* + w_i^*)]$$

$$= \Phi_{i+1,i}\, E[Y_i X_{i,i-1}^{*T}]S_i^* + \Phi_{i+1,i}\, E[Y_i w_i^*] +$$

$$+ \Gamma_i\, E[V_i X_{i,i-1}^{*T}]S_i^* +$$

$$+ \Gamma_i\, E[V_i w_i^*] \qquad (6.3.28)$$

Since Y_i depends only on Y_{i-1} and V_{i-1} (equation 6.3.1) and V_i and w_i are uncorrelated (equation 6.3.8), $E[Y_i w_i^*] = 0$. Also $E[V_i X_{i,i-1}^{*T}] = 0$ since $X_{i,i-1}$ is independent of V_i whose mean is a zero vector (Equations 6.3.26 and 6.3.1). Thus equation 6.3.28 reduces to,

$$E[Y_{i+1}e^{*}_{i,i-1}] = \Phi_{i+1,i}\, E[Y_i X^{*T}_{i,i-1}]S^{*}_i \qquad (6.3.29)$$

But, from equation 6.3.26, Y_i may be expressed in terms of the prediction error as,

$$Y_i = Y^{'}_{i,i-1} + X_{i,i-1} \qquad (6.3.30)$$

Substituting Y_i from equation 6.3.30 into equation 6.3.29 gives,

$$E[Y_{i+1}e^{*}_{i,i-1}] = \Phi_{i+1,i}\, E[Y^{'}_{i,i-1}X^{*T}_{i,i-1}]S^{*}_i +$$

$$+ \Phi_{i+1,i}\, E[X_{i,i-1}X^{*T}_{i,i-1}]S^{*}_i \qquad (6.3.31)$$

By virtue of the orthogonal projection theorem[114], $E[Y^{'}_{i,i-1}X^{*T}_{i,i-1}] = 0$. Also, by defining

$$P_{i,i-1} = E[X_{i,i-1}X^{*T}_{i,i-1}] \qquad (6.3.32)$$

equation 6.3.31 simplies to,

$$E[Y_{i+1}e^{*}_{i,i-1}] = \Phi_{i+1,i}\, P_{i,i-1}S^{*}_i \qquad (6.3.33)$$

Let us now consider the term $E[e_{i,i-1}e^{*}_{i,i-1}]$ on the right-hand side of equation 6.3.23. This term may be expanded using equation 6.3.27 to give,

$$E[e_{i,i-1}e^{*}_{i,i-1}] = E[(X^{T}_{i,i-1}S_i + w_i)(X^{*T}_{i,i-1}S_i^{*} + w_i^{*})] \tag{6.3.34}$$

Since $X^{T}_{i,i-1}S_i = S^{T}_i X_{i,i-1}$, equation 6.3.34 becomes

$$E[e_{i,i-1}e^{*}_{i,i-1}] = S^{T}_i E[X_{i,i-1}X^{*T}_{i,i-1}]S^{*}_i + S^{T}_i E[X_{i,i-1}w^{*}_i] +$$

$$+ E[w_i X^{*T}_{i,i-1}]S^{*}_i + E[w_i w^{*}_i] \tag{6.3.35}$$

The second and third terms on the right-hand side of equation 6.3.35 are obviously zero, so that from equations 6.3.32 and 6.3.8, equation 6.3.35 reduces to,

$$E[e_{i,i-1}e^{*}_{i,i-1}] = S^{T}_i P_{i,i-1} S^{*}_i + \sigma^2 \tag{6.3.36}$$

Using equations 6.3.36, 6.3.33 and 6.3.14 to substitute for the terms on the right-hand side of equation 6.3.23, we have,

$$\hat{E}[Y_{i+1}|e_{i,i-1}] = \Phi_{i+1,i}P_{i,i-1}S^{*}_i\,(S^{T}_i P_{i,i-1}S^{*}_i + \sigma^2)^{-1}\ x$$

$$x\ (r_i - Y'^{T}_{i,i-1}\,S_i) \tag{6.3.37}$$

If we denote

$$K_{i+1,i} = \Phi_{i+1,i}\,P_{i,i-1}S^{*}_i\,(S^{T}_i P_{i,i-1}S^{*}_i + \sigma^2)^{-1} \tag{6.3.38}$$

then equation 6.3.37 becomes,

$$\hat{E}[Y_{i+1}|e_{i,i-1}] = K_{i+1,i}\ (r_i - Y'^{T}_{i,i-1}\ S_i) \qquad (6.3.39)$$

Hence, using values from equations 6.3.22 and 6.3.39, the 1-step prediction of Y_{i+1} is given from equation 6.3.17 by,

$$Y'_{i+1,i} = \Phi_{i+1,i}\ Y'_{i,i-1} + K_{i+1,i}\ (r_i - Y'^{T}_{i,i-1}\ S_i) \quad (6.3.40)$$

In order to use equation 6.3.40, we need to specify $P_{i,i-1}$ for the calculation of $K_{i+1,i}$ (equation 6.3.38). Alternatively, we may determine $P_{i+1,i}$, and this is obtained as follows. The error in the 1-step prediction of Y_{i+1} is given by,

$$X_{i+1,i} = Y_{i+1} - Y'_{i+1,i} \qquad (6.3.41)$$

Substituting for Y_{i+1} (equation 6.3.1) and $Y'_{i+1,i}$ (equation 6.3.40), we have

$$X_{i+1,i} = \Phi_{i+1,i}\ Y_i + \Gamma_i V_i - \Phi_{i+1,i}\ Y'_{i,i-1} -$$

$$- K_{i+1,i}\ (r_i - Y'^{T}_{i,i-1}\ S_i) \qquad (6.3.42)$$

Substituting for r_i from equation 6.3.5 and noting that $Y'^{T}_{i,i-1}\ S_i$ $= S_i^T\ Y'_{i,i-1}$, equation 6.3.42 becomes,

$$X_{i+1,i} = \Phi_{i+1,i}\,(Y_i - Y'_{i,i-1}) - K_{i+1,i}S_i^T\,(Y_i - Y'_{i,i-1}) -$$

$$- K_{i+1,i}w_i + \Gamma_i V_i$$

$$= \Phi_{i+1,i}\,X_{i,i-1} - K_{i+1,i}\,S_i^T X_{i,i-1} -$$

$$- K_{i+1,i}\,w_i + \Gamma_i V_i$$

$$= (\Phi_{i+1,i} - K_{i+1,i}\,S_i^T)X_{i,i-1} -$$

$$- K_{i+1,i}w_i + \Gamma_i V_i \qquad (6.3.43)$$

From the definition of $P_{i,i-1}$ (equation 6.3.32), we have

$$P_{i+1,i} = E[X_{i+1,i}\,X_{i+1,i}^{*T}]$$

From equation 6.3.43 and since $X_{i,i-1}$, w_i and V_i are statistically orthogonal, we have

$$P_{i+1,i} = E[(\Phi_{i+1,i} - K_{i+1,i}\, S_i^T)X_{i,i-1}X_{i,i-1}^{*T}\,(\Phi_{i+1,i} - K_{i+1,i}S_i^T)^{*T} +$$

$$+ K_{i+1,i}\, w_i w_i^*\, K_{i+1,i}^{*T} + \Gamma_i V_i V_i^{*T} \Gamma_i^{*T}]$$

$$= \Phi_{i+1,i}\, P_{i,i-1} \Phi_{i+1,i}^{*T} -$$

$$- K_{i+1,i}\, S_i^T P_{i,i-1}\, \Phi_{i+1,i}^{*T} -$$

$$- \Phi_{i+1,i}\, P_{i,i-1} S_i^*\, K_{i+1,i}^{*T} +$$

$$+ K_{i+1,i}\, S_i^T P_{i,i-1}\, S_i^* K_{i+1,i}^{*T} +$$

$$+ K_{i+1,i}\, \sigma^2 K_{i+1,i}^{*T} +$$

$$+ \Gamma_i\, Q_i \Gamma_i^{*T}$$

$$= \Phi_{i+1,i}\, P_{i,i-1} \Phi_{i+1,i}^{*T} -$$

$$- K_{i+1,i}\, S_i^T P_{i,i-1}\, \Phi_{i+1,i}^{*T} -$$

$$- \Phi_{i+1,i}\, P_{i,i-1} S_i^*\, K_{i+1,i}^{*T} +$$

$$+ K_{i+1,i}\, (S_i^T P_{i,i-1} S_i^* + \sigma^2)\, K_{i+1,i}^{*T} +$$

$$+ \Gamma_i\, Q_i \Gamma_i^{*T} \qquad (6.3.44)$$

Substituting for $K_{i+1,i}$ (equation 6.3.38) in equation 6.3.44, we have,

$$P_{i+1,i} = \Phi_{i+1,i} P_{i,i-1} \Phi^{*T}_{i+1,i} -$$

$$- \Phi_{i+1,i} P_{i,i-1} S^*_i (S^T_i P_{i,i-1} S^*_i + \sigma^2)^{-1} S^T_i P_{i,i-1} \Phi^{*T}_{i+1,i} -$$

$$- \Phi_{i+1,i} P_{i,i-1} S^*_i K^{*T}_{i+1,i} +$$

$$+ \Phi_{i+1,i} P_{i,i-1} S^*_i (S^T_i P_{i,i-1} S^*_i + \sigma^2)^{-1} (S^T_i P_{i,i-1} S^*_i + \sigma^2) K^{*T}_{i+1,i} +$$

$$+ \Gamma_i Q_i \Gamma^{*T}_i$$

$$= \Phi_{i+1,i} P_{i,i-1} \Phi^{*T}_{i+1,i} -$$

$$- \Phi_{i+1,i} P_{i,i-1} S^*_i (S^T_i P_{i,i-1} S^*_i + \sigma^2)^{-1} S^T_i P_{i,i-1} \Phi^{*T}_{i+1,i} +$$

$$+ \Gamma_i Q_i \Gamma^{*T}_i \qquad (6.3.45)$$

Now, it can be seen from equations 6.3.1 and 6.3.5 that Y_i and r_i depend on V_j for $j<i$, which mean that R_i contains no information about V_i. Therefore, the prediction of Y_{i+1} based on R_i could simply be obtained by a 1-step prediction from Y'_i, with the estimate of V_i being set equal to a zero vector. Thus,

$$Y'_{i+1,i} = \Phi_{i+1,i} Y'_i \qquad (6.3.46)$$

Clearly, the two predictions given by equations 6.3.40 and 6.3.46 are the same, and so replacing $Y'_{i+1,i}$ in equation 6.3.40 by its value in equation 6.3.46, we have,

$$\Phi_{i+1,i} Y'_i = \Phi_{i+1,i} Y'_{i,i-1} + K_{i+1,i}(r_i - S_i^T \Phi_{i,i-1} Y'_{i-1}) \tag{6.3.47}$$

Premultiplying equation 6.3.47 by $\Phi_{i,i+1}$ and using the properties of the transition matrix[114] that $\Phi_{i+1,i} = (\Phi_{i,i+1})^{-1}$, we have,

$$Y'_i = \Phi_{i,i-1} Y'_{i-1} + \Phi_{i,i+1} K_{i+1,i} (r_i - S_i^T \Phi_{i,i-1} Y'_{i-1}) \tag{6.3.48}$$

If we define

$$K_i = \Phi_{i,i+1} K_{i+1,i} \tag{6.3.49}$$

then, using the value of $K_{i+1,i}$ from equqtion 6.3.38, we have,

$$K_i = P_{i,i-1} S_i^* (S_i^T P_{i,i-1} S_i^* + \sigma^2)^{-1} \tag{6.3.50}$$

and equation 6.3.48 simplifies to,

$$Y'_i = \Phi_{i,i-1} Y'_{i-1} + K_i (r_i - S_i^T \Phi_{i,i-1} Y'_{i-1}) \tag{6.3.51}$$

An alternative form to equation 6.3.51 is obtained by substituting

$\Phi_{i,i-1} Y'_{i-1}$ by $Y'_{i,i-1}$ (equation 6.3.46), so that

$$Y'_i = Y'_{i,i-1} + K_i (r_i - S_i^T Y'_{i,i-1}) \qquad (6.3.52)$$

Next, we obtain an expression for the covariance of the error vector in the estimate Y'_i. Using the definition for X_i (equation 6.3.11) and the expression for Y'_i above, we have,

$$X_i = Y_i - Y'_{i,i-1} - K_i (r_i - S_i^T Y'_{i,i-1})$$

$$= (Y_i - Y'_{i,i-1}) - K_i (S_i^T (Y_i - Y'_{i,i-1}) + w_i)$$

$$= X_{i,i-1} - K_i (S_i^T X_{i,i-1} + w_i) \qquad (6.3.53)$$

Since $X_{i,i-1}$ and w_i are statistically orthogonal, we have,

$$P_{i,i} = E[X_i X_i^{*T}]$$

$$= E[X_{i,i-1} X_{i,i-1}^{*T}] -$$

$$- E[X_{i,i-1} X_{i,i-1}^{*T}] S_i^* K_i^{*T} -$$

$$- K_i S_i^T E[X_{i,i-1} X_{i,i-1}^{*T}] +$$

$$+ K_i S_i^T E[X_{i,i-1} X_{i,i-1}^{*T}] S_i^* K_i^{*T} +$$

$$+ K_i E[w_i w_i^*] K_i^{*T}$$

$$= P_{i,i-1} - P_{i,i-1}S_i^*K_i^{*T} - K_iS_i^TP_{i,i-1} +$$

$$+ K_iS_i^TP_{i,i-1}S_i^*K_i^{*T} + K_i\sigma^2K_i^{*T}$$

$$= (I - K_iS_i^T)P_{i,i-1} - P_{i,i-1}S_i^*K_i^{*T} +$$

$$+ K_i\,(S_i^TP_{i,i-1}S_i^* + \sigma^2)K_i^{*T} \qquad (6.3.54)$$

where I is a (g+1)x(g+1) identity matrix. Substituting the value of K_i (equation 6.3.50) into the last term on the right-hand side of equation 6.3.54 gives,

$$P_{i,i} = (I - K_iS_i^T)P_{i,i-1} - P_{i,i-1}S_i^*K_i^{*T} +$$

$$+ P_{i,i-1}S_i^*\,(S_i^TP_{i,i-1}S_i^* + \sigma^2)^{-1}\,x$$

$$x\,(S_i^TP_{i,i-1}S_i^* + \sigma^2)\,K_i^{*T}$$

$$= (I - K_iS_i^T)P_{i,i-1} \qquad (6.3.55)$$

It can be seen that the expression for $P_{i,i}$ contains $P_{i,i-1}$ which can be obtained from $P_{i+1,i}$ (equation 6.3.45). First we rewrite equation 6.3.45 as,

$$P_{i+1,i} = \Phi_{i+1,i} (P_{i,i-1} - K_i S_i^T P_{i,i-1}) \Phi_{i+1,i}^{*T}$$

$$+ \Gamma_i Q_i \Gamma_i^{*T}$$

$$= \Phi_{i+1,i} (I - K_i S_i^T) P_{i,i-1} \Phi_{i+1,i}^{*T} + \Gamma_i Q_i \Gamma_i^{*T} \qquad (6.3.56)$$

Thus, from equation 6.3.55,

$$P_{i+1,i} = \Phi_{i+1,i} P_{i,i} \Phi_{i+1,i}^{*T} + \Gamma_i Q_i \Gamma_i^{*T} \qquad (6.3.57)$$

Clearly, $P_{i,i-1}$ could be obtained from equation 6.3.57, i.e.,

$$P_{i,i-1} = \Phi_{i,i-1} P_{i-1,i-1} \Phi_{i,i-1}^{*T} + \Gamma_{i-1} Q_{i-1} \Gamma_{i-1}^{*T} \qquad (6.3.58)$$

Hence, equations 6.3.46, 6.3.50, 6.3.52, 6.3.55 and 6.3.58 constitute the Kalman filter estimator giving the minimum error-variance unbiased estimate of Y_i based on the channel model of equation 6.3.1 and the measurement model of equation 6.3.4. These equations are summarized below.

$$Y'_{i,i-1} = \Phi_{i,i-1} Y'_{i-1} \qquad (6.3.59a)$$

$$P_{i,i-1} = \Phi_{i,i-1} P_{i-1,i-1} \Phi_{i,i-1}^{*T} + \Gamma_{i-1} Q_{i-1} \Gamma_{i-1}^{*T} \qquad (6.3.59b)$$

$$K_i = P_{i,i-1} S_i^* (S_i^T P_{i,i-1} S_i^* + \sigma^2)^{-1} \qquad (6.3.59c)$$

$$P_{i,i} = (I - K_i S_i^T) P_{i,i-1} \qquad (6.3.59d)$$

$$Y'_i = Y'_{i,i-1} + K_i (r_i - S_i^T Y'_{i,i-1}) \qquad (6.3.59e)$$

The flow chart and the block diagram of the Kalman filter estimator are shown in Figures 6.3.1 and 6.3.2, respectively.

Before using the Kalman filter estimator, it is necessary to assign proper initial conditions for the estimate of Y and also the covariance matrix P. In practice, Y_o is unlikely to be available so that a random initial condition is most appropriate[51,114]. Suppose therefore that Y_o is a random vector with mean $\bar{Y}_o$ and covariance matrix P_o, that is,

$$\left.\begin{aligned} E[Y_o] &= \bar{Y}_o \\ E[(Y_o - \bar{Y}_o)(Y_o - \bar{Y}_o)^{*T}] &= P_o \end{aligned}\right\} \qquad (6.3.60)$$

then, clearly, the best estimate of Y_o, prior to the arrival of any received signal is given by

$$Y_o' = E[Y_o] = \bar{Y}_o \qquad (6.3.61)$$

Consequently, the estimate (or prediction) of Y_1, given no received signal, is simply

$$Y_{1,o}' = \Phi_{1,o} Y_o' = \Phi_{1,o} \bar{Y}_o \qquad (6.3.62)$$

If we examine the algorithms for computing the Kalman gain vector K_i, the a priori covariance matrix $P_{i,i-1}$ and the a posteriori covariance matrix $P_{i,i}$, we would observe that they do not depend on the received

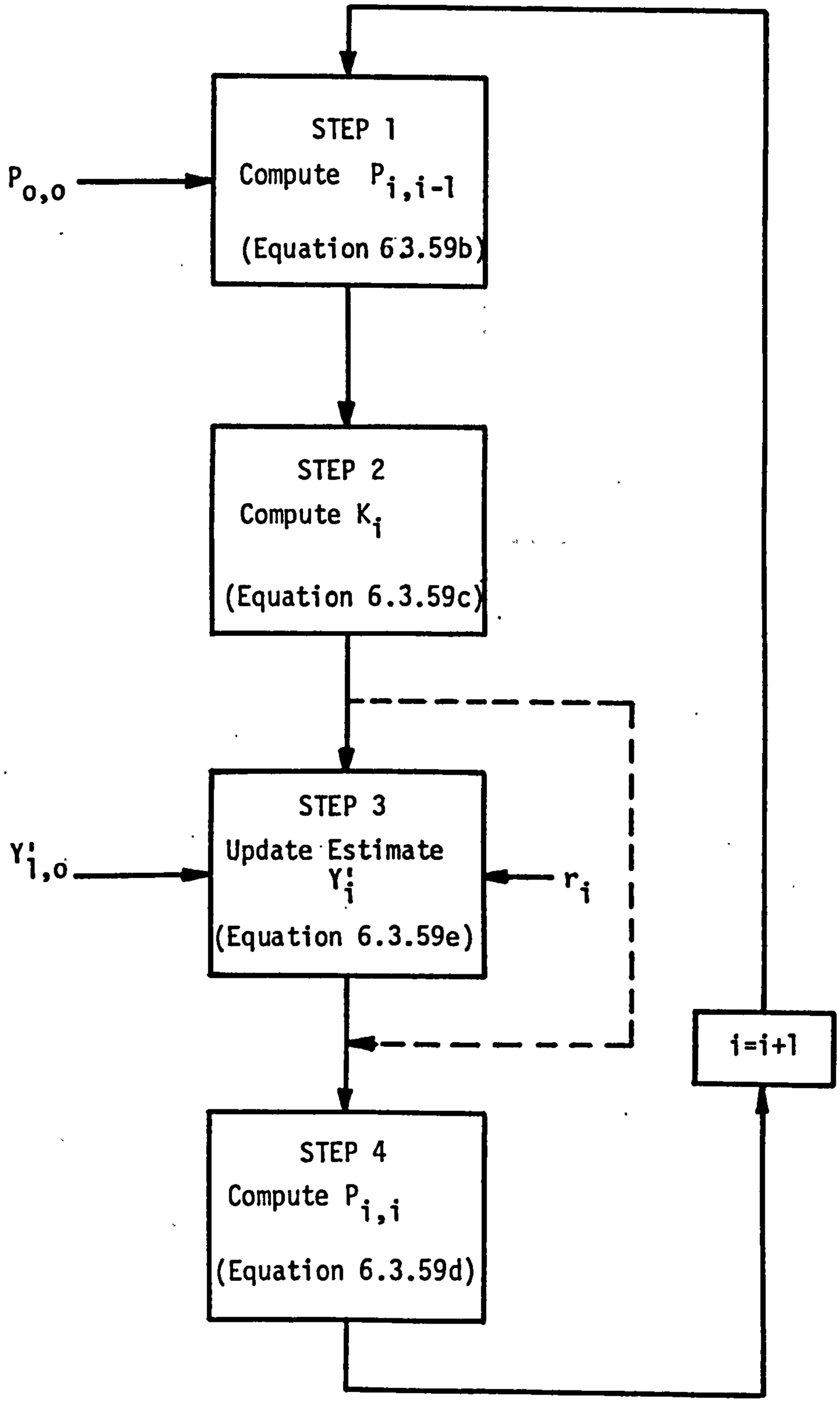

FIGURE 6.3.1: FLOW CHART OF THE CONVENTIONAL KALMAN FILTER ESTIMATOR

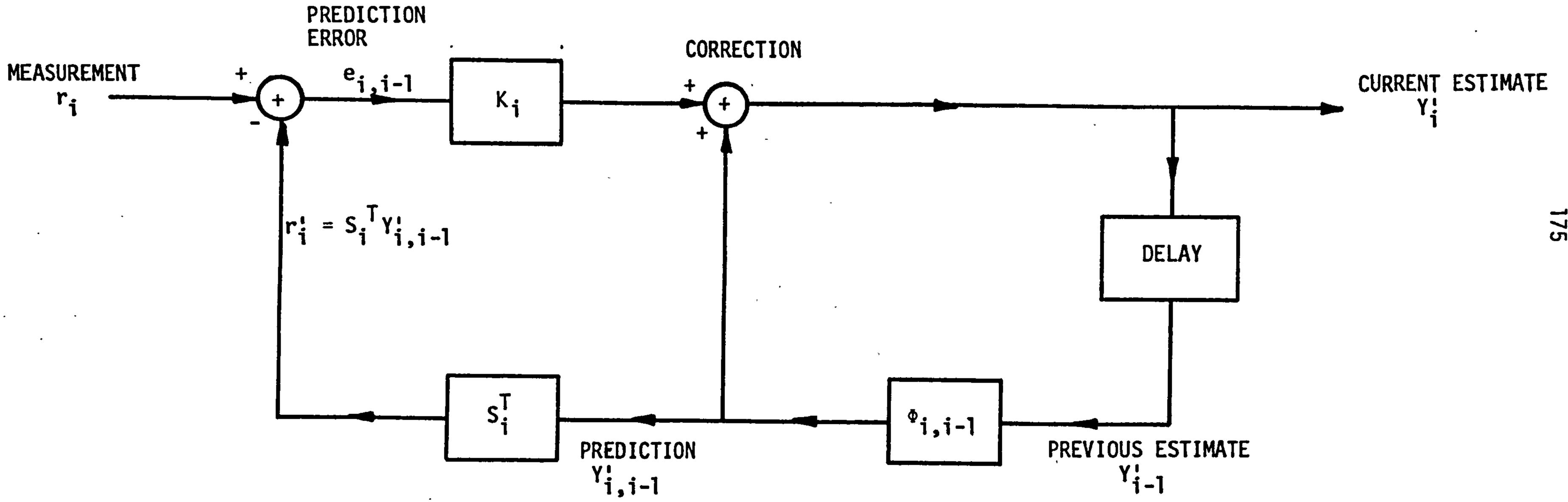

FIGURE 6.3.2: BLOCK DIAGRAM OF THE CONVENTIONAL KALMAN FILTER ESTIMATOR

signals $\{r_i\}$, and so, for example, the gain vector K may be computed beforehand and kept in store. This is obviously advantageous if the cost of storage is cheaper than real-time computation.

An important feature of the Kalman algorithm is that in addition to providing a recursive solution to the least-squares problem that can be implemented directly, it also computes the error covariance matrix P which may be used to judge the accuracy of the estimates.

In practice, the actual value of the matrices Φ and Γ are not known to the receiver. However, intuitively, one may consider the HF channel, over a sufficiently long time interval, to be randomly varying about some mean value, then,

$$Y_{i+1} = Y_i + V_i' \tag{6.3.63}$$

where V_i' is a noise vector. Clearly, in this case, both matrices can be set to the identity matrices of the appropriate dimensions. Consequently algorithm 6.3.59 reduces to

$$P_{i,i-1} = P_{i-1,i-1} + Q_{i-1} \tag{6.3.64a}$$

$$K_i = P_{i,i-1} S_i^* (S_i^T P_{i,i-1} S_i^* + \sigma^2)^{-1} \tag{6.3.64b}$$

$$P_{i,i} = (I - K_i S_i^T) P_{i,i-1} \tag{6.3.64c}$$

$$Y_i' = Y_{i-1}' + K_i (r_i - S_i^T Y_{i-1}') \tag{6.3.64d}$$

because the one-step prediction $Y'_{i,i-1}$ is now simply given by the estimate Y'_{i-1} (see equation 6.3.59a).

Clearly, equation 6.3.59a computes the prediction of Y_i from the updated estimate Y'_{i-1}. Perhaps, a better arrangement is that where Φ and Γ are still the identity matrices, but Y_i is predicted using a suitable arrangement of prediction. Among the various predictors that have been studied in Ref. 89, for applications involving the HF channel, the most promising is the degree-1 least-squares fading-memory predictor. Therefore, the Kalman filter is now of the form

$$Y'_{i,i-1} = \text{obtained by degree-1 least-squares fading-memory prediction} \tag{6.3.65a}$$

$$P_{i,i-1} = P_{i-1,i-1} + Q_{i-1} \tag{6.3.65b}$$

$$K_i = P_{i,i-1} S_i^* \left(S_i^T P_{i,i-1} S_i^* + \sigma^2\right)^{-1} \tag{6.3.65c}$$

$$P_{i,i} = (I - K_i S_i^T) P_{i,i-1} \tag{6.3.65d}$$

$$Y'_i = Y'_{i,i-1} + K_i (r_i - S_i^T Y'_{i,i-1}) \tag{6.3.65e}$$

The matrix Q_{i-1} in equations 6.3.64a and 6.3.65b is the covariance matrix of V'_{i-1}, i.e.,

$$Q_{i-1} = E[V'_{i-1} (V'_{i-1})^{*T}] \tag{6.3.66}$$

In practice, Q is also not known and, in fact, it may be estimated as outlined by Jazwinski[49]. Earlier, we have assigned Φ and Γ each

to be an identity matrix. Clearly, these assumptions have resulted in a different model from that assumed by the Kalman filter. However, one may choose the matrix Q such that model errors are 'covered' with noise. Here, we assign the matrix Q_{i-1} as

$$Q_{i-1} = cI \tag{6.3.67}$$

where c is a small positive real constant and I is an identity matrix. This means that the components of V_i' are statistically independent. Another alternative for the value of Q_{i-1} is

$$Q_{i-1} = q\, P_{i-1,i-1} \tag{6.3.68}$$

where q is a small positive constant. The potential weakness of having Q_{i-1} as in equation 6.3.68 is that after repeated application of the Kalman filter, the matrix $P_{i,i-1}$ may cease to be a positive definite matrix which means that it is no longer the correct error covariance matrix. Therefore, in order to impose $P_{i,i-1}$ to be a positive definite matrix, one may use,

$$Q_{i-1} = q\, P_{i-1,i-1} + cI \tag{6.3.69}$$

When the various possible values of Q_{i-1} are incorporated into algorithms 6.3.64 and 6.3.65, the following algorithms are obtained.

Kalman Estimator 1

$$P_{i,i-1} = P_{i-1,i-1} + cI$$

$$K_i = P_{i,i-1} S_i^* \ (S_i^T P_{i,i-1} S_i^* + \sigma^2)^{-1}$$

$$P_{i,i} = (I - K_i S_i^T) P_{i,i-1}$$

$$Y_i' = Y_{i-1}' + K_i \ (r_i - S_i^T Y_{i-1}')$$

Kalman Estimator 2

$Y_{i,i-1}'$ = obtained by degree-1 least-squares fading-memory prediction

$$P_{i,i-1} = P_{i-1,i-1} + cI$$

$$K_i = P_{i,i-1} S_i^* \ (S_i^T P_{i,i-1} S_i^* + \sigma^2)^{-1}$$

$$P_{i,i} = (I - K_i S_i^T) P_{i,i-1}$$

$$Y_i' = Y_{i,i-1}' + K_i \ (r_i - S_i^T Y_{i,i-1}')$$

Kalman Estimator 3

$Y'_{i,i-1}$ = obtained by degree-1 least-squares fading-memory prediction

$$P_{i,i-1} = P_{i-1,i-1} + q\,P_{i-1,i-1}$$

$$K_i = P_{i,i-1}\,S_i^*(S_i^T\,P_{i,i-1}\,S_i^* + \sigma^2)^{-1}$$

$$P_{i,i} = (I - K_i S_i^T)\,P_{i,i-1}$$

$$Y'_i = Y'_{i,i-1} + K_i\,(r_{i.} - S_i^T\,Y'_{i,i-1})$$

Kalman Estimator 4

$Y'_{i,i-1}$ = obtained by degree-1 least-squares fading-memory prediction

$$P_{i,i-1} = P_{i-1,i-1} + q\,P_{i-1,i-1} + cI$$

$$K_i = P_{i,i-1}S_i^*\,(S_i^T P_{i,i-1}S_i^* + \sigma^2)^{-1}$$

$$P_{i,i} = (I - K_i S_i^T)\,P_{i,i-1}$$

$$Y'_i = Y'_{i,i-1} + K_i\,(r_i - S_i^T\,Y'_{i,i-1})$$

Kalman Estimator 5

$$P_{i,i-1} = P_{i-1,i-1} + q P_{i-1,i-1}$$

$$K_i = P_{i,i-1} S_i^* (S_i^T P_{i,i-1} S_i^* + \sigma^2)^{-1}$$

$$P_{i,i} = (I - K_i S_i^T) P_{i,i-1}$$

$$Y_i' = Y_{i-1}' + K_i (r_i - S_i^T Y_{i-1}')$$

In all cases the optimum values of σ^2, c and q are found by trial and error.

6.4 COMPLEX FEEDFORWARD TRANSVERSAL-FILTER ESTIMATOR

The structure of the complex feedforward transversal-filter estimator is as shown in Figure 6.4.1. It is basically a modification of the linear feedforward transversal-filter estimator in Section 3.5. but the estimator is required here to handle complex-valued signals. It operates as follows.

Upon the reception of r_{i+n} and before the detection of s_{i+1}, the signals along the delay line are the detected data-symbols s_i', s_{i-1}', ... s_{i-g}'. Each symbol s_{i-h}' for h = 0, 1, ..., g is multiplied by the corresponding component $y_{i-1,h}'$ of the previous estimate Y_{i-1}'. The resulting products are added to form an estimate r_i' of the received signal r_i, that is

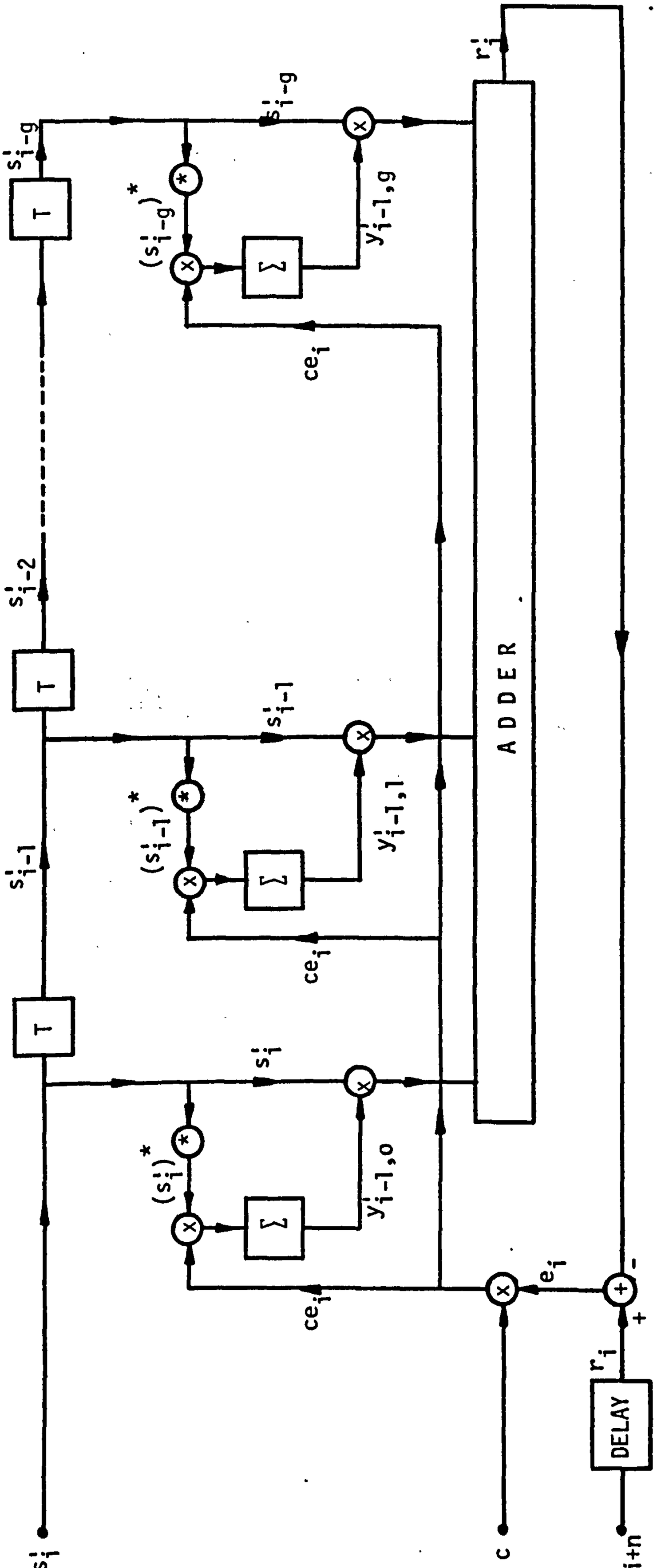

FIGURE 6.4.1: COMPLEX FEEDFORWARD TRANSVERSAL-FILTER

$$r'_i = \sum_{h=0}^{g} s'_{i-h}\, y'_{i-1,h} \qquad (6.4.1)$$

The estimate r'_i is subtracted from the corresponding received sample r_i which was previously held in store to give the error signal

$$e_i = r_i - r'_i \qquad (6.4.2)$$

e_i is then multiplied by a small positive real quantity c. The resulting signal ce_i multiplies each of the complex conjugates $(s'_i)^*$, $(s'_{i-1})^*$, ...,$(s'_{i-g})^*$ of the detected data-symbols s'_i, s'_{i-1}, ..., s'_{i-g}. The resulting products are added to the corresponding components of Y'_{i-1} to give the updated estimate Y'_i of Y_i. Thus, the $(h+1)^{th}$ component of Y'_i is

$$y'_{i,h} = y'_{i-1,h} + ce_i(s'_{i-h})^* \qquad (6.4.3)$$

In vector notation, the estimate of Y_i is given by,

$$Y'_i = Y'_{i-1} + ce_i\, S^*_i \qquad (6.4.4)$$

where S^*_i is a (g+1)-component column vector with components $\{(s'_{i-h})^*\}$, that is

$$S^*_i = [(s'_i)^*\ (s'_{i-1})^*\ \ldots\ (s'_{i-g})^*]^T \qquad (6.4.5)$$

The positive real quantity c in equations 6.4.3 and 6.4.4 is known as the step size of the estimator. The smaller the value of c, the smaller is the effect of additive noise on the estimate Y_i'. However, with small values of c, the rate of response of Y_i' to variations in Y_i is slow.

The algorithm given by equation 6.4.4 is the well known gradient or steepest descent algorithm[21,26-27,89,116-121]. We will call this algorithm the Feedforward Estimator 1. The algorithm, is, in fact, a recursive solution to the least-squares estimation problem of Section 3.3, but modified to handle complex quantities. Basically, the estimator starts with an initial estimate Y_0' and measures the gradient of the mean square error function that it to be minimized, and updates the estimate according to the gradient. When the process is repeated, the error in the estimate is successively reduced and the estimate converges to the optimum estimate of the channel.

A comparison of various channel estimators[26] has shown that the overall performance of the gradient algorithm is as good as the least-squares estimator in applications where the channel is time-invariant or slowly time-varying, as for example, a random walk channel. Over HF radio links, rapid variations may occur in the characteristics of the channel. Thus, more sophisticated techniques are required for the estimation of this type of channel. It has been shown[89] that when the gradient algorithm is employed in the estimation of a linear baseband channel that includes an HF radio link; a useful improvement in performance is obtained by including a predictor. The Feedforward

Estimator 1 is then modified to

$$Y_i' = Y_{i,i-1}' + ce_i\, S_i^* \tag{6.4.6}$$

where $Y_{i,i-1}'$ is the prediction of Y_i at time t=(i-1)T. Various arrangements of prediction have been studied in Ref. 89. The most promising arrangement is the degree-1 least-squares fading-memory predictor. Detailed descriptions of the predictor will be given in the next section. We will call the algorithm given by equation 6.4.6 the Feedforward Estimator 2.

6.5 LEAST-SQUARES FADING-MEMORY PREDICTION

With a receiver that employs a maximum likelihood detector, there is an inherent delay of several sampling intervals, say n-1, in the detection of a data symbol. For example, s_i is detected after the reception of r_{i+n-1}. This means that the estimate Y_i' of Y_i produced by the feedforward transversal-filter estimator (Section 6.4) or the Kalman filter estimator (Section 6.3) is only available to the detector on the receipt of r_{i+n} so that s_{i+1} may then be detected. Therefore, the delay in the estimation of Y_i is n sampling intervals. The error in using Y_i' instead of Y_{i+n}' in the detection of s_{i+1} becomes excessive when n is large or when the sampled impulse-response of the channel changes rapidly. Thus, it is necessary to make a prediction of Y_{i+n}, which can be derived from the estimates Y_i', Y_{i-1}', ... In addition to the n-step prediction $Y_{i+n,i}'$, a 1-step prediction $Y_{i+1,i}'$ of Y_{i+1} is also required so that Y_i' can be replaced

by $Y'_{i+1,i}$ when forming the updated estimate Y'_{i+1} in the channel estimator. Clark and McVerry[89] have tested several arrangements of prediction on a model of an HF radio link with two independent Rayleigh fading sky waves. The most promising of the predictors is the degree-1 least-squares fading-memory predictor, and so, in this part of the investigation, we have used this predictor for determining $Y'_{i+1,i}$ and $Y'_{i+n,i}$. The degree-1 least-squares fading memory predictor will now be described.

Here, the predicted value of a variable parameter at any time instant in the future is taken as the value of a polynomial, at the particular instant, the polynomial being designed to give the best fit to the sequence of past observations in the sense that it minimizes an appropriately weighted sum of the squares of the errors. Morrison[44] has suggested that the weight factor be an exponentially decaying function so that the older observations have less influence on the choice of the polynomial. The name least-squares that is given to this type of predictor comes from the fact that the criterion for choosing a polynomial is that the weighted sum of the squares of the errors in the predictions of the received signals $\{r_i\}$ be minimized, where the predictions of the $\{r_i\}$ are themselves derived from the predictions of the sampled impulse-response of the channel. The least-squares fading-memory prediction as applied by Morrison[44] derived the prediction from past observations of the parameter in question. However, Clark and McVerry[89] have obtained the prediction using past updated estimates of the parameter. The latter arrangement seems more likely to become unstable when the estimates are themselves

in error. The results of extensive computer simulation tests[89] have however shown that, with proper setting, the predictor is stable under a variety of channel conditions.

Clearly, each of the g+1 components of the sampled impulse-response of the channel can be considered as a variable parameter, and so in the prediction of these components, g+1 polynomials of a given degree are determined, each of which gives the weighted least-squares fit to the components in the corresponding locations in the vector Y'_i, Y'_{i-1}, ... Degree-1 prediction is now given as follows.

$$(Y'_{i+1,i})' = (Y'_{i,i-1})' + (1-\theta)^2 E_i \qquad (6.5.1)$$

$$Y'_{i+1,i} = Y'_{i,i-1} + (Y'_{i+1,i})' + (1-\theta^2) E_i \qquad (6.5.2)$$

$$Y'_{i+n,i} = Y'_{i+1,i} + (n-1)(Y'_{i+1,i})' \qquad (6.5.3)$$

where $(Y'_{i+1,i})'$ is a function of the first differential of $Y'_{i+1,i}$ with respect to time. θ is a real constant with a value in the range 0 to 1, but normally close to 1. The vector E_i is the error in the prediction $Y'_{i,i-1}$ with respect to Y'_i, that is,

$$E_i = Y'_i - Y'_{i,i-1} \qquad (6.5.4)$$

The updated estimate Y'_i used in the above equations is provided by the channel estimator. In order to start the whole process of estimation and prediction, the following initial values may be used.

$$Y'_{1,o} = Y'_o \simeq Y_o \qquad (6.5.5)$$

$$(Y'_{1,o})' = 0 \qquad (6.5.6)$$

The channel estimator uses $Y'_{1,o}$ to determine Y'_1 so that E_1 can be obtained. The predictor, in turn, uses E_1 and the initial values in equations 6.5.5 and 6.5.6 to form $Y'_{2,1}$ which is subsequently used by the estimator to obtain Y'_2. The process continues in this way.

6.6 RESULTS AND ANALYSIS OF COMPUTER SIMULATION TESTS

Extensive tests have been carried out to investigate the possible application of the Kalman filter to the estimation of the sampled impulse-response of an HF radio channel which forms part of a synchronous serial data-transmission system. The digital data is to be transmitted at the data rate of 9600 bit/s, using quadrature amplitude modulation. All the tests have been performed by computer-simulation using the powerful CDC 7600 computer at the University of Manchester Regional Computer Centre. An example of the simulation programs are given in Appendices A3 and A4.

The model of the HF radio link that is used in the tests has two independent Rayleigh fading sky waves. Each sky wave introduces the same average attenuation and the same frequency spread of 1 Hz into the data signal, such that the average attenuation over the radio link is 0 dB. The relative delay in transmission between the two sky waves is 2 milliseconds. For ease of simulation, we are confined here to a fixed delay which can be altered to other values if required.

For the purpose of assessing the cost effectiveness of the Kalman filter estimator, we compare its performance with a feedforward transversal-filter estimator. The latter has been suggested as the basis of the most cost-effective estimator for applications involving an HF radio link. Clark and McVerry[89], in fact, have tested the feedforward transversal-filter estimator with various arrangements of prediction on a model of an HF channel with the above specifications. However, the tests were carried out at the data rate of 2400 bit/s with 4-level QAM signal. Our tests are at 9600 bit/s with 16-level QAM signal, which, therefore, has shorter sampling interval (when sampling once per data symbol) and so increases the number of components in the sampled impulse-response of the channel. Consequently, we would expect our results for the feedforward transversal-filter estimator to show a possible degradation when compared with the corresponding estimator in Ref. 89. However, a fair comparison cannot be made between these results for several reasons. Firstly, although the channel used in these tests has the same values for the relative transmission delay of the two sky waves and for the frequency spread, different random number sequences used for generating the fading sequences in the model of the HF channel can cause appreciable difference in the performance of the estimator. Secondly, the optimum values of the various parameters associated with the estimator are not the same due to the absence of any exact procedure for obtaining these values. However, if we compare the general behaviour of the estimator, the two results are in agreement.

The performances of the estimators are summarized in Figures 6.6.1-6.6.11 and Table 6.6.4. The quantity that is used for checking the convergence of the estimators is ξ_i which is the square of the error in the n-step prediction $Y'_{i,i-n}$, and is given by,

$$\xi_i = |Y_i - Y'_{i,i-n}|^2 \qquad (6.6.1)$$

As explained previously, n is the delay in the estimation of Y_i which is typically 17 sampling intervals[95]. In order to minimize the influence of a particular sequence of input data symbols on the performance of the estimator, we calculate $\bar{\xi}_i$ instead, which, for each value of i, is the ensemble average of 20 values of ξ_i obtained from the transmission of 20 different sequences of $\{s_i\}$ together with 20 different sequences of $\{w_i\}$. Although the process of evaluating $\bar{\xi}_i$ is rather tedious, we can consider each curve obtained in this way as representing the 'average' behaviour of the estimator. The other quantity that is used to judge the performance of the estimator is ξ, which is the mean-square error in the n-step prediction $Y'_{i,i-n}$, measured in dB relative to unity, and is given by

$$\xi = 10 \log_{10} \left(\frac{1}{19200} \sum_{i=1938}^{21137} |Y_i - Y'_{i,i-n}|^2 \right) \qquad (6.6.2)$$

In the foregoing equation, we have deliberately omitted the first 1937 n-step predictions of Y_i, so that any transient behaviour of the estimator just after it commences operation will not affect ξ.

Consequently, ξ can be taken as representing the 'steady-state' performance of the estimator. The number 1937 has not been chosen for any particular reason, it was merely selected for the convenience of simulating the estimators. Clearly, from equation 6.6.2, each value of ξ is the result of the transmission of over 21000 data symbols and also involving the same number of $\{Y_i\}$ in the prediction/estimation process.

The average transmitted energy per bit of information at the input and output of the HF radio link is arranged to be unity. The additive noise that corrupts the signal at the output of the HF radio link is Gaussian with two-sided power spectral density of $\frac{1}{2}N_o$. Thus, the signal-to-noise ratio ψ, defined as the ratio in dB of the average transmitted energy per bit to the two sided noise power spectral density at the receiver input, is given by,

$$\psi = 10 \log_{10} (1/\tfrac{1}{2}N_o) \qquad (6.6.3)$$

In all tests on the Kalman estimators, the quantity σ^2 that appears in the Kalman gain equation is assumed to be known. In practice, σ^2 should be adjusted by trial and error to obtain the optimum performance of the estimator.

Figure 6.6.1 summarizes the results of extensive computer simulation tests, comparing the performances of the Feedforward Estimators 1 and 2 with the Kalman Estimators 1 and 2. The delay in estimation is 17 sampling intervals. The parameters that can be adjusted are

θ and c, and so when these are set to their respective optimum values, the performances of the estimators are the best obtainable under the given conditions. Thus, at every point on each curve in Figure 6.6.1, the parameters θ and c have been given values as close as possible to their optimum values. The adjustments of the parameters have taken up a considerable amount of computing time. Basically, the method involves the alternate adjustment of each parameter, for example, with θ, say, fixed at a certain value, c is varied to find the optimum value of ξ under the given condition. The value of c for which ξ is optimum is noted and, in the next step, c is fixed at this value while θ is varied. A second minimum value of ξ is obtained. The value of θ at the second minimum is noted and used in the next step to find another minimum value of ξ in the same way as before. The process continues in this way until no further improvement is obtained in the value of ξ by adjusting θ and c. Therefore, at the end of these adjustments, the particular combination of θ and c gives the best obtainable performance of each estimator, and the values of θ and c are considered as the optimum values (see Tables 6.6.1 and 6.6.3 for the optimum values of θ and c). From these curves, we observe that at high signal-to-noise ratios (ψ>30), both types of estimators (Kalman and feedforward) give a considerable improvement in performance when a prediction is involved in updating an estimate. The advantage is less obvious at the lower signal-to-noise ratios. This is as expected because the predictor is clearly less effective in 'noisy' environments. We also observed that at lower signal-to-noise ratios (ψ<20) the performance of the Kalman Estimator 1 is almost identical to that of the Feedforward Estimator 1.

Figure 6.6.2 shows the variation of the mean-square error in the 1-step prediction of Y_i with ψ. The 1-step prediction $Y'_{i,i-1}$ is required by the predictor in forming the n-step prediction $Y'_{i,i-n}$, and in addition, it is required by the Feedforward Estimator 2, Kalman Estimators 2, 3 and 4 in updating the estimate Y_i. The mean-square error in the 1-step prediction $Y'_{i,i-1}$ is defined as

$$\xi' = 10 \log_{10} \left(\frac{1}{19200} \sum_{i=1938}^{21137} |Y_i - Y'_{i,i-1}|^2\right) \tag{6.6.4}$$

The values of θ and c at every point on each curve are the same as the corresponding set of values in Figure 6.6.1. This means that these parameters may not give the optimum value of ξ' at each value of ψ, and so further improvements in ξ' may be obtained for all the estimators. However, in most cases, the optimum values of θ and c which give the minimum value of ξ also give the minimum value of ξ'. Thus, Figure 6.6.2 is very close to that where θ and c are adjusted for the minimum value of ξ'. The objective here is to obtain the most accurate n-step prediction of Y_i as it is the n-step predictions which are required by the detector in the detection of the data symbols. Consequently, θ and c have not been optimized for the mean-square error ξ'. Figure 6.6.2 has been included so as to show approximately the accuracy of the 1-step predictions.

In Figure 6.6.3, the mean-square error ξ'' in the updated estimated Y'_i is shown for values of ψ in the range of 5 to 60. The mean-square error is defined as

$$\xi'' = 10 \log_{10} \left(\frac{1}{19200} \sum_{i=1938}^{21137} |Y_i - Y_i'|^2 \right) \qquad (6.6.5)$$

The parameters θ and c at each signal-to-noise ratio are here not the values which minimize ξ''. They are in fact the values which give the minimum value of ξ at each value of ψ. Therefore, Figure 6.6.3 has been included merely to show the accuracy of the updated estimate of Y_i when the parameters θ and c are optimized for the n-step prediction of Y_i. It can be seen that errors in the updated estimates also follow the same behaviour as in the previous two figures.

From these three figures, it is clear that the Kalman Estimator 2 and the Feedforward Estimator 2 are worthy of further consideration.

Figures 6.6.4 and 6.6.5 show the variation of the error in the n-step prediction $Y'_{i,i-n}$ with the parameter c at various signal-to-noise ratios for the Kalman Estimator 2 and the Feedforward Estimator 2, respectively. The parameter θ is set to its optimum value at each signal-to-noise ratio for the optimum value of c and it is held fixed along each curve. The parameter c used with the Kalman Estimator 2 is the value of each diagonal component of the matrix Q_{i-1} in the equation for the a priori error covariance matrix $P_{i,i-1}$. In the case of the Feedforward Estimator 2, c is the step size of the estimator. It can be seen that, with the Kalman Estimator 2, as the signal-to-noise ratio increases, the optimum value of c decreases. At a signal-to-noise ratio of 5 dB, the optimum value of c is 10^{-4}, at $\psi = 60$, the optimum value of c is 10^{-7}. The performance of the Kalman Estimator 2 deteriorates rapidly when c falls below its optimum value. However, the estimator remains almost optimum for values

of c above the optimum value, at least over the range tested. As for the Feedforward Estimator 2, very small values of c are to be avoided because then the estimator cannot adequately track the received signal. The optimum values of c for both estimators at different values of ψ are given in Table 6.6.1.

The variations of ξ with θ at various signal-to-noise ratios for the Kalman Estimator 2 and the Feedforward Estimator 2 are given in Figures 6.6.6 and 6.6.7, respectively. For each curve, the parameter c is fixed at the optimum value for the particular signal-to-noise ratio. Both sets of curves exhibit the same behaviour, that is, the optimum value of θ increases as the signal-to-noise ratio decreases. The optimum values of θ are given in Table 6.6.1.

Figures 6.6.8-6.6.11 show the convergence of the Kalman Estimators 1 and 2 and the Feedforward Estimators 1 and 2 under various initial conditions. Each of these curves is the ensemble average of 20 convergence curves which have been obtained using 20 different sequences of $\{s_i\}$ and 20 different sequences of $\{w_i\}$. The initial conditions are given in Table 6.6.2, where I is a (g+1)x(g+1) identity matrix, and 0 is a (g+1)-component column vector with all its components equal to zero. It is assumed in all cases that the estimators do not know the rate of change of Y_i at the start of transmission, so that $(Y'_{0,-1})' = 0$. In all tests, the signal-to-noise ratio is 60 dB and the parameters θ and c are optimum.

Figure 6.6.8 shows the convergence of the Kalman Estimator 1 and the Feedforward Estimator 1 at the start of transmission when

both estimators have no prior knowledge of Y_i. Accordingly, we set the a priori error covariance matrix $P_{o,o}$ for the Kalman Estimator 1 to a diagonal matrix with large diagonal elements (= 10^6). If we consider the convergence of the estimators to their respective values of the steady-state mean square error ξ, the Kalman Estimator 1 converges in about 160 sampling intervals, while the Feedforward Estimator 1 takes about 280 sampling intervals. When the estimators have prior knowledge of Y_i at the start of transmission (Figure 6.6.9) both estimators take very little time to converge to the steady-state mean-square error. The little 'hump' that appears at the beginning of each convergence curve is most likely due to the delay in obtaining sufficiently accurate estimate of the rate of change of Y_i by the predictor. When Figure 6.6.8 is compared with Figure 6.6.9, we can see that the performance of the Kalman Estimator 1 in Figure 6.6.8 becomes identical to that in Figure 6.6.9 after about 200 sampling intervals, while the corresponding value for the Feedforward Estimator 1 is 440 sampling intervals. Thus, the Kalman Estimator 1 recovers relatively quickly from the absence of the prior knowledge of Y_i.

Figure 6.6.10 shows the convergence of the Kalman Estimator 2 and the Feedforward Estimator 2 when both have no prior knowledge of Y_i at the start of transmission. The Feedforward Estimator 2 converges to its steady-state mean-square error ξ in about 840 sampling intervals, while the corresponding value for the Kalman Estimator 2 is 1240 sampling intervals. The convergence of both estimators are slower than the case in Figure 6.6.8 because the 1-step predictor of

the sampled impulse-response is here part of the updating algorithm for Y_i', and clearly, the absence of any prior knowledge of Y_o', $Y_{o,-1}'$ and $(Y_{o,-1}')'$ means that the predictor requires a longer time to obtain sufficiently accurate estimates of these quantities and therefore slows down considerably the convergence of both estimators. In Figure 6.6.11, the convergence of both estimators is more rapid because of the prior knowledge of Y_1 at the start of transmission. However, the Kalman Estimator 2 still converges more slowly to its steady-state mean-square error than the Feedforward Estimator 2.

So far, we have seen that the performance of the Feedforward Estimator 1 follows quite closely that of the Kalman Estimator 1. In fact, the two estimators are almost identical in performance below $\psi \simeq 20$ (see Figure 6.6.1). At these signal-to-noise ratios, the optimum values of θ for both estimators are the same (see Table 6.6.3). This means that both estimators are using the same predictor. Thus, the almost identical performances of both estimators suggest that probably the Kalman Estimator 1 effectively degenerates into the Feedforward Estimator 1. This will only happen when the matrix $P_{i,i-1}$ is set to kI, where k is a scalar constant and I is the $(g+1)x(g+1)$ identity matrix, so that

$$(S_i^T P_{i,i-1} S_i^* + \sigma^2)^{-1} = (k \sum_{h=0}^{g} |s_{i-h}|^2 + \sigma^2)^{-1} \tag{6.6.6}$$

which is a scalar quantity. Therefore the Kalman gain vector becomes

$$K_i = k\ (k \sum_{h=0}^{g} |s_{i-h}|^2 + \sigma^2)^{-1}\ s_i^* \qquad (6.6.7)$$

A comparison between the updating equation for the Kalman Estimator 1 (equation 6.3.64d), with K_i given by equation 6.6.7, and the corresponding equation for the Feedforward Estimator 1 (equation 6.4.4) suggests that

$$k\ (k \sum_{h=0}^{g} |s_{i-h}|^2 + \sigma^2)^{-1} \simeq c \qquad (6.6.8)$$

where c is a scalar positive constant and is the step size of the Feedforward Estimator 1. Close examination of the foregoing equation reveals that in order for the relationship to be maintained, $\sum_{h=0}^{g} |s_{i-h}|^2$ must remain almost a constant. However, the data-symbols $\{s_i\}$ are statistically independent and equally likely to have any of their 16 possible values as given by equation 6.2.1, and so it is most likely that $\sum_{h=0}^{g} |s_{i-h}|^2$ will not remain a constant. Also, in our tests, we have not deliberately made $P_{i,i-1} = kI$ and checks have been made on the actual matrix $P_{i,i-1}$ which show that it is not equal to kI. Thus, the Kalman Estimator 1 has not degenerated into the Feedforward Estimator 1. We can deduce that the Kalman Estimator 1 as applied to our problem here is not optimum. This, in a way, is what we might have expected because with the Kalman Estimator, we have assumed that the matrices Φ and Γ (equation 6.3.1) both to be the identity matrices. Therefore, the channel is modelled simply as in equation 6.3.63, and so we rely on Q_{i-1} (equation 6.3.66) to compensate for any modelling errors. In all the tests above, $Q_{i-1} = cI$, where c is a

small positive constant. Hsu[126] has suggested setting Q_{i-1} to be proportional to $P_{i-1,i-1}$, that is,

$$Q_{i-1} = q\, P_{i-1,i-1} \tag{6.6.9}$$

where q (<<1) is a small positive constant. We have also considered Q_{i-1} as a combination of these two schemes, that is,

$$Q_{i-1} = q\, P_{i-1,i-1} + cI \tag{6.6.10}$$

With c given a positive value, the scheme given by equation 6.6.10 ensures that the matrix $P_{i,i-1}$ remains a positive definite matrix. Table 6.6.4 gives the performances of the Kalman Estimators using various schemes, with all the parameters optimum.

With reference to Table 6.6.4, the entries for the Kalman Estimator 2 enclosed within the brackets are the actual values of the steady-state mean-square error ξ in the n-step prediction of Y_i. The figures for the other estimators give their performance, measured in dB, relative to the Kalman Estimator 2. Clearly, from Table 6.6.4, the best performance is given by the Kalman Estimator 2 followed by the Kalman Estimator 4.

Let us now re-examine why the Kalman Estimator 1 is not optimum as an estimator of the sampled impulse-response of the linear baseband channel in Figure 6.2.1, which includes a model of an HF radio link. Modelling of the HF radio channel is the subject of the CCIR Report

No. 549 of the CCIR XII Plenary Assembly (1974)[77]. It is recommended that the HF channel be modelled theoretically as a complex tapped delay line with the number of taps corresponding to the number of sky waves present (Section 4.4). The signal on each tap is multiplied by a complex narrow-band baseband Gaussian waveform which imposes the Rayleigh fading. Alternatively, we can consider the signal to be separately multiplied by two real-valued narrow-band baseband Gaussian waveforms as in Figure 4.4.2. Thus, four Gaussian waveforms are involved in the two-sky-wave model. It is well known that the transfer function and impulse response of a Bessel filter tend towards Gaussian as the order of the filter is increased. Therefore, in our simulation the required Gaussian spectrum is approximated using a fifth order digital Bessel filter (Section 4.4) which is implemented as three separate filters connected in cascade. Each fading sequence $\{q_{h,i}\}$ for any given h (= 1, 2, 3 or 4) that multiplies the signal at each tap is then generated by filtering a sequence of statistically independent Gaussian random variables $\{v_{h,i}\}$ using the Bessel filter. Ref. 89 gives a clearer idea of how $\{v_{h,i}\}$ is processed into $\{q_{h,i}\}$, which we have simply reproduced here in Figure 6.6.12. From Figure 6.6.12, it is clear that the $\{q_{h,i}\}$ and therefore Y_i are not first-order Markov processes, where, the present state at time t=iT is dependent on the previous state at time t=(i-1)T and a white noise component. In fact, here, the present state depends on the last five of the previous states. The derivation of the Kalman filter estimator assumes that the channel can be modelled as a first-order Markov process. Obviously, any higher-order process can easily be reduced

to first-order by simple algebraic manipulations. However, if we are to do this here, all the matrices in the resultant Kalman filter estimator will be extended five fold, and thus become considerably more complex and require excessive computation. The feedforward transversal-filter estimator is far simpler to implement and requires far fewer computations. When it is modified to include a predictor and also utilizes some prior knowledge of the channel, the performance is far superior to the Kalman estimators (Section 7).

Due to the above fundamental weakness of the Kalman filter and its poor performance as a channel estimator, we have not pursued the study of other variants of the Kalman filter, such as the fast Kalman[128] and the square-root Kalman[51,126] algorithms. In any case, these algorithms merely improve certain aspects of the conventional Kalman filter. For instance, the fast Kalman reduces the number of operations per cycle from n^2 to n. The square-root Kalman requires roughly equivalent number of multiplications per cycle as the conventional Kalman filter but it has improved stability and increased numerical accuracy.

Kalman Estimator 2			Feedforward Estimator 2		
ψ	c	θ	ψ	c	θ
5	10^{-4}	0.96	5	0.03	0.98
10	10^{-4}	0.96	10	0.04	0.98
20	10^{-4}	0.95	20	0.04	0.97
30	10^{-6}	0.92	30	0.02	0.94
40	10^{-6}	0.89	40	0.03	0.93
50	10^{-7}	0.86	50	0.08	0.94
60	10^{-7}	0.81	60	0.05	0.91

TABLE 6.6.1: OPTIMUM VALUES OF θ AND c FOR THE KALMAN ESTIMATOR 2 AND THE FEEDFORWARD ESTIMATOR 2

		Y'_0	$Y'_{0,-1}$	$(Y'_{0,-1})'$	$P_{0,0}$
Figure 6.6.8	Kalman Estimator 1	0	0	0	$10^6 I$
	Feedforward Estimator 1	0	0	0	-
Figure 6.6.9	Kalman Estimator 1	Y_0	Y_0	0	I
	Feedforward Estimator 1	Y_0	Y_0	0	-
Figure 6.610	Kalman Estimator 2	0	0	0	$10^6 I$
	Feedforward Estimator 2	0	0	0	-
Figure 6.6.11	Kalman Estimator 2	Y_0	Y_0	0	I
	Feedforward Estimator 2	Y_0	Y_0	0	-

TABLE 6.6.2: VARIOUS INITIAL CONDITIONS FOR THE KALMAN ESTIMATORS 1 AND 2 AND THE FEEDFORWARD ESTIMATORS 1 AND 2

Kalman Estimator 1			Feedforward Estimator 1		
ψ	c	θ	ψ	c	θ
5	10^{-5}	0.99	5	0.003	0.99
10	10^{-5}	0.99	10	0.006	0.99
20	10^{-4}	0.99	20	0.010	0.99
30	10^{-4}	0.98	30	0.015	0.98
40	10^{-2}	0.97	40	0.020	0.98
50	10^{-3}	0.96	50	0.020	0.98
60	10^{-4}	0.96	60	0.020	0.98

TABLE 6.6.3: OPTIMUM VALUES OF θ AND c FOR THE KALMAN ESTIMATOR 1 AND THE FEEDFORWARD ESTIMATOR 1

Estimator \ Signal-to-noise ratio, ψ	60	30
Kalman Estimator 2 ($Q_i = cI$)	(-49.6638 dB) 0	(-32.0351 dB) 0
Kalman Estimator 3 ($Q_i = q\, P_{i-1,i-1}$)	1.40	0.23
Kalman Estimator 4 ($Q_i = q\, P_{i-i,i-1} + cI$)	0.28	0.11
Kalman Estimator 1 ($Q_i = cI$)	14.27	1.36
Kalman Estimator 5 ($Q_i = q\, P_{i-1,i-1}$)	13.35	1.28

TABLE 6.6.4: COMPARISON OF THE MEAN-SQUARE ERRORS GIVEN BY THE KALMAN ESTIMATORS, MEASURED IN dB, RELATIVE TO THE KALMAN ESTIMATOR 2

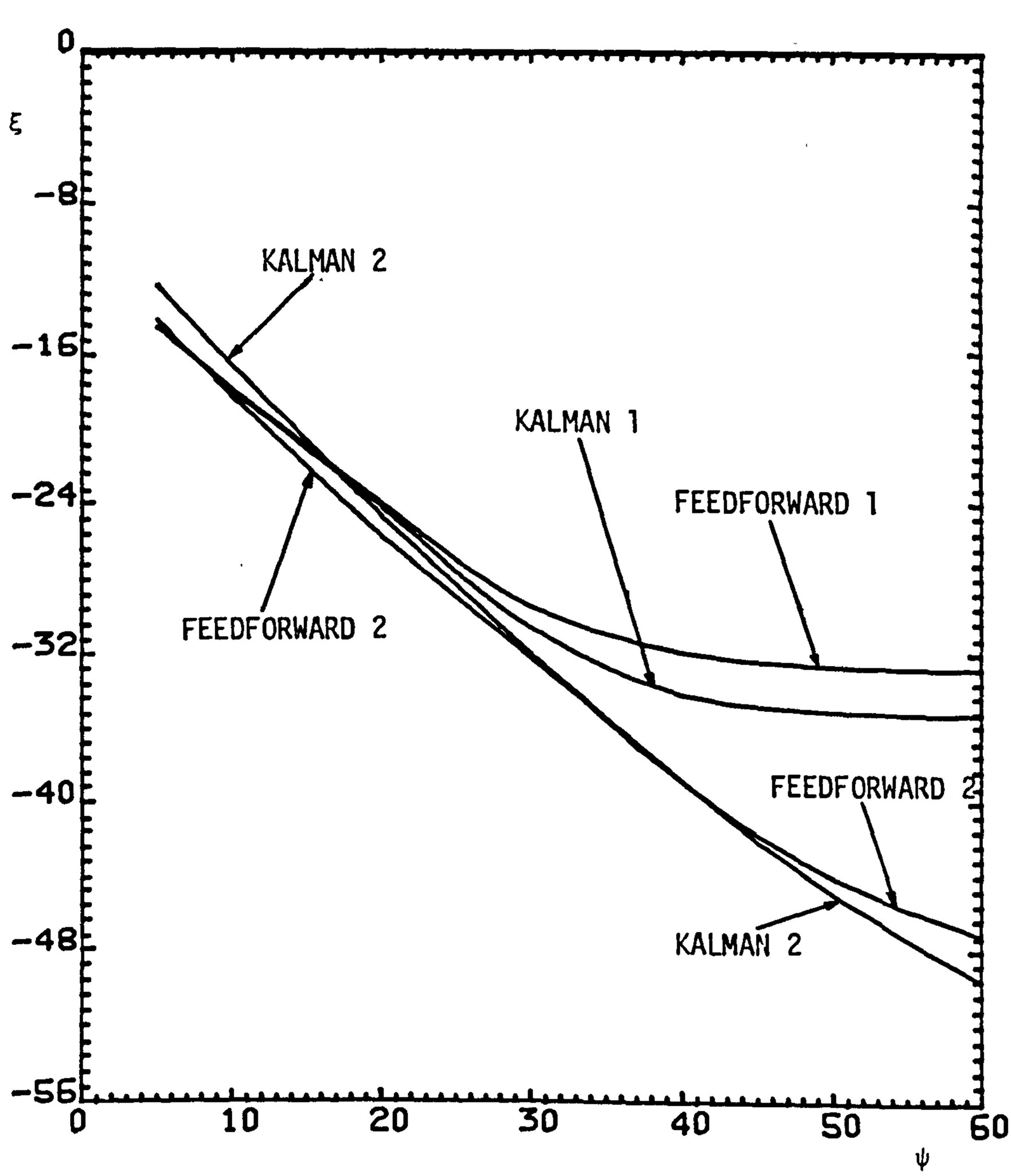

FIGURE 6.6.1: PERFORMANCE OF ESTIMATORS MEASURED BY THE n-STEP PREDICTION
θ AND c OPTIMUM AT EACH ψ

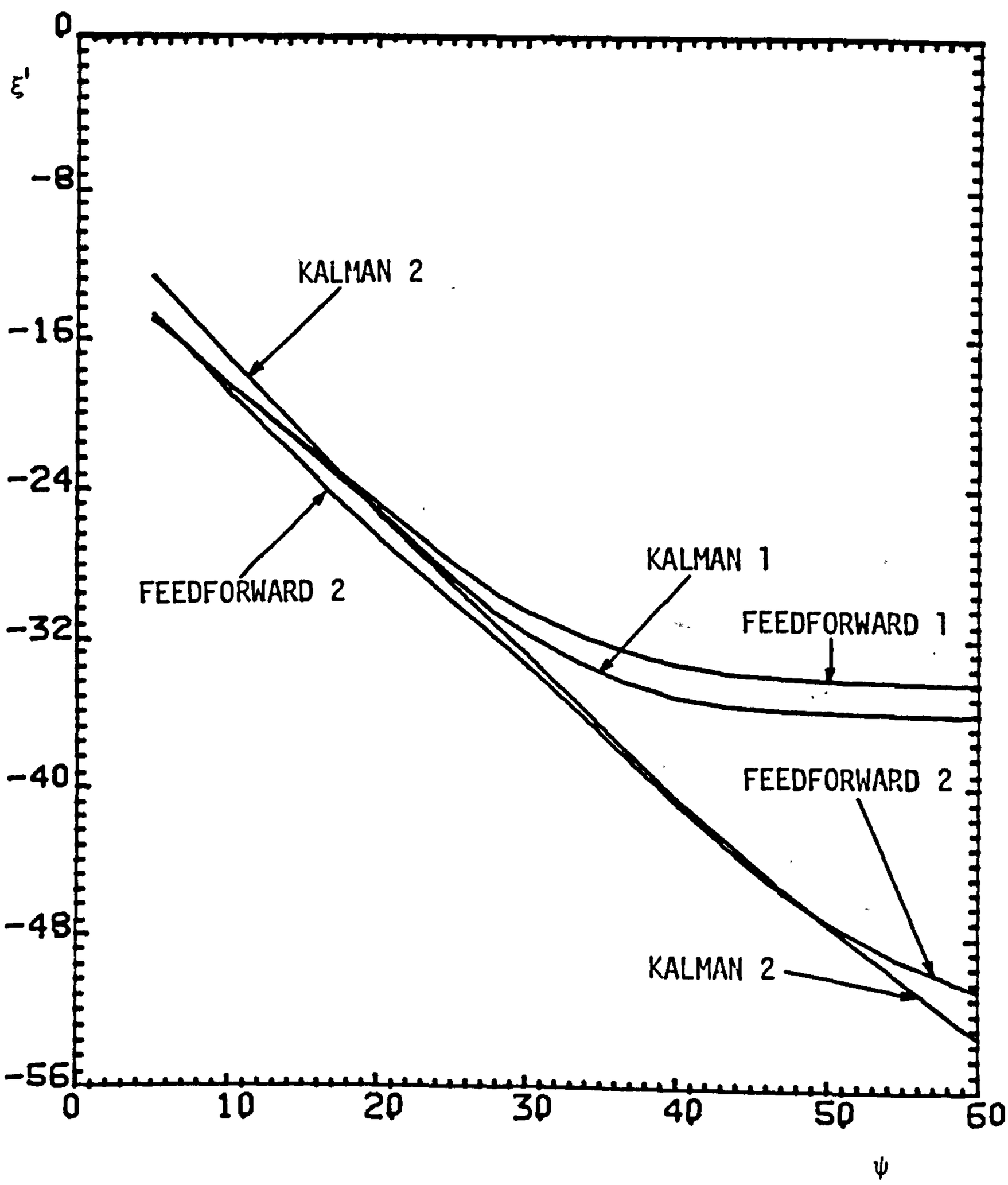

FIGURE 6.6.2: PERFORMANCE OF ESTIMATORS MEASURED BY THE 1-STEP PREDICTION
θ AND c AS FOR FIGURE 6.6.1

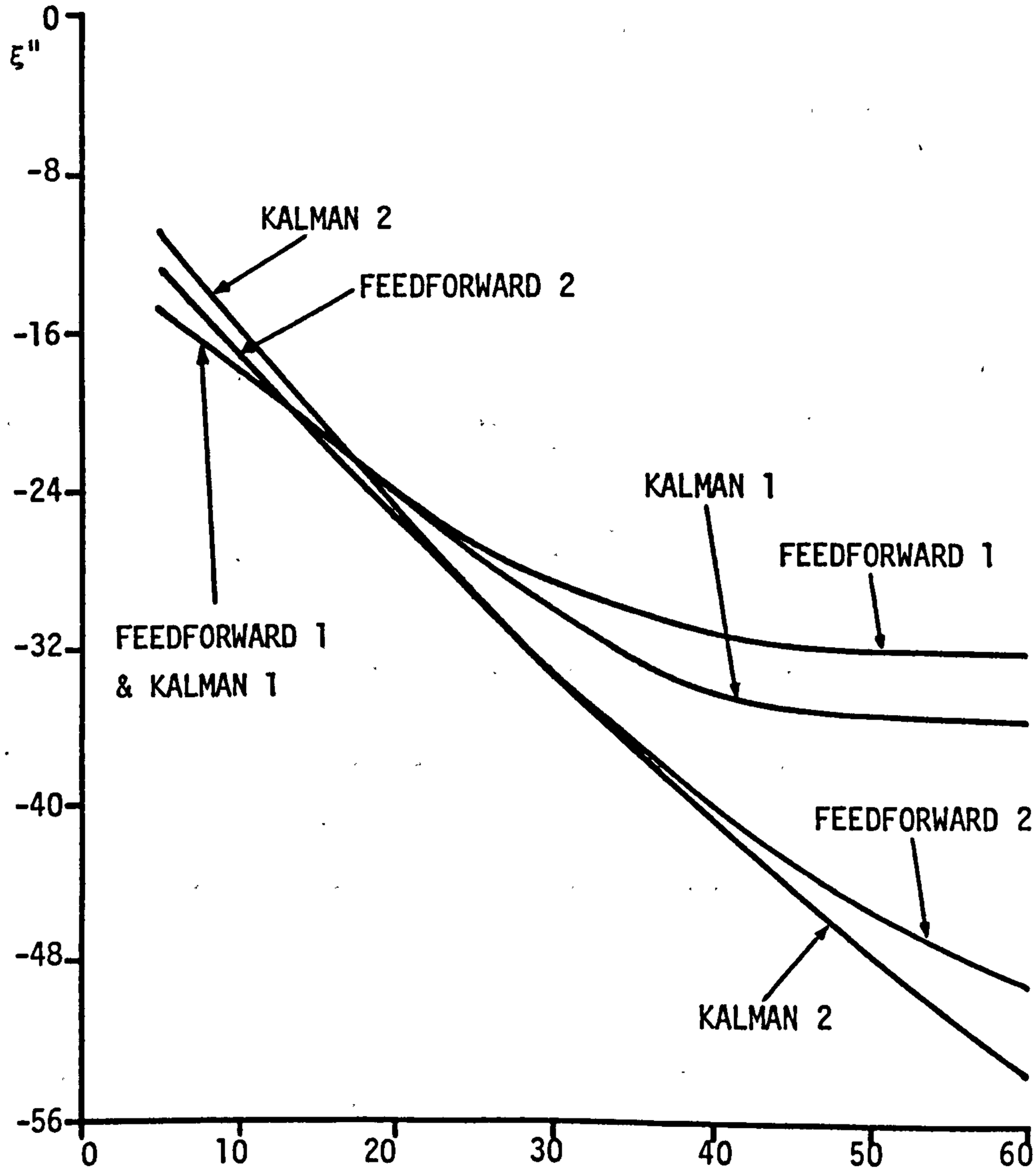

FIGURE 6.6.3: PERFORMANCE OF ESTIMATORS MEASURED BY THE UPDATED ESTIMATE
θ AND c AS FOR FIGURE 6.6.1

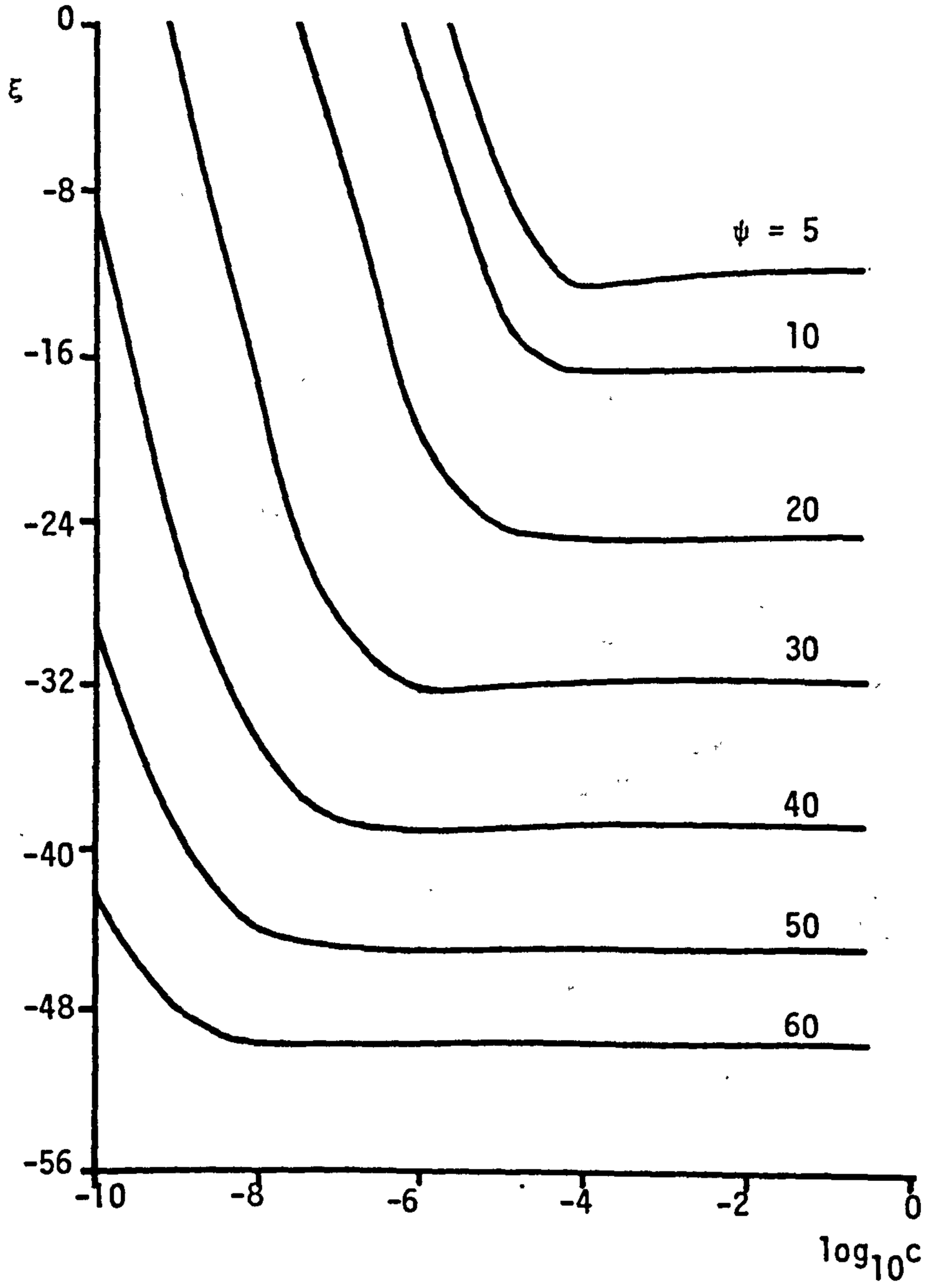

FIGURE 6.6.4: VARIATION OF ξ WITH c FOR KALMAN ESTIMATOR 2
θ OPTIMUM AT EACH ψ

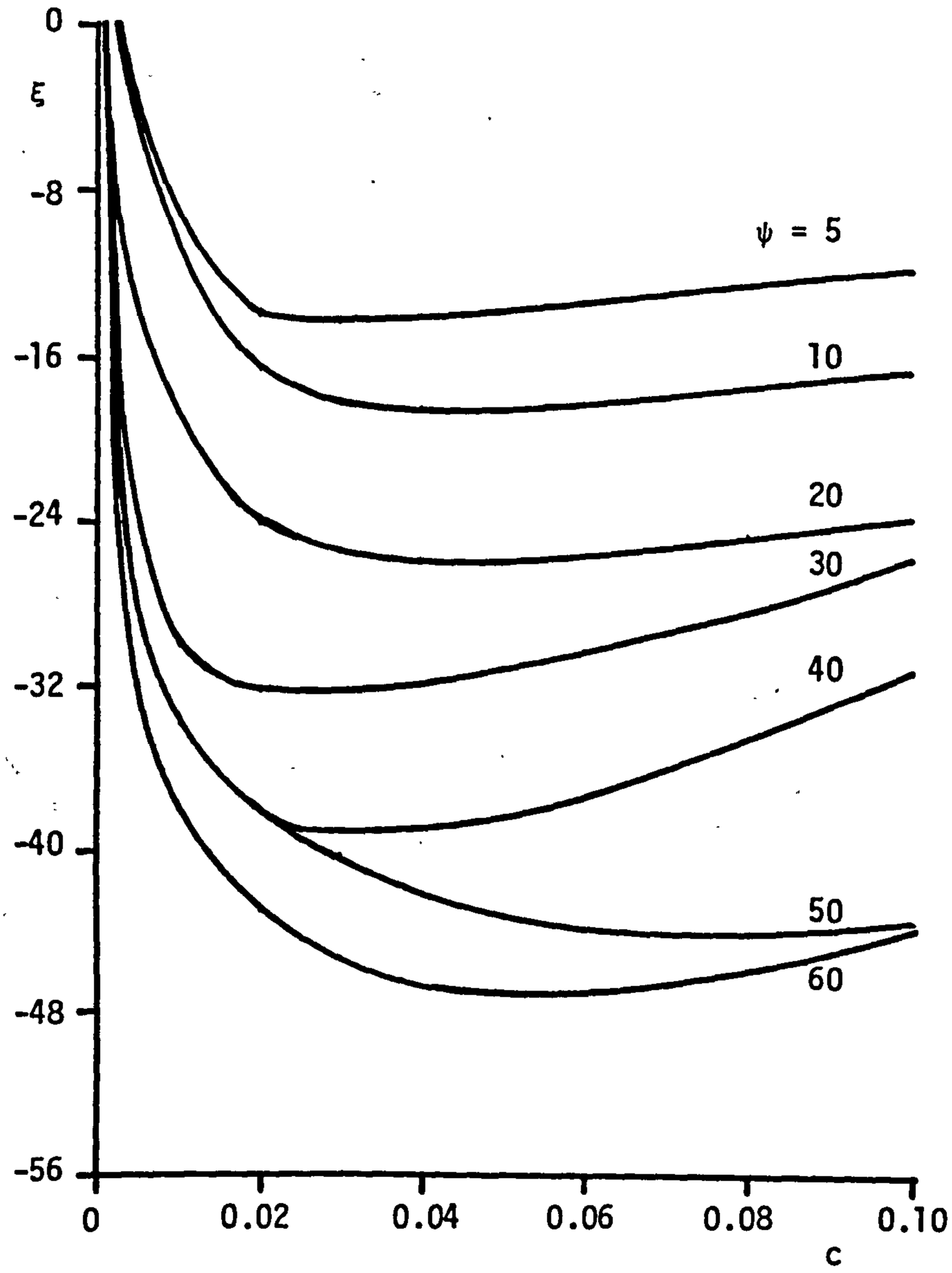

FIGURE 6.6.5: VARIATION OF ξ WITH c FOR FEEDFORWARD ESTIMATOR 2
θ OPTIMUM AT EACH ψ

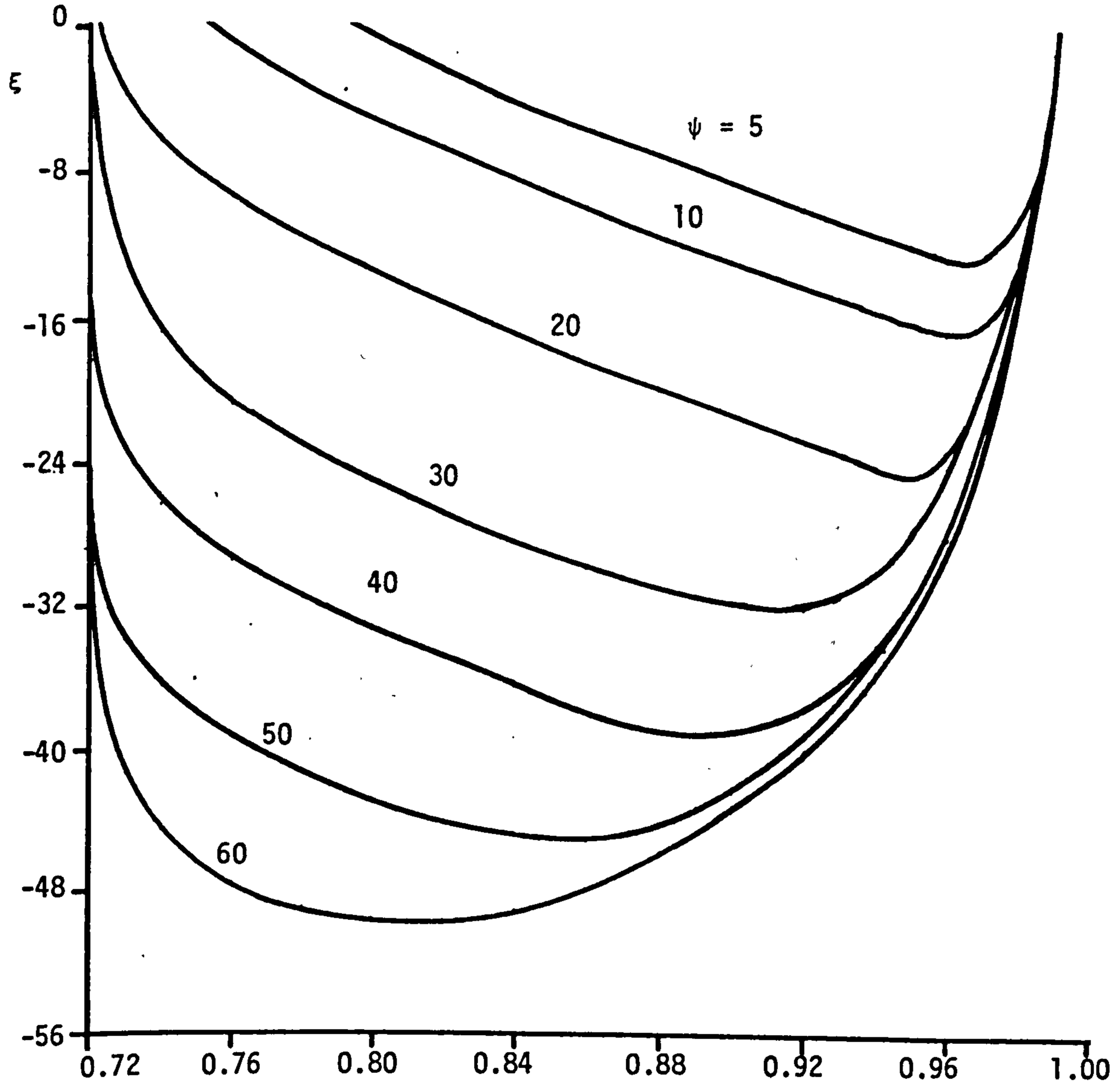

FIGURE 6.6.6: VARIATION OF ξ WITH θ FOR KALMAN ESTIMATOR 2
c OPTIMUM AT EACH ψ

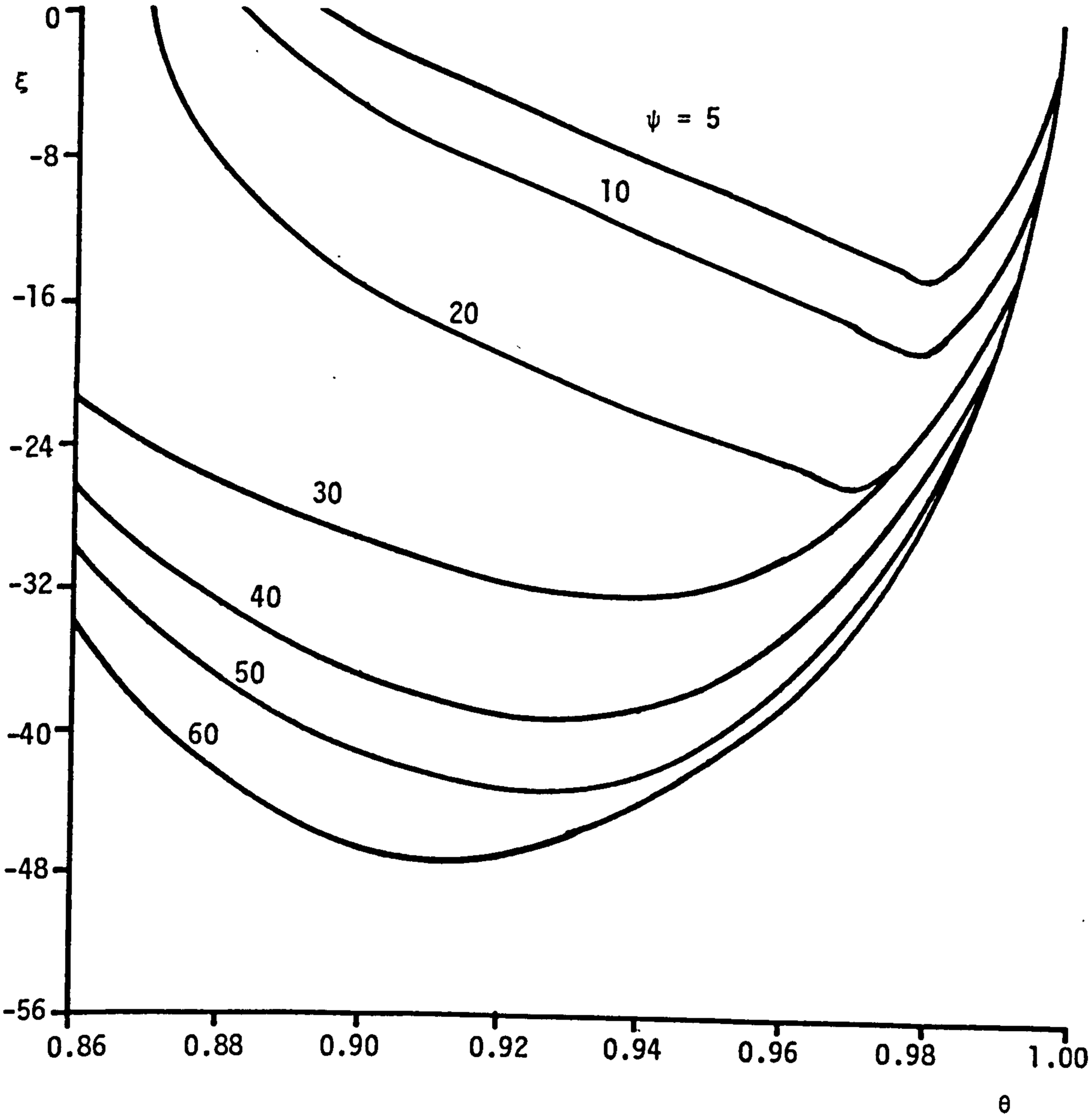

FIGURE 6.6.7: VARIATION OF ξ WITH θ FOR FEEDFORWARD ESTIMATOR 2
c OPTIMUM AT EACH ψ

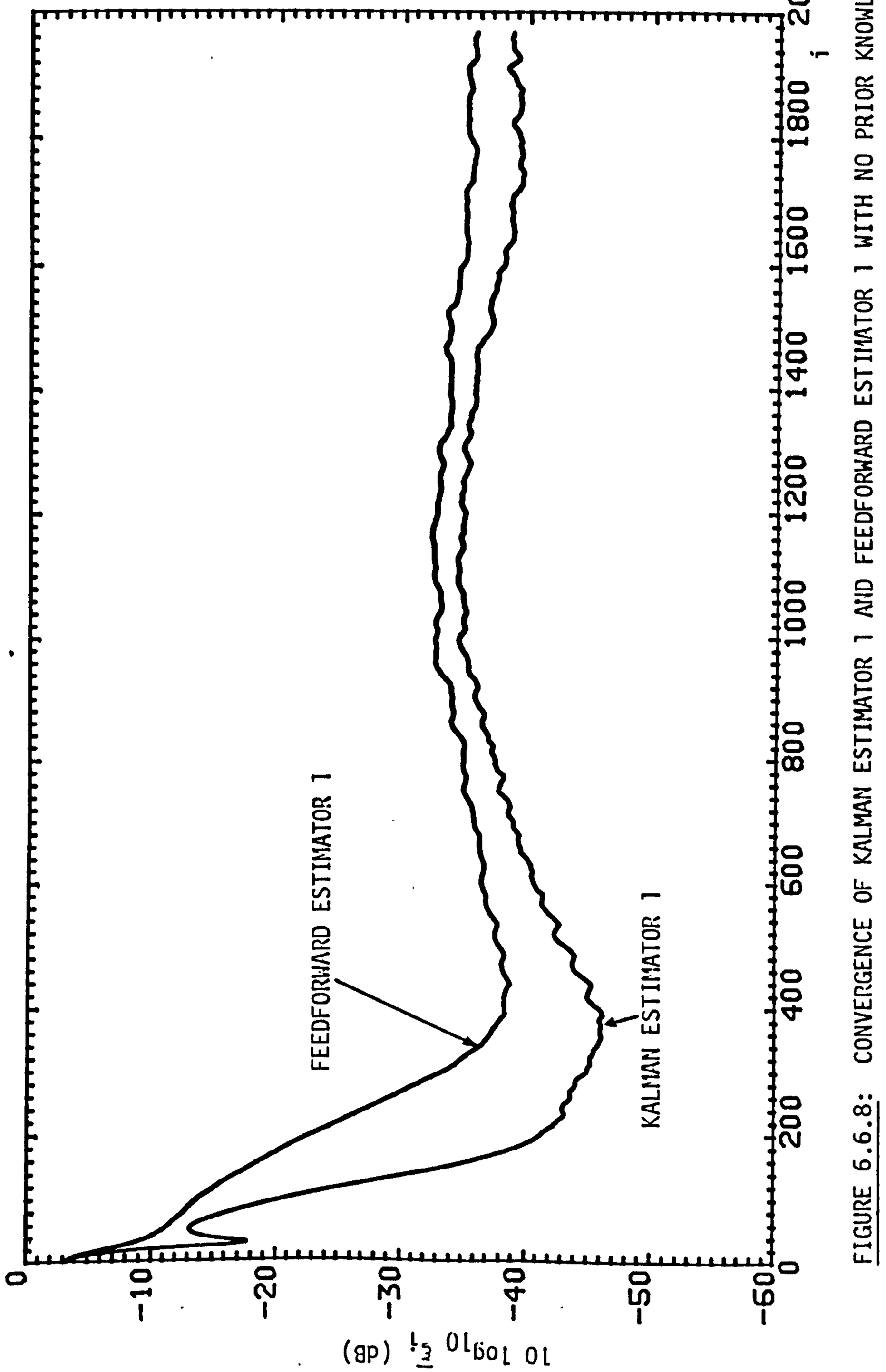
10 log10 ε̄i (dB)
0
-10
-20
-30
-40
-50
-60
0
200
400
600
800
1000
1200
1400
1600
1800
2000
i
FEEDFORWARD ESTIMATOR 1
KALMAN ESTIMATOR 1
CONVERGENCE OF KALMAN ESTIMATOR 1 AND FEEDFORWARD ESTIMATOR 1 WITH NO PRIOR KNOWLEDGE Yi

FIGURE 6.6.8:

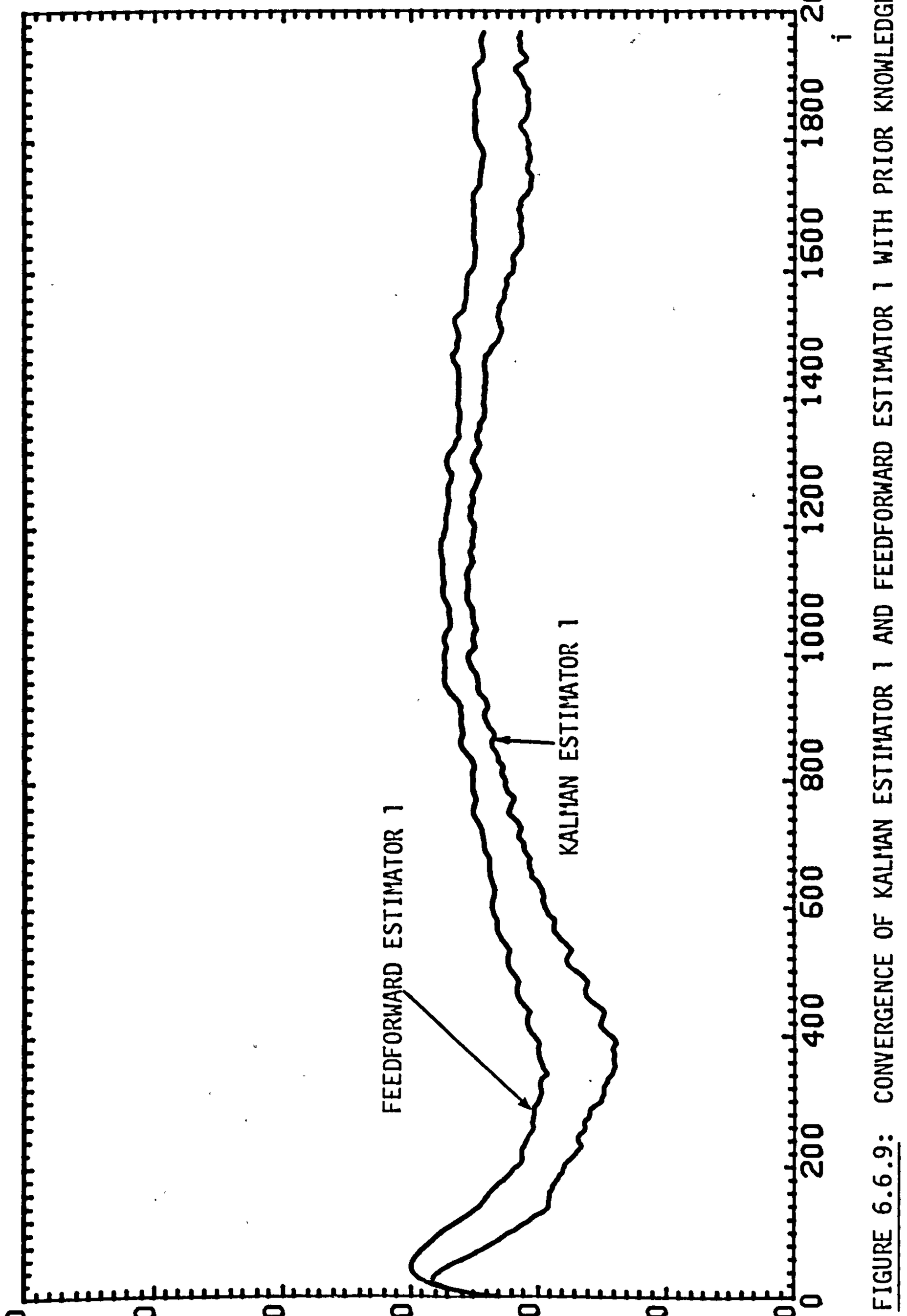

FIGURE 6.6.9: CONVERGENCE OF KALMAN ESTIMATOR 1 AND FEEDFORWARD ESTIMATOR 1 WITH PRIOR KNOWLEDGE OF Y_i

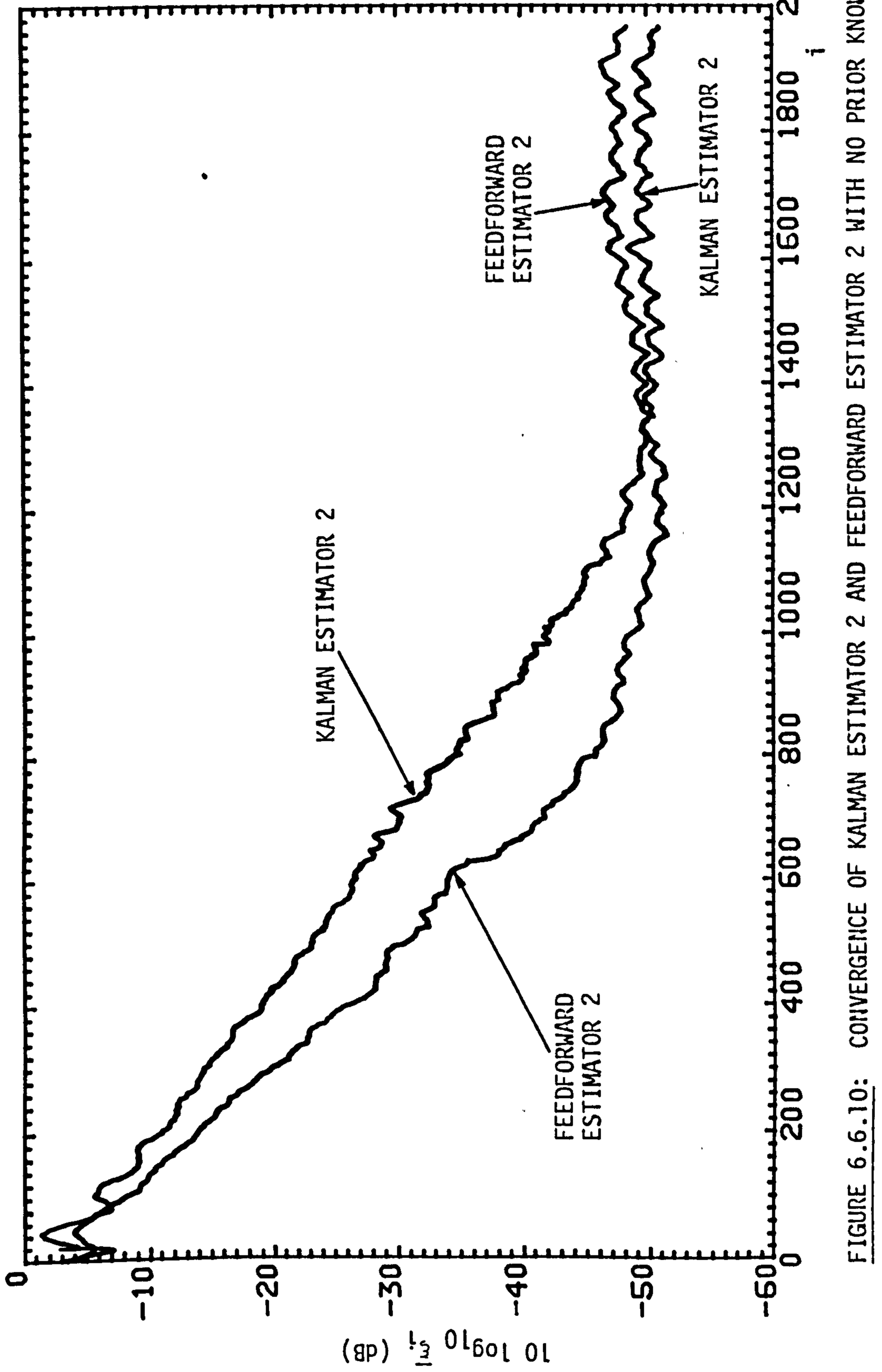

FIGURE 6.6.10: CONVERGENCE OF KALMAN ESTIMATOR 2 AND FEEDFORWARD

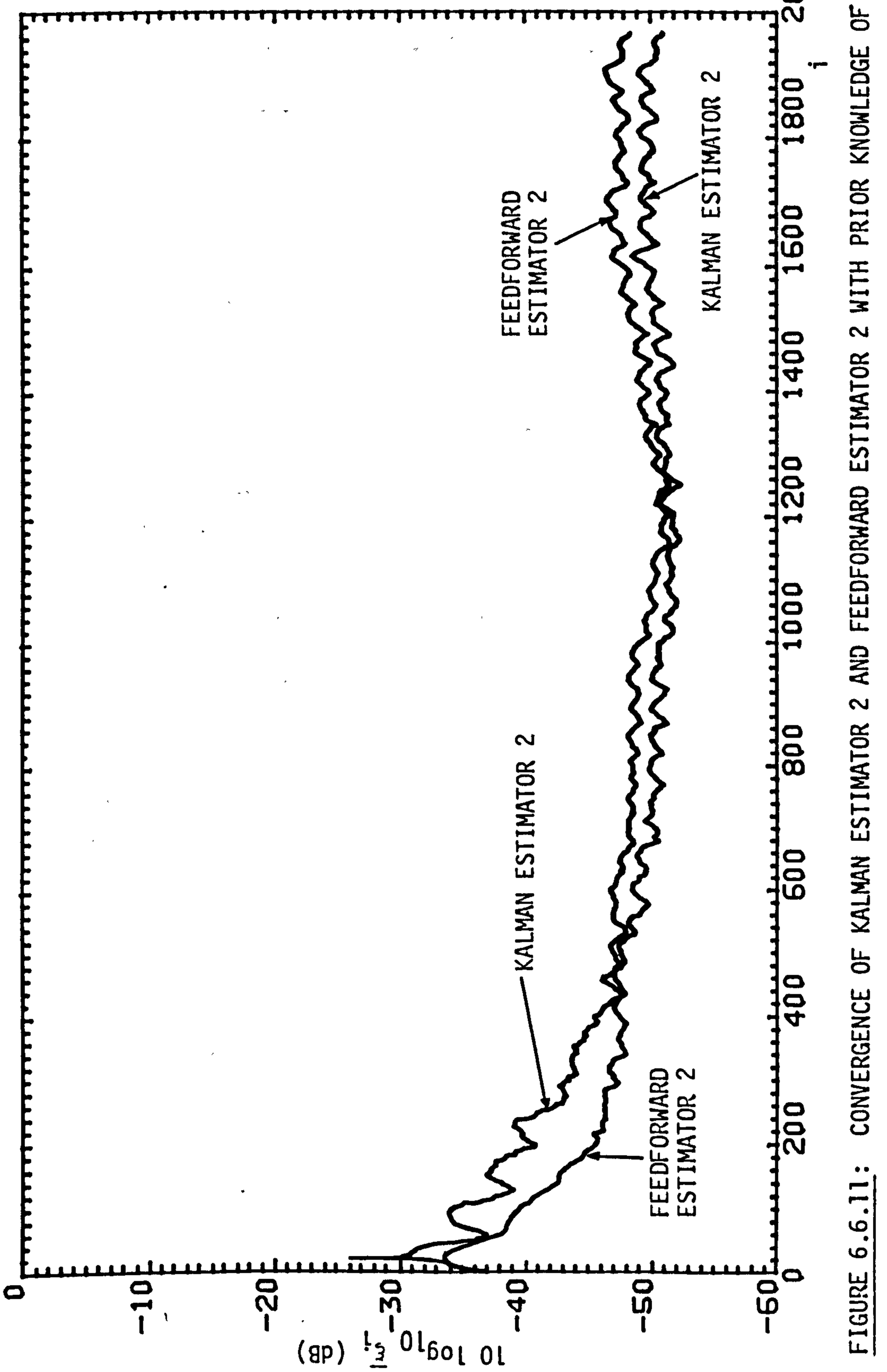

FIGURE 6.6.11: CONVERGENCE OF KALMAN ESTIMATOR 2 AND FEEDFORWARD ESTIMATOR 2 WITH PRIOR KNOWLEDGE OF Y_i

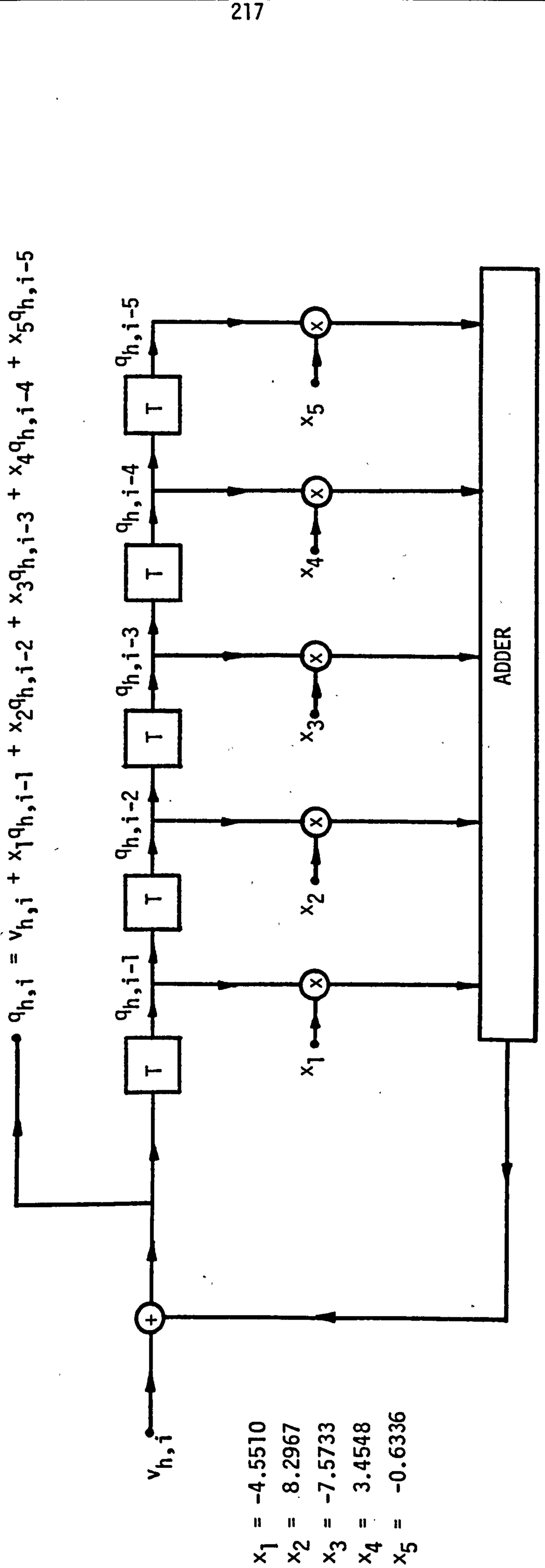

FIGURE 6.6.12: FIFTH ORDER LOWPASS BESSEL FILTER USED FOR GENERATING THE GAUSSIAN RANDOM VARIABLES $\{q_{h,i}\}$

7. IMPROVED CHANNEL ESTIMATOR

7.1 INTRODUCTION

Recently, some computer simulation tests have shown that the performance of a feedforward transversal-filter channel estimator is improved considerably if the estimator knows the basic structure of the HF channel[95]. Specifically, the estimator requires knowledge of the number of sky waves present and assumes that the relative delays in transmission between these sky waves are fixed. This a priori information appears to be of limited use, but as we shall see later, it is exploited very well by the estimator when making an estimate of the channel. These conclusions are drawn from tests carried out using a model of an HF radio link that has two Rayleigh fading sky waves[95]. The HF radio link is part of a synchronous serial data transmission system which transmits data at the rate of 9600 bit/s using quadrature amplitude modulation.

The improved channel estimator is further studied here so as to gain deeper insights into the structure and the method of operation of the estimator. [The essential difference in the conditions under which the estimator is tested, from those in Ref. 95, where a two-sky-wave model of the channel is used, is that three sky waves are now present.] The latter is considered as a typical poor channel condition over actual HF radio links. The model of the data-transmission system used here, is basically the same as that in Section 6, but with several differences which are outlined in Section 7.2. One of these involves the property of the sampled

impulse-responses of the transmitter and receiver filters. Here, the impulse responses of the filters are made minimum phase. The conversion of the impulse responses to minimum phase is described in Appendix A1. The derivation of the improved channel estimator is given in Section 7.3. The estimator is tested by computer simulation and the results are presented and analysed in Sections 7.4.1-7.4.8.

7.2 MODEL OF DATA-TRANSMISSION SYSTEM USED IN THE TESTS

The model of the data-transmission system that is used in the computer simulation tests, the results of which are presented in Section 7.4 is basically the same as that previously described in Section 6.2, but with the following exceptions:

1. It is assumed that the data signal is here transmitted via three independent Rayleigh fading sky waves. This represents typical poor channel conditions over actual HF radio links[111,123]. In the model of the HF radio link (Section 4.4), six waveforms $q_h(t)$, where $h = 1,2,\ldots,6$, are now required for generating the corresponding fading sequences $\{q_{h,i}\}$. The variance of each $q_h(t)$ is arranged to be $\frac{1}{6}$, so that the sum of the variances is still equal to 1. Thus, the sky waves, here, also do not introduce, on average, any gain or attenuation into the transmitted data signal. The required variances are achieved by adjusting the gain K at the input of the digital Bessel filter (Section 4.4, Figure 4.4.5). Table 4.4.2 gives, for each filter,

the value of K which sets the variance of each sequence $\{q_{h,i}\}$ to $\frac{1}{4}$. Clearly, the gain K is different here. Table 7.2.1 gives the values of K (or, in fact, K^{-1}) for the three filters. The relative delays in transmission between the different sky waves are also given in Table 7.2.1. In this table, τ_1 is the relative delay in transmission between the first and the second sky waves, and τ_2 is that between the first and the third sky waves. As before, the average attenuation introduced by the HF radio link is zero.

Channel		1	2	3
Frequency spread, f_{sp} (Hz)		$\frac{1}{2}$	1	2
Constant, K^{-1}		398805.63	19744.873	1093.7761
Relative delay in transmission	τ_1 (ms)	$\frac{1}{3}$	1	$\frac{2}{3}$
	τ_2 (ms)	1	2	3

TABLE 7.2.1: VARIOUS PARAMETERS ASSOCIATED WITH THE MODEL OF THE HF RADIO LINK

(2.) The sampled impulse-responses of the transmitter and receiver filters are here minimum phase. These filters represent the overall filtering carried out at the appropriate ends of the system. The reasons and method used for converting the sampled impulse-responses to minimum phase are discussed in Appendix A1.

Apart from these two exceptions, all the assumptions made in Section 6.2 are valid here.

7.3 DERIVATION OF IMPROVED CHANNEL ESTIMATOR

In the analysis to be presented here, it is assumed that the data signal is transmitted via three independent sky waves and that the time delay introduced in transmission over each of the sky waves is taken to be fixed over the duration of the data signal. It is also assumed that correct sampling frequency is used at the receiver. Now, since the resultant impulse response of the combined transmitter and receiver filters extends over only a few sampling intervals and the rate of fading in the received data signal is very small compared with the signal-element rate, the sampled impulse-response of the linear baseband channel, at time t=iT, can be taken to be,

$$Y_i = \lambda_i L + \mu_i M + \rho_i N \qquad (7.3.1)$$

where L, M and N are fixed (g+1)-component vectors with complex-valued components and, λ_i, μ_i and ρ_i are complex-valued scalars which vary with i. Clearly, from the properties of $q_h(t)$ (Section 4.4), the real and imaginary part of λ_i, μ_i and ρ_i are statistically independent Gaussian random variables with zero mean and the same variance. Therefore $\{\lambda_i\}$, $\{\mu_i\}$ and $\{\rho_i\}$ are uncorrelated; however, neighbouring values of each random variable are highly correlated. Each of the terms in Y_i (equation 7.3.1) corresponds to the sampled impulse-response of the corresponding sky wave, so that, Y_i has the value

$\lambda_i L$, $\mu_i M$ or $\rho_i N$ if only the first, second or third sky wave is present, respectively.

Equation 7.3.1 is correct at all times if the data signal in the demodulated waveform r(t) is shaped entirely by the linear filters (Figure 6.2.1) that precede the HF radio link; but when the receiver filter also introduces some signal shaping, equation 7.3.1 is no longer accurate, especially during the deepest fades. However, results of an investigation[16] have indicated that with the filter actually used, equation 7.3.1 is still, for practical purposes, correct for the data-transmission system assumed.

Clearly, from equation 7.3.1, if the receiver can determine the time-invariant vectors L, M and N, then an estimate of Y_i is obtained by estimating only the random variables λ_i, μ_i and ρ_i. However, the vectors L, M and N are not easily determined; they are not normally orthogonal or even related in any very simple manner. But it is evident from equation 7.3.1 that the vector Y_i must lie in a three-dimensional subspace spanned by L, M and N, in the (g+1)-dimensional unitary vector space containing all (g+1)-component vectors over the complex field. Since, L, M and N are fixed the subspace spanned by these vectors is also fixed, so that the receiver needs only estimate the subspace. This is achieved by estimating three orthonormal vectors A, B and C which also span the subspace, such that

$$Y_i = a_i A + b_i B + c_i C \qquad (7.3.2)$$

for all {i}. The scalars, a_i, b_i and c_i and the components of A, B and C are all complex-valued. The vectors A, B and C are all of unit length and they could lie anywhere in the subspace, but are orthogonal to each other at all times.

Just prior to the reception of r_{i+n}, the receiver holds the vectors

$$A_i = [a_{i,0}\ a_{i,1} \cdots a_{i,g}]^T \tag{7.3.3}$$

$$B_i = [b_{i,0}\ b_{i,1} \cdots b_{i,g}]^T \tag{7.3.4}$$

and

$$C_i = [c_{i,0}\ c_{i,1} \cdots c_{i,g}]^T \tag{7.3.5}$$

which are the estimates of A, B and C, respectively. The formation of these vectors will be described later. Since A_i, B_i and C_i are only estimates of A, B and C, they do not lie exactly in the subspace spanned by A, B and C, but lie close to the subspace. At time $t=(i+n)T$, r_i and the detected symbol s_i' are fed to the feedforward transversal-filter estimator, which, together with the value of the 1-step prediction of Y_i, form an estimate Y_i' of Y_i (see Section 6.4). Since Y_i' normally does not lie in the three-dimensional subspace spanned by A_i, B_i and C_i, an improved estimate of Y_i is formed by projecting Y_i' orthogonally onto the three-dimensional subspace. The vector that lies in the subspace resulting from the projection is given by,

$$F_i = \alpha_i A_i + \beta_i B_i + \gamma_i C_i \qquad (7.3.6)$$

where α_i, β_i and γ_i are obtained as follows. Since $Y_i' - F_i$ is orthogonal to the three-dimensional subspace, it is also orthogonal to the vectors A_i, B_i and C_i. Thus,

$$A_i^{*T} (Y_i' - F_i) = 0 \qquad (7.3.7)$$

$$B_i^{*T} (Y_i' - F_i) = 0 \qquad (7.3.8)$$

and

$$C_i^{*T} (Y_i' - F_i) = 0 \qquad (7.3.9)$$

where A_i^{*T}, B_i^{*T} and C_i^{*T} are the conjugate transposes of A_i, B_i and C_i, respectively. Substituting the value of F_i from equation 7.3.6 into equations 7.3.7-7.3.9, we have,

$$A_i^{*T} (Y_i' - \alpha_i A_i - \beta_i B_i - \gamma_i C_i) = 0 \qquad (7.3.10)$$

$$B_i^{*T} (Y_i' - \alpha_i A_i - \beta_i B_i - \gamma_i C_i) = 0 \qquad (7.3.11)$$

and

$$C_i^{*T} (Y_i' - \alpha_i A_i - \beta_i B_i - \gamma_i C_i) = 0 \qquad (7.3.12)$$

A_i, B_i and C_i are orthonormal vectors which means

$$A_i^{*T} A_i = B_i^{*T} B_i = C_i^{*T} C_i = 1 \qquad (7.3.13)$$

and $$A_i^{*T}B_i = B_i^{*T}A_i = C_i^{*T}A_i = C_i^{*T}B_i = A_i^{*T}C_i = B_i^{*T}C_i = 0 \qquad (7.3.14)$$

Using this property, the values of α_i, β_i and γ_i are obtained from equations 7.3.10, 7.3.11 and 7.3.12, respectively

$$\alpha_i = A_i^{*T}Y_i' \qquad (7.3.15)$$

$$\beta_i = B_i^{*T}Y_i' \qquad (7.3.16)$$

and $$\gamma_i = C_i^{*T}Y_i' \qquad (7.3.17)$$

As previously mentioned, A_i, B_i and C_i are unlikely to lie exactly in the three-dimensional subspace containing Y_i and, in addition, the vectors L, M and N may in fact vary slowly with time, so also may the subspace. Therefore, for satisfactory operation, the subspace spanned by A_i, B_i and C_i should be adjusted adaptively to track the received signal. The adjustment is made using Y_i' such that the new subspace spanned by A_{i+1}, B_{i+1} and C_{i+1} is slightly closer to Y_i'. For the minimum change in the subspace spanned by A_i, B_i and C_i, corresponding to a given small reduction in the distance $|Y_i' - F_i|$, the subspace must be rotated towards Y_i', the rotation being pivoted about a two-dimensional subspace which lies in the subspace spanned by A_i, B_i and C_i and also is orthogonal to F_i. If we let

$$E_i = Y_i' - F_i \qquad (7.3.18)$$

then, the vectors in the new three-dimensional subspace that correspond to the vectors $\alpha_i A_i$, $\beta_i B_i$ and $\gamma_i C_i$ in the original subspace are approximately,

$$\alpha_i A'_{i+1} = \alpha_i A_i + \eta|\alpha_i|^2 E_i \qquad (7.3.19)$$

$$\beta_i B'_{i+1} = \beta_i B_i + \eta|\beta_i|^2 E_i \qquad (7.3.20)$$

and

$$\gamma_i C'_{i+1} = \gamma_i C_i + \eta|\gamma_i|^2 E_i \qquad (7.3.21)$$

where η is a small positive real quantity. Simplifying equations 7.3.19-7.3.21, gives,

$$A'_{i+1} = A_i + \eta\alpha_i^* E_i \qquad (7.3.22)$$

$$B'_{i+1} = B_i + \eta\beta_i^* E_i \qquad (7.3.23)$$

and

$$C'_{i+1} = C_i + \eta\gamma_i^* E_i \qquad (7.3.24)$$

where α_i^*, β_i^* and γ_i^* are the conjugates of α_i, β_i and γ_i, respectively. The vectors A'_{i+1}, B'_{i+1} and C'_{i+1} form a basis of a new three-dimensional subspace. Clearly, from equations 7.3.22-7.3.24, the vectors A'_{i+1}, B'_{i+1} and C'_{i+1} are not exactly orthonormal and so they are orthonormalized using the Gram-Schmidt orthonormalization process[98], as follows. First the receiver sets

$$A_{i+1} = |A'_{i+1}|^{-1}A'_{i+1} \tag{7.3.25}$$

so that $|A_{i+1}| = 1$, and then

$$B''_{i+1} = B'_{i+1} - A^{*T}_{i+1}B'_{i+1}A_{i+1} \tag{7.3.26}$$

and $$B_{i+1} = |B''_{i+1}|^{-1}B''_{i+1} \tag{7.3.27}$$

so that $|B_{i+1}| = 1$ and $A^{*T}_{i+1}B_{i+1} = 0$, and finally

$$C''_{i+1} = C'_{i+1} - B^{*T}_{i+1}C'_{i+1}B_{i+1} - A^{*T}_{i+1}C'_{i+1}A_{i+1} \tag{7.3.28}$$

and $$C_{i+1} = |C''_{i+1}|^{-1}C''_{i+1} \tag{7.3.29}$$

so that $|C_{i+1}| = 1$ and $A^{*T}_{i+1}C_{i+1} = B^{*T}_{i+1}C_{i+1} = 0$.

The receiver next predicts the values of α_{i+1}, β_{i+1} and γ_{i+1} using least-squares fading-memory prediction[44]. If $\alpha_{i,i-1}$, $\beta_{i,i-1}$ and $\gamma_{i,i-1}$ are the previously derived predictions of α_i, β_i and γ_i, respectively, then the errors in these predictions are,

$$\varepsilon_{\alpha,i} = \alpha_i - \alpha_{i,i-1} \tag{7.3.30}$$

$$\varepsilon_{\beta,i} = \beta_i - \beta_{i,i-1} \tag{7.3.31}$$

and $$\varepsilon_{\gamma,i} = \gamma_i - \gamma_{i,i-1} \tag{7.3.32}$$

where α_i, β_i and γ_i have been found using equations 7.3.15, 7.3.16 and 7.3.17, respectively. The 1-step predictions are obtained as follows.

Degree-0 prediction:

$$\alpha_{i+1,i} = \alpha_{i,i-1} + (1-\theta)\varepsilon_{\alpha,i} \qquad (7.3.33)$$

$$\beta_{i+1,i} = \beta_{i,i-1} + (1-\theta)\varepsilon_{\beta,i} \qquad (7.3.34)$$

$$\gamma_{i+1,i} = \gamma_{i,i-1} + (1-\theta)\varepsilon_{\gamma,i} \qquad (7.3.35)$$

Degree-1 prediction:

$$\alpha'_{i+1,i} = \alpha'_{i,i-1} + (1-\theta)^2\varepsilon_{\alpha,i} \qquad (7.3.36)$$

$$\beta'_{i+1,i} = \beta'_{i,i-1} + (1-\theta)^2\varepsilon_{\beta,i} \qquad (7.3.37)$$

$$\gamma'_{i+1,i} = \gamma'_{i,i-1} + (1-\theta)^2\varepsilon_{\gamma,i} \qquad (7.3.38)$$

$$\alpha_{i+1,i} = \alpha_{i,i-1} + \alpha'_{i+1,i} + (1-\theta^2)\varepsilon_{\alpha,i} \qquad (7.3.39)$$

$$\beta_{i+1,i} = \beta_{i,i-1} + \beta'_{i+1,i} + (1-\theta^2)\varepsilon_{\beta,i} \qquad (7.3.40)$$

$$\gamma_{i+1,i} = \gamma_{i,i-1} + \gamma'_{i+1,i} + (1-\theta^2)\varepsilon_{\gamma,i} \qquad (7.3.41)$$

Degree-2 prediction:

$$\alpha''_{i+1,i} = \alpha''_{i,i-1} + \frac{1}{2}(1-\theta)^3\varepsilon_{\alpha,i} \qquad (7.3.42)$$

$$\beta''_{i+1,i} = \beta''_{i,i-1} + \frac{1}{2}(1-\theta)^3\varepsilon_{\beta,i} \qquad (7.3.43)$$

$$\gamma''_{i+1,i} = \gamma''_{i,i-1} + \frac{1}{2}(1-\theta)^3\varepsilon_{\gamma,i} \qquad (7.3.44)$$

$$\alpha'_{i+1,i} = \alpha'_{i,i-1} + 2\alpha''_{i+1,i} + \frac{3}{2}(1-\theta)^2(1+\theta)\varepsilon_{\alpha,i} \qquad (7.3.45)$$

$$\beta'_{i+1,i} = \beta'_{i,i-1} + 2\beta''_{i+1,i} + \frac{3}{2}(1-\theta)^2(1+\theta)\varepsilon_{\beta,i} \qquad (7.3.46)$$

$$\gamma'_{i+1,i} = \gamma'_{i,i-1} + 2\gamma^{u}_{i+1,i} + \frac{3}{2}(1-\theta)^2(1+\theta)\varepsilon_{\gamma,i} \qquad (7.3.47)$$

$$\alpha_{i+1,i} = \alpha_{i,i-1} + \alpha'_{i+1,i} - \alpha''_{i+1,i} + (1-\theta^3)\varepsilon_{\alpha,i} \qquad (7.3.48)$$

$$\beta_{i+1,i} = \beta_{i,i-1} + \beta'_{i+1,i} - \beta''_{i+1,i} + (1-\theta^3)\varepsilon_{\beta,i} \qquad (7.3.49)$$

$$\gamma_{i+1,i} = \gamma_{i,i-1} + \gamma'_{i+1,i} - \gamma''_{i+1,i} + (1-\theta^3)\varepsilon_{\gamma,i} \qquad (7.3.50)$$

where $\alpha'_{i+1,i}$, $\beta'_{i+1,i}$ and $\gamma'_{i+1,i}$ are measures of the rates of change of α_i, β_i and γ_i respectively; and $\alpha''_{i+1,i}$, $\beta''_{i+1,i}$ and $\gamma''_{i+1,i}$ give an

indication of the corresponding accelerations. θ is a positive real constant in the range of 0 to 1 and generally close to 1. Having obtained the 1-step predictions $\alpha_{i+1,i}$, $\beta_{i+1,i}$ and $\gamma_{i+1,i}$ and also the vectors A_{i+1}, B_{i+1} and C_{i+1}, the receiver forms the prediction of Y_{i+1} as,

$$Y'_{i+1,i} = \alpha_{i+1,i}A_{i+1} + \beta_{i+1,i}B_{i+1} + \gamma_{i+1,i}C_{i+1} \quad (7.3.51)$$

$Y'_{i+1,i}$ is required by the complex feedforward transversal-filter estimator, on the receipt of r_{i+1} at the input of the estimator, firstly to form an estimate of r_{i+1} (equation 6.4.1) and secondly, after forming the error signal e_{i+1} (equation 6.4.2), to form the updated estimate Y'_{i+1} of Y_{i+1} (equation 6.4.4).

The receiver is also required to determine the n-step prediction $Y'_{i+n,i}$ of Y_{i+n} for use in the detection of s_{i+1} at time $t=(i+n)T$. This is obtained as follows. First, the receiver computes the n-step predictions of α_{i+n}, β_{i+n} and γ_{i+n} as,

Degree-0 prediction:

$$\alpha_{i+n,i} = \alpha_{i+1,i} \quad (7.3.52)$$

$$\beta_{i+n,i} = \beta_{i+1,i} \quad (7.3.53)$$

$$\gamma_{i+n,i} = \gamma_{i+1,i} \quad (7.3.54)$$

Degree-1 prediction:

$$\alpha_{i+n,i} = \alpha_{i+1,i} + (n-1)\alpha'_{i+1,i} \tag{7.3.55}$$

$$\beta_{i+n,i} = \beta_{i+1,i} + (n-1)\beta'_{i+1,i} \tag{7.3.56}$$

$$\gamma_{i+n,i} = \gamma_{i+1,i} + (n-1)\gamma'_{i+1,i} \tag{7.3.57}$$

Degree-2 prediction:

$$\alpha_{i+n,i} = \alpha_{i+1,i} + (n-1)\alpha'_{i+1,i} + (n-1)^2\alpha''_{i+1,i} \tag{7.3.58}$$

$$\beta_{i+n,i} = \beta_{i+1,i} + (n-1)\beta'_{i+1,i} + (n-1)^2\beta''_{i+1,i} \tag{7.3.59}$$

$$\gamma_{i+n,i} = \gamma_{i+1,i} + (n-1)\gamma'_{i+1,i} + (n-1)^2\gamma''_{i+1,i} \tag{7.3.60}$$

The n-step prediction $Y'_{i+n,i}$ is given by

$$Y'_{i+n,i} = \alpha_{i+n,i}A_{i+1} + \beta_{i+n,i}B_{i+1} + \gamma_{i+n,i}C_{i+1} \tag{7.3.61}$$

The performance of the estimator is judged by the accuracy of the n-step prediction $Y'_{i+n,i}$ as this is the information that is used in the detection of the data symbols. It is evident that a single estimation process involves many steps and these will be listed below in the order of use. In this listing, it is assumed that the vectors A'_i,

B_i' and C_i' are orthonormalized at each i, and degree-1 prediction is used.

Step 1 $$r_i' = \sum_{h=0}^{q} s_{i-h}' y_{i,i-1,h}'$$

Step 2 $$e_i = r_i - r_i'$$

Step 3 $$Y_i' = Y_{i,i-1}' + ce_i S_i^*$$

Step 4 $$\alpha_i = A_i^{*T} Y_i'$$

$$\beta_i = B_i^{*T} Y_i'$$

$$\gamma_i = C_i^{*T} Y_i'$$

Step 5 $$F_i = \alpha_i A_i + \beta_i B_i + \gamma_i C_i$$

Step 6 $$E_i = Y_i' - F_i$$

Step 7 $$A_{i+1}' = A_i + \eta\alpha_i^* E_i$$

$$B_{i+1}' = B_i + \eta\beta_i^* E_i$$

$$C_{i+1}' = C_i + \eta\gamma_i^* E_i$$

Step 8

$$A_{i+1} = |A'_{i+1}|^{-1}A'_{i+1}$$

$$B''_{i+1} = B'_{i+1} - A^{*T}_{i+1}B'_{i+1}A_{i+1}$$

$$B_{i+1} = |B''_{i+1}|^{-1}B''_{i+1}$$

$$C''_{i+1} = C'_{i+1} - B^{*T}_{i+1}C'_{i+1}B_{i+1} - A^{*T}_{i+1}C'_{i+1}A_{i+1}$$

$$C_{i+1} = |C''_{i+1}|^{-1}C''_{i+1}$$

Step 9

$$\varepsilon_{\alpha,i} = \alpha_i - \alpha_{i,i-1}$$

$$\varepsilon_{\beta,i} = \beta_i - \beta_{i,i-1}$$

$$\varepsilon_{\gamma,i} = \gamma_i - \gamma_{i,i-1}$$

$$\alpha'_{i+1,i} = \alpha'_{i,i-1} + (1-\theta)^2\varepsilon_{\alpha,i}$$

$$\beta'_{i+1,i} = \beta'_{i,i-1} + (1-\theta)^2\varepsilon_{\beta,i}$$

$$\gamma'_{i+1,i} = \gamma'_{i,i-1} + (1-\theta)^2\varepsilon_{\gamma,i}$$

$$\alpha_{i+1,i} = \alpha_{i,i-1} + \alpha'_{i+1,i} + (1-\theta^2)\varepsilon_{\alpha,i}$$

$$\beta_{i+1,i} = \beta_{i,i-1} + \beta'_{i+1,i} + (1-\theta^2)\varepsilon_{\beta,i}$$

$$\gamma_{i+1,i} = \gamma_{i,i-1} + \gamma'_{i+1,i} + (1-\theta^2)\varepsilon_{\gamma\, i}$$

Step 10 $$\gamma'_{i+1,i} = \alpha_{i+1,i}A_{i+1} + \beta_{i+1,i}B_{i+1} + \gamma_{i+1,i}C_{i+1}$$

Step 11 $$\alpha_{i+n,i} = \alpha_{i+1,i} + (n-1)\alpha'_{i+1,i}$$

$$\beta_{i+n,i} = \beta_{i+1,i} + (n-1)\beta'_{i+1,i}$$

$$\gamma_{i+n,i} = \gamma_{i+1,i} + (n-1)\gamma'_{i+1,i}$$

Step 12 $$\gamma'_{i+n,i} = \alpha_{i+n,i}A_{i+1} + \beta_{i+n,i}B_{i+1} + \gamma_{i+n,i}C_{i+1}$$

Clearly, before the estimator can start to operate, the initial values of the vectors A_i, B_i and C_i and also the scalars α_i, β_i, γ_i, $\alpha_{i,i-1}$, $\beta_{i,i-1}$, $\gamma_{i,i-1}$, $\alpha'_{i,i-1}$, $\beta'_{i,i-1}$ and $\gamma'_{i,i-1}$ must be available. The vectors A_0, B_0 and C_0 may be determined as follows. Using a conventional estimation method, such as those in Section 3.7, estimates of the sampled impulse-response of the channel are obtained at three well-spaced time instances, $t = -2kT$, $t = -kT$ and $t = 0$ and let these estimates be Y'_{-2k}, Y'_{-k} and Y'_0, respectively. The constant k is a reasonably large positive integer, say 1000. In addition, the receiver also determines an estimate $Y'_{-\ell}$ or $Y_{-\ell}$, at time $t = -\ell T$,

which will be required later. ℓ is also a positive integer but not as large as k; typical value of ℓ is 64. It is assumed that these estimates are reasonably correct and that the estimates are significantly 'different', so that they are not collinear. The estimates Y'_{-2k}, Y'_{-k} and Y'_0 are then orthonormalized to give the orthonormal vectors,

$$A_0 = |Y'_{-2k}|^{-1}Y'_{-2k} \tag{7.3.62}$$

$$B_0 = |B'_0|^{-1}B'_0 \tag{7.3.63}$$

$$C_0 = |C'_0|^{-1}C'_0 \tag{7.3.64}$$

where

$$B'_0 = Y'_{-k} - A_0^{*T}Y'_{-k}A_0 \tag{7.3.65}$$

and

$$C'_0 = Y'_0 - B_0^{*T}Y'_0B_0 - A_0^{*T}Y'_0A_0 \tag{7.3.66}$$

The vectors A_0, B_0 and C_0, therefore, form an orthonormal basis of the three-dimensional subspace spanned by Y'_{-2k}, Y'_{-k} and Y'_0. The initial values of the scalars $\alpha_{i,i-1}$, $\beta_{i,i-1}$, $\gamma_{i,i-1}$, α_i, β_i and γ_i are then given by,

$$\alpha_{0,-1} = \alpha_0 = A_0^{*T}Y'_0 \tag{7.3.67}$$

$$\beta_{0,-1} = \beta_0 = B_0^{*T}Y'_0 \tag{7.3.68}$$

$$\gamma_{o,-1} = \gamma_o = C_o^{*T} Y'_o \tag{7.3.69}$$

The reason for obtaining the estimate $Y'_{-\ell}$ of $Y_{-\ell}$ is to enable the receiver to form reasonably accurate initial estimates of the rates of change of α, β and γ. These are obtained as follows. The receiver forms

$$\alpha_{-\ell} = A_o^{*T} Y'_{-\ell} \tag{7.3.70}$$

$$\beta_{-\ell} = B_o^{*T} Y'_{-\ell} \tag{7.3.71}$$

$$\gamma_{-\ell} = C_o^{*T} Y'_{-\ell} \tag{7.3.72}$$

and uses these values to calculate the rates of change

$$\alpha'_{1,o} = (\alpha_o - \alpha_{-\ell})/\ell \tag{7.3.73}$$

$$\beta'_{1,o} = (\beta_o - \beta_{-\ell})/\ell \tag{7.3.74}$$

$$\gamma'_{1,o} = (\gamma_o - \gamma_{-\ell})/\ell \tag{7.3.75}$$

The rates of change of α, β and γ may have been derived either from the estimate Y'_{-2k} or Y'_{-k}, but since k is so large, the values obtained are most likely to be inaccurate.

With all the initial values now specified, the improved channel estimator operates exactly as previously indicated starting from step 1 and arriving at the required value of the n-step prediction of the sampled impulse-response of the channel at step 12.

7.4 RESULTS AND ANALYSIS OF COMPUTER SIMULATION TESTS

Extensive computer simulation tests have been carried out on the improved channel estimator for the proposed use in a synchronous serial data-transmission system (Figure 6.2.1) that operates at the data rate of 9600 bit/s over HF radio links. These tests were performed using the CDC 7600 computer at the University of Manchester Regional Computer Centre. An example of the simulation which also includes the channel simulator is given in Appendix A5. In the simulation of the HF radio link, it is assumed that three independent Rayleigh fading sky waves are present. This represents typical poor channel conditions over actual HF radio links[111,123]. Each sky wave introduces the same average attenuation and the same frequency spread into the data signal, such that the average attenuation over the radio link is 0 dB. Three channels with different rates of fading were used in the tests. It is assumed that the relative delays in transmission between the different sky waves are time-invariant, but may be changed if desired. All the relevant parameters for each channel are summarized in Table 7.4.1. τ_1 is here the relative time delay between the first and second sky waves and τ_2 is the relative time delay between the first and third sky waves.

Channel	Frequency Spread (Hz)	Relative delay in transmission	
		τ_1 (ms)	τ_2 (ms)
1	$\frac{1}{2}$	$\frac{1}{3}$	1
2	1	1	2
3	2	$\frac{2}{3}$	3

TABLE 7.4.1: PARAMETERS OF THE CHANNELS USED IN THE TESTS

The results of the tests are shown in Figures 7.4.1-7.4.39. In many of these graphs, the parameter that is plotted is ξ_i which is the square of the error in the n-step prediction $Y'_{i,i-n}$ and is given by,

$$\xi_i = |Y_i - Y'_{i,i-n}|^2 \qquad (7.4.1)$$

Another parameter that is also used to judge the performance of the estimator is ξ, which is the mean-square error in the prediction $Y'_{i,i-n}$, measured in dB relative to unity, and is given by,

$$\xi = 10 \log_{10} \left(\frac{1}{48000} \sum_{i=1873}^{49872} |Y_i - Y'_{i,i-n}|^2\right) \qquad (7.4.2)$$

It can be seen that, in the above equation, the first 1872 values of the square of the error in $Y'_{i,i-n}$, i.e. $|Y_i - Y'_{i,i-n}|^2$ have been omitted. This is done deliberately so that any transient behaviour of the estimator which may occur immediately after the estimator

commences operation will have settled and so will not affect the value of ξ. No particular significance is attached to the value of 1872 which is a compromise between the need to ensure that the initial transients have decayed to zero and the need to avoid a needless increase in the number of data symbols transmitted in any one test. Later, it will be shown that this value is more than adequate for preventing the initial transients from affecting ξ. Thus, ξ gives a measure of the performance of the estimator when it is already operating properly. In other words, we can consider ξ as a measure of the 'steady-state' performance of the estimator. Also, it can be seen from equation 7.4.2 that each test involves the transmission of nearly 50,000 data-symbols $\{s_i\}$ over the appropriate channel. Each of the three channels has been represented by a particular sequence of nearly 50,000 vectors $\{Y_i\}$. The six fading sequences $\{q_{h,i}\}$ have been selected such that the influence of the chosen sequences on the performance of the estimator is minimized. In all tests,

$$n = 17 \tag{7.4.3}$$

$$k = 1440 \tag{7.4.4}$$

$$\ell = 64 \tag{7.4.5}$$

where n sampling intervals is the delay in estimation, and -2kT, -kT and -ℓT are the time instants when the estimates Y'_{-2k}. Y'_{-k} and $Y'_{-\ell}$ are determined, respectively. The estimates Y'_{-2k} and Y'_{-k} are

required together with the estimate Y'_0 for the formation of the initial vectors A_0, B_0 and C_0 (equations 7.3.62-7.3.64). The estimate $Y'_{-\ell}$ is used to calculate $\alpha_{-\ell}$, $\beta_{-\ell}$ and $\gamma_{-\ell}$ (equations 7.3.70-7.3.72) which are subsequently used in equations 7.3.73-7.3.75 to calculate the initial valuesof the rates of change of α β and γ. The chosen value of n is typical of that likely to be used in practice[89,95]. The signal-to-noise ratio is measured as ψ dB, where,

$$\psi = 10 \log_{10} (1/\tfrac{1}{2}N_0) \qquad (7.4.6)$$

This equation uses the fact that the average transmitted energy per bit of information, at the input and output of the HF radio link, is unity, and the two-sided power spectral density of the additive white Gaussian noise at the output of the HF radio link is $\frac{1}{2}N_0$.

In all tests, except where stated, the estimates Y'_{-2k}, Y'_{-k} and Y'_0 are taken as their actual values Y_{-2k}, Y_{-k} and Y_0, respectively. Thus, the orthonormal vectors A_0, B_0 and C_0 derived from these estimates span the correct subspace containing Y_{-2k}, Y_{-k}, Y_0 and, in fact, all the $\{Y_i\}$. Obviously, the subspace must be held fixed and this is achieved by setting the parameter n to zero. In this case, steps 5 to 8 of the improved channel estimator are omitted from the estimation process. Thus, when the parameters θ and c have their optimum values, the performance of the improved channel estimator is the upper bound to its actual performance.

7.4.1 Convergence of Estimator

Each of the convergence curves presented in the following pages, with the exception of Figure 7.4.1, is in fact the variation of $10 \log_{10} \bar{\xi}_i$ with i, where $\bar{\xi}_i$ is the ensemble average of 20 values of ξ_i obtained using 20 different sequences of $\{s_i\}$ and 20 different sequences of the additive noise $\{w_i\}$. Where this is the case, we can consider the convergence curve as representing the approximate behaviour of the estimator in the mean.

Figure 7.4.1 shows the performance of the improved channel estimator immediately after the starting-up procedure. Channel 3 has been used when investigating the convergence properties of the estimator because it represents a particularly bad channel with a fading rate of over 88 fades per minute. Channels 1 and 2 are not so severe, so that a good performance of the estimator over channel 3 most likely will mean a good or even better performance over channels 1 and 2. The result shown in Figure 7.4.1 has been obtained using a single sequence of the values $\{s_i\}$ and a single sequence of $\{w_i\}$, with the signal-to-noise ratio set to 60 dB. The predictor uses degree-1 least-squares fading-memory prediction. The parameters θ and c are given the values of 0.80 and 0.05, respectively. The given combination of θ and c are the optimum values of these parameters at the particular signal-to-noise ratio. The method of finding the optimum values will be discussed later. Each point on the convergence curve is the square of the error in the n-step prediction of Y_i (equation 7.4.1). In Figure 7.4.2, an ensemble average of 20 convergence curves is presented. As expected, the errors in the n-step predictions converge

rapidly to the steady-state mean value of about -44 dB, but a more prominent feature of the two convergence curves is the "high-frequency oscillation" of the prediction errors. Here, the frequency of oscillation is about 50 Hz and the peak-to-peak value is about 10 dB. The rapid convergence of the estimator is as expected since the correct subspace has been used throughout and also the estimator has fairly accurate knowledge of the initial values of the rates of change of α, β and γ. When the correct subspace is used, the rapidity of convergence is determined here by the accuracy of the prior knowledge of the rates of change of α, β and γ; the more accurate they are, the faster is the convergence. The behaviour of the estimator was also investigated at a lower signal-to-noise ratio. Figure 7.4.5 shows, among other information, the convergence of the estimator (curved marked Degree 1) at the signal-to-noise ratio of 20 dB. It can be seen that, unlike the corresponding case (ψ = 60) above, $\bar{\xi}_i$ fluctuates randomly about the mean value. Thus, the oscillation of the errors as shown in Figures 7.4.1 and 7.4.2 is not a typical behaviour of the estimator. The reason for the oscillation is likely to be the small value of the parameter θ used by the predictor. θ is an important parameter and its role is explained as follows. We will only consider the formation of the n-step prediction of α_{i+n} because the same method is also used to find $\beta_{i+n,i}$ and $\gamma_{i+n,i}$. The predictor is required here to predict a single variable parameter, α. Now, the prediction $\alpha_{i+n,i}$ is calculated in two stages. Firstly, the predictor forms the 1-step prediction $\alpha_{i+1,i}$ (equation 7.3.39) and the rate of change $\alpha'_{i+1,i}$ (equation 7.3.36)

using the degree-1 least-squares fading-memory prediction, and secondly it uses these values to calculate $\alpha_{i+n,i}$ by linear interpolation. The prediction $\alpha_{i+1,i}$ is the value, at time t=(i+1)T, of the polynomial of degree 1 which has been fitted to the sequence of updated estimates α_i, α_{i-1}, α_{i-2}, ... The polynomial has been chosen such that the weighted sum of the squares of the errors in the 1-step prediction is minimized. The weighting function is the exponential function θ^r, where r = 0,1,2,... and θ is real and its value lies in the range $0 < \theta < 1$. The value r = 0 corresponds to the current time instant and as r increases time recedes into the past, i.e. i decreases. By using an exponential weighting function, the older estimates have less influence on the prediction. When the estimating polynomial has the given degree, a small value of θ results in large oscillation of the prediction errors but small systematic (or bias) errors. Here, systematic errors are defined as the errors due to the inadequate fitting of the sequence of the updated estimates α_i, α_{i-1}, α_{i-2}, ... by the chosen polynomial. When θ has the value closer to 1, a small regular oscillation is obtained but the penalty is the large systematic errors. This behaviour is evident from the results given in Figure 7.4.3, which shows that increasing θ from 0.8 to 0.9 has apparently reduced the amplitude of the oscillation but the value of ξ has increased due to the rise in systematic errors.

We have seen that when θ is small the systematic errors are small, and at the same time the weighting function θ^r dies out more rapidly. This means that the prediction is then based on very few

recent updated estimates. When the estimates themselves are seriously in error, it is likely that the resulting prediction will be in error. Any recursive algorithm is potentially unstable, more so when, in this case, the prediction is derived from past updated estimates rather than from a sequence of observations as described in Ref. 44. However, the results presented here as well as others[89,95,97] have shown that the predictor is stable if sensible values of the parameters θ and c are used.

The discussion above has shown that in order to reduce the oscillation in the prediction errors, the parameter θ must be increased to a value closer to 1. However, this results in an increase in the systematic errors which increases the steady-state mean value ξ. One possible solution is to increase the degree of the estimating polynomial to degree 2, so that the systematic errors are reduced. Intuitively, this must be so because increasing the degree of the estimating polynomial should result in a better fit on the data and therefore reducing the systematic errors. In addition, the optimum value of θ is now higher than in the previous case and so a smaller oscillation is achieved. This is in fact what we have observed. In Figure 7.4.4, we have plotted the convergence curves of the estimator for channel 3 using degree-2 least-squares fading-memory prediction at the signal-to-noise ratios of 20 dB and 60 dB. The optimum value of θ for the curve with $\psi = 20$ is 0.97 and that for $\psi = 60$ is 0.94. In order to give a better comparison, in Figure 7.4.5 we have superimposed the convergence curves using degree-2 prediction onto the corresponding curves which uses degree-1 prediction. It can

be seen that the curve for ψ = 60 and using degree-2 prediction converges to a lower steady-state mean value compared to the corresponding curve using degree-1 prediction. However, the convergence is now slower. The reason is that while the estimator knows the correct subspace when forming a prediction, it only has accurate prior knowledge of the rates of change (first differentials) of α, β and γ, and no prior knowledge at all of the accelerations (second differentials) of these quantities. Therefore, it takes some time before the estimator can obtain sufficiently accurate estimates of the accelerations. Also, the curves for ψ = 60 in Figure 7.4.5 show that by increasing the degree of the estimating polynomial, systematic errors are reduced which results in an improvement in the steady-state mean value of ξ. In addition, a smaller oscillation in the prediction errors is obtained as a larger value of θ is now used. At ψ = 20 there is very little difference in the behaviour of the estimator when using degree-1 or degree-2 prediction. The optimum values of θ are 0.95 and 0.97 respectively. Here, the signal-to-noise ratio is low and so the performance of the estimator is large affected by the additive noise.

7.4.2 Optimum Values of θ and c

One of the factors that determines the performance of the estimator is the choice of θ and c. The parameter θ used by the least-squares fading-memory prediction has a value in the range 0 to 1, and is usually

set close to 1[95]. The larger the value of θ, the longer is the 'memory' of the predictor, which means that more estimates are effectively involved in forming a prediction[89]. On the other hand, the step size of the feedforward transversal filter (parameter c) is preferably small so that the estimate Y_i' will be less affected by additive noise, however, the convergence of the estimator to its steady-state performance will now be slow.

The search for θ and c that results in the optimum performance of the estimator is not too difficult but is very time consuming. Here, a systematic approach is taken and is illustrated in Figures 7.4.6 and 7.4.7. In the first stage, a parameter (say, θ) is varied over a certain range while keeping the other parameter (c) at some fixed value. A minimum value of ξ is obtained corresponding to the given value of c (point 1, Figure 7.4.6). In the second stage, θ is fixed at the value corresponding to the first minimum value of ξ and c is now varied. A second minimum value of ξ is found at point 2 in Figure 7.4.7. The third stage involves varying the parameter θ while fixing c at the value corresponding to the previous minimum. The process of adjusting θ and c continues alternately in this way until no further improvements in the value of ξ are obtained. The valuesof θ and c which correspond to the best performance of the estimator are considered as the optimum values of the parameters. The process of adjusting θ and c as outlined above is dependent on their starting values. Obviously, fewer adjustments are required if their starting values are chosen closer to their respective optimum values. Otherwise, many laborious adjustments are required.

Generally, the optimum values of θ and c are not the same at different channel conditions or with different arrangements of prediction. Thus, for each of the three channels used in the tests, we have used the above method to find the optimum values of θ and c at signal-to-noise ratios of 5, 10, 20, 30, 40, 50 and 60 dB. Figures 7.4.8-7.4.16 show the variation of ξ with the parameter c at various signal-to-noise ratios with θ optimum and held fixed along each curve. The predictor is the least-squares fading-memory type of degree 0, 1 or 2. The three-dimensional subspace which contain the $\{Y_i\}$ is assumed to be known. Table 7.4.2 gives the optimum values of c. Clearly, from these curves, values of c greater than zero but not too large are to be used so that the estimator can adequately track the received signal (equation 6.4.6). Figures 7.4.17-7.4.25 show the variations of ξ with θ, where c is now optimum and it is held constant along each curve. As θ approaches 1, systematic errors are large so that ξ increases very rapidly, and the estimates (predictions) finally diverge when $\theta = 1$. We have seen before that the optimum value of θ when using degree-1 prediction can become quite small, especially over channels 2 and 3 at the higher signal-to-noise ratios, apparently resulting in large oscillations of the prediction errors. However, from Figures 7.4.21 and 7.4.24, the value of θ can be increased while keeping the estimating polynomial to degree 1 at the expense of only a few dB reduction in performance. The optimum values of θ for the different degrees of the estimating polynomials are summarized in Table 7.4.3.

Degree of estimating polynomial	Signal-to-Noise Ratio / Channel	ψ=5	10	20	30	40	50	60
0	1	0.01	0.01	0.01	0.03	0.06	0.10	0.11
	2	0.01	0.01	0.02	0.05	0.08	0.10	0.11
	3	0.01	0.02	0.04	0.07	0.10	0.11	0.11
1	1	0.07	0.10	0.06	0.07	0.09	0.09	0.07
	2	0.05	0.07	0.08	0.10	0.08	0.06	0.07
	3	0.13	0.09	0.08	0.07	0.04	0.05	0.05
2	1	0.07	0.07	0.08	0.11	0.08	0.11	0.08
	2	0.08	0.09	0.18	0.39	0.17	0.13	0.11
	3	0.07	0.08	0.08	0.08	0.08	0.08	0.06

TABLE 7.4.2: OPTIMUM VALUES OF c

Degree of estimating polynomial	Signal-to-Noise Ratio / Channel	ψ=5	10	20	30	40	50	60
0	1,2,3	θ = 0						
1	1	0.99	0.99	0.98	0.97	0.96	0.94	0.90
	2	0.98	0.98	0.97	0.96	0.93	0.88	0.85
	3	0.98	0.97	0.95	0.92	0.86	0.82	0.80
2	1	0.99	0.99	0.99	0.99	0.98	0.98	0.97
	2	0.99	0.99	0.99	0.99	0.98	0.97	0.96
	3	0.98	0.98	0.97	0.96	0.95	0.94	0.94

TABLE 7.4.3: OPTIMUM VALUES OF θ

7.4.3 Steady-State Performance of Estimator

Figures 7.4.26-7.4.28 show the steady-state performance of the improved channel estimator when operating over channels 1, 2 and 3. On each graph, three curves are plotted showing the performance of the estimator when it uses degree-0, 1 or 2 least-squares fading-memory prediction. At every point on each curve, the parameters θ and c have their optimum values. Now, when the estimator uses degree-0 prediction, the optimum value of θ, in every case, is zero (Table 7.4.3). Thus, for instance, $\alpha_{i+1,i}$ and $\alpha_{i+n,i}$ are given by (equations 7.3.33 and 7.3.52),

$$\alpha_{i+1,i} = \alpha_i \tag{7.4.7}$$

and

$$\alpha_{i+n,i} = \alpha_i \tag{7.4.8}$$

which mean that the predictions of α_{i+1} and α_{i+n} are simply the present estimate α_i, and as such the arrangement represents no prediction. Since α (also β and γ) is time-varying, the larger the value of n the poorer is the prediction given by equation 7.4.8. Obviously, degree-0 prediction is inferior in performance when it is compared with degree-1 or degree-2 prediction, and this is demonstrated by the performance curves in Figures 7.4.26-7.4.28. The performance of the estimator over all three channels follows a similar pattern. At the higher signal-to-noise ratios (ψ = 40 to 60), degree-1 or degree-2 prediction gives a considerable improvement of the order of 15 to 20 dB over degree-0 prediction. As the signal-to-

noise ratio decreases, the advantage remains significant but not as much as when little or no additive noise is present. When making the above comparisons, degree-1 and degree-2 predictions have been grouped together because they have comparable performances. However, noticeable difference exists between the performance of degree-1 and degree-2 prediction. With the value of ψ greater than about 20, degree-2 prediction offers a significant improvement over degree-1 prediction. For example, at $\psi = 60$, degree-2 prediction is better by 2.3, 3.8 and 3.8 dB for channels 1, 2 and 3, respectively. At low signal-to-noise ratios, the performance of degree-1 prediction is now better than degree-2 prediction, but the improvement is only marginal.

A comparison between the results obtained here for channels 1 and 3 and the corresponding channels with the same frequency spreads in Ref. 95 shows that when the sky wave increases from two to three, there is only a marginal deterioration in the performance of the estimator, roughly in the region of 1 or 2 dB.

7.4.4 Influence of Prior Knowledge of Rates of Change of α, β and γ on Convergence of Estimator

During the starting-up of the estimator, predictions of the rates of change of α, β and γ at time $t=T$ are made and the values are fed to the estimator to help improve the initial response. These predictions are accurate since the correct values of the appropriate vectors in $\{Y_i\}$ have been used in the calculations (equations 7.3.73-7.3.75). In Figure 7.4.29, the convergence of the estimator when it

uses the predictions of the rates of change of α, β and γ is compared with the case where these predictions are not available. In the latter case, $\alpha'_{i,o}$, $\beta'_{i,o}$ and $\gamma'_{i,o}$ (equations 7.3.73-7.3.75) are all set to zero, so that the estimate $Y'_{-\ell}$ need not be determined. Clearly, when the estimator has no knowledge of the rates of change of α, β and γ, the errors in the n-step predictions of the $\{Y_i\}$ are initially large. However, the curve quickly converges to that where the rates of change are known after about 90 sampling intervals.

7.4.5 Effects of the Accuracy of the Initial Estimates of the Subspace on the Performance of Estimator

Figure 7.4.30 gives a comparison of the behaviour of the estimator over channel 3 when operating under two different conditions. Firstly, the estimator knows at all times the correct three-dimensional subspace containing the $\{Y_i\}$ and secondly, it has no knowledge of the subspace and so must estimate this subspace. For each curve the signal-to-noise ratio is 60 dB. Now, as described previously, when the correct subspace is used, the parameter η is simply set to zero. In Figure 7.4.30, two curves are shown marked $\eta = 0$. One of these curves uses θ and c(0.80 and 0.05, respectively) which are optimum for steady-state operation. This curve is in fact the same as that plotted in Figure 7.4.2. The second curve marked $\eta = 0$ uses θ and c (0.81 and 0.12, respectively) which are optimized for the starting-up procedure. As explained previously, because the two values of θ are very nearly the same, both curves oscillate at about the same frequency and roughly of equal peak-to-peak amplitude.

However, in the latter case, the optimum value of c is larger and so marginally improves the convergence, but the steady-state performance of the estimator as indicated by the value of ξ (equation 7.4.2) has increased by a small amount. This must be so because it is the property of the feedforward transversal-filter estimator (Figure 6.4.1) that a large value of c results in faster convergence at the expense of greater sensitivity to additive noise. The curves for $n \neq 0$ show the behaviour of the estimator when it has no prior knowledge of the correct three-dimensional subspace. Previously, the correct subspace was available because the estimates Y'_{-2k}, Y'_{-k} and Y'_o are assumed to be the correct vectors Y_{-2k}, Y_{-k} and Y_o, respectively. In practice the correct vectors are not known and so they must be estimated using other estimation processes (Section 3.7). It is inevitable that these estimates are to some degree in error but surprisingly accurate estimates can be obtained using a suitable estimator. In the simulation, the errors in the estimates are modelled as statistically independent Gaussian random variables with zero mean and variance that reflects the degree of error[95]. Thus, the estimates Y'_{-2k}, Y'_{-k} and Y'_o are assumed to be,

$$Y'_{-2k} = Y_{-2k} + Z_{-2k} \qquad (7.4.9)$$

$$Y'_{-k} = Y_{-k} + Z_{-k} \qquad (7.4.10)$$

and

$$Y'_o = Y_o + Z_o \qquad (7.4.11)$$

where Z_{-2k}, Z_{-k} and Z_o are complex-valued (g+1)-dimensional vectors. The real and imaginary parts of these vectors are sample values of statistically independent Gaussian random variables with zero mean and variance σ_Z^2. For the three curves (η = 0.001, η= 0.01 and η = 0.1), θ, c and σ_Z^2 are given the values 0.80, 0.05 and 10^{-6}, respectively. In addition to these convergence curves, Table 7.4.4 gives the values of the steady-state mean-square error ξ, for different values of η and also for different vectors A_o, B_o and C_o which span the initial three-dimensional subspace. Under the given condition, the curve for η = 0 converges to the best steady-state performance of the estimator. When the initial three-dimensional subspace is fairly accurate ($\sigma_Z^2 = 10^{-6}$), the curve for η = 0 is approached quite closely by the curve for η = 0.1 (Figure 7.4.30) and this is maintained even in the steady-state (Table 7.4.4). When a larger value of σ_Z^2 is used, say 10^{-3}, the initial estimate of the subspace is poor and using η = 0.1 still gives a better performance than η = 0.001, but this arrangement is now almost 8 dB inferior to that with η= 0. Thus, as expected, an accurate initial estimate of the subspace must be obtained in order to achieve the best initial performance of the estimator. Also shown in Table 7.4.4 is the quantity $\xi_{initial}$ which gives a rough indication of the initial performance of the estimator. $\xi_{initial}$ is calculated in the same way as ξ (equation 7.4.2), but, here, only the first 1872 n-step predictions of the $\{Y_i\}$ are used. Clearly, when the initial estimate of the subspace is poor, the initial performance of the estimator is improved by using η = 0.1.

			ξ (dB)	$\xi_{initial}$ (dB)
Variance of Z_{-2k}, Z_{-k} & Z_o	$\sigma_Z^2 = 0$	$\eta = 0$	-44.20	-44.83
	$\sigma_Z^2 = 10^{-6}$	$\eta = 0.001$	-40.72	-39.06
		$\eta = 0.1$	-42.38	-42.89
	$\sigma_Z^2 = 10^{-3}$	$\eta = 0.001$	-13.38	-12.15
		$\eta = 0.1$	-36.37	-19.81

TABLE 7.4.4: COMPARISON OF THE VALUES OF ξ AND $\xi_{initial}$ FOR CHANNEL 3, $\psi = 60$, $c = 0.05$, $\theta = 0.80$

7.4.6 Near-Orthonormal Property of Vectors

One of the essential processes undertaken by the improved channel estimator is the estimation of the three-dimensional subspace containing the $\{Y_i\}$. Due to the difficulty in determining the vectors L, M and N (equation 7.3.1) that span the subspace, the estimator forms estimates A_i, B_i and C_i of the three orthonormal vectors A, B and C which also span the subspace. Usually the subspace spanned by the estimates A_i, B_i and C_i is unlikely to be the correct subspace that contains the $\{Y_i\}$ and so A_i, B_i and C_i are adjusted (equations 7.3.22-7.3.24), so that the new subspace spanned by A_{i+1}, B_{i+1} and C_{i+1} is slightly closer to Y_i'. Clearly, from equations 7.3.22-7.3.24, if A_i, B_i and C_i are orthonormal, the new vectors A_{i+1}, B_{i+1} and C_{i+1} cannot be orthonormal. The length of A_{i+1}, B_{i+1} and C_{i+1} is slightly greater than 1 and they are unlikely

to be orthogonal. In the formulation of the improved channel estimator, these vectors have been assumed orthonormal, in particular, α_i, β_i and γ_i (equations 7.3.15-7.3.17) are derived using this property. Thus, the vectors A_i, B_i and C_i, ideally, must be orthonormalized at all times. The orthonormalization of the vectors (equations 7.3.25-7.3.29) involves a considerable amount of computation per received signal. However, tests have shown that when A_o, B_o and C_o are orthonormal, the subsequent vectors A_i, B_i and C_i remain very nearly orthonormal. Figures 7.4.31-7.4.34 show the lengths $|A_i|$, $|B_i|$ and $|C_i|$ for i = 0,1,...,50000. The estimator is here operating over the worst channel, i.e. channel 3 and the signal-to-noise ratio (ψ) is 60 dB. As before, the parameters θ (0.80) and c(0.05) are optimum for steady-state operation at the particular value of ψ and $\eta = 0$. In Figures 7.4.31 and 7.4.32, σ_Z^2 has the value 10^{-6} and the corresponding value for Figures 7.4.33 and 7.4.34 is 10^{-3}. This means that, in the latter case, the estimator begins operation with a subspace which is further away from the correct subspace. Two values of η have been used for each value of σ_Z^2. In Figures 7.4.31 and 7.4.33, $\eta = 0.001$, while in Figures 7.4.32 and 7.4.34, $\eta = 0.1$. The main feature of the four graphs is the capability of the vectors to (almost) self-normalize themselves, even after a sudden increase in their lengths. It can be seen that $\eta = 0.001$ causes less increase in the lengths of the vectors from unity but the steady-state performance is poor. In addition to the self-normalizing property, the vectors are also very nearly orthogonal. Figures 7.4.35 and 7.4.36 attempt to

demonstrate this property. The relevant parameters, here, are $\sigma_Z^2 = 10^{-6}$, $\psi = 60$, $c = 0.05$, $\theta = 0.80$, $\eta = 0.001$ (Figure 7.4.35) and $\eta = 0.1$ (Figure 7.4.36). By definition, for the vectors to be orthogonal, their inner products $A_i \cdot B_i$, $A_i \cdot C_i$ and $B_i \cdot C_i$ must be zero or, in fact, 0+j0 as the vectors have complex values. The inner products could have been presented as points on the complex number plane. However, by the nature of the results, this representation will show many points clustered together near the origin and it would be difficult to indicate the value of i for each point. Therefore, we have plotted, instead, the variation of the magnitudes of the inner products with i. Clearly, for both cases (η = 0.001 and 0.1), the orthogonality of the vectors is very nearly maintained at all times. Although Figures 7.4.35 and 7.4.36 demonstrate the approximate orthogonality of the first 3000 sets of vectors, similar behaviour has also been observed for the subsequent vectors. Also, it has been observed that the vectors tend to orthonormalize themselves when degree-2 prediction is used.

The results above are indeed astonishing because they are contrary to our expectation that the lengths of the vectors will keep increasing and also the orthogonality between the vectors will be lost if they are not made orthonormal at least once in a while. Here, we will present a simple intuitive argument as to why the vectors A_i, B_i and C_i remain very nearly orthonormal.

At the start of the estimation process, the vectors A_o, B_o and C_o which are derived from the vectors Y'_{-2k}, Y'_{-k} and Y'_o are made orthonormal. Using these starting vectors, α_o, β_o and γ_o are formed

using equations 7.3.15, 7.3.16 and 7.3.17, respectively. Since the estimator assumes that the vectors are orthonormal, which they are, α_o, β_o and γ_o obtained from these equations have their correct values. The vector F_o, which is given by

$$F_o = \alpha_o A_o + \beta_o B_o + \gamma_o C_o \qquad (7.4.12)$$

is then the correct orthogonal projection of Y_o' onto the three-dimensional subspace spanned by A_o, B_o and C_o. This means that the vector E_o, which is given by

$$E_o = Y_o' - F_o \qquad (7.4.13)$$

is orthogonal to the three-dimensional subspace spanned by A_o, B_o and C_o. At the next sampling instant, the vectors A_o, B_o and C_o are updated to A_1, B_1 and C_1 according to equations 7.3.22, 7.3.23 and 7.3.24, respectively. It is clear from these equations that if A_o, B_o and C_o are orthonormal, then the new vectors A_1, B_1 and C_1 are no longer orthogonal and each of length slightly greater than 1. The next step in the estimation process involves the calculation of α_1, β_1 and γ_1 according to equations 7.3.15, 7.3.16 and 7.3.17, respectively. These equations have been derived assuming the vectors are orthonormal. As this is not the case, values of α_1 β_1 and γ_1 obtained using these equations are obviously incorrect and, in fact, the magnitudes $|\alpha_1|$, $|\beta_1|$ and $|\gamma_1|$ are greater than they should be. Since the vector F_1 is obtained using the equation

$$F_1 = \alpha_1 A_1 + \beta_1 B_1 + \gamma_1 C_1 \qquad (7.4.14)$$

the length of F_1 is greater than it should be. Thus, the vector F_1 is not the orthogonal projection of Y_1' onto the subspace spanned by A_1, B_1 and C_1. This, in turn, means that E_1, as given by

$$E_1 = Y_1' - F_1 \qquad (7.4.15)$$

is not orthogonal to the subspace spanned by A_1, B_1 and C_1. In fact, E_1 contains a component which is proportional to $-F_1$. Therefore, when the vectors are updated in the next sampling interval using

$$A_2 = A_1 + n\alpha_1^* E_1 \qquad (7.4.16)$$

$$B_2 = B_1 + n\beta_1^* E_1 \qquad (7.4.17)$$

$$C_2 = C_1 + n\gamma_1^* E_1 \qquad (7.4.18)$$

then, clearly, the lengths $|A_2| < |A_1|$, $|B_2| < |B_1|$ and $|C_2| < |C_1|$, and the inner products between any two vectors A_2, B_2 and C_2 are greater than that corresponding to the previous vectors A_1, B_1 and C_1.

Obviously, similar arguments can be used for the case where, say, at some time instant iT, the length of the vector F_i as derived from equation 7.3.6 is smaller than it should be. In this case, the new vectors A_{i+1}, B_{i+1} and C_{i+1} will be greater in length when

compared to the previous vectors A_i, B_i and C_i, respectively. The inner products between any two of the vectors A_{i+1}, B_{i+1} and C_{i+1} are now smaller than that corresponding pair of the previous vectors A_i, B_i and C_i. Thus, it is sufficient to make only the vectors A_o, B_o and C_o orthonormal. The subsequent vectors A_i, B_i and C_i are nearly orthonormal because the error vector E_i is not orthogonal to the subspace spanned by A_i, B_i and C_i. Due to this 'built-in' compensating mechanism that keeps the vectors nearly orthonormal, it is therefore not essential for them to be made orthonormal. The results obtained have confirmed this conclusion. The advantage of leaving out the Gram-Schmidt orthonormalization process (equations 7.3.25-7.3.29) in terms of the reduction in computational requirement is clearly enormous. For the three-sky-wave model, the number of computations is reduced by

	36 (g+1)	equivalent scalar multiplications
	9 (g+1)	equivalent scalar additions or subtractions
	3	square-root operations
and	3	scalar divisions

7.4.7 Effects of Quantization Noise

The performance of degree-0, degree-1 and degree-2 predictions have so far been compared assuming that, in all calculations, the quantization is that introduced by the accuracy of the computer itself. This is obviously not true in practice. For instance, when two b bits numbers are multiplied, the result requires a

storage of 2b bits and when the product occurs in a recursive structure, the storage required will grow at each successive iteration. Therefore, practical limitation forces the result to be quantized to a fixed number of bits. Figures 7.4.37-7.4.39 show the effects of quantization noise, in particular, the errors due to rounding off the results of multiplications, on degree-0, degree-1 and degree-2 predictions. The detailed descriptions of how these results are obtained are given in Appendix A2. Briefly, the roundoff noise is accounted for by assuming the multiplication to be done in infinite precision and the roundoff noise is simply added to the result[93]. Each noise sample is a sample value of a uniform random variable with zero mean and variance $2^{-2b}/12$, where b+1 is the number of bits of each register. In all cases, the signal-to-noise ratio is 60 dB. The parameters θ and c are the optimum values. $\eta = 0$, so that the correct three-dimensional subspace is used throughout. It can be seen that, in terms of word length, degree-0 requires the least number of bits but the performance is greatly inferior to degree-1 or degree-2 prediction. For all three channels, the optimum performance when using degree-1 prediction is obtained with register length of about 20 bits, while degree-2 requires an additional 8 bits.

7.4.8 Summary of Results and Recommendation

From the results, it is obvious that the degree-0 estimating polynomial is totally inadequate for use as a predictor of the sampled impulse-response of the channel. The choice between degree-1 and

degree-2 is not so clear. At high signal-to-noise ratios, degree-2 prediction offers a significant improvement in steady-state performance over degree-1 prediction. However, at low signal-to-noise ratios, degree-1 gives a better performance, albeit only by a very small amount. With degree-1 prediction, it is possible for the accuracy of the predictions (of the $\{Y_i\}$) to vary in an oscillatory manner. Therefore, although the value of the steady-state mean-square error (ξ) is low, sometimes the errors in these predictions are quite large, which means that the detector is fed at these times with poor estimates of the channel. With degree-2 prediction, the oscillatory effect is effectively eliminated as the optimum value of θ is now higher. The disadvantages of degree-2 prediction are that it requires slightly more computations per received signal and also slightly larger word length for the optimum performance of the estimator. As a comparison, degree-1 prediction requires 3N complex multiplications and 5N complex additions or subtractions in generating the n-step predictions of α, β and γ, where N is the number of sky waves. Degree-2 prediction requires 6N complex multiplications and 9N complex additions or subtractions, which, however, are still relatively small because N is usually 2 or 3. In terms of word size, the number of bits required by degree-1 and degree-2 predictions are 20 and 28 bits, respectively, both of which are not excessive. Therefore, degree-2 prediction appears to be a better choice because of its improved performance at the higher signal-to-noise ratios and also for its good performance over all signal-to-noise ratios. In addition, we have not encountered any stability problem in using the higher degree prediction. Also, it

was found that only the vectors that spanned the initial estimate of the subspace need be orthonormalized. The estimator remains stable even though the subsequent vectors are not orthonormalized. This reduces considerably the amount of computation required in the prediction of the sampled impulse-response.

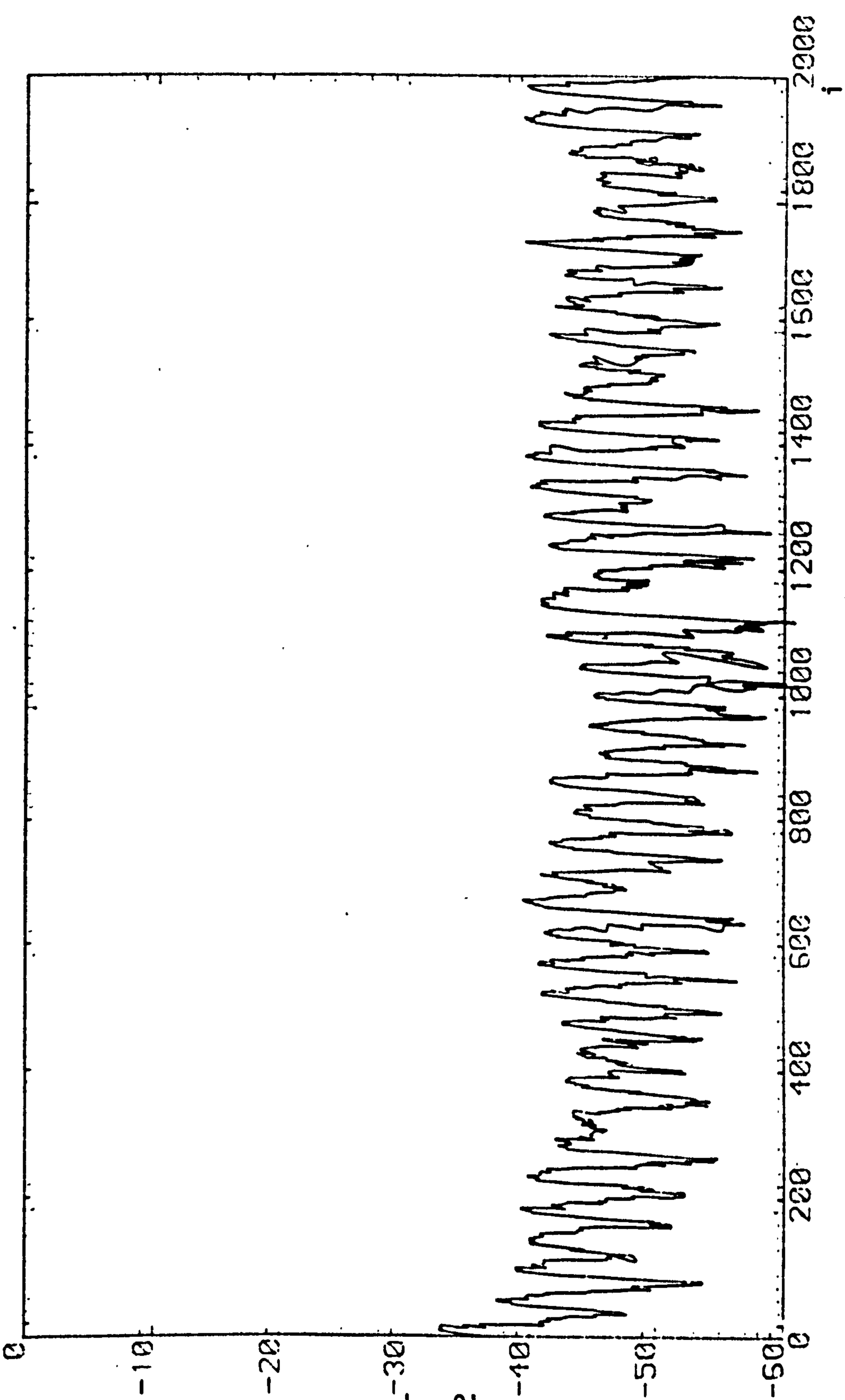

FIGURE 7.4.1: A SINGLE CONVERGENCE CURVE OF THE IMPROVED CHANNEL ESTIMATOR
CHANNEL 3, $\psi = 60$, DEGREE-1 PREDICTION, CORRECT SUBSPACE,
$\eta = 0$, $\theta = 0.80$, $c = 0.05$

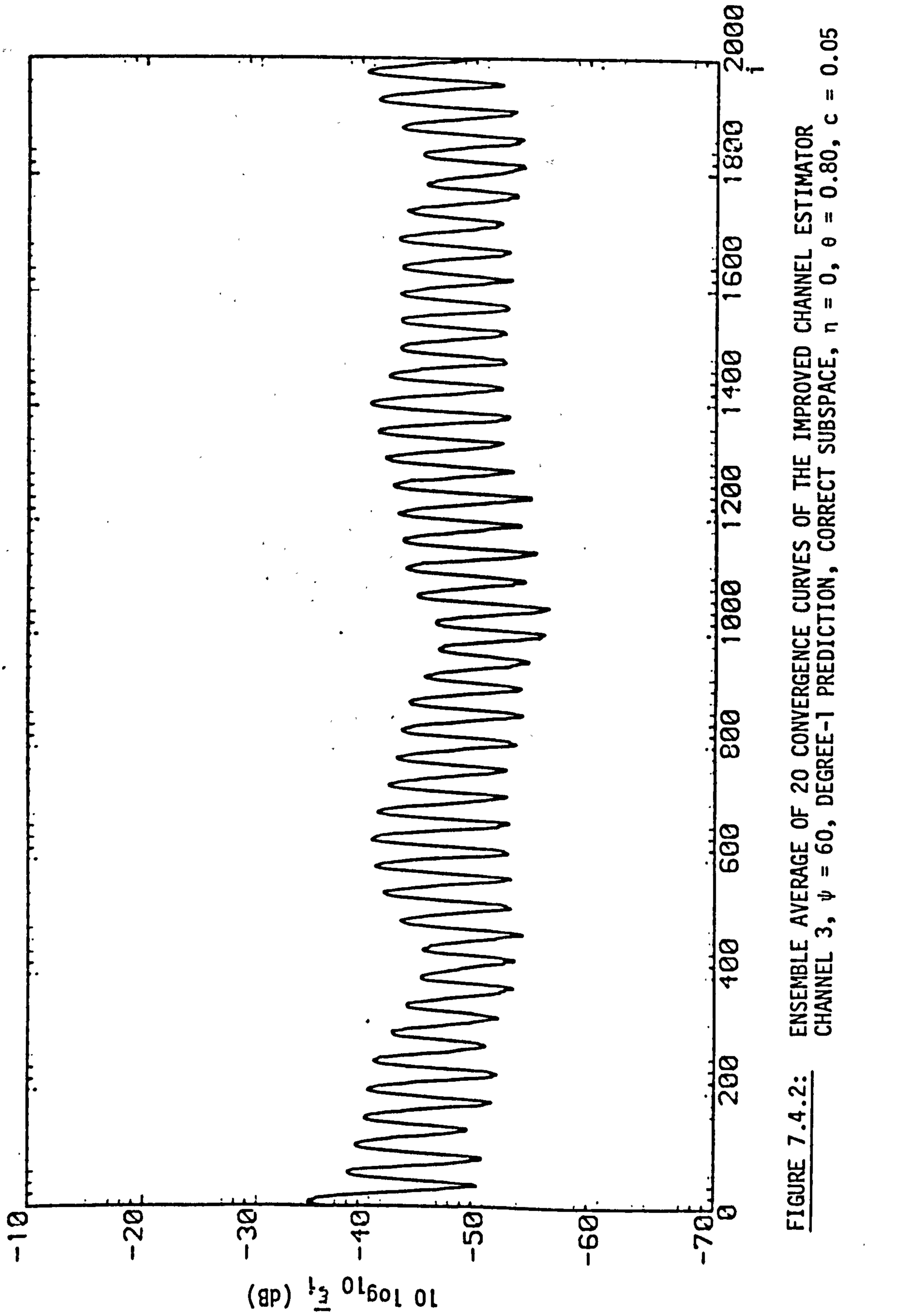

FIGURE 7.4.2: ENSEMBLE AVERAGE OF 20 CONVERGENCE CURVES OF THE IMPROVED CHANNEL ESTIMATOR CHANNEL 3, $\psi = 60$, DEGREE-1 PREDICTION, CORRECT SUBSPACE, $\eta = 0$, $\theta = 0.80$, c = 0.05

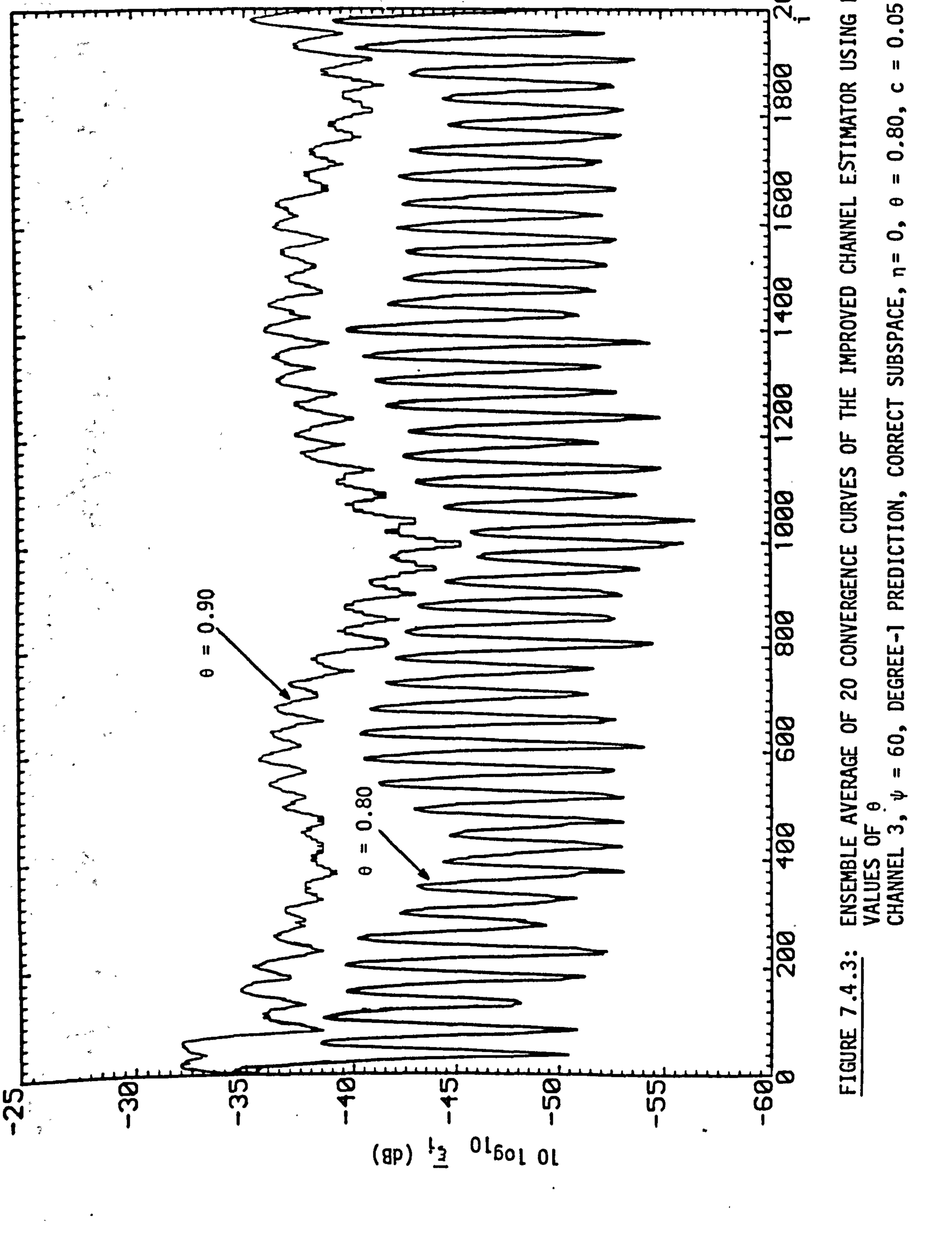

FIGURE 7.4.3: ENSEMBLE AVERAGE OF 20 CONVERGENCE CURVES OF THE IMPROVED CHANNEL ESTIMATOR USING DIFFERENT VALUES OF θ
CHANNEL 3, ψ = 60, DEGREE-1 PREDICTION, CORRECT SUBSPACE, η= 0, θ = 0.80, c = 0.05

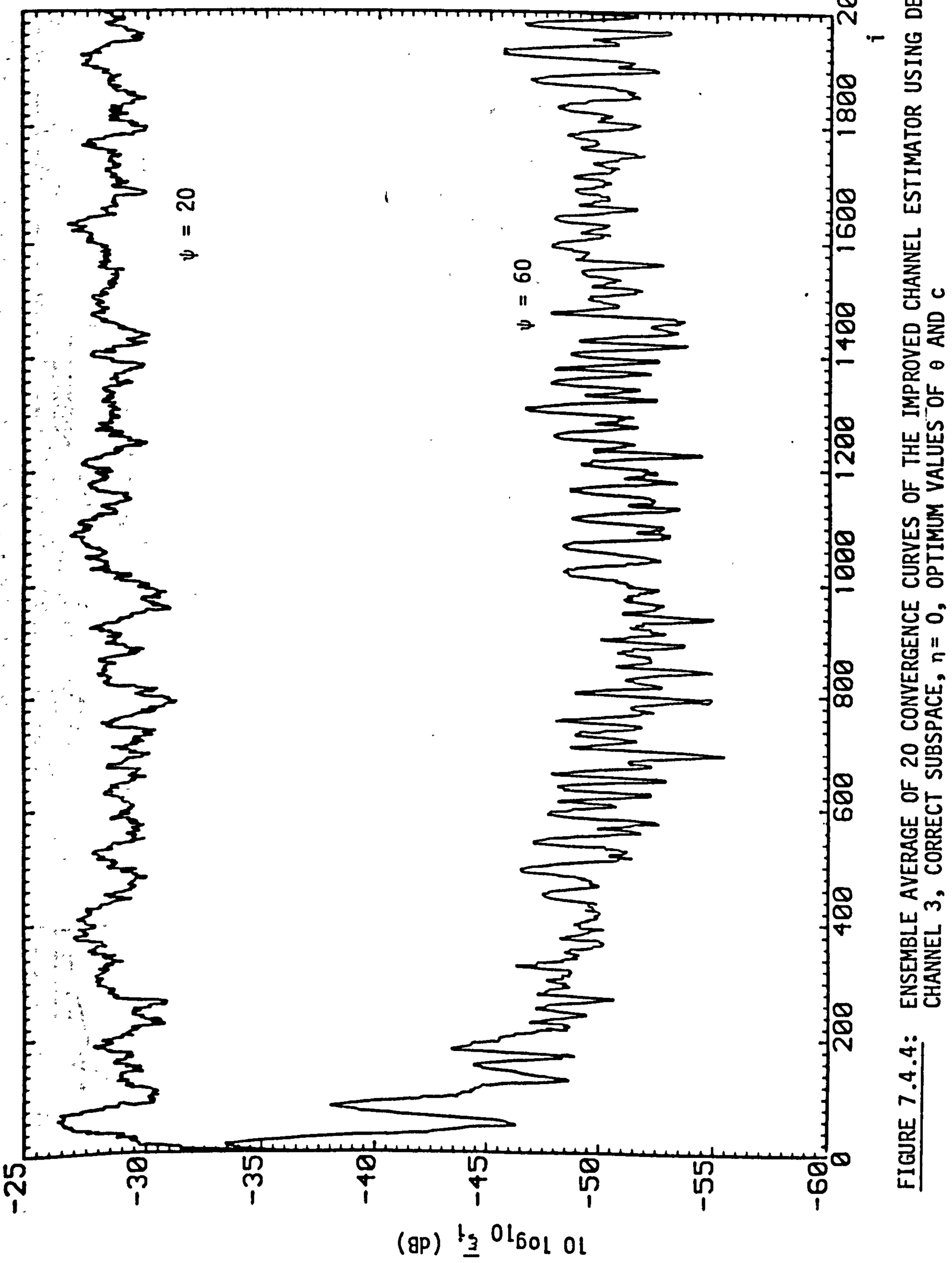

FIGURE 7.4.4: ENSEMBLE AVERAGE OF 20 CONVERGENCE CURVES OF THE IMPROVED CHANNEL ESTIMATOR USING DEGREE-2 PREDICTION CHANNEL 3, CORRECT SUBSPACE, η= 0, OPTIMUM VALUES OF θ AND c

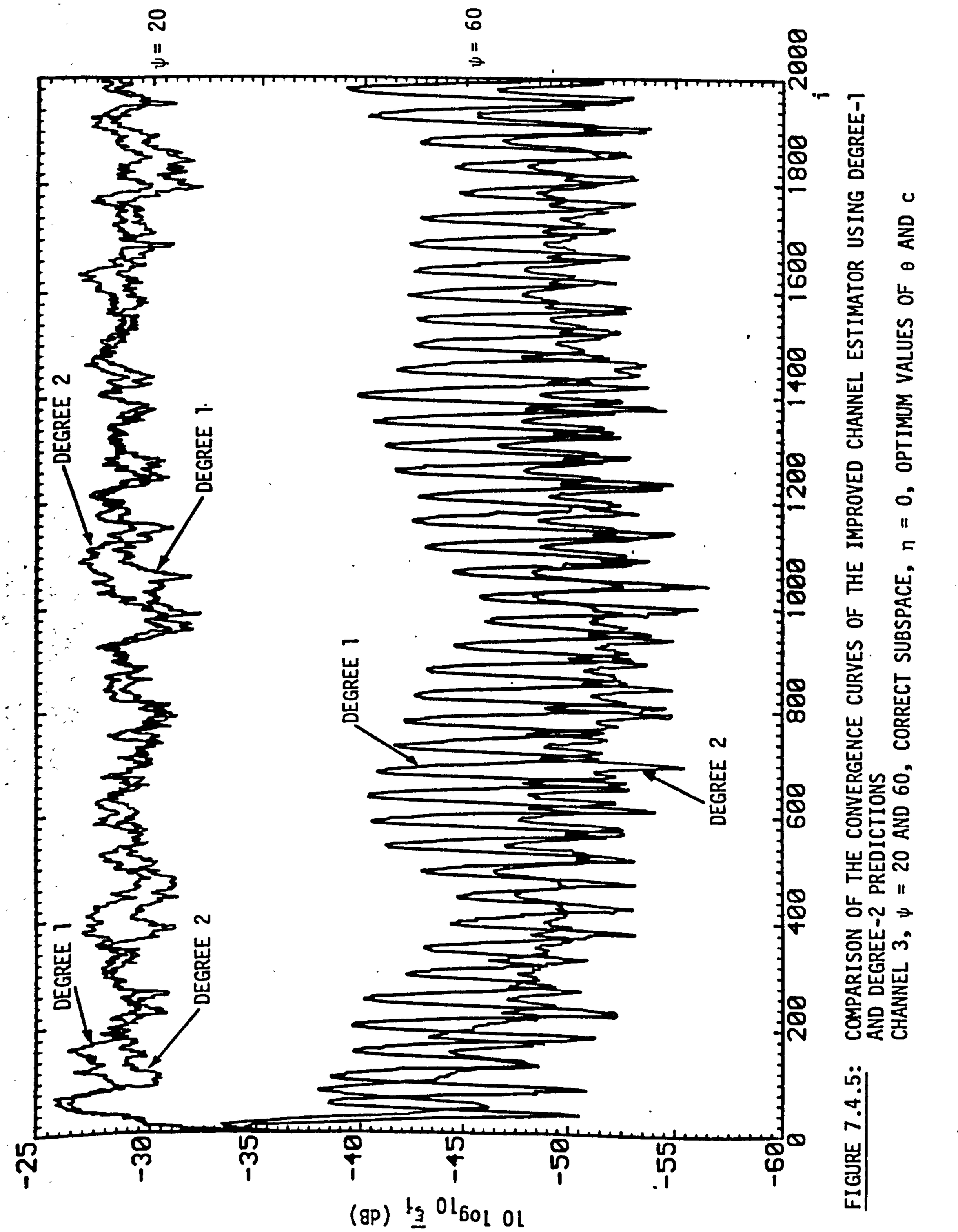

FIGURE 7.4.5: COMPARISON OF THE CONVERGENCE CURVES OF THE IMPROVED CHANNEL ESTIMATOR USING DEGREE-1 AND DEGREE-2 PREDICTIONS
CHANNEL 3, ψ = 20 AND 60, CORRECT SUBSPACE, η = 0, OPTIMUM VALUES OF θ AND c

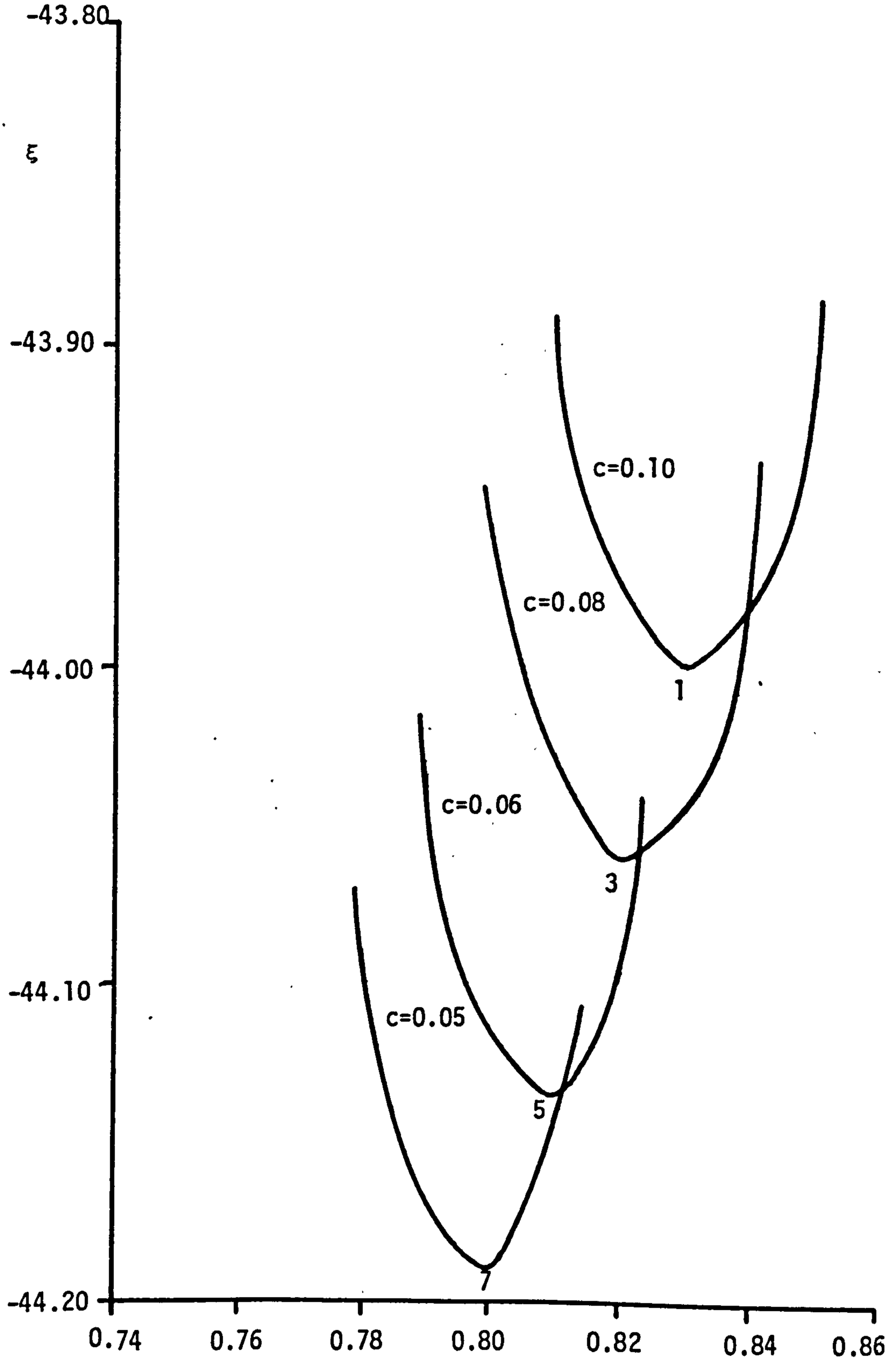

FIGURE 7.4.6: OPTIMIZATION OF θ

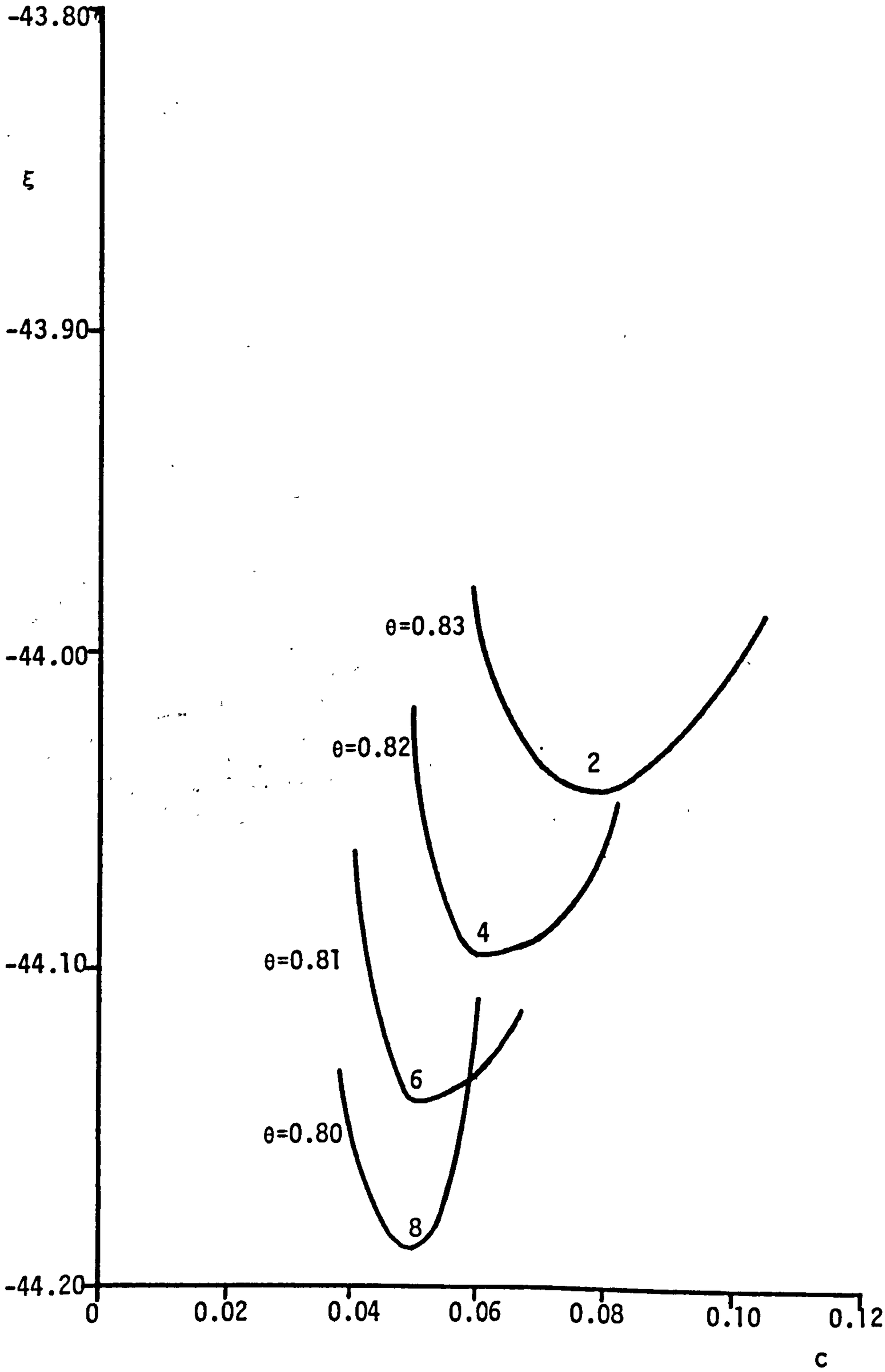

FIGURE 7.4.7: OPTIMIZATION OF c

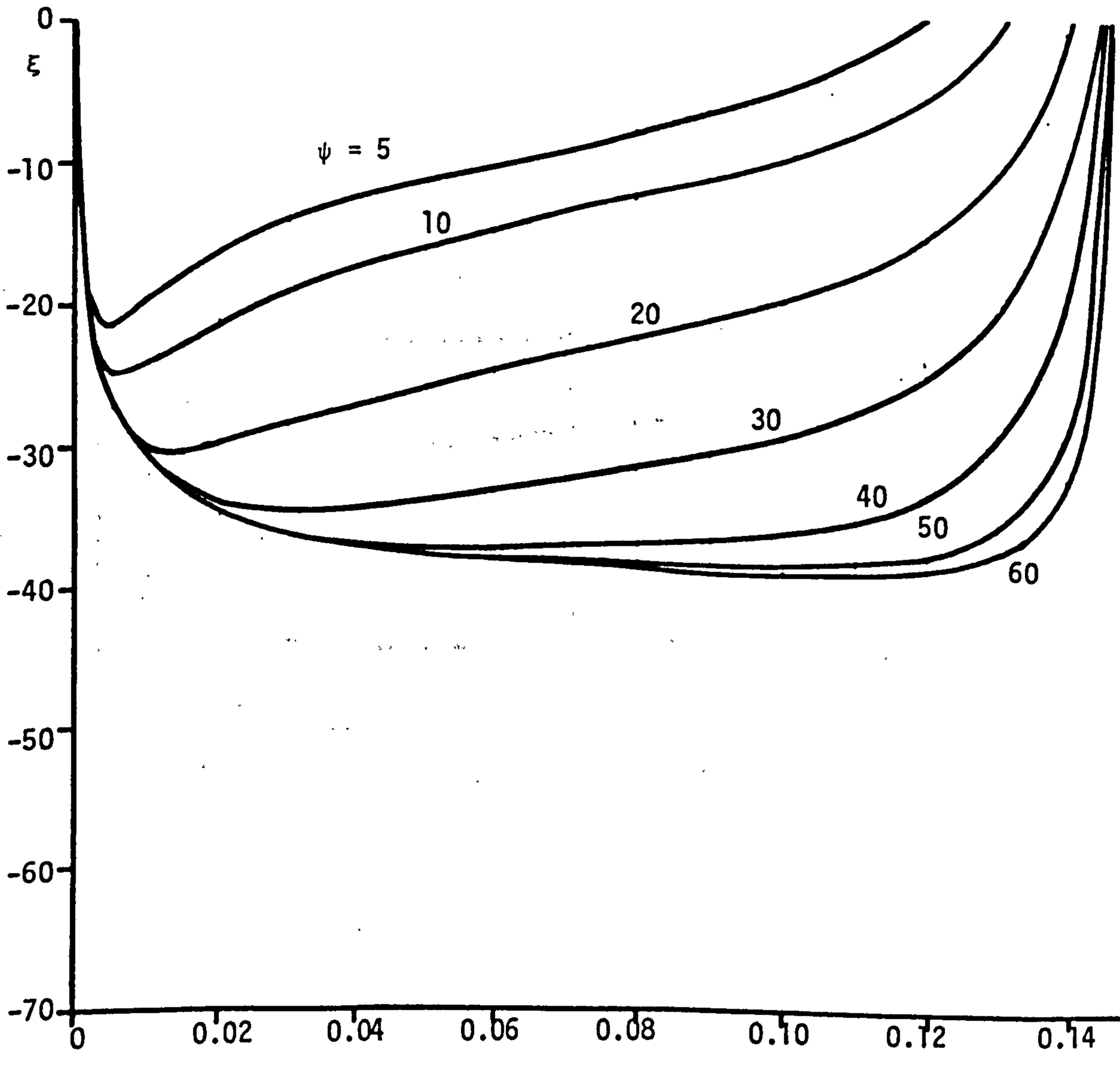

FIGURE 7.4.8: VARIATION OF ξ WITH c
CHANNEL 1, DEGREE-0 PREDICTION, CORRECT SUBSPACE
$\eta = 0$, θ OPTIMUM AT EACH ψ

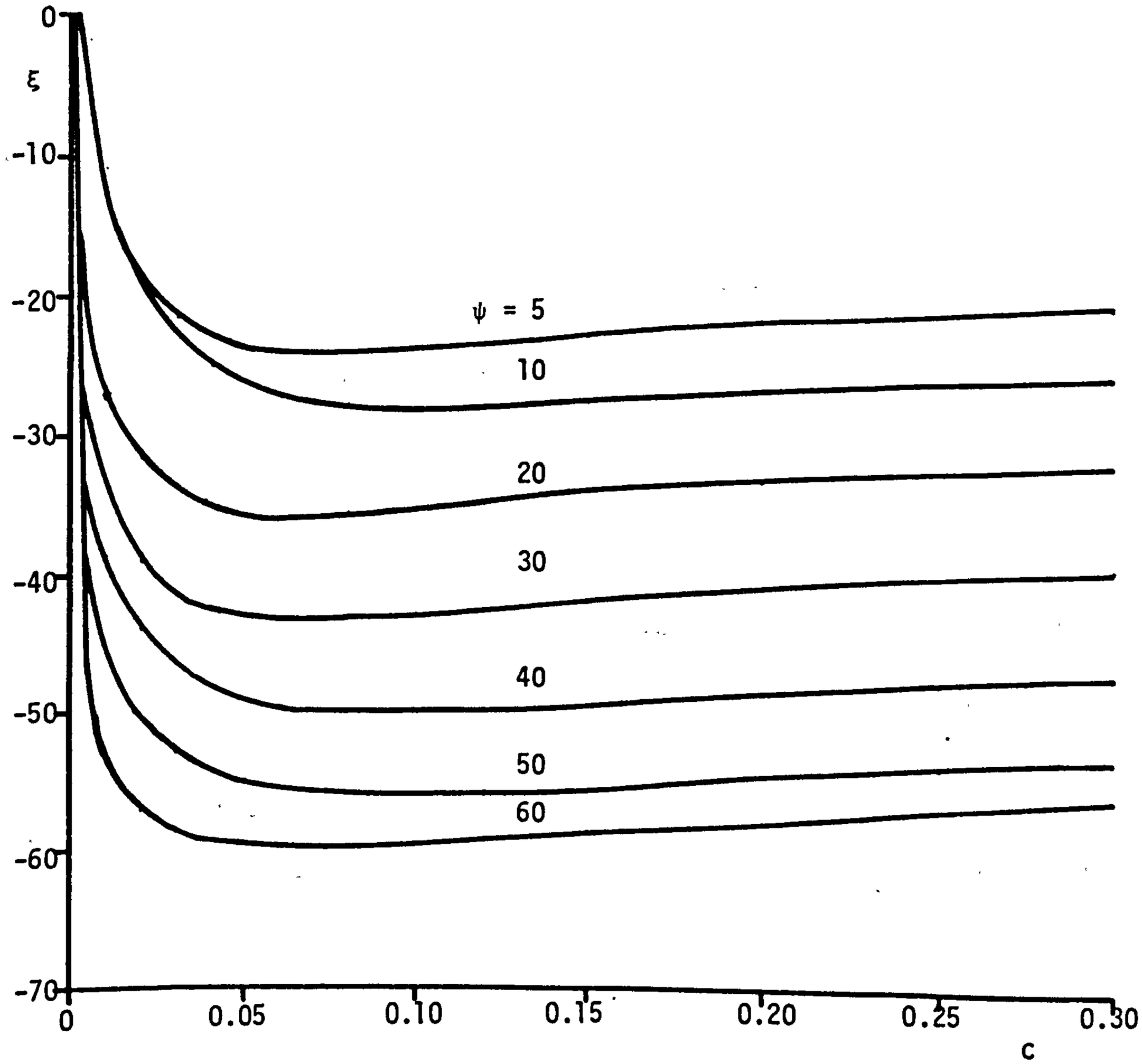

FIGURE 7.4.9: VARIATION OF ξ WITH c
CHANNEL 1, DEGREE-1 PREDICTION, CORRECT SUBSPACE
$\eta = 0$, θ OPTIMUM AT EACH ψ

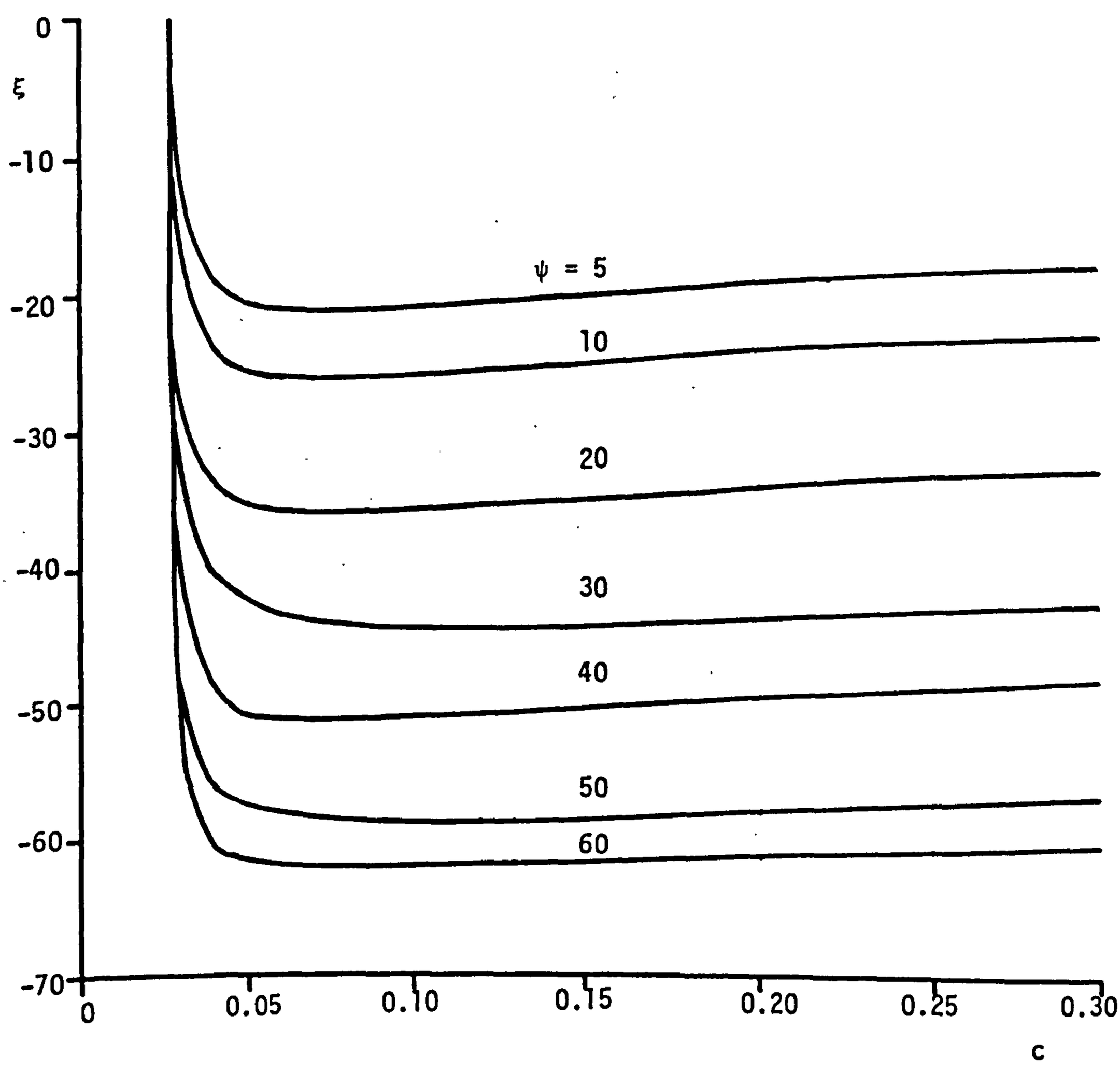

FIGURE 7.4.10: VARIATION OF ξ WITH c
CHANNEL 1, DEGREE-2 PREDICTION, CORRECT SUBSPACE
$\eta = 0$, θ OPTIMUM AT EACH ψ

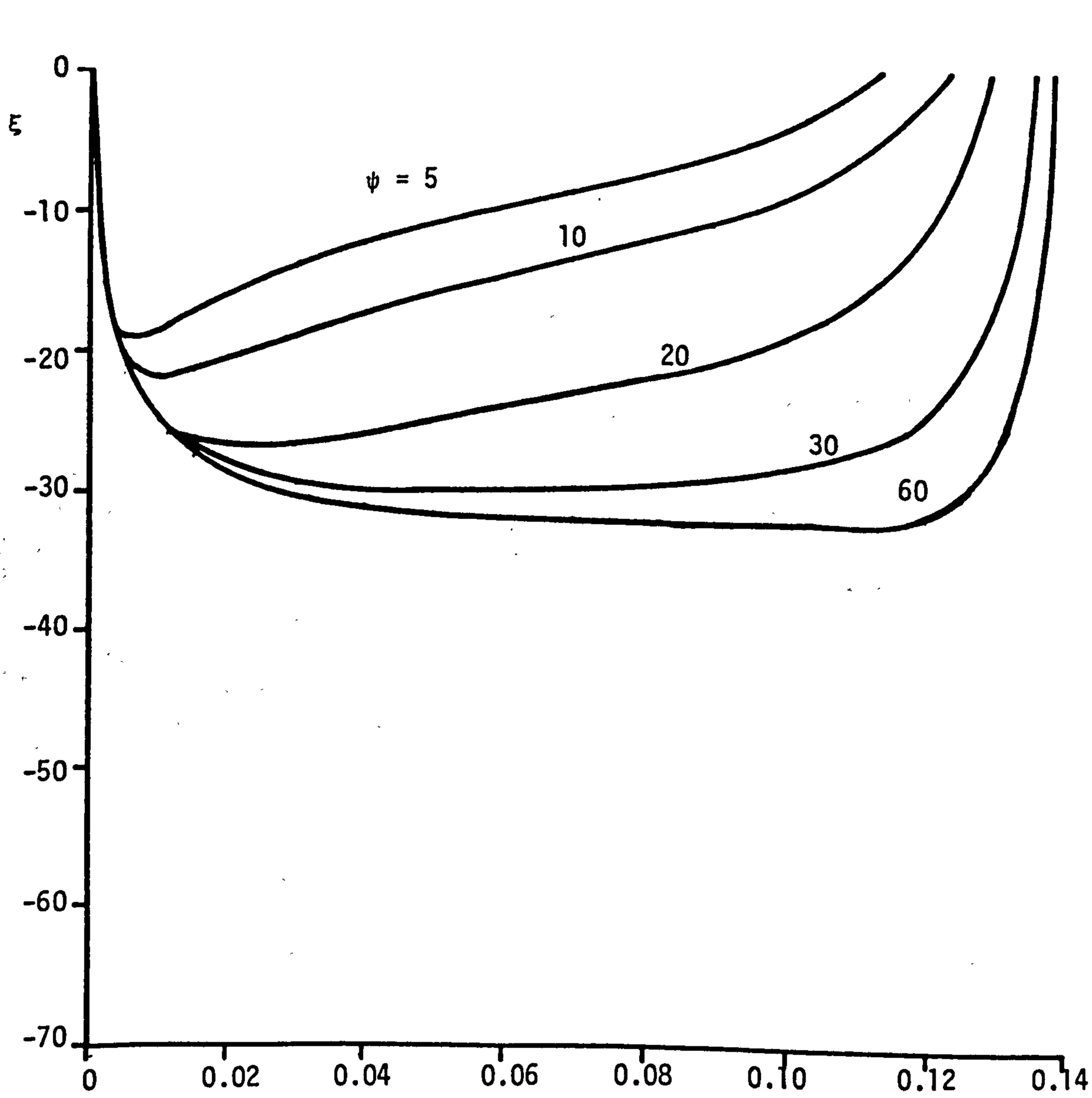

FIGURE 7.4.11: VARIATION OF ξ WITH c
CHANNEL 2, DEGREE-0 PREDICTION, CORRECT SUBSPACE
$\eta = 0$, θ OPTIMUM AT EACH ψ

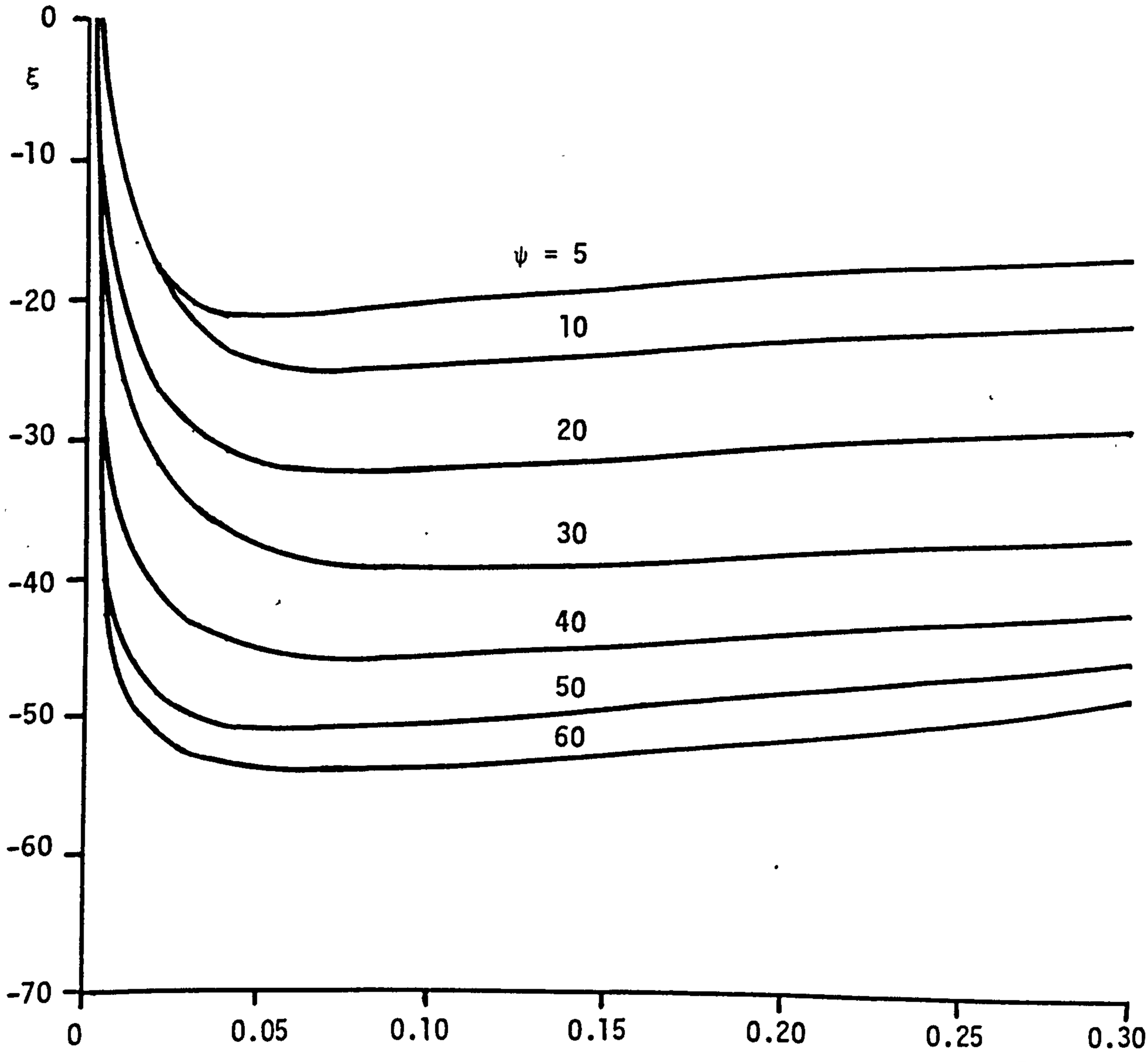

FIGURE 7.4.12: VARIATION OF ξ WITH c
CHANNEL 2, DEGREE-1 PREDICTION, CORRECT SUBSPACE
$\eta = 0$, θ OPTIMUM AT EACH ψ

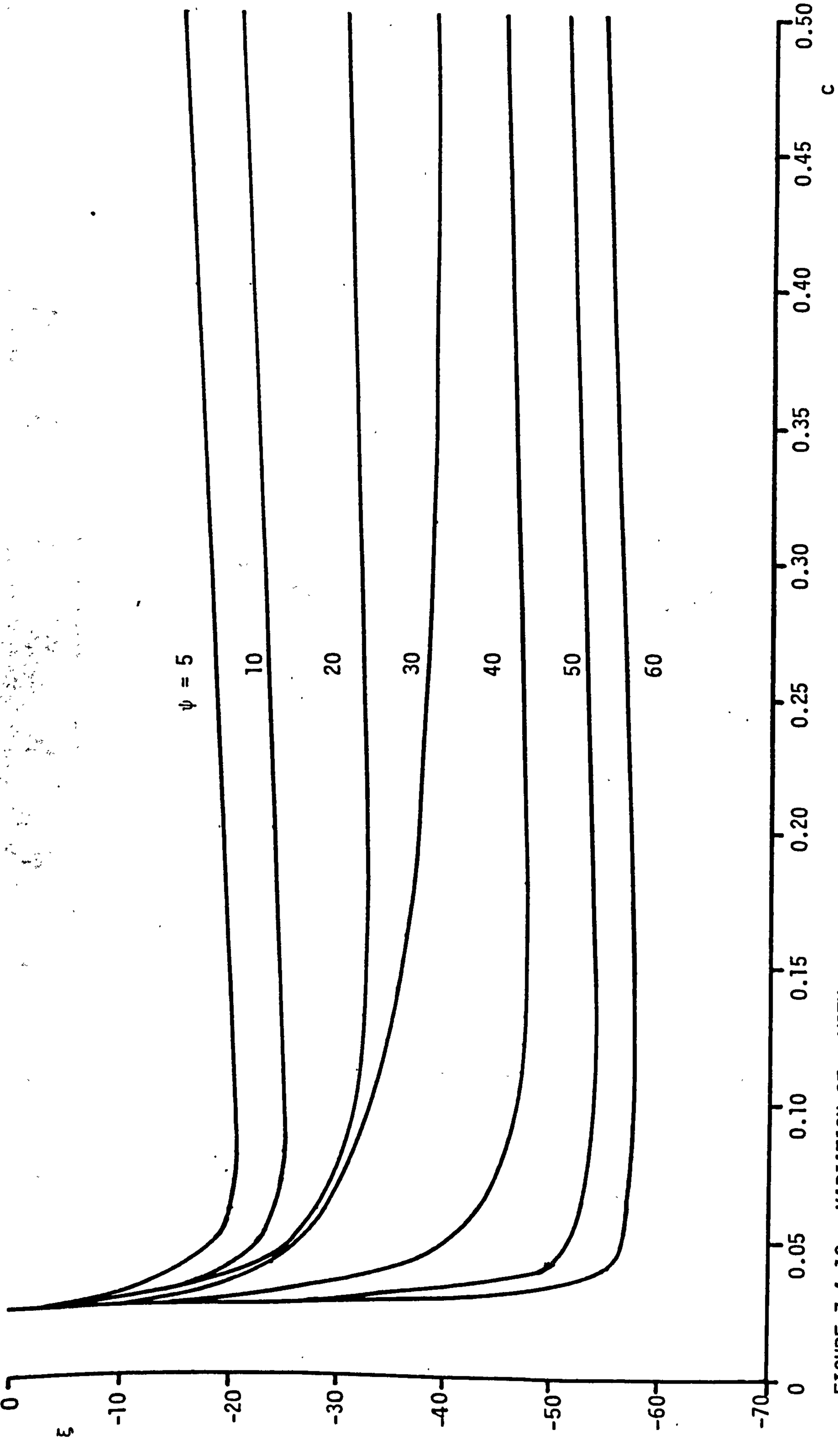
ψ = 5
10
20
30
40
50
60
ε
0
-10
-20
-30
-40
-50
-60
-70
0
0.05
0.10
0.15
0.20
0.25
0.30
0.35
0.40
0.45
0.50
c
η = 0,θ OPTIMUM AT EACH ψ
DEGREE-2 PREDICTION, CORRECT SUBSPACE, η =
CHANNEL 2, D
OF ε WITH c
VARIATION

FIGURE 7.4.13:

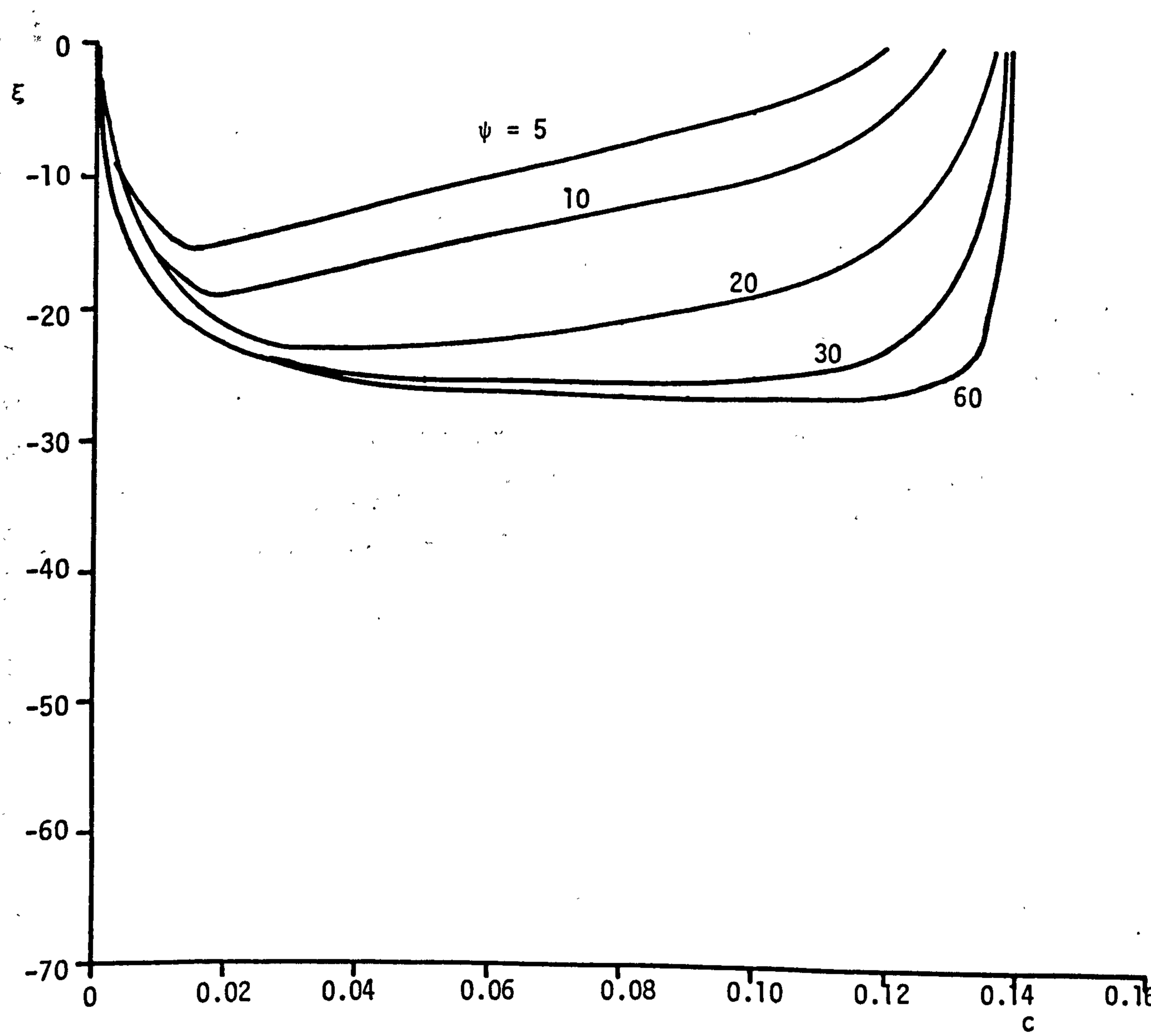

FIGURE 7.4.14: VARIATION OF ξ WITH c
CHANNEL 3, DEGREE-0 PREDICTION, CORRECT SUBSPACE
$\eta = 0$, θ OPTIMUM AT EACH ψ

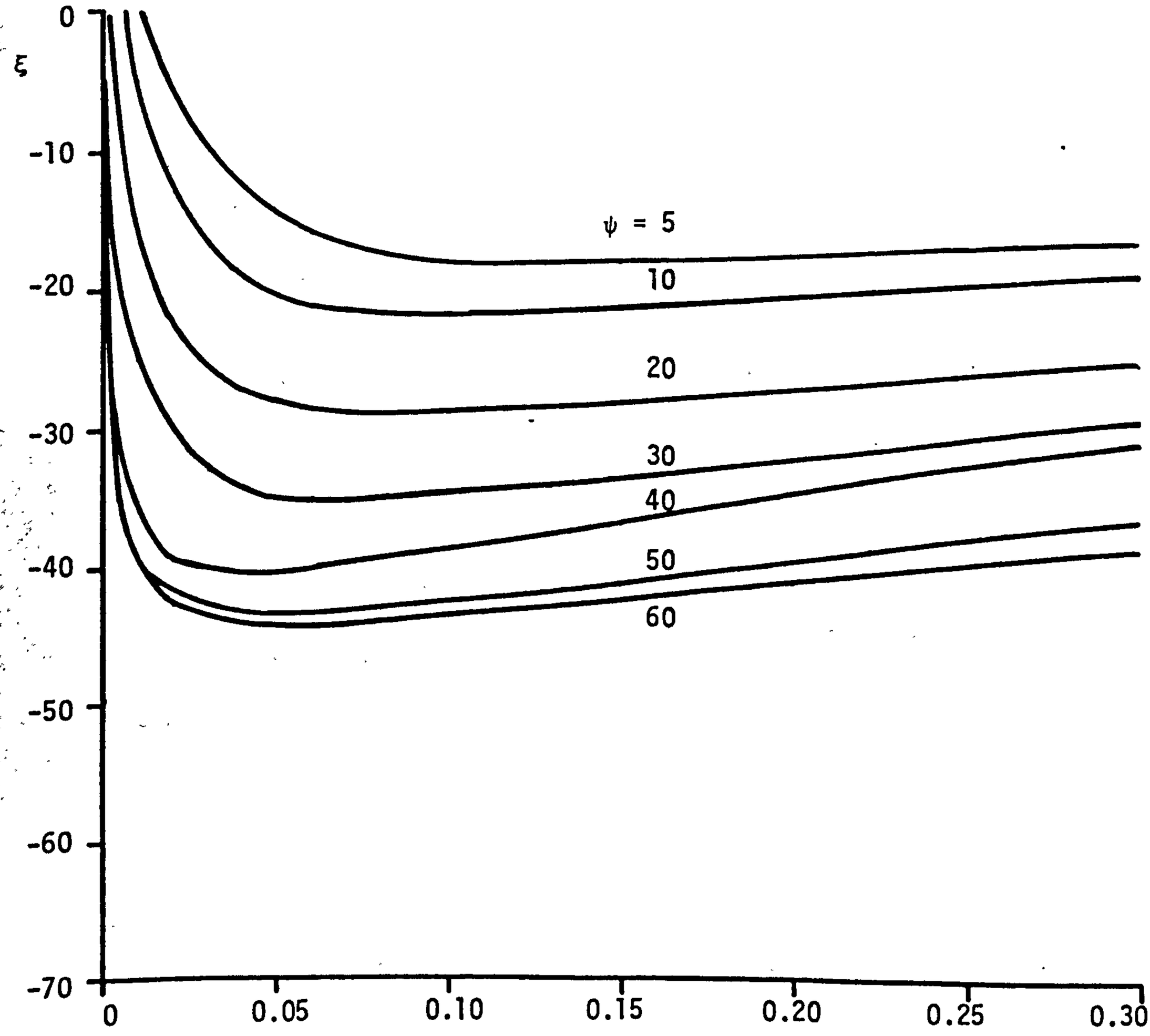

FIGURE 7.4.15: VARIATION OF ξ WITH c
CHANNEL 3, DEGREE-1 PREDICTION, CORRECT SUBSPACE
$\eta = 0$, θ OPTIMUM AT EACH ψ

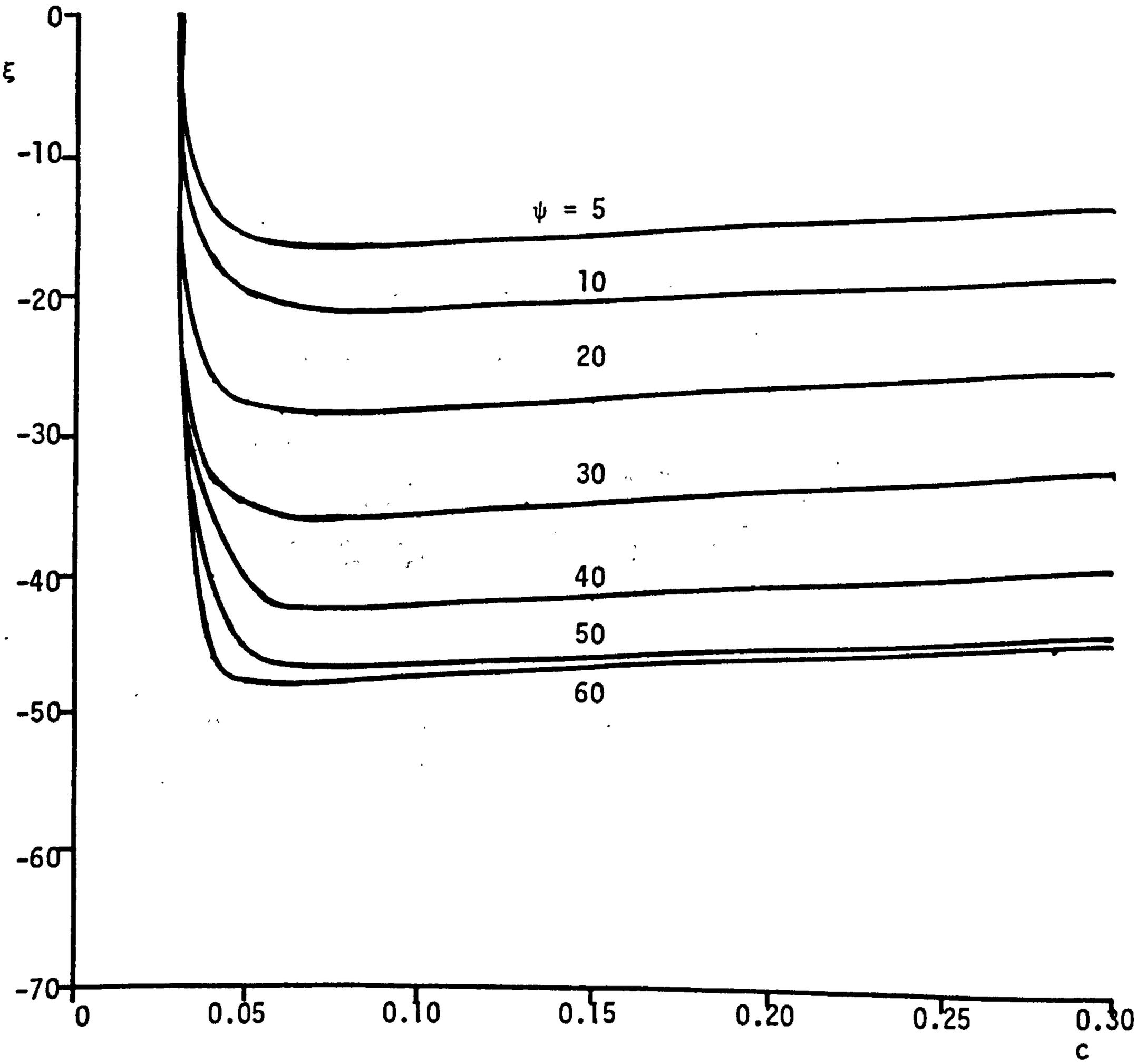

FIGURE 7.4.16: VARIATION OF ξ WITH c
CHANNEL 3, DEGREE-2 PREDICTION, CORRECT SUBSPACE
$\eta = 0$, θ OPTIMUM AT EACH ψ

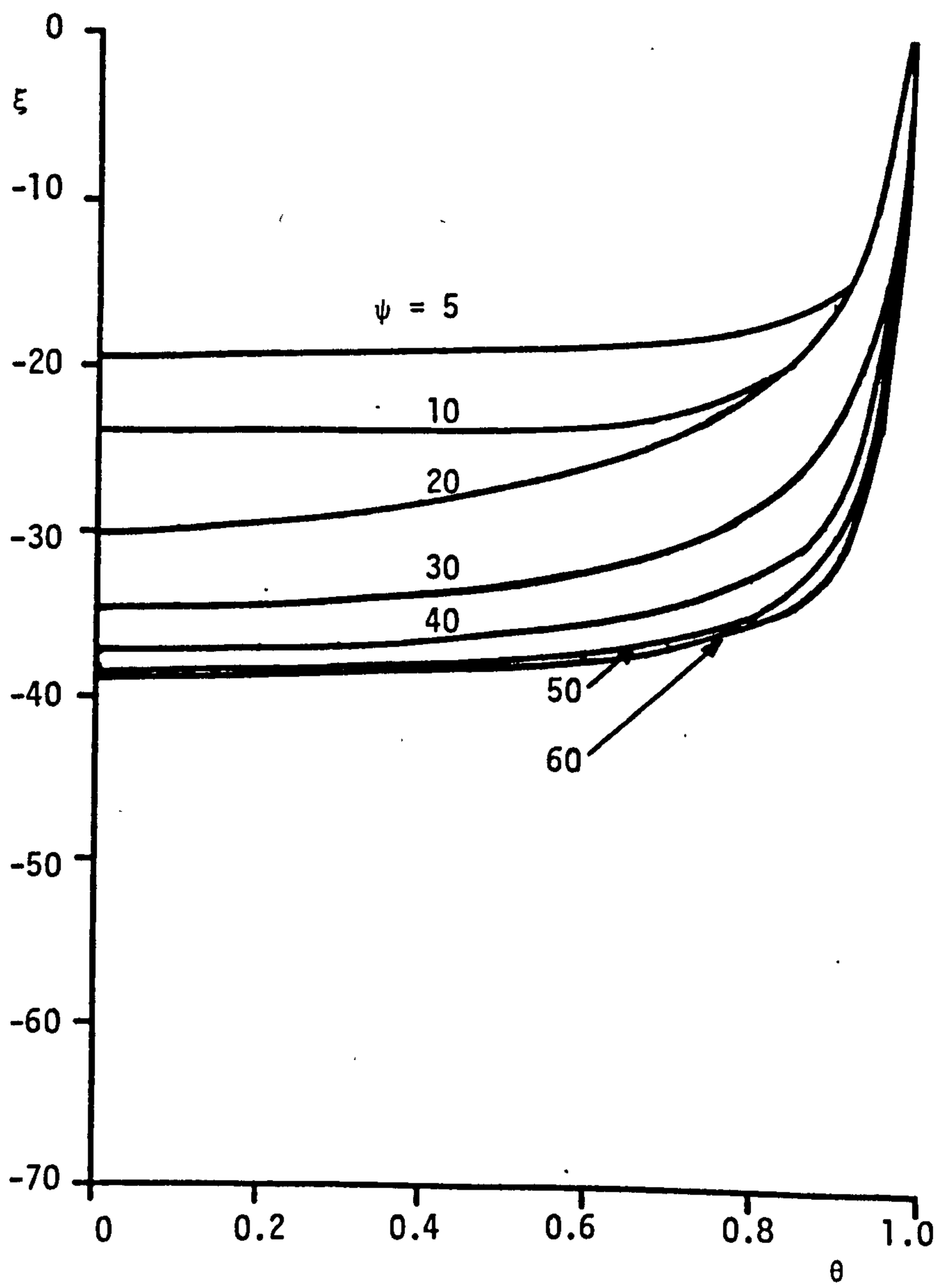

FIGURE 7.4.17: VARIATION OF ξ WITH θ
CHANNEL 1, DEGREE-0 PREDICTION, CORRECT SUBSPACE
η = 0, c OPTIMUM AT EACH ψ

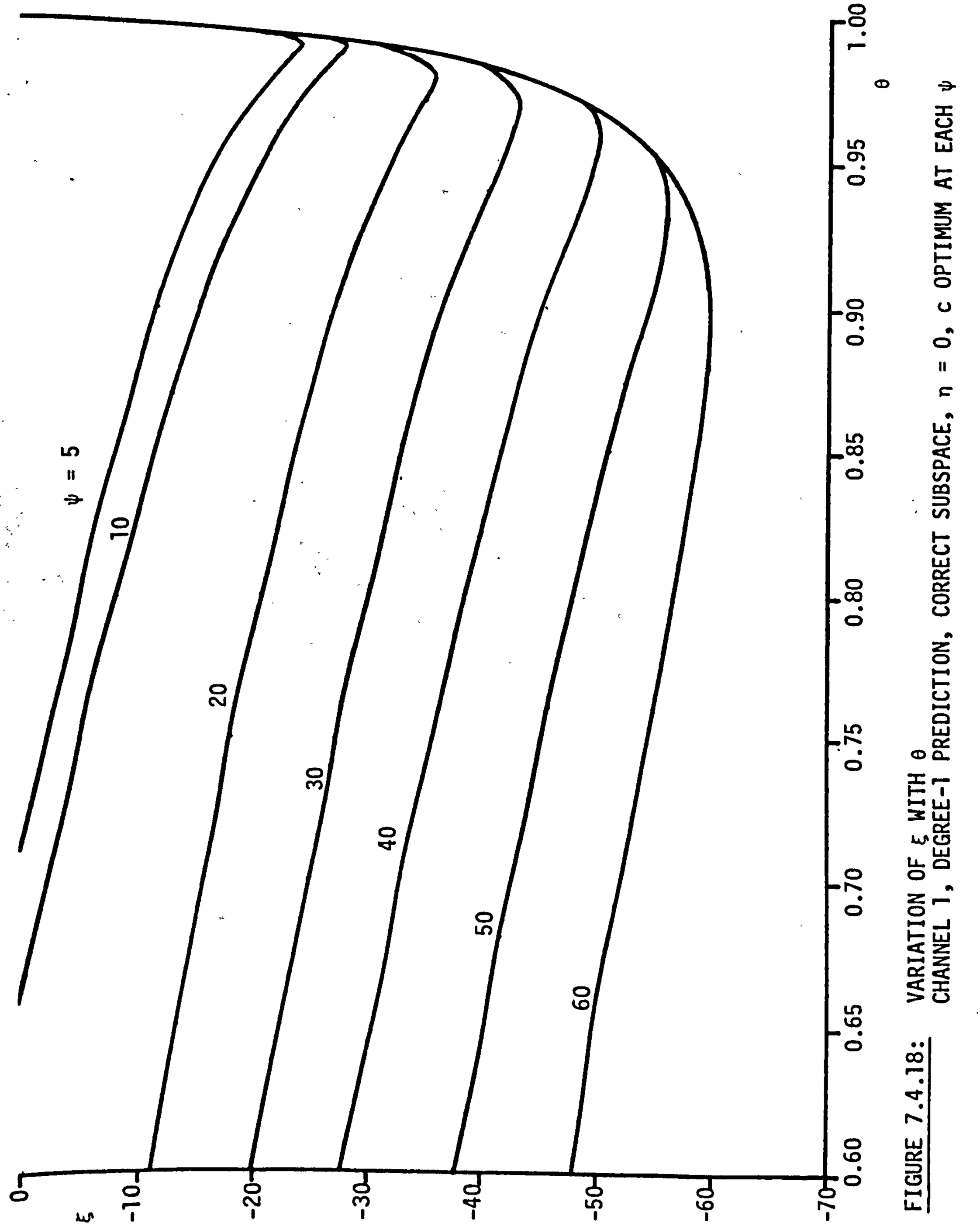
ψ = 5
10
20
30
40
50
60
ξ
0
-10
-20
-30
-40
-50
-60
-70
0.60
0.65
0.70
0.75
0.80
0.85
0.90
0.95
1.00
θ
VARIATION OF ξ WITH θ
CHANNEL 1, DEGREE-1 PREDICTION, CORRECT SUBSPACE, η = 0, c OPTIMUM AT EACH ψ

FIGURE 7.4.18:

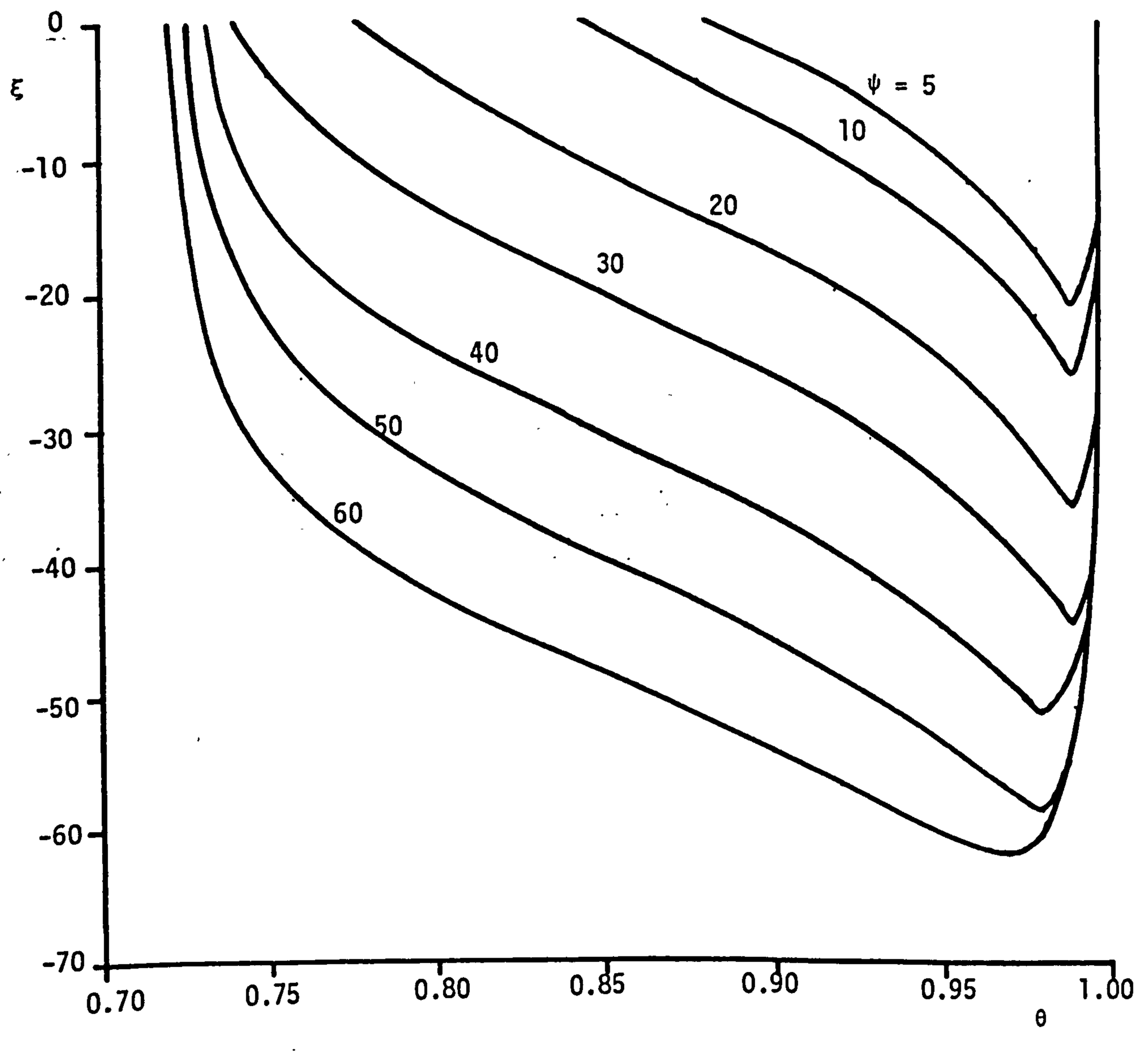

FIGURE 7.4.19: VARIATION OF ξ WITH θ
CHANNEL 1, DEGREE-2 PREDICTION, CORRECT SUBSPACE
$\eta = 0$, c OPTIMUM AT EACH ψ

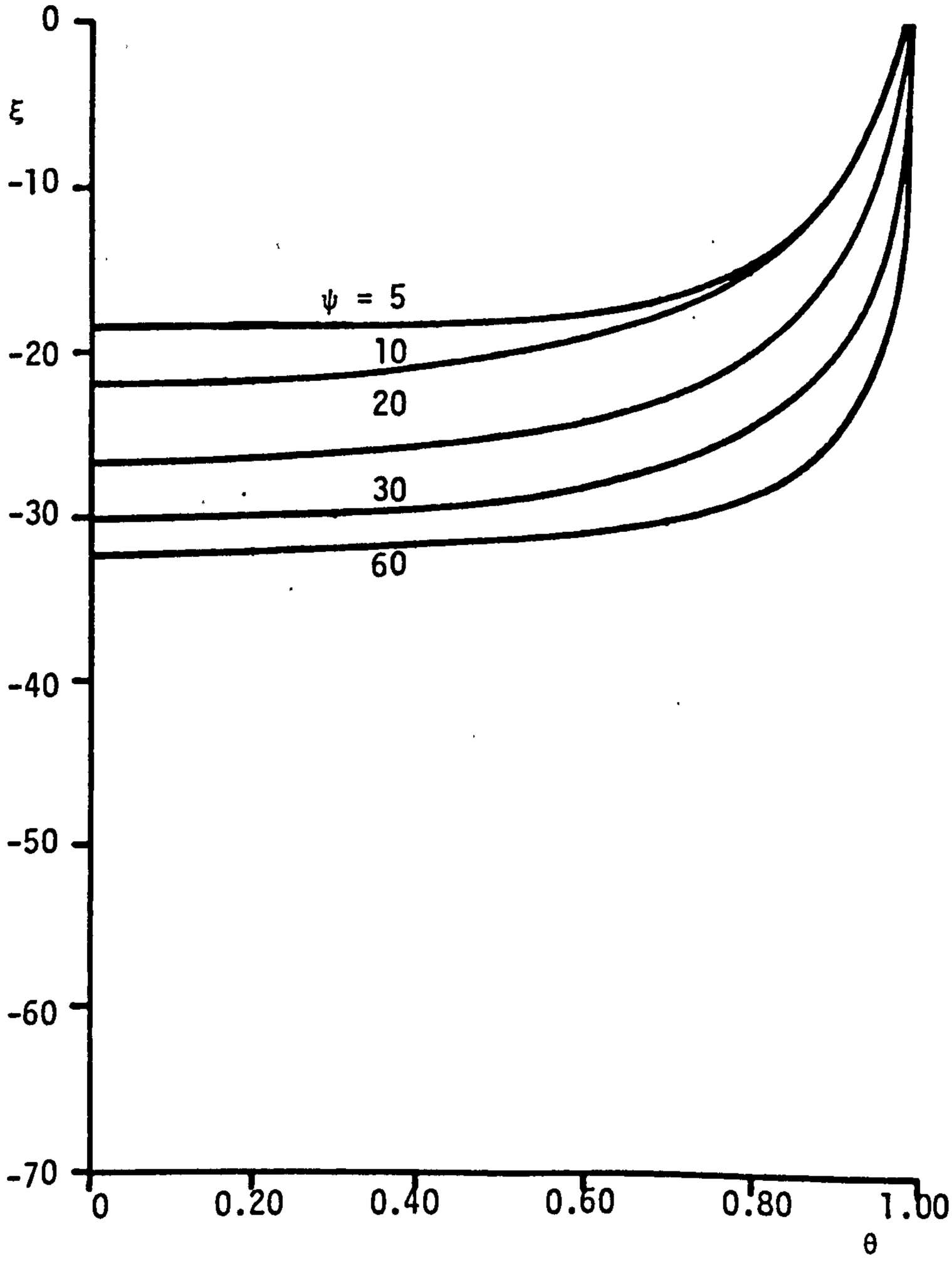

FIGURE 7.4.20: VARIATION OF ξ WITH θ
CHANNEL 2, DEGREE-0 PREDICTION, CORRECT SUBSPACE
$\eta = 0$, c OPTIMUM AT EACH ψ

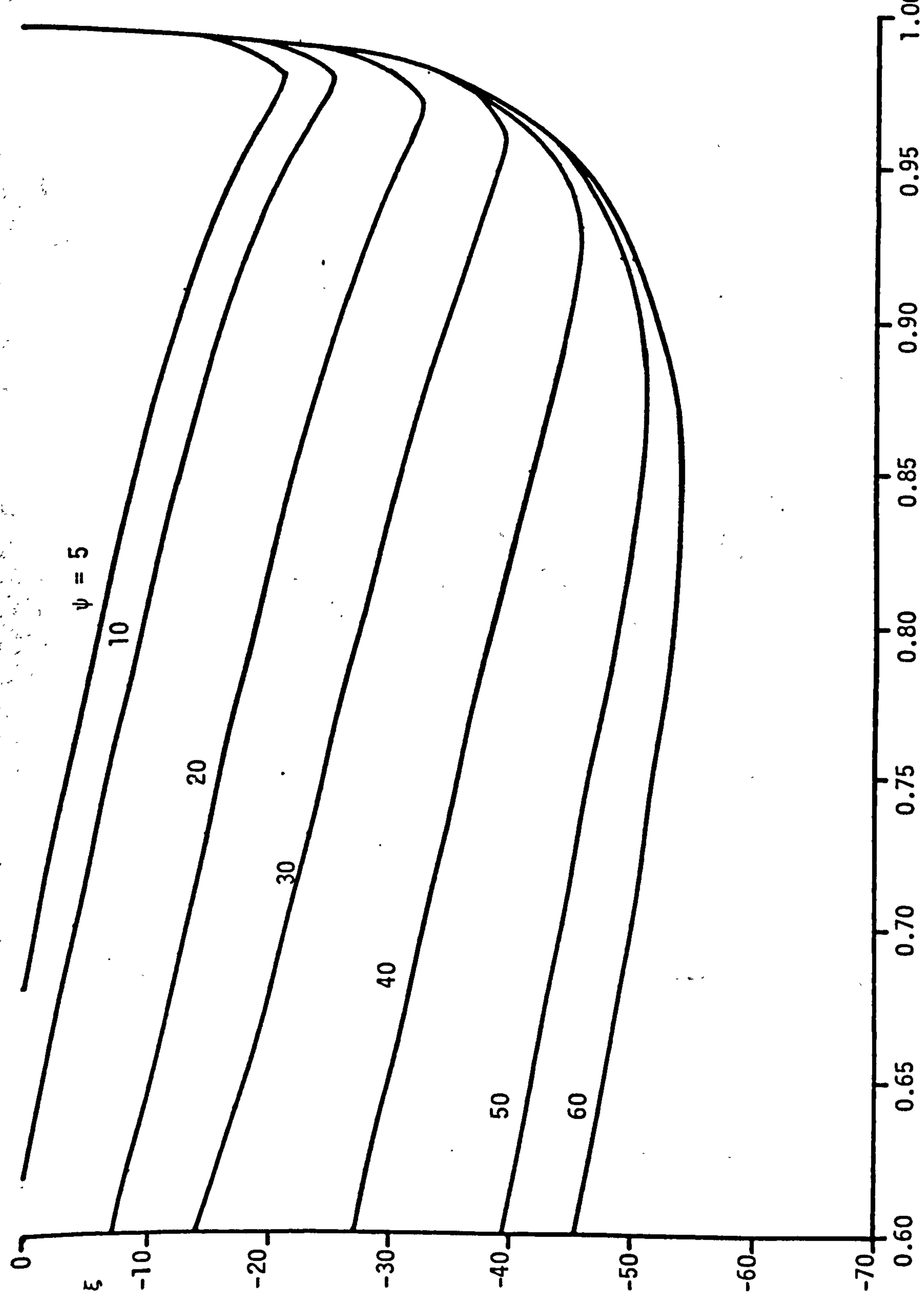

FIGURE 7.4.21: VARIATION OF ξ WITH θ AT EACH ψ. CHANNEL 2, DEGREE-1 PREDICTION, CORRECT SUBSPACE, η = 0, c OPTIMUM ...

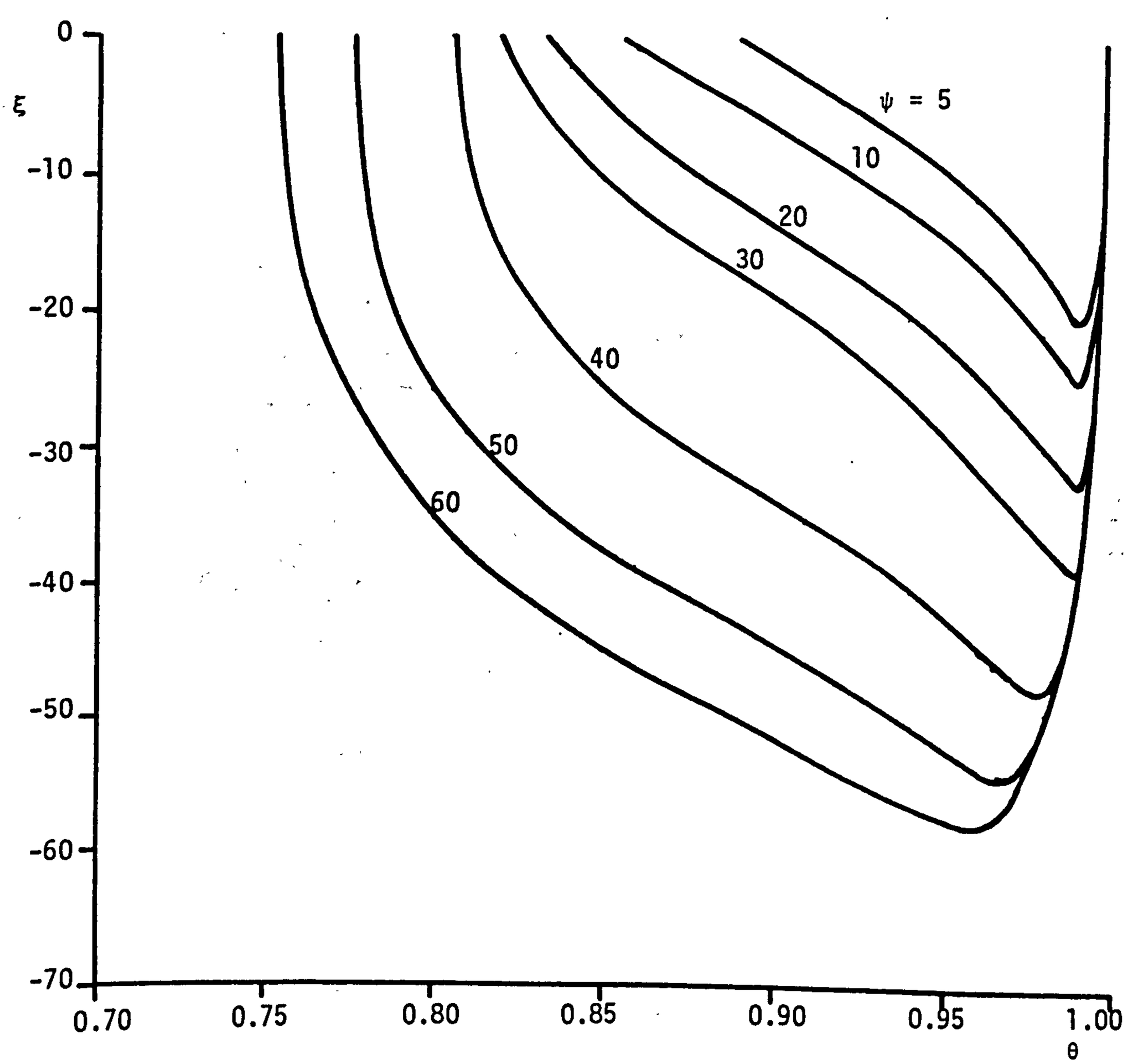

FIGURE 7.4.22: VARIATION OF ξ WITH θ
CHANNEL 2, DEGREE-2 PREDICTION, CORRECT SUBSPACE
η = 0, c OPTIMUM AT EACH ψ

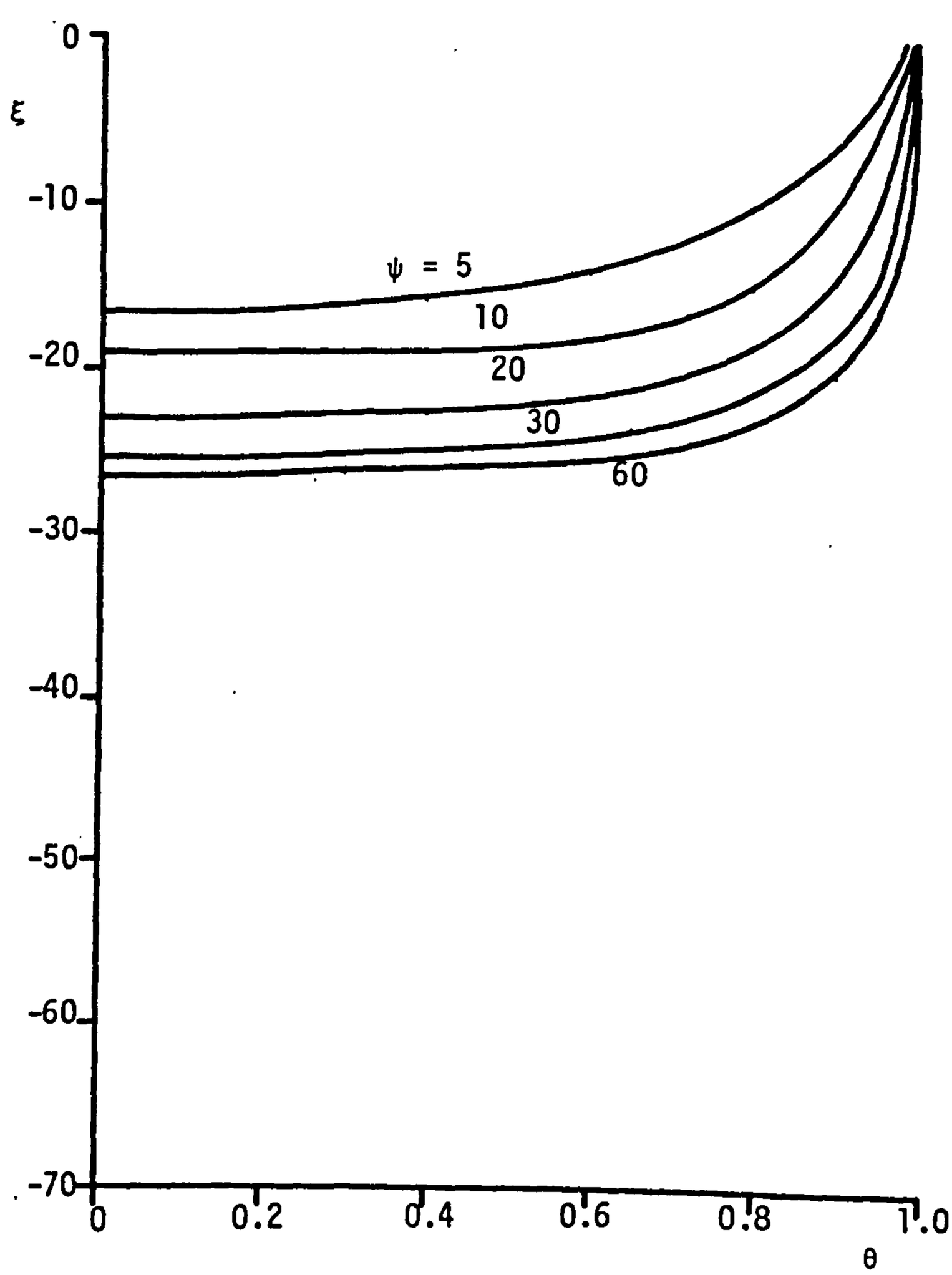

FIGURE 7.4.23: VARIATION OF ξ WITH θ
CHANNEL 3, DEGREE-0 PREDICTION, CORRECT SUBSPACE
$\eta = 0$, c OPTIMUM AT EACH ψ

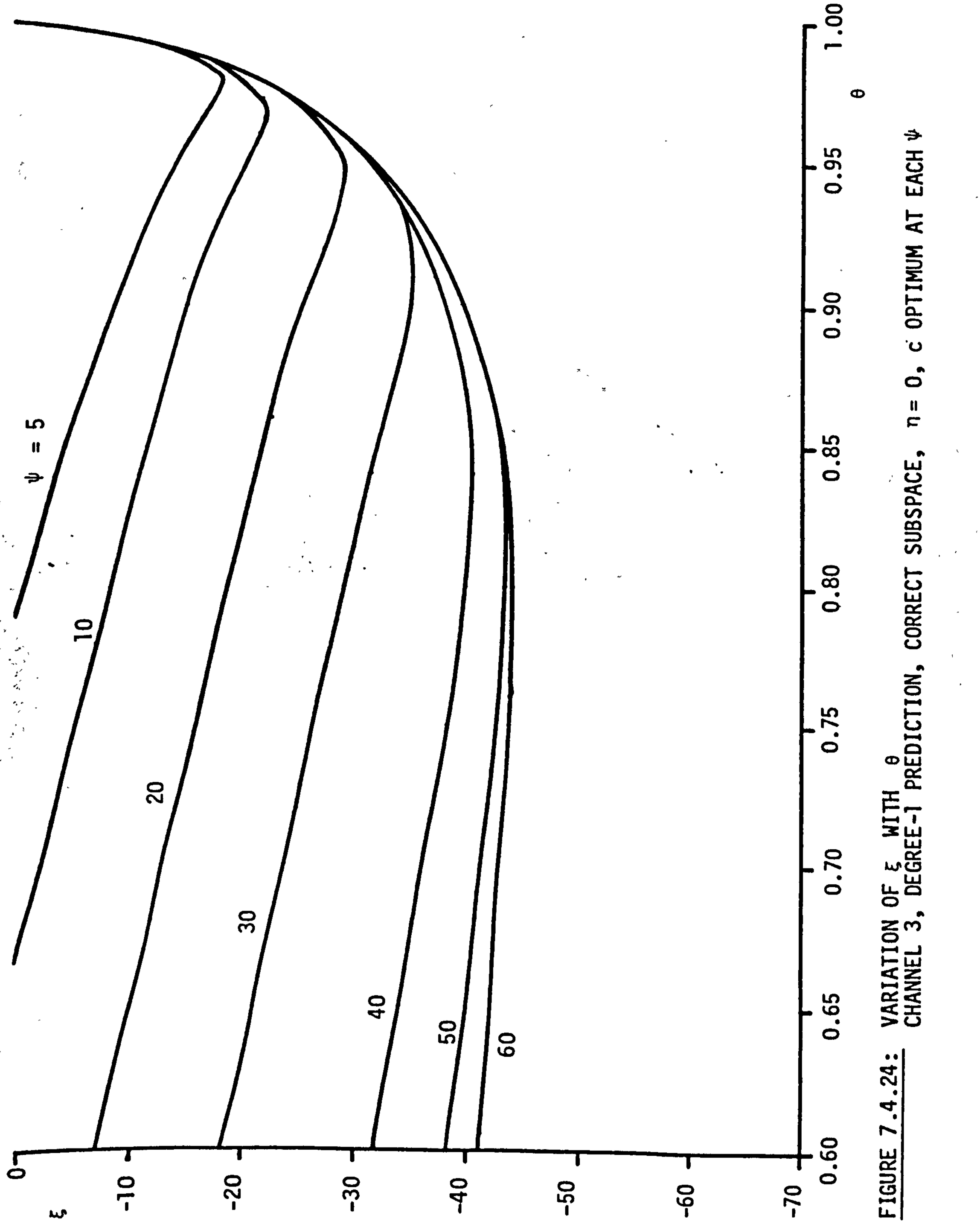

FIGURE 7.4.24: VARIATION OF ξ WITH θ
CHANNEL 3, DEGREE-1 PREDICTION, CORRECT SUBSPACE, η = 0, c OPTIMUM AT EACH ψ

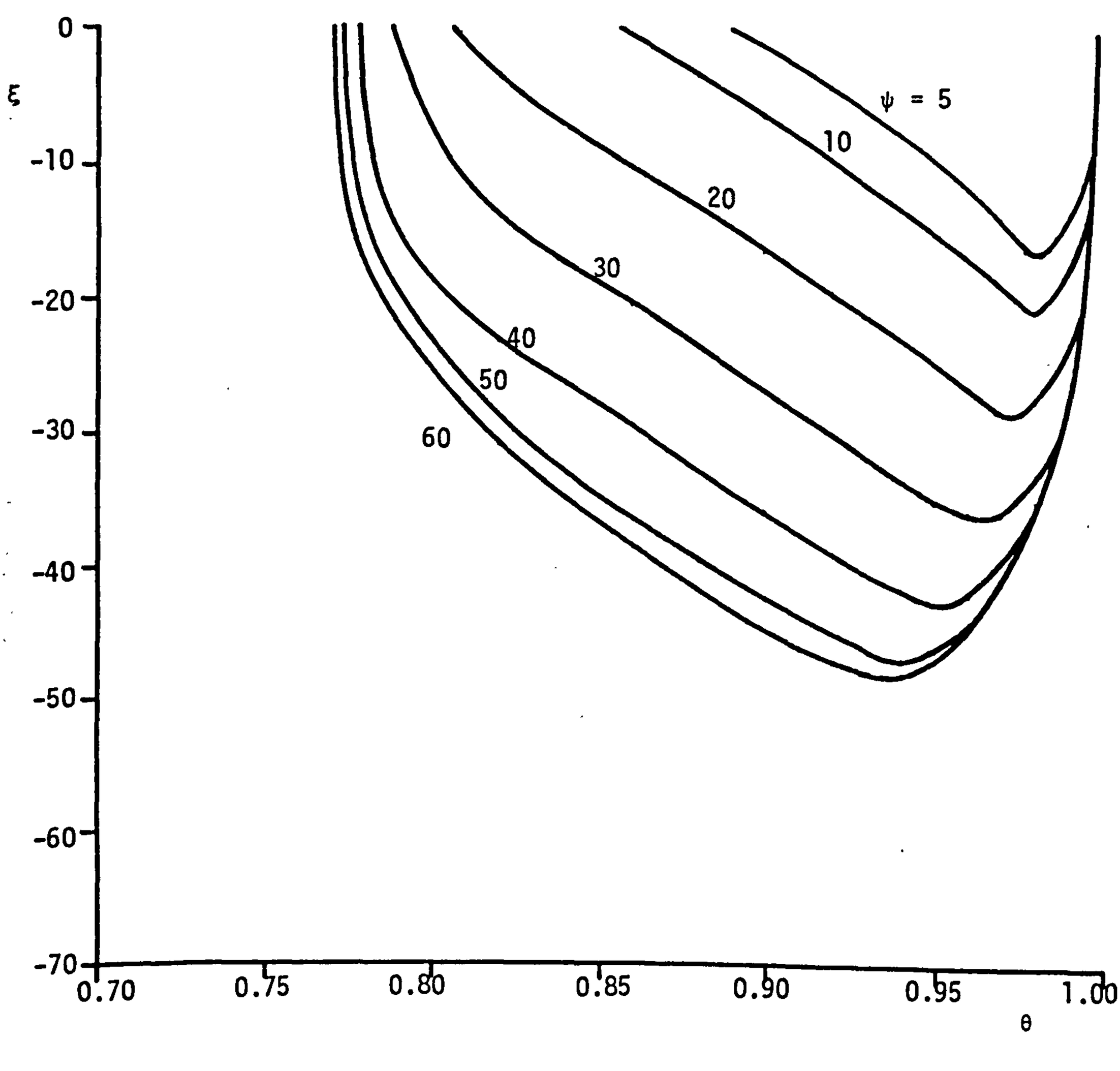

FIGURE 7.4.25: VARIATION OF ξ WITH θ
CHANNEL 3, DEGREE-2 PREDICTION, CORRECT SUBSPACE
$\eta = 0$, c OPTIMUM AT EACH ψ

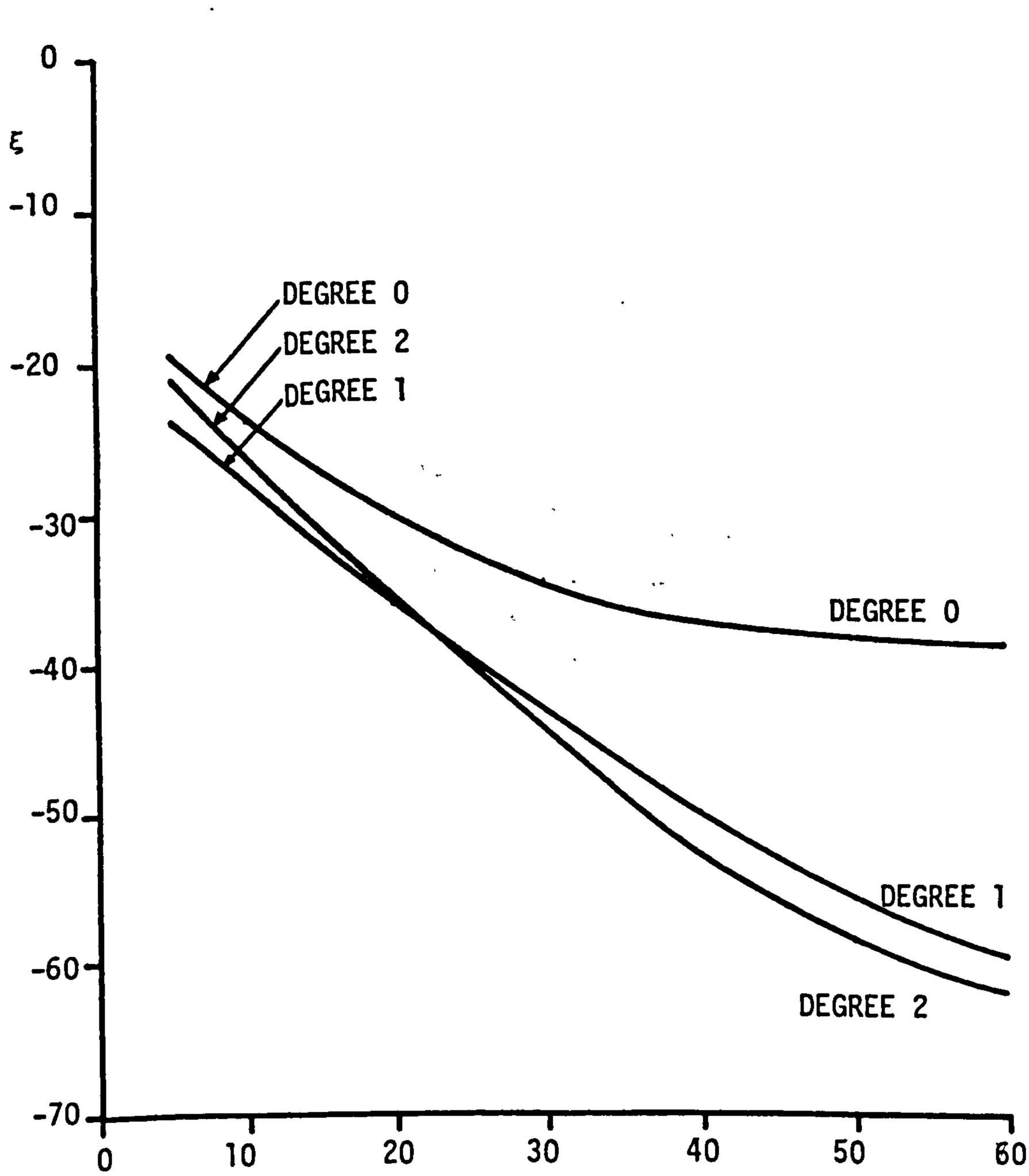

FIGURE 7.4.26: STEADY-STATE PERFORMANCE OF IMPROVED CHANNEL ESTIMATOR WITH CHANNEL 1
θ AND c ARE OPTIMUM AT EACH ψ, $\eta = 0$

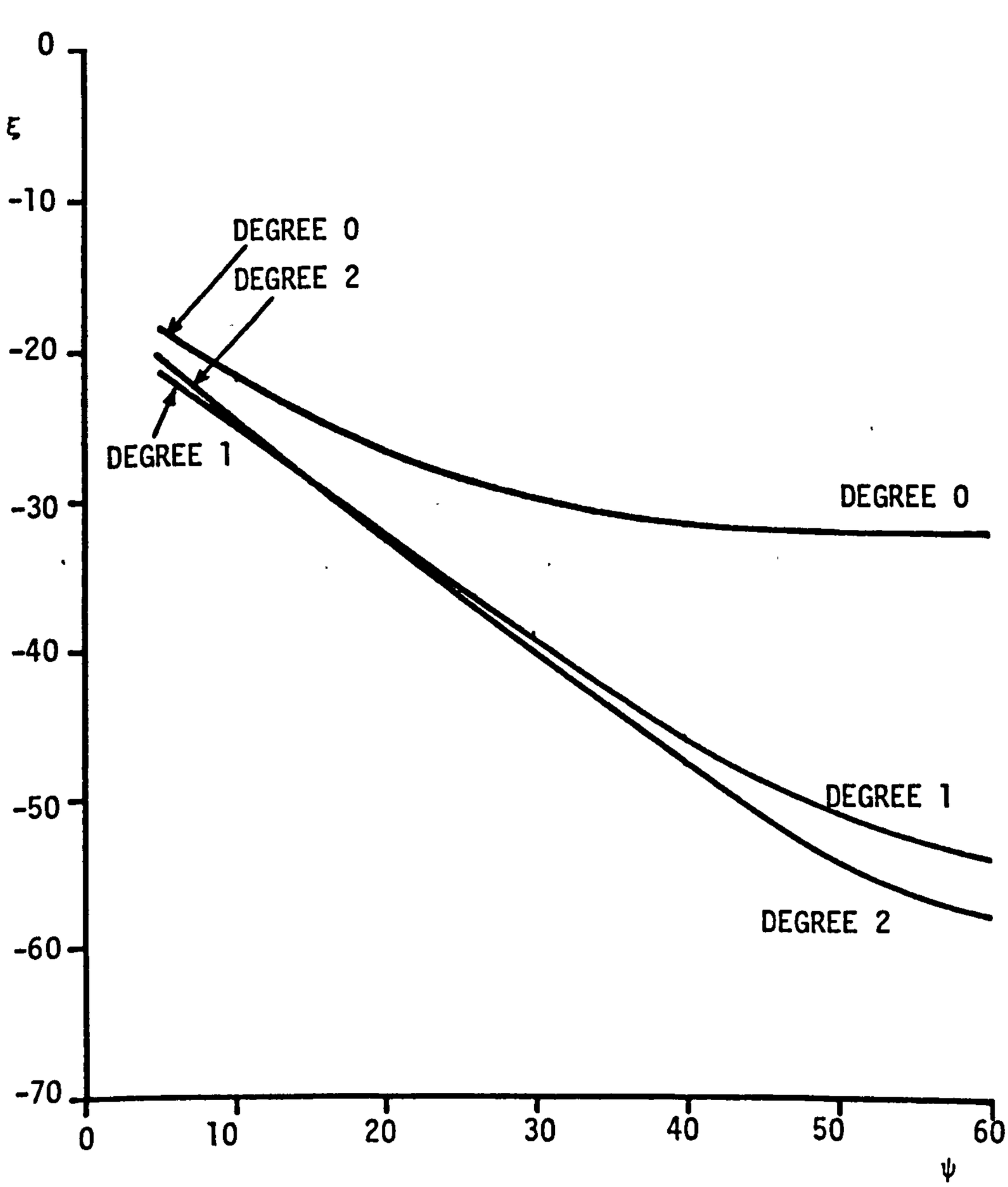

FIGURE 7.4.27: STEADY-STATE PERFORMANCE OF IMPROVED CHANNEL ESTIMATOR WITH CHANNEL 2
θ AND c ARE OPTIMUM AT EACH ψ, $\eta = 0$

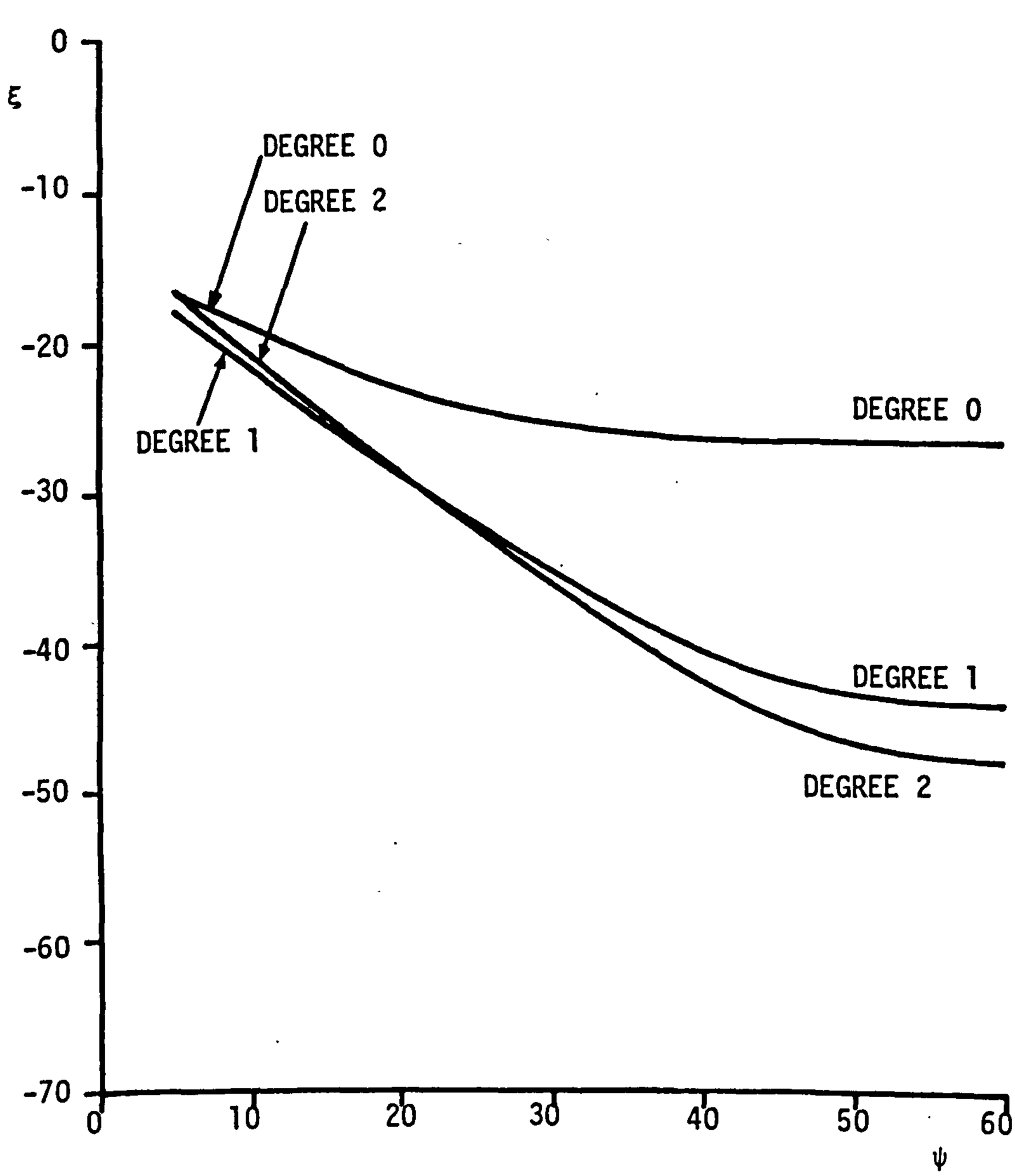

FIGURE 7.4.28: STEADY-STATE PERFORMANCE OF IMPROVED CHANNEL ESTIMATOR WITH CHANNEL 3
θ AND c ARE OPTIMUM AT EACH ψ, $\eta = 0$

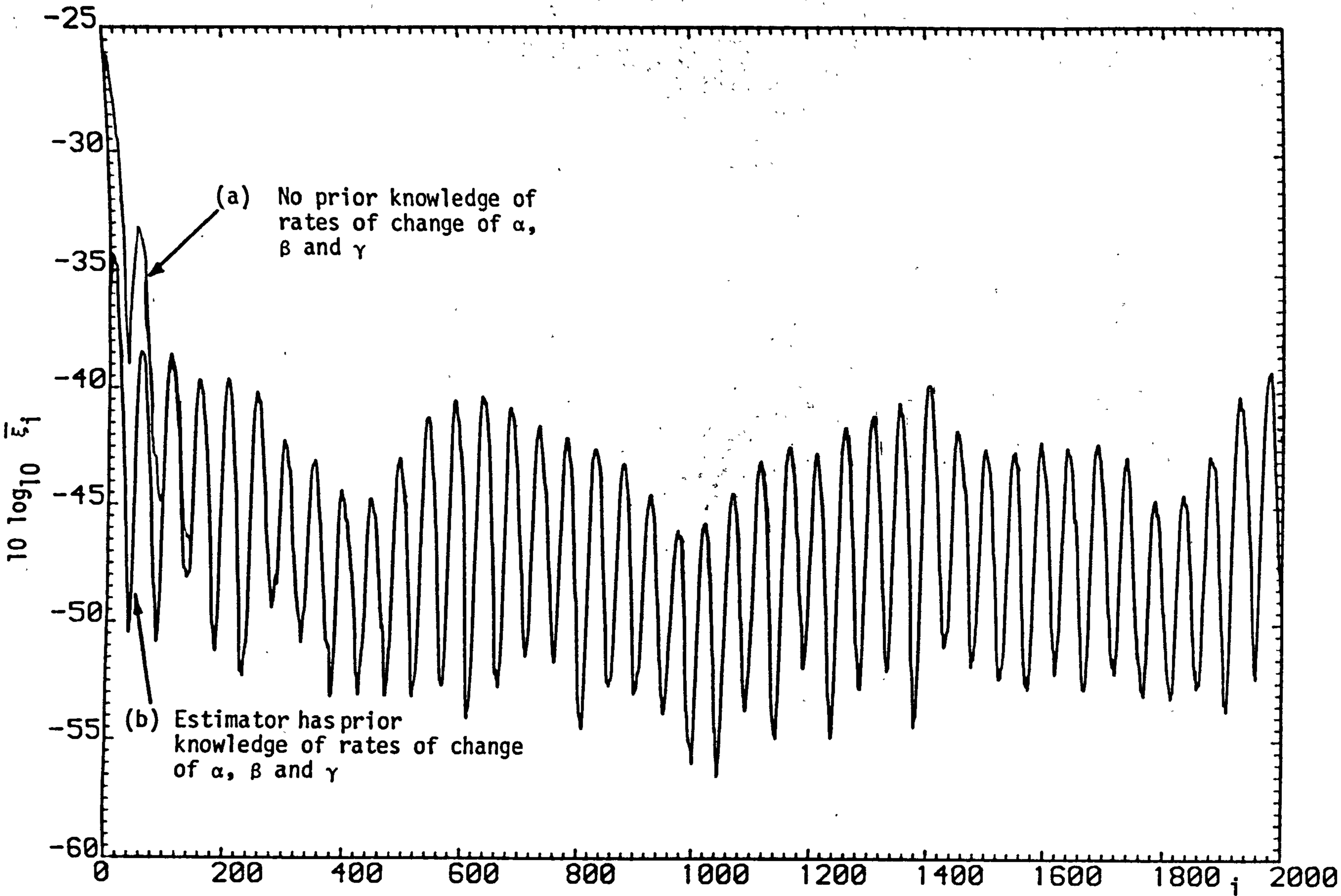

FIGURE 7.4.29: COMPARISON OF THE CONVERGENCE OF THE IMPROVED CHANNEL ESTIMATOR FOR THE CASES (a) IT HAS KNOWLEDGE OF THE RATES OF CHANGE OF α, β AND γ, AND (b) IT HAS NO PRIOR KNOWLEDGE OF THESE VALUES. CHANNEL 3, $\psi = 60$, DEGREE-1 PREDICTION, CORRECT SUBSPACE, $\eta = 0$, $\theta = 0.8$, $c = 0.05$

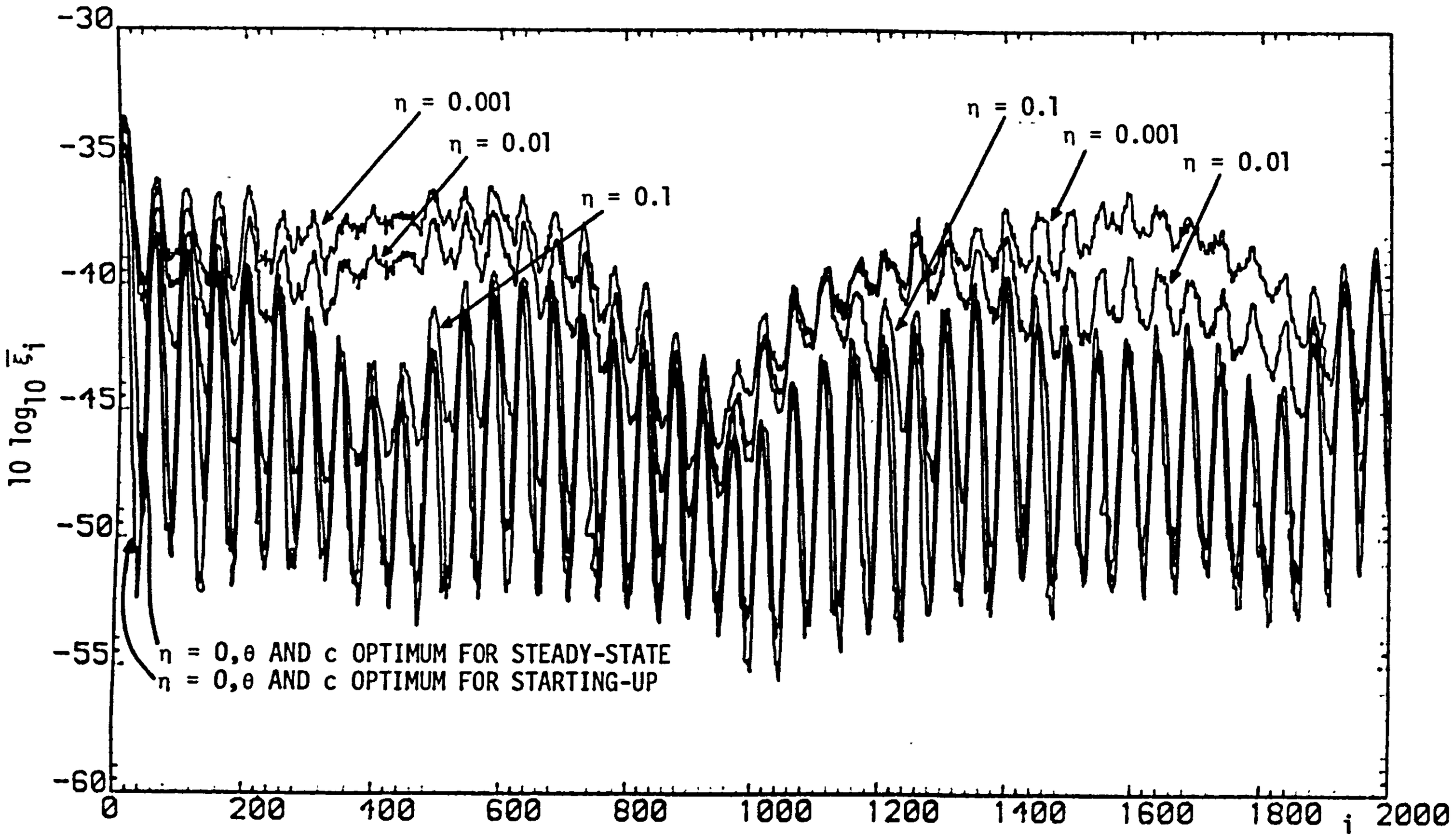

FIGURE 7.4.30: COMPARISON OF THE PERFORMANCE OF THE IMPROVED CHANNEL ESTIMATOR FOR THE CASES (a) THE CORRECT THREE-DIMENSIONAL SUBSPACE IS KNOWN (η=0), AND (b) THE SUBSPACE IS NOT KNOWN ($\eta \neq 0$) CHANNEL 3, ψ = 60, DEGREE-1 PREDICTION, θ = 0.80, c = 0.05, $\sigma_Z^2 = 10^{-6}$

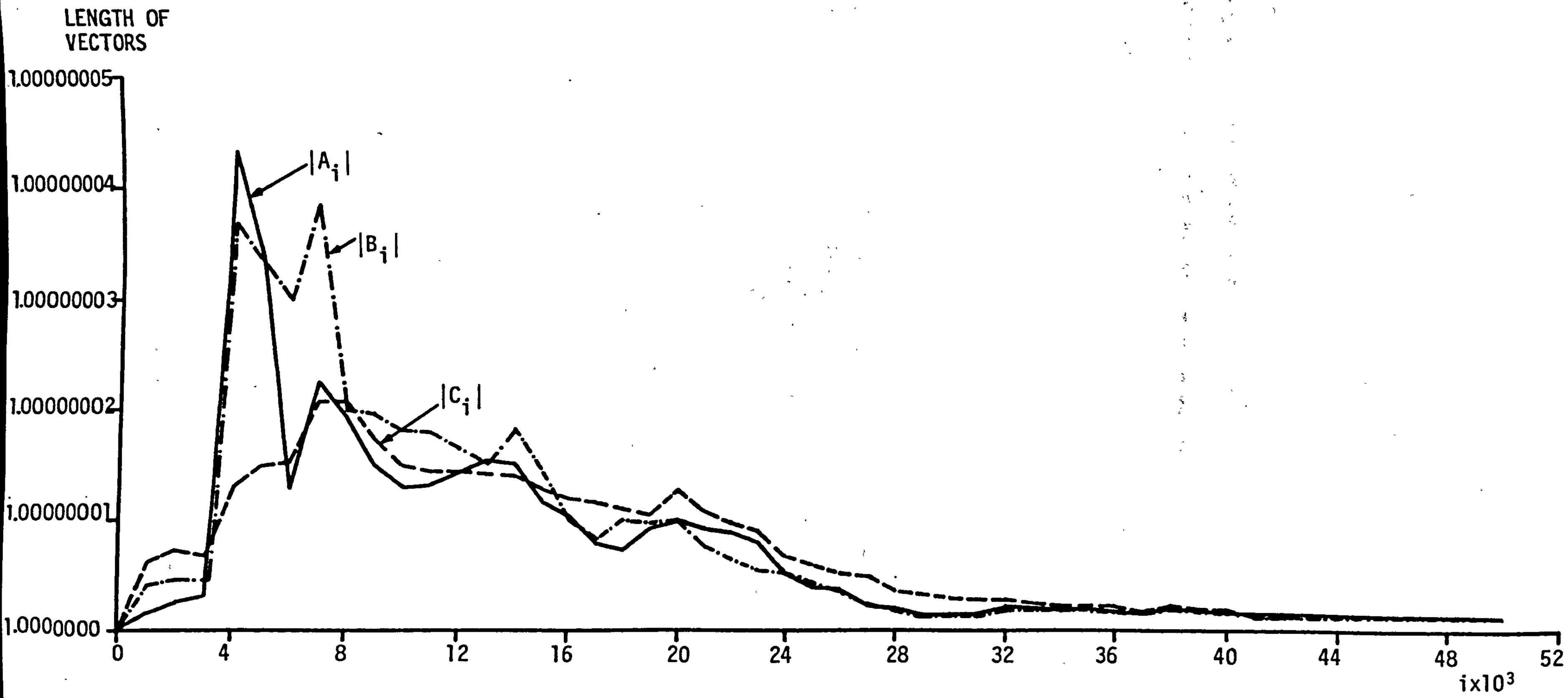

FIGURE 7.4.31: VARIATION OF THE LENGTH OF VECTORS A_i, B_i AND C_i
CHANNEL 3, $\psi = 60$, DEGREE-1 PREDICTION, $\eta = 0.001$, $\sigma_Z^2 = 10^{-6}$, $\theta = 0.80$, $c = 0.05$

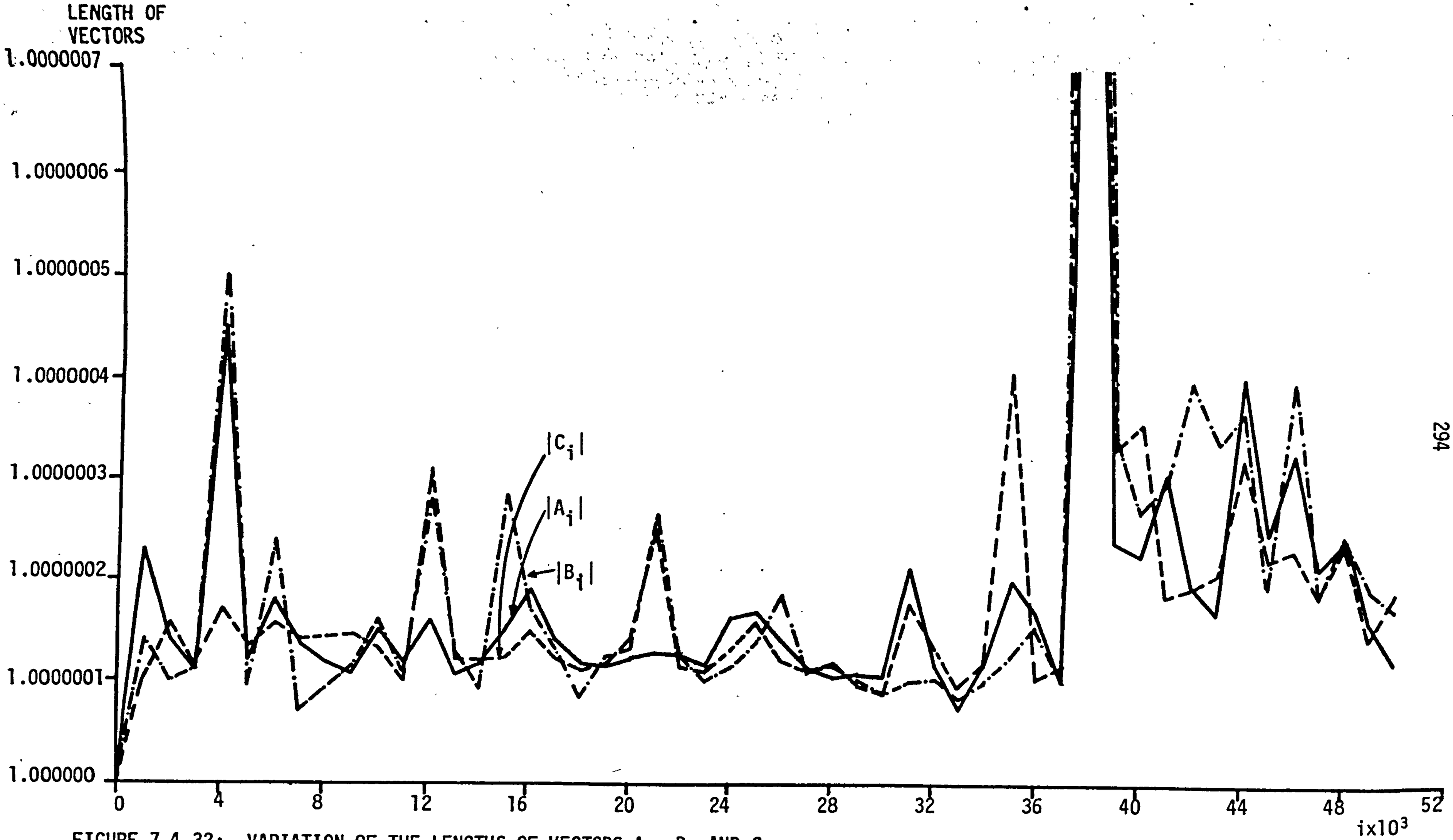

FIGURE 7.4.32: VARIATION OF THE LENGTHS OF VECTORS A_i, B_i AND C_i
CHANNEL 3, $\psi = 60$, DEGREE-1 PREDICTION, $\eta = 0.1$, $\sigma_Z^2 = 10^{-6}$, $\theta = 0.80$, $c = 0.05$

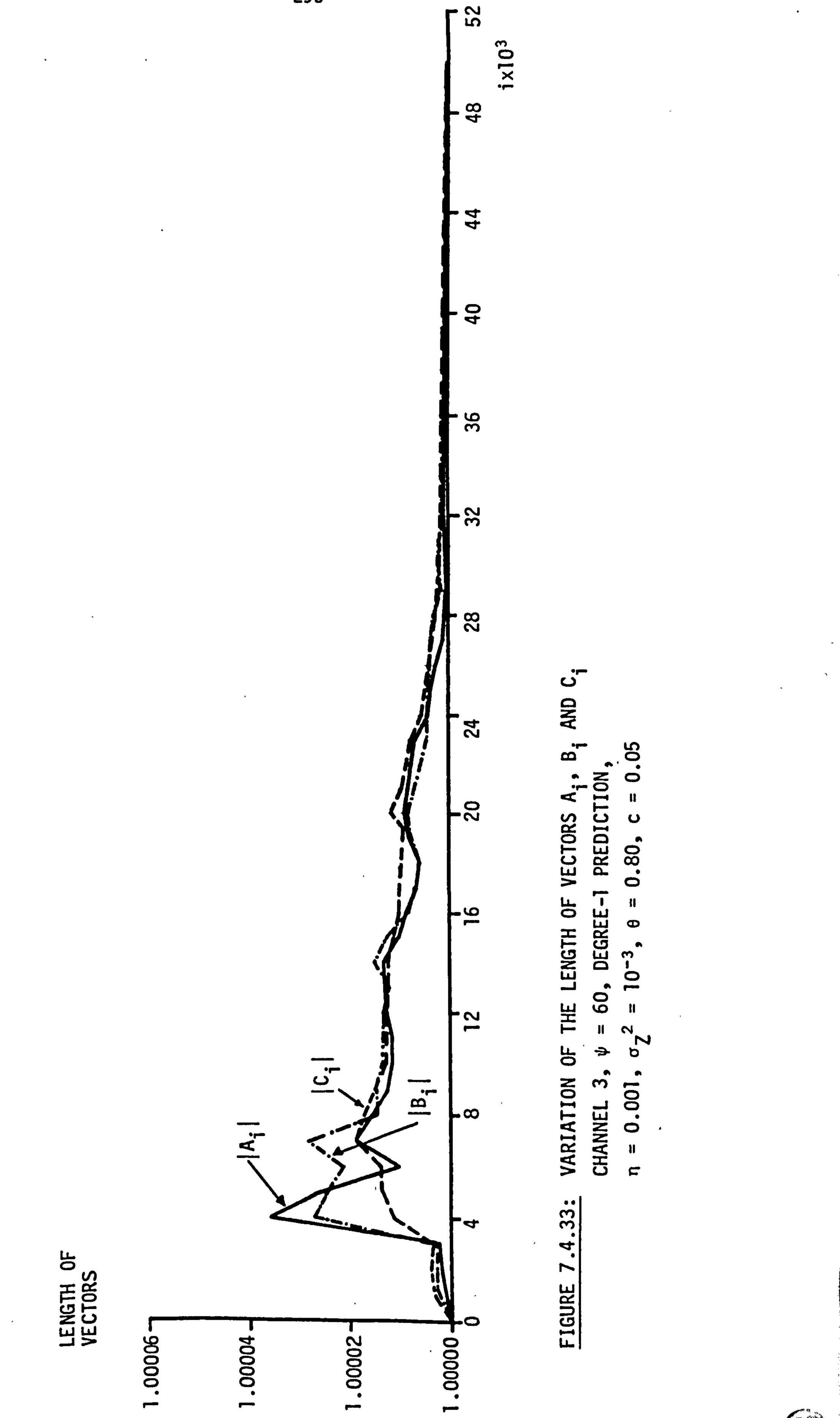

FIGURE 7.4.33: VARIATION OF THE LENGTH OF VECTORS A_i, B_i AND C_i CHANNEL 3, ψ = 60, DEGREE-1 PREDICTION, η = 0.001, $\sigma_Z^2 = 10^{-3}$, θ = 0.80, c = 0.05

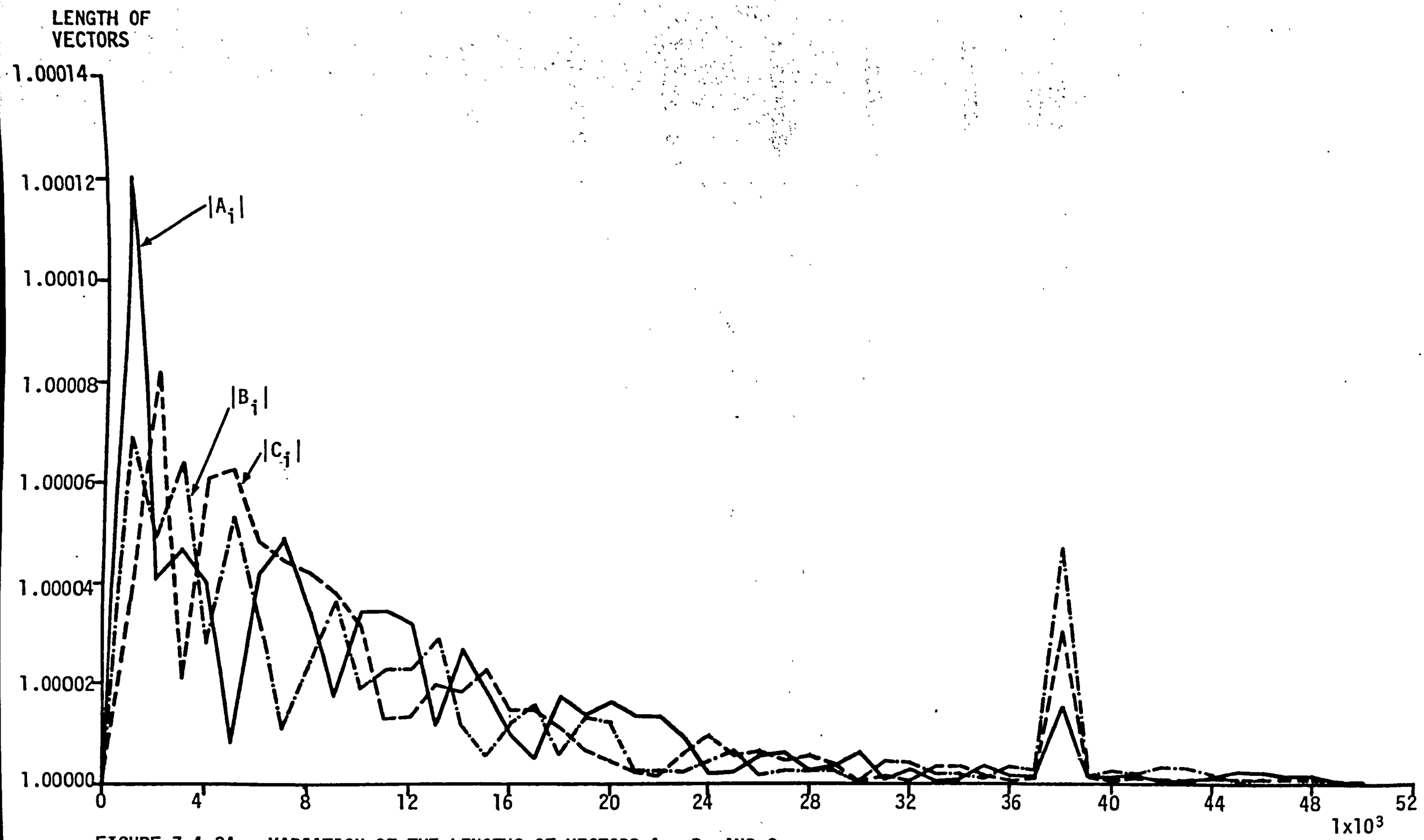

FIGURE 7.4.34: VARIATION OF THE LENGTHS OF VECTORS A_i, B_i AND C_i CHANNEL 3, ψ= 60, DEGREE-1 PREDICTION, η= 0.1, $\sigma_Z^2 = 10^{-3}$, θ= 0.80, c = 0.05

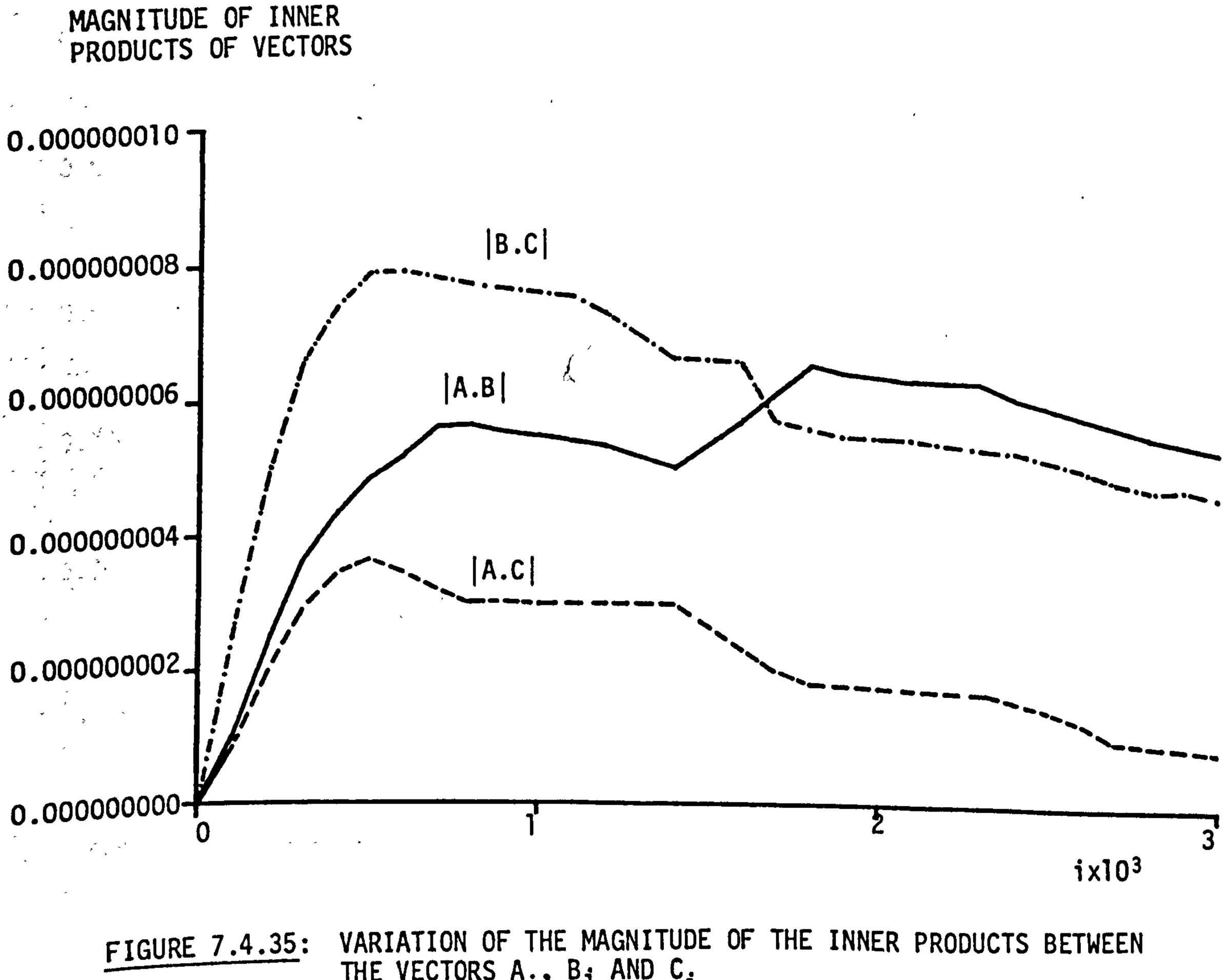

FIGURE 7.4.35: VARIATION OF THE MAGNITUDE OF THE INNER PRODUCTS BETWEEN THE VECTORS A_i, B_i AND C_i
CHANNEL 3, ψ = 60, DEGREE-1 PREDICTION,
η = 0.001, $\sigma_Z^2 = 10^{-6}$, θ = 0.80, c = 0.005

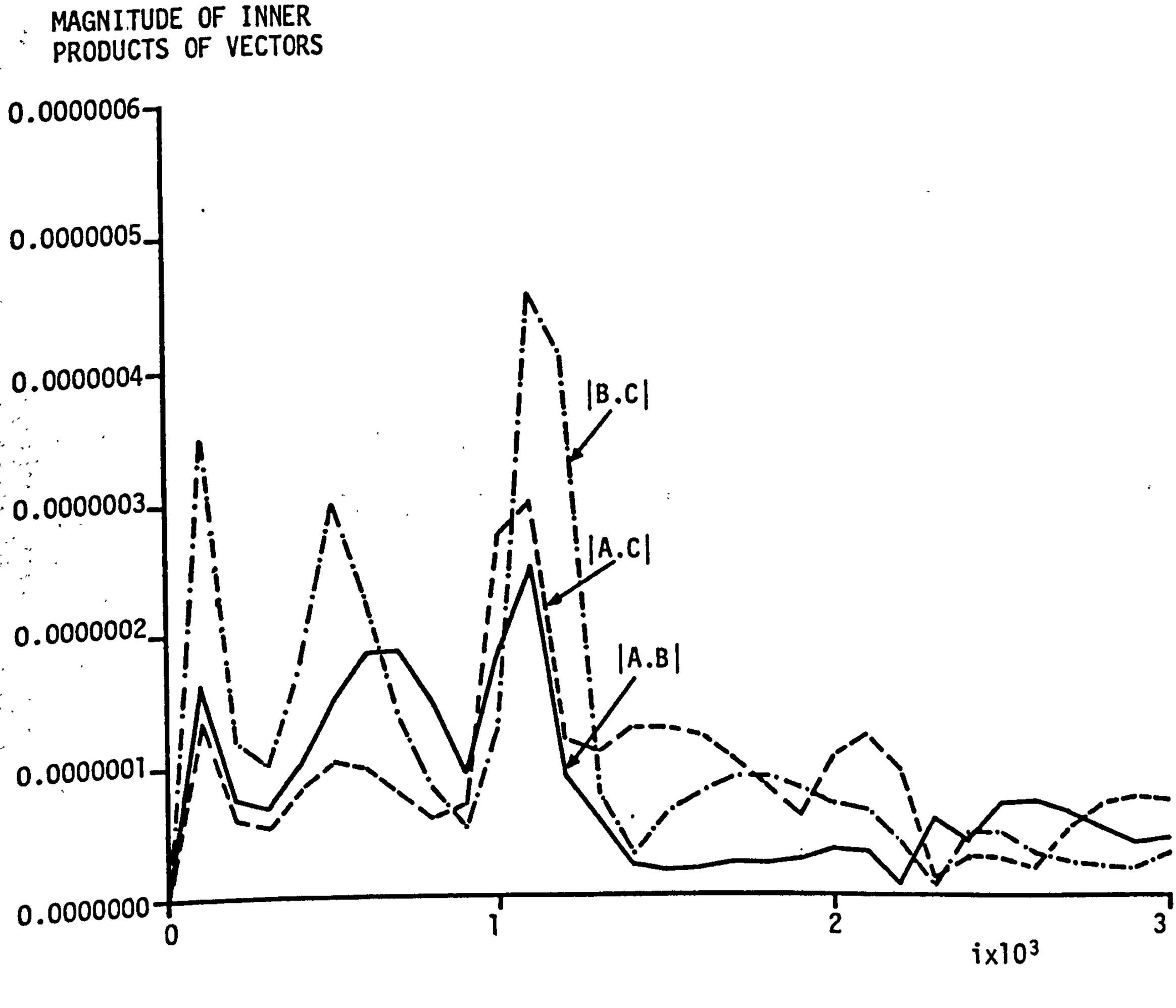

FIGURE 7.4.36: VARIATION OF THE MAGNITUDE OF THE INNER PRODUCTS BETWEEN THE VECTORS A_i, B_i AND C_i
CHANNEL 3, ψ = 60, DEGREE-1 PREDICTION,
η = 0.1, $\sigma_Z^2 = 10^{-6}$, θ= 0.80, c = 0.05

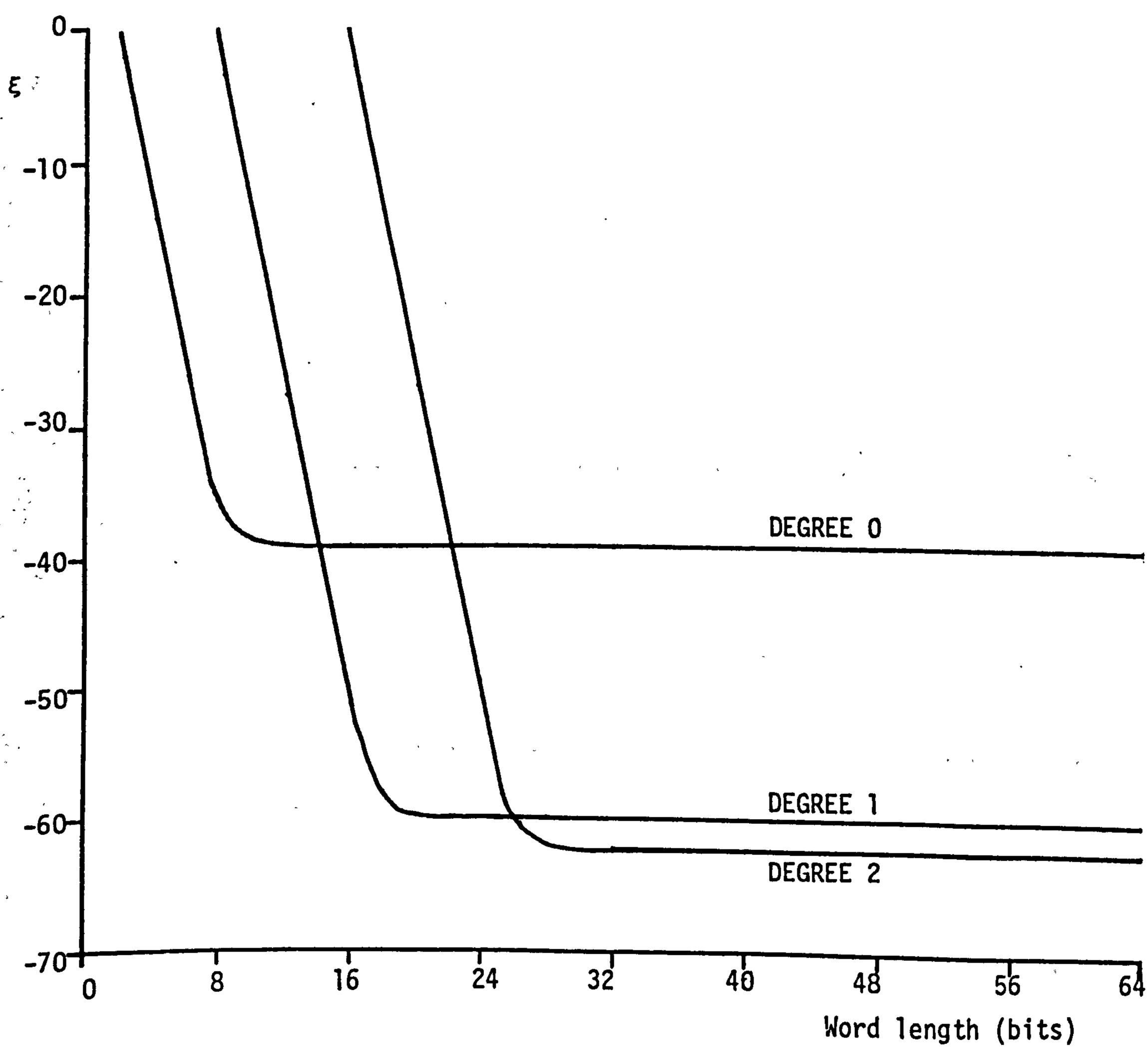

FIGURE 7.4.37: EFFECTS OF QUANTIZATION NOISE
CHANNEL 1, $\psi = 60$, CORRECT SUBSPACE $\eta = 0$, θ AND c ARE OPTIMUM

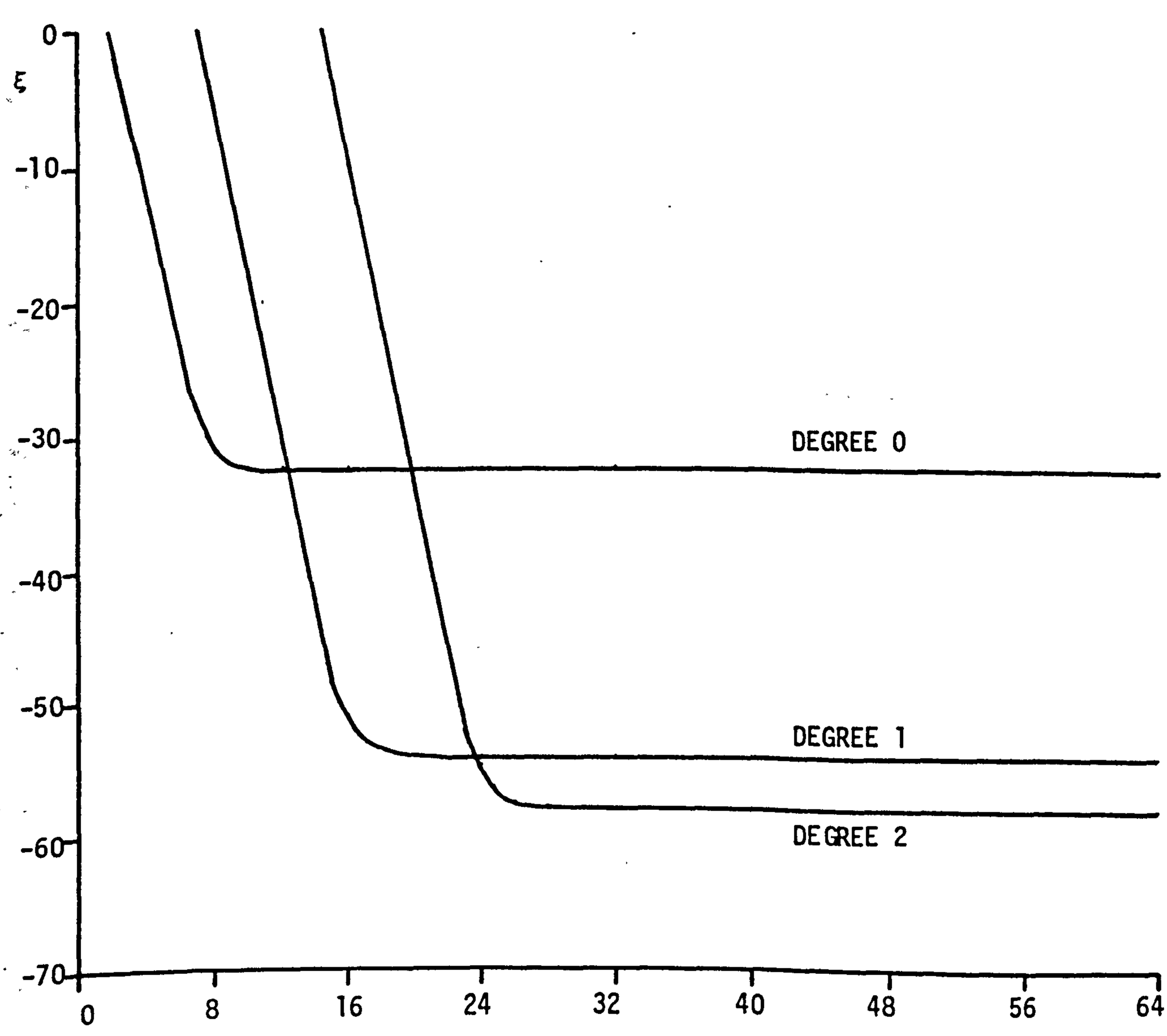

FIGURE 7.4.38: EFFECTS OF QUANTIZATION NOISE
CHANNEL 2, ψ = 60, CORRECT SUBSPACE,
η = 0, θ AND c ARE OPTIMUM

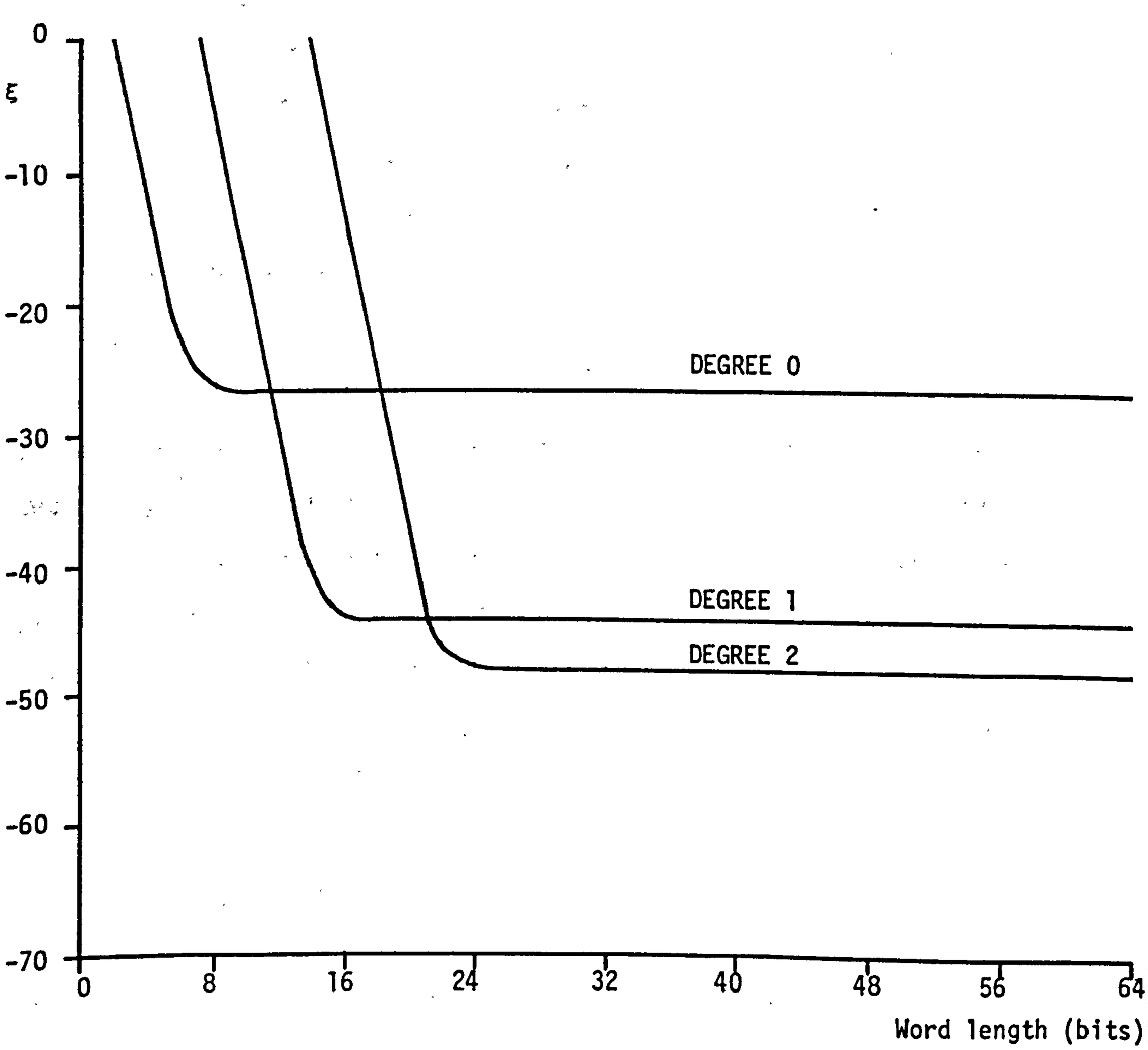

FIGURE 7.4.39: EFFECT OF QUANTIZATION NOISE
CHANNEL 3, ψ = 60, CORRECT SUBSPACE,
η = 0, θ AND c ARE OPTIMUM

8. SUGGESTIONS FOR FURTHER WORK

The main conclusion of Section 6 is that the performance of the conventional Kalman estimator as tested on a model of an HF channel is not optimum. This is due to the fact that the Kalman estimator has been formulated with the assumption that the channel can be modelled as a first-order Markov process. However, when the model of the channel is reduced to the required form, the complexity of the resulting Kalman estimator is increased, in our case, by five times. The estimator is now too complex to be implemented. In recent years, a new type of algorithm, the adaptive lattice algorithm, has received much interest in the published literature. The lattice algorithm does not make any assumption like the Kalman filter concerning the HF channel. It is basically a simple structure which decorrelates the input samples so that rapid convergence is possible. The convergence properties of the lattice algorithm are identical to the Kalman filter, and its computational requirement is comparable to the fast Kalman algorithm. Obviously, this is far too complex when compared with the feedforward transversal-filter estimator. Nevertheless, with the superior tracking capability of the lattice algorithm compared to the feedforward transversal-filter estimator, it may prove worthwhile to develop the former in a similar fashion to the feedforward transversal-filter estimator as in the improved channel estimator.

In Section 7, we have tested the improved channel estimator assuming that it is started correctly. We have seen that the three starting-up vectors must be reasonably accurate in order for the

estimator to have a performance close to the best that can be obtained. Therefore, a suitable channel estimator is required for the starting-up procedure that can give fast and reasonably accurate estimates of the channel at the appropriate times.

In the formulation of the improved channel estimator, it is assumed that the number of sky waves is fixed to some number and the relative delays in transmission between the sky waves are fixed. Obviously, this is not the case in practice. If the estimator can recognise the correct number of sky waves present, obviously this leads to a more effective arrangement as this avoids the unnecessary computation when the estimator is higher than the required dimension. Therefore, the channel simulator must first be modified to simulate the above effects and the estimator tested before implementing it in hardware. This is also a test on the effectiveness of the estimator when the channel no longer obeys the above assumptions..

9. CONCLUSIONS

The investigation has been concerned with techniques of estimating the sampled impulse-response of HF radio links. The channel estimators are either based on the Kalman filter or the feedforward transversal-filter estimator.

Computer simulation tests have shown that the performance of the conventional Kalman filter estimator is not optimum. The reason has been attributed to the assumption by the Kalman filter that the channel is modelled as a first-order Markov process. This is not true for the model of the HF radio link used in the tests which, in fact, conform to CCIR recommendation. If the model of the channel is to be reduced to a first-order Markov process, the complexity of the resulting Kalman estimator increases five fold and consequently is not worthy of further consideration. However, it has been shown that several modifications of the conventional Kalman estimator give an improved performance particularly at high signal-to-noise ratios (Section 6.6).

The results of the investigation on the improved channel estimator are presented in Section 7.4. This estimator is based on the feedforward transversal-filter estimator but has been modified to include a predictor and also utilizes some prior knowledge of the basic structure of the channel in the estimation process. Comparison of these results with that of the conventional Kalman estimator shows the considerable superiority of the improved channel estimator. It

is also shown that when the predictor is the degree-1 least-squares fading-memory predictor, it is possible for the accuracy of the estimation (prediction) to oscillate over a large range of values (Section 7.4.1). This is remedied by increasing the degree of the predictor to degree 2. Simulation results have also revealed the self-orthonormalizing property of the estimator (Section 7.4.6) which allows a considerable reduction in equipment complexity to be achieved by omitting the orthonormalization process.

APPENDIX A1

CONVERSION OF THE SAMPLED IMPULSE-RESPONSES OF THE TRANSMITTER AND RECEIVER FILTERS TO MINIMUM PHASE

The sampled impulse-responses of the transmitter and receiver filters used in Figure 6.2.1 are nonminimum phase which means that the responses rise slowly towards their respective peaks. This has the effect of reducing the tolerance of the detection process to additive noise and also increasing the minimum value of n, where n-1 is the delay in the detection of a data symbol[16], so that the estimator is required to make predictions over a large interval. Obviously, large-interval predictions are likely to be less accurate than short-interval predictions. Therefore, due to these two reasons, it is necessary to make the transmitter and receiver filters minimum phase. Ideally, for the optimum performance of the detector, the sampled impulse-response of the linear baseband channel must be made minimum phase, and, for a time-invariant channel, this is achieved by introducing an adaptive linear filter ahead of the detector[2]. The linear filter replaces the roots of the z-transform of the sampled impulse-response of the linear baseband channel, which lie outside the unit circle in the z-plane, by the complex conjugates of their reciprocals[93]. However, the relatively rapid variations in the characteristics of the HF radio link mean that the adjustment of the adaptive linear filter is difficult. Therefore, the best that can be done is to restrict the minimum phase condition to the sampled impulse-responses of the transmitter and receiver filters.

The transmitter filter, with impulse response a'(t) is in fact a cascade of several filters which include the baseband signal shaping filter (lowpass), the post-modulation filter (bandpass) and the radio transmitter filter. It is assumed that exactly half of the total radio filter frequency response is present at the transmitter end of the transmission system and the remaining half at the receiver end. The receiver filter, with impulse response b'(t) is also a cascade of several filters which include the radio receiver filter, the pre-demodulation filter (bandpass) and the post-demodulation filter (lowpass). The characteristics of the radio filter are those of an actual radio set, i.e. the Clansman VRC 321. The characteristics of these filters (or their combinations) are already given in Section 4.5. The impulse responses a'(t) and b'(t) here are, of course, the same as a(t) and b(t) in Section 4.5. a'(t) and b'(t) are the nonminimum phase impulse responses of the transmitter and receiver filters, respectively. The change in notation is found necessary so that the minimum phase impulse responses that result from the conversion of a'(t) and b'(t) can be denoted by a(t) and b(t). Therefore, a(t) and b(t) still represent the overall filtering at the transmitter and receiver, respectively.

The conversion of the sampled impulse-responses of the transmitter and receiver filters to minimum phase is as follows[93].

The impulse responses a'(t) and b'(t) were supplied by F. McVerry in the form of sampled values (Table A1.1), where the sampling rate is 4800 samples/second. It is assumed that the impulse responses a'(t) and b'(t) are of finite duration, so that the sampled values $\{a'_h\}$ and

$\{b'_h\}$ for h<0 and h>g' are zero. The integer g'+1 is the number of samples in the sampled impulse-response. Clearly, from the characteristics of the filters (Section 4.5), a sampling rate of 4800 samples/second is well above the Nyquist rate of these filters. Thus, by virtue of the uniform sampling theorem, a'(t) and b'(t) can be completely reconstructed from the samples $\{a'_h\}$ and $\{b'_h\}$, respectively, using an ideal lowpass filter[99-101], in this case, with a cut-off frequency of f_c = 2400 Hz. The conversion to minimum phase is outlined here only for the $\{a'_h\}$ as the same procedure is also applicable for the $\{b'_h\}$. The waveform which is reconstructed using the ideal lowpass filter is given by[99-101,125],

$$a'(t) = \sum_{h=-\infty}^{\infty} a'_h \text{ sinc } 4800\ (t - h\ \frac{1}{4800}) \qquad \text{(A1.1)}$$

where the sampled values $\{a'_h\}$ are given in Table A1.1. Clearly, from equation A1.1, the sampled values $\{a'_h\}$ are recovered at the sampling instants $\{\frac{h}{4800}\}$ because at these times all the sinc functions have the values zero except for one whose value is $a'_h = a'(\frac{h}{4800})$. At all other times, a'(t) is the sum of the values of the sinc functions at the particular instant weighted by the $\{a'_h\}$ (equation A1.1).

Before finding the roots of the z-transform of the sampled impulse-response $\{a'_h\}$, we have chosen first to oversample a'(t). The reason for this will become clear later. The new sampling rate is 9600 samples/second which means that an additional value of a'(t) is required at half-way between any two given samples $\{a'_h\}$. These

values are easily calculated using equation A1.1. Let us denote the resulting sequence of the finely-sampled values by $\{a''_h\}$ (Table A1.2). It is convenient to represent the sampled impulse-response in the form of a polynomial

$$A'(z) = \sum_{h=0}^{q} a''_h z^{-h} \qquad (A1.2)$$

where $z = \exp(j \frac{2\pi f}{9600})$ and $j = \sqrt{-1}$. The integer q+1 is the number of samples $\{a''_h\}$ which, in this case, is equal to 32. A'(z) is also known as the z-transform of the sequence of values $\{a''_h\}$. The polynomial A'(z) can also be expressed as

$$A'(z) = a''_o \prod_{h=1}^{q} (1 - \delta'_h z^{-1}) \qquad (A1.3)$$

where $\delta'_1, \delta'_2, \ldots, \delta'_q$ are the q roots of the polynomial A'(z). All the roots are complex-valued and are determined using the root-finding algorithm CØ2ADF[104]. The values of these roots are given in Table A1.3. All roots which lie outside the unit circle in the z-plane are then replaced by the complex conjugate of their reciprocals[93]. The roots which are already inside the unit circle remain unchanged. Let $\delta_1, \delta_2, \ldots, \delta_q$ represent the new set of roots where all of these are now inside the unit circle. Therefore, the minimum phase sampled impulse-response is given by,

$$A(z) = a''_o k_a \prod_{h=1}^{q} (1 - \delta_h z^{-1}) \qquad (A1.4)$$

where k_a is a constant that is required in order to preserve the discrete energy-density of a'(t), so that the transformation is merely a pure phase transformation[2] and does not introduce any gain or attenuation in the signal energy. The value of k_a is simply the product of the distances from the origin of the z-plane of all the roots of $\{a''_h\}$ which lie outside the unit circle. Table A1.4 gives the values of the minimum phase sampled impulse-response which are found by expanding equation A1.4. It can be seen from Table A1.4 that the rise time to the peak value is now shorter than the non-minimum sampled impulse-response. Also, the energy of the minimum phase sampled impulse-response is concentrated around an earlier sample (h=6) for both the transmitter and receiver filters, whereas, for the nonminimum phase sampled impulse-responses, h=12 and h=13, respectively (Figures A1.1 and A1.2). The quantity plotted in Figures A1.1 and A1.2 is the energy contribution of the first p+1 samples of the impulse response, e.g.,

$$E(p) = \sum_{h=0}^{p} |a_h|^2 \qquad \text{(A1.5)}$$

It can be seen that,

$$\sum_{h=0}^{p} |a'_h|^2 \leq \sum_{h=0}^{p} |a_h|^2, \text{ for all } p \qquad \text{(A1.6)}$$

which means that the minimum phase sampled impulse-response introduces the minimum amount of delay[93]. This is also true for the receiver filter.

Having obtained the minimum phase sampled impulse-response $\{a_h\}$, the ideal lowpass filter is used, as previously, to reconstruct the impulse response a(t) from the samples $\{a_h\}$. The cut-off frequency of the filter is 4800 Hz. Thus, a(t) is given by,

$$a(t) = \sum_{h=-\infty}^{\infty} a_h \text{ sinc } 9600\ (t - h\ \frac{1}{9600}) \qquad \text{(A1.7)}$$

Now, the impulse response c(t) of the ideal lowpass filter is non-causal[99], i.e.,

$$c(t) \neq 0, \qquad \text{for } t < 0 \qquad \text{(A1.8)}$$

Therefore, the response of the ideal lowpass filter with the sequence $\{a_h\}$ as the input is of a significant magnitude for $t < 0$. This is due to the presence of the tails of the sinc functions. The actual value of the response at any time instant is given by the sum of the weighted sinc functions (equation A1.7). However, as the rate of sampling of the response of the transmitter filter is increased, the magnitude of the tails at both ends of the response of the ideal lowpass filter gets smaller. Thus, the sampling rate of 9600 samples/second is chosen as a compromise between having small ripples in the lowpass filter response when $t < 0$ and a manageable number of samples in the transmitter filter response to be used by the root-finding algorithm. The reconstruction of the impulse response a(t) is necessary so that values of a(t) can be obtained at any other sampling phase and sampling rate. Clearly, from equation 4.5.25, each sky wave is multiplied by the sampled impulse-response of the transmitter filter

which is sampled at a certain phase. Let $\{a_{1,h}\}$, $\{a_{2,h}\}$ and $\{a_{3,h}\}$, be the sampled impulse-responses of the transmitter filter sampled at 4800 samples/second which correspond to the impulse responses $a(t)$, $a(t-\tau_1)$ and $a(t-\tau_2)$, respectively. τ_1 and τ_2 are, respectively, the multipath propagation delays of the second and the third sky waves with respect to the first sky wave. The delays are expressed as a whole number of sampling periods plus a sampling phase[16], e.g.,

$$\tau_1 = \rho_1 \frac{T}{2} + \rho_1' \qquad \text{(A1.9)}$$

where ρ_1 is the number of sampling periods and T is the signalling interval ($= \frac{1}{2400}$) and ρ_1' is the sampling phase ($< \frac{T}{2}$). As an example, for the channel with the delays $\tau_1 = \frac{2}{3}$ ms and $\tau_2 = 3$ ms, the relevant values are,

$$\left.\begin{aligned} \rho_1 &= 3 \\ \rho_2 &= 14 \\ \rho_1' &= 0.2/4800 \\ \rho_2' &= 0.4/4800 \end{aligned}\right\} \qquad \text{(A1.10)}$$

and the sampled impulse-responses $\{a_{1,h}\}$, $\{a_{2,h}\}$, $\{a_{3,h}\}$ and $\{b_h\}$ are shown in Table A1.5.

Finally, the sequence of noise samples $\{w_i\}$ which is added to the data signals at the output of the linear baseband channel

(Figure 6.2.1) is obtained by filtering a sequence of complex-valued statistically independent Gaussian random variables with zero mean and variance σ_w^{2}[16]. The sampled impulse-response of the filter is $\{b_h''\}$, where the $\{b_h''\}$ is given by,

$$b_h'' = \frac{b_h}{\sum |b_h|^2} \tag{A1.11}$$

so that

$$\sum |b_h''|^2 = 1 \tag{A1.12}$$

Therefore, it can be shown[16] that the variances of the input and the output noise samples are the same, but the output noise sequence is slightly correlated.

TABLE A1.1: THE NONMINIMUM PHASE SAMPLED IMPULSE-RESPONSES OF THE TRANSMITTER AND RECEIVER FILTERS SAMPLED AT 4800 SAMPLES/ SECOND

Sampled impulse-response of the transmitter filter, $\{a'_h\}$		Sampled impulse-response of the receiver filer, $\{b'_h\}$	
Real part	Imaginary part	Real part	Imaginary part
-0.0382	-0.5007	-0.4107	0.2882
0.2457	1.3823	-0.2050	0.6548
0.0557	2.3229	0.2219	2.0303
4.3052	1.6233	1.4222	3.4222
22.3184	-2.3123	11.5059	1.8432
44.8006	-7.0695	33.8749	-5.1777
42.0069	-5.2753	46.7973	-11.4399
9.6632	2.7801	28.1107	-5.1152
-13.7143	5.0775	-2.5666	7.5627
-7.1940	0.3151	-12.3912	8.1280
4.7637	-0.6568	-2.6308	-0.8993
2.6054	1.3191	4.3105	-2.9923
-1.9526	-0.0767	2.0033	0.8730
-0.2429	-1.0017	-1.2050	1.1213
0.7289	0.5064	-0.7537	-0.6766
-0.4394	0.3751	0.4731	-0.3189

TABLE A1.2: THE NONMINIMUM PHASE SAMPLED IMPULSE-RESPONSES OF THE TRANSMITTER AND RECEIVER FILTERS SAMPLED AT 9600 SAMPLES/ SECOND

Sampled impuse-response of the transmitter filter, $\{a_n''\}$		Sampled impulse-response of the receiver filter, $\{b_n''\}$	
Real part	Imaginary part	Real part	Imaginary part
-0.0382	0.5007	-0.4107	0.2882
0.1028	0.8954	-0.4323	0.4191
0.2457	1.3823	-0.2050	0.6548
0.1670	1.9185	0.0847	1.1921
0.0557	2.3229	0.2219	2.0303
0.9140	2.3162	0.3858	2.8989
4.3052	1.6233	1.4222	3.4222
11.4730	0.0630	4.7111	3.2167
22.3184	-2.3123	11.5059	1.8432
34.7403	-5.0150	21.8845	-1.0427
44.8006	-7.0695	33.8749	-5.1777
48.0903	-7.3538	43.5905	-9.2903
42.0069	-5.2753	46.7973	-11.4399
27.6243	-1.3579	41.2284	-10.0760
9.6632	2.7801	28.1107	-5.1152
-5.6773	5.2497	11.7500	1.7134
-13.7143	5.0775	-2.5666	7.5627
-13.3492	2.8632	-10.9678	9.9369
-7.1340	0.3151	-12.3912	8.1280
0.1670	-0.9961	-8.5298	3.6243
4.7637	-0.6568	-2.6308	-0.8993
5.1605	0.5273	2.1945	-3.2794
2.6054	1.3191	4.3105	-2.9923
-0.4127	1.0165	3.8518	-1.0659

Continued...

TABLE A1.2 continued

-1.9526	-0.0767	2.0033	0.8730
-1.5886	-0.9945	0.0364	1.6495
-0.2429	-1.0017	-1.2050	1.1213
0.7567	-0.2414	-1.3974	0.0404
0.7289	0.5064	-0.7537	-0.6766
0.0461	0.6718	0.0808	-0.6862
-0.4394	0.3751	0.4731	-0.3189
-0.3401	0.0792	0.3129	-0.0471

TABLE A1.3: ROOTS OF THE NONOMINIMUM PHASE SAMPLED IMPULSE-RESPONSES OF THE TRANSMITTER AND RECEIVER FILTERS

Roots of the sampled impulse-response of the transmitter filter		Roots of the sampled impulse-response of the receiver filter	
Real Part	Imaginary part	Real part	Imaginary part
1.542713	0.375924	1.141239	-0.992131
-0.923559	0.323485	1.259681	1.076074
1.183257	-1.030641	-0.930914	-0.292618
-0.201917	-0.972178	1.564782	0.277184
0.511298	0.984301	-0.656985	0.717809
-0.890323	-0.400737	0.395981	-1.053240
0.115413	1.017592	0.234388	0.978854
0.722994	-0.245218	-0.470449	-0.850972
-0.680373	-0.703588	-0.182849	0.970264
-0.609533	0.775278	0.372906	-0.646634
0.571004	1.322234	-0.871534	0.423016
0.404667	-0.988114	0.684503	0.297149
-0.975522	-0.041948	-0.748088	-0.614189
0.735817	0.190313	0.074496	-0.996252
-0.022479	-1.020884	0.408216	0.936265
-0.287358	0.953022	-0.964082	0.069910
-0.376043	-0.910869	0.743087	-0.166141
0.631750	0.412323	-0.513406	0.830456
-0.741692	0.645077	-0.304536	-0.927783
-0.537503	-0.821000	0.542441	0.867407
0.346879	0.997610	-0.620157	-0.745439
0.484888	-0.435231	-0.016778	1.003321
-0.847649	0.492744	0.326867	-0.932239
0.197426	-0.957681	-0.934374	0.250826
-0.112229	0.995169	0.739256	0.065513
0.400470	-0.807719	-0.777901	0.580480
-0.456069	0.879016	0.597154	-0.305347

TABLE A1.3 continued

0.767182	-0.044329	-0.352912	0.915072
-0.966696	0.143160	-0.129193	-0.975133
-0.799427	-0.561965	-0.849567	-0.461511
-0.949746	-0.225377	-0.959548	-0.113384

TABLE A1.4: THE MINIMUM PHASE SAMPLED IMPULSE-RESPONSES OF THE TRANSMITTER AND RECEIVER FILTERS SAMPLED AT 9600 SAMPLES/SECOND

Sampled impulse-response of the transmitter filter $\{a_h\}$		Sampled impulse-response of the receiver filter, $\{b_h\}$	
Real part	Imaginary part	Real part	Imaginary part
-0.1795896	2.3539405	-1.9417691	1.3625952
-1.0126608	9.1023947	-7.1672741	5.0809811
-3.0773455	20.7590237	-15.9797864	11.5941040
-6.3729500	34.6175663	-26.4837803	19.8575657
-9.9409021	45.5584592	-35.1417733	27.3342937
-12.1892194	48.5737623	-38.4036552	30.8364948
-11.7869473	41.4909978	-34.4788717	28.0870086
-8.5086317	26.3691069	-24.3073589	19.2456629
-3.4618271	8.7045826	-11.2301982	7.2714615
1.4399026	-5.2922114	0.5324620	-3.4220063
4.4438154	-11.7869820	7.8155160	-9.2602472
4.8093491	-10.8377828	9.7283726	-9.2402194
3.0642536	-5.5819054	7.5124057	-5.0954462
0.5572495	-0.0043047	3.4078680	-0.0090979
-1.3596576	3.1582131	-0.5057505	3.2326498
-1.9971243	3.3428704	-2.9068417	3.5893140
-1.4973528	1.7365460	-3.3707125	1.8975352
-0.5158362	0.0226668	-2.3084858	-0.1488969
0.2925598	-0.7776891	-0.6759166	-1.2813604
0.6217121	-0.646187	0.5852576	-1.2373936
0.5180829	-0.1292556	1.0482656	-0.4830313
0.1794357	0.2537894	0.8502824	0.3399562
-0.1842786	0.2880296	0.3621876	0.7614804
-0.3807598	0.0471432	-0.0950895	0.6378702
-0.3167778	-0.2324818	-0.3105902	0.1979014
-0.1118142	-0.3298345	-0.2141025	-0.1413245

TABLE A1.4 continued

0.0021899	-0.2107548	0.0438410	-0.1532672
-0.0314648	-0.0348275	0.1793671	0.0155204
-0.0443806	0.0392056	0.0738947	0.0940330
0.0400357	0.0206312	-0.0843017	0.0287380
0.051533	0.0098505	-0.0646936	-0.0312132
-0.0723509	0.0168479	0.0661712	-0.0099654

TABLE A1.5: EXAMPLES OF THE SAMPLED IMPULSE-RESPONSES OF THE TRANSMITTER AND RECEIVER FILTERS USED IN THE COMPUTER SIMULATION TESTS

$\{a_{1,h}\}$		$\{a_{2,h}\}$		$\{a_{3,h}\}$		$\{b_k\}$	
Real part	Imaginary part	Real part	Imaginary part	Real part	Imaginary part	Real part	Imaginary part
-0.1795896	2.3539405	-0.0622160	0.9639589	-0.0105240	0.1932385	-1.9417691	1.3625952
-3.0773455	20.7590237	-2.0820312	15.5920086	-1.3136537	11.0688962	-15.9797864	11.5941040
-9.9409021	45.5584592	-8.5764574	41.8806123	-7.1104051	37.2136597	-35.1417733	27.3342937
-11.7869473	41.4909978	-12.3102829	45.4936549	-12.3469721	47.9575159	-34.4788717	28.0870086
-3.4618271	8.7045826	-5.5766967	15.6491184	-7.5848703	22.8262482	-11.2301982	7.2714615
4.4438154	-11.7869820	3.5478141	-10.1779415	2.2353854	-7.2498590	7.8155160	-9.2602472
3.0642536	-5.5819054	3.9398962	-7.9404850	4.5938614	-10.0026703	7.5124057	-5.0954462
-1.3596576	3.1582131	-0.7258700	2.2650217	0.0931639	0.8695437	-0.5057505	3.2326498
-1.4973528	1.7365460	-1.7957047	2.4780490	-1.9704176	3.1072800	-3.3707125	1.8975352
0.2925598	-0.7776891	0.0207712	-0.5908297	-0.3233694	-0.2261096	-0.6759166	-1.2813604
0.5180829	-0.1292556	0.6018517	-0.3459233	0.6313238	-0.5552906	1.0482656	-0.4830313
-0.1842786	0.2880296	-0.0464514	0.3143350	0.1035718	0.2882096	0.3621876	0.7614804
-0.3167778	-0.2324818	-0.3680978	-0.1350979	-0.3865939	-0.0156703	-0.3105902	0.1979014
0.0021899	-0.2107548	-0.0182370	-0.2790169	-0.0734526	-0.3215770	0.0438410	-0.1532672
-0.0443806	0.0392056	-0.0471151	0.0231422	-0.0386471	-0.0107706	0.0738947	0.0940330
0.0515533	0.0098505	0.0789564	0.0071662	0.0608046	0.0140909	-0.0646936	-0.0312132

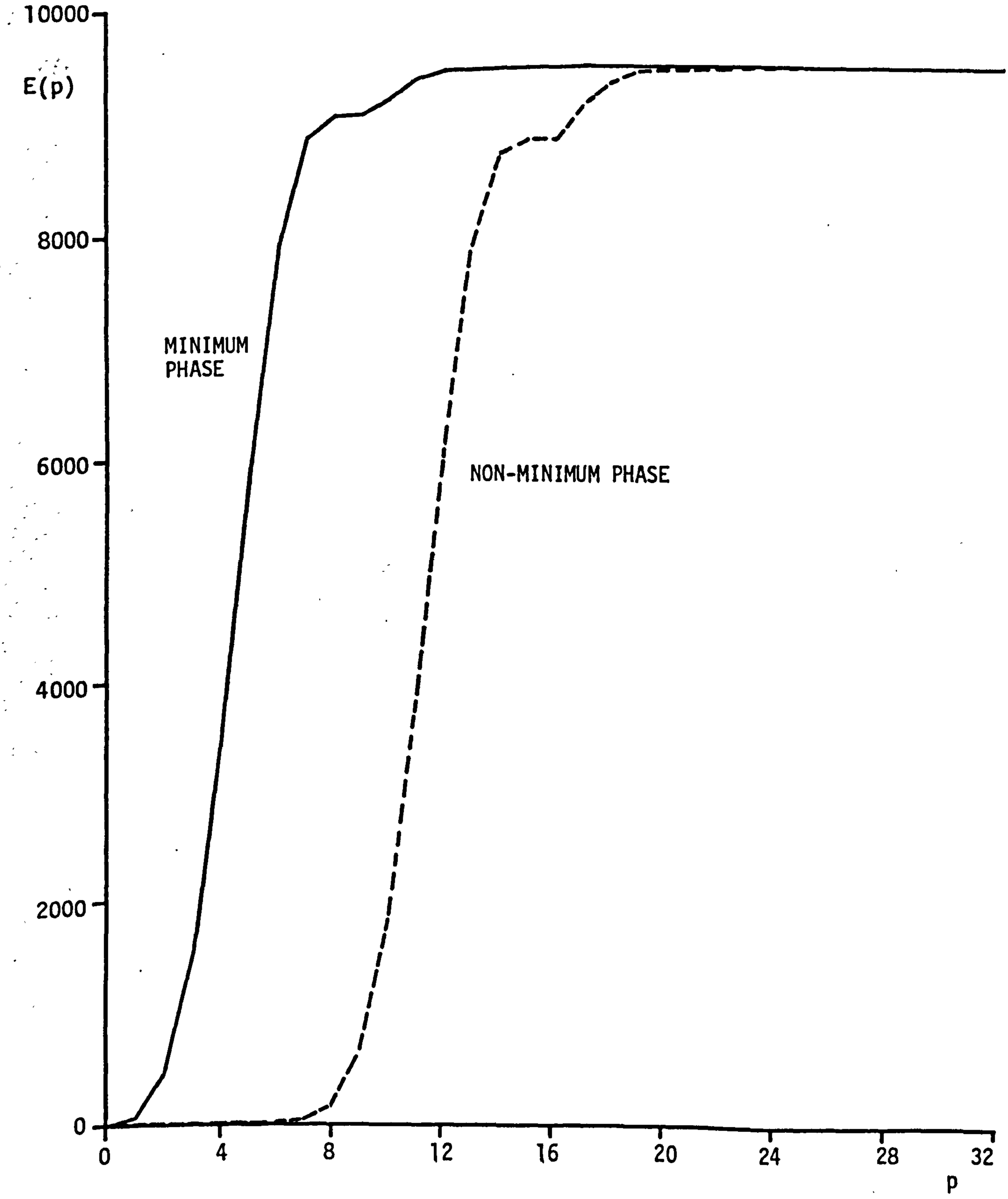

FIGURE A1.1: ENERGY CONTRIBUTION OF THE FIRST p+1 SAMPLES OF THE IMPULSE RESPONSE OF TRANSMITTER FILTER

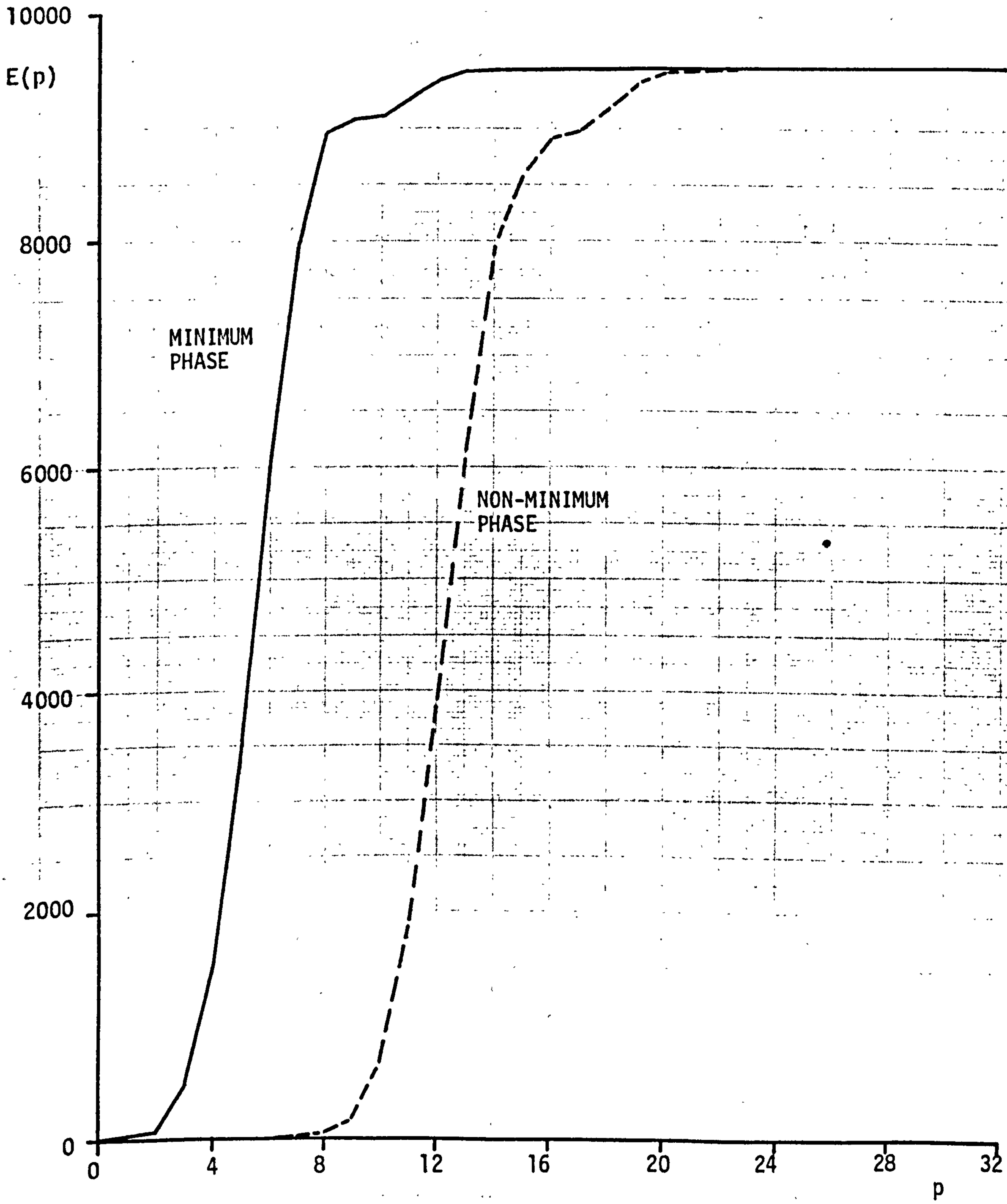

FIGURE A1.2: ENERGY CONTRIBUTION OF THE FIRST p+1 SAMPLES OF THE IMPULSE RESPONSE OF RECEIVER FILTER

APPENDIX A2

EFFECTS OF QUANTIZATION NOISE ON LEAST-SQUARES FADING-MEMORY PREDICTOR

Perhaps the most interesting source of quantization noise is the error introduced by quantizing the results of multiplications[112]. For example, if two numbers are each quantized to b bits, the result of their multiplication will require $2b$ bits of register length for storage. If the length of this product is not reduced, and if the product occurs in a recursive structure, then on successive iterations, the storage required will grow linearly to a considerable amount. Therefore, practical limitations force the numbers to be quantized. There are two standard methods of eliminating the low-order bits resulting from the multiplications and these are truncation and rounding. The latter is preferred because of its desirable properties, i.e. the error signal is independent of the type of arithmetic (floating or fixed point), its mean is zero and no other method yields lower variance[92]. To account for the round-off noise, the multiplication is first assumed to be performed in infinite precision, the round-off noise being then added to the results. Each noise sample is a sample value of a uniform random variable with zero mean and variance of $2^{-2b}/12$, where b+1 is the number of bits of each word.

Consider the degree-1 least-squares fading-memory prediction as an example (see Section 7.3). Figure A2.1 shows a possible implementation of the algorithm in infinite precision arithmetic. In Figure A2.2 the position of the three noise sources e_1, e_2 and e_3 are shown.

The effects of quantization noise on the degree-0, 1, and 2 least-squares fading-memory predictors are presented in Section 7.4.7.

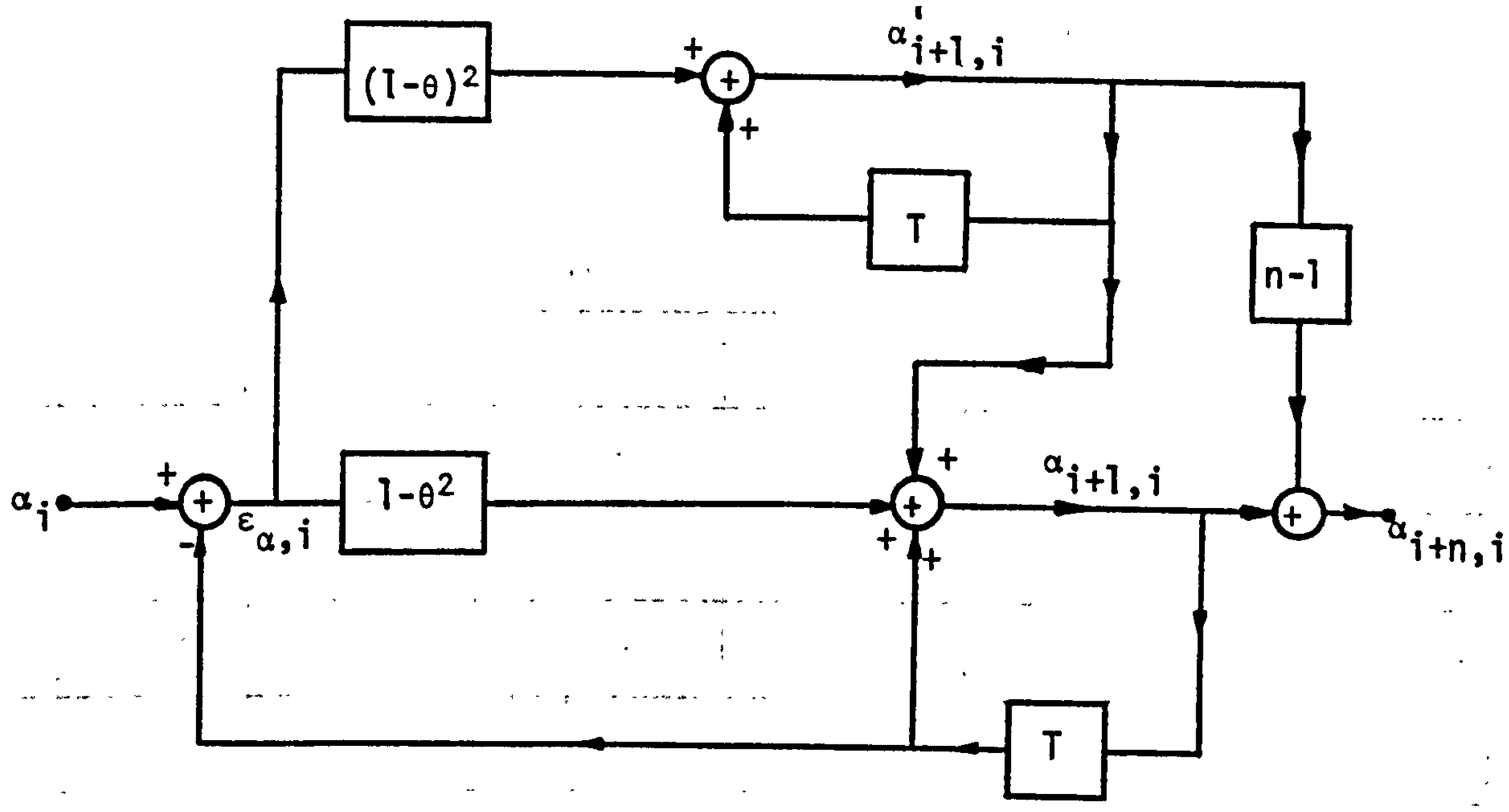

FIGURE A2.1: DEGREE-1 LEAST SQUARES FADING-MEMORY PREDICTOR ASSUMING INFINITE PRECISION

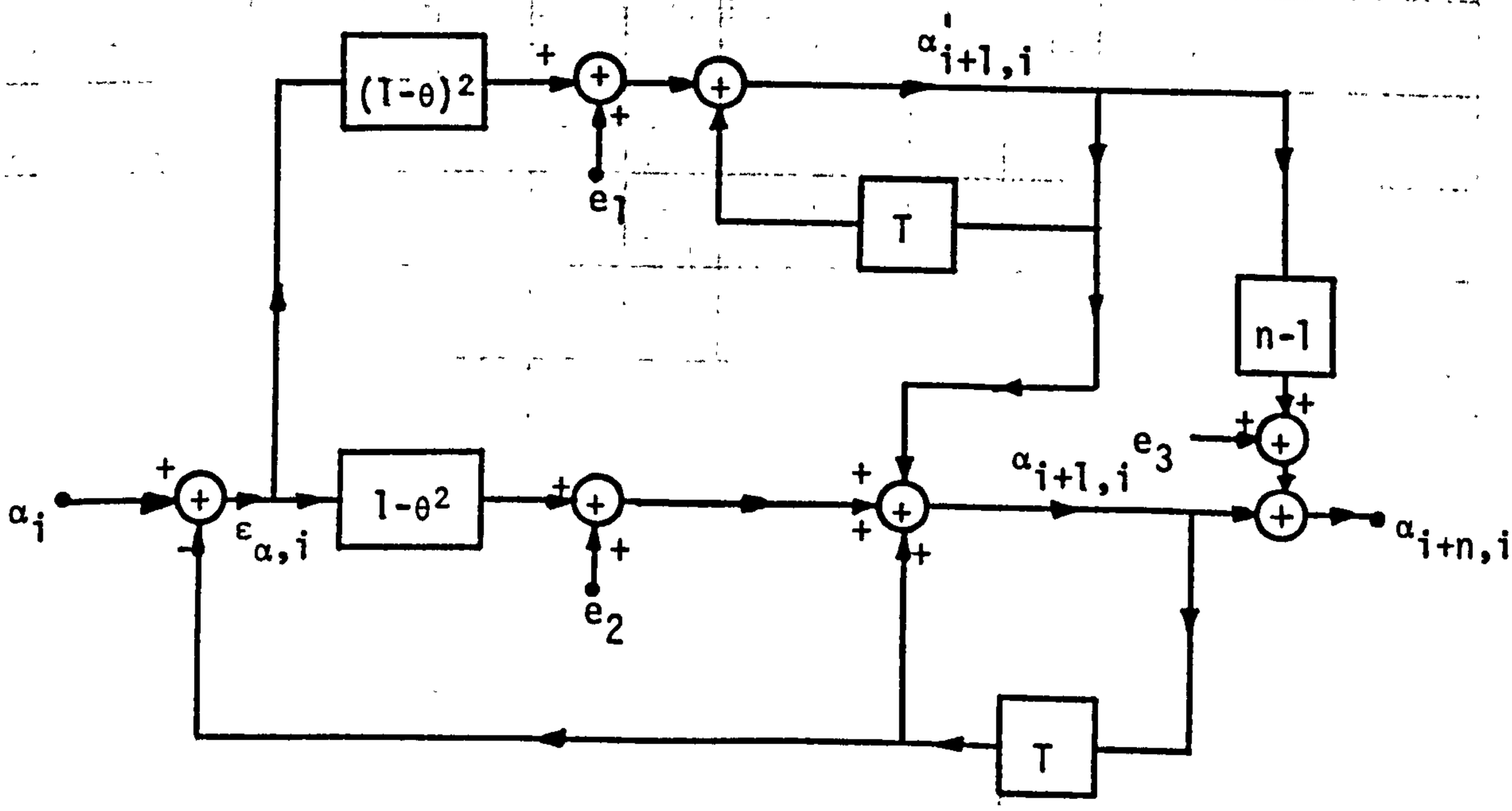

FIGURE A2.2: DEGREE-1 LEAST-SQUARES FADING-MEMORY PREDICTOR WITH QUANTIZATION NOISE ADDED

APPENDIX A3

AN EXAMPLE OF THE SIMULATION OF THE KALMAN FILTER ESTIMATOR

```
      PROGRAM R0002(INPUT,OUTPUT,TAPE1=INPUT,TAPE2=OUTPUT)
C
C
C     KALMAN FILTER ESTIMATOR APPLIED TO 2-SKYWAVE H.F LINK
C     PREDICTION : LEAST-SQUARES FADING-MEMORY USING POLYNOMIAL OF
C                  DEGREE 1
C     INPUT SIGNAL : 16-POINT QAM
C     AVERAGE TRANSMITTED ENERGY PER BIT IS UNITY
C     BIT RATE IS 9600 BITS/SEC
C     CHANNEL VECTOR IS NOT NORMALISED
C     CHANNEL SIMULATED - CH. 2 -- 1 HZ AND 2 MILLISECS
C     INITIAL VALUES ARE
C               S(0,0) = I
C                   Q(I) = C * S(I-1,I-1)
C               X(1,0) = Y(0)
C     DELAY IN ESTIMATION = 17 SAMPLING INTERVALS
C     ------------------------------------------
C
C
      DIMENSION RAYLI1(5),RAYLQ1(5),RAYLI2(5),RAYLQ2(5),COEFF(5),
     1X1(2),Y1(2),X2(2),Y2(2),R(4,50),Q(4,50)
      DIMENSION OPI1(4),OPQ1(4),OPI2(4),OPQ2(4)
      DIMENSION RAY1(1100),RAY2(1100),RAY3(1100),RAY4(1100)
      DIMENSION CI(16),CQ(16),CID(16),CQD(16)
      DIMENSION WSI(30),WSQ(30)
      DIMENSION ANOIR(30),ANOIQ(30)
      DIMENSION TI(30,30),TQ(30,30)
      DIMENSION HIT(50,50),HQT(50,50),CRI(30),CRQ(30)
      DIMENSION SER(25),SEQ(25),CER(25),CEQ(25),PPR(25,25),PPQ(25,25),
     1PR(25,25),PQ(25,25),QVR(25,25),QVQ(25,25),SPR(25),SPQ(25),
     2PSR(25),PSQ(25),GSR(25,25),GSQ(25,25),GR(25),GQ(25),
     3GSPR(25,25),GSPQ(25,25)
      DIMENSION XX1R(25),XX1Q(25),XXOR(25),XXOQ(25),XXNR(25),XXNQ(25),
     1EPR(25),EPQ(25)
      DIMENSION XSR(16),XSQ(16)
      DIMENSION SSR(60),SSQ(60),RRR(60),RRQ(60)
      INTEGER SDEL,SDEL1
      DATA WSI/-0.0059,-0.003,0.0032,0.0205,0.1662,0.4893,0.6759,
     1 0.406,-0.0371,-0.179,-0.038,0.0623,0.0289,-0.0174,-0.0109,
     2-0.0068,0.,0.,0.,0.,0.,0.,0.,0.,0.,0.,0.,0.,0./
      DATA WSQ/0.0042,0.0095,0.0293,0.0494,0.0266,-0.0748,-0.1652,
     1 -0.0739,0.1092,0.1174,-0.013,-0.0432,0.0126,0.0162,-0.0098,
     2 -0.0046,0.,0.,0.,0.,0.,0.,0.,0.,0.,0.,0.,0.,0./
      DATA CRI/-0.4107,-0.205,0.2219,1.4222,11.5059,33.8749,46.7973,
     1 28.1107,-2.5666,-12.3912,-2.6308,4.3105,2.0033,-1.205,
     2 -0.7537,0.4731,0.,0.,0.,0.,0.,0.,0.,0.,0.,0.,0.,0./
      DATA CRQ/0.2882,0.6548,2.0303,3.4222,1.8432,-5.1777,-11.4399,
```

```
     1 -5.1152,7.5627,8.128,-0.8993,-2.9923,0.873,1.1213,-0.6766,
     2 -0.3189,0.,0.,0.,0.,0.,0.,0.,0.,0.,0.,0.,0.,0./
      DATA CI/-0.0382,0.2457,0.0557,4.3052,22.3184,44.8006,42.0069,
     19.6632,-13.7143,-7.1940,4.7637,2.6054,-1.9526,-0.2429,0.7289,
     2-0.4394/
      DATA CQ/0.5007,1.3823,2.3229,1.6233,-2.3123,-7.0695,-5.2753,
     12.7801,5.0775,0.3151,-0.6568,1.3191,-0.0767,-1.0017,0.5064,
     20.3751/
      DATA CID/-0.1703,0.2024,0.0702,1.4971,13.8791,37.6942,47.5134,
     123.1819,-8.4805,-12.2511,1.6847,4.7107,-1.0031,-1.2512,0.8066,
     2-0.06/
      DATA CQD/0.3445,0.9827,2.0572,2.2102,-0.4665,-5.6382,-7.0769,
     1-0.245,5.4433,2.2094,-1.0544,0.8176,0.778,-1.0643,-0.0624,0.7109/
      DATA XSR/1.,3.,3.,1.,-1.,-3.,-3.,-1.,1.,3.,3.,1.,-1.,-3.,-3.,-1./
      DATA XSQ/1.,1.,3.,3.,1.,1.,3.,3.,-1.,-1.,-3.,-3.,-1.,-1.,-3.,-3./
      CALL DARRAY(1000,10,10,1)
C
C
      WRITE(2,2060)
      WRITE(2,2070)
      READ(1,*)IXX
      READ(1,*)ILOOPS
      READ(1,*)(COEFF(I),I=1,5),DEL,DCGAIN
      READ(1,*) IMPL,SR
      READ(1,*)SDEL
      READ(1,*)C
      READ(1,*)AMEAN,SIGMA
      READ(1,*)THETA
      DCGAIN=1.0/DCGAIN
      CALL G05CBF(IXX)
      DO 3 I=1,50
      DO 3 J=1,50
      HIT(I,J)=0.0
3     HQT(I,J)=0.0
      IDEL=INT(DEL*2*SR)
      IMP1=IMPL+IDEL
      IM1=IMP1-1
      IMPR=(2*IMPL+IDEL-1)/2
      IMPES=IMPR
      SCALE=2.0/SQRT(10.0)
      IS=0
      IC=0
      LB=31
      LB1=LB+1
      ITDEL=LB+SDEL
      SDEL1=SDEL-1
      MM1=50
      MM1=MM1+1
      MM2=MM1+10
      SIN=0.0
      ROT=0.0
      TSQERR=0.0
      TSQ1=0.0
      TSQN=0.0
      THETA1=(1.0-THETA)**2
      THETA2=1.0-THETA**2
      DO 790 I=1,IMPR
      XX1R(I)=0.0
790   XX1Q(I)=0.0
```

```
      DO 794 I=1,IMPR
      DO 794 J=I,IMPR
      IF(I.NE.J)GO TO 796
      PR(I,J)=1.0
      PQ(I,J)=0.0
      GO TO 794
  796 PR(I,J)=0.0
      PQ(I,J)=0.0
      PR(J,I)=PR(I,J)
      PQ(J,I)=-PQ(I,J)
  794 CONTINUE
      POS=-1.0
      DO  8 I=1,IMP1
      DO  8 J=1,IMP1
      TI(I,J)=0.0
    8 TQ(I,J)=0.0
      IMPP=IMPR+2
      IMPRP=IMPR+1
      ISTEP=20* 2*SR
      STIP=1.0/ISTEP
      DO 10 I=1,5
      RAYLI1(I)=0.0
      RAYLQ1(I)=0.0
      RAYLI2(I)=0.0
   10 RAYLQ2(I)=0.0
C
C
      DO 40 J=1,50
      OPI1(1)=G05DDF(0.0,1.0)-(RAYLI1(1)*COEFF(1)+RAYLI1(2)*COEFF(2))
      OPQ1(1)=G05DDF(0.0,1.0)-(RAYLQ1(1)*COEFF(1)+RAYLQ1(2)*COEFF(2))
      OPI2(1)=G05DDF(0.0,1.0)-(RAYLI2(1)*COEFF(1)+RAYLI2(2)*COEFF(2))
      OPQ2(1)=G05DDF(0.0,1.0)-(RAYLQ2(1)*COEFF(1)+RAYLQ2(2)*COEFF(2))
      OPI1(2)=OPI1(1)-(RAYLI1(3)*COEFF(3)+RAYLI1(4)*COEFF(4))
      OPQ1(2)=OPQ1(1)-(RAYLQ1(3)*COEFF(3)+RAYLQ1(4)*COEFF(4))
      OPI2(2)=OPI2(1)-(RAYLI2(3)*COEFF(3)+RAYLI2(4)*COEFF(4))
      OPQ2(2)=OPQ2(1)-(RAYLQ2(3)*COEFF(3)+RAYLQ2(4)*COEFF(4))
      X1(2)=OPI1(2)-RAYLI1(5)*COEFF(5)
      Y1(2)=OPQ1(2)-RAYLQ1(5)*COEFF(5)
      X2(2)=OPI2(2)-RAYLI2(5)*COEFF(5)
      Y2(2)=OPQ2(2)-RAYLQ2(5)*COEFF(5)
      RAYLI1(5)=X1(2)
      RAYLQ1(5)=Y1(2)
      RAYLI2(5)=X2(2)
      RAYLQ2(5)=Y2(2)
      X1(2)=X1(2)*DCGAIN
      Y1(2)=Y1(2)*DCGAIN
      X2(2)=X2(2)*DCGAIN
      Y2(2)=Y2(2)*DCGAIN
      RAYLI1(4)=RAYLI1(3)
      RAYLI1(3)=OPI1(2)
      RAYLI1(2)=RAYLI1(1)
      RAYLI1(1)=OPI1(1)
      RAYLQ1(4)=RAYLQ1(3)
      RAYLQ1(3)=OPQ1(2)
      RAYLQ1(2)=RAYLQ1(1)
      RAYLQ1(1)=OPQ1(1)
      RAYLI2(4)=RAYLI2(3)
      RAYLI2(3)=OPI2(2)
      RAYLI2(2)=RAYLI2(1)
      RAYLI2(1)=OPI2(1)
      RAYLQ2(4)=RAYLQ2(3)
      RAYLQ2(3)=OPQ2(2)
      RAYLQ2(2)=RAYLQ2(1)
   40 RAYLQ2(1)=OPQ2(1)
```

```
C
C
      ILOP=100+ILOOPS
C
C
      DO  45 K=1,ILOP
      OPI1(1)=G05DDF(0.0,1.0)-(RAYLI1(1)*COEFF(1)+RAYLI1(2)*COEFF(2))
      OPQ1(1)=G05DDF(0.0,1.0)-(RAYLQ1(1)*COEFF(1)+RAYLQ1(2)*COEFF(2))
      OPI2(1)=G05DDF(0.0,1.0)-(RAYLI2(1)*COEFF(1)+RAYLI2(2)*COEFF(2))
      OPQ2(1)=G05DDF(0.0,1.0)-(RAYLQ2(1)*COEFF(1)+RAYLQ2(2)*COEFF(2))
      OPI1(2)=OPI1(1)-(RAYLI1(3)*COEFF(3)+RAYLI1(4)*COEFF(4))
      OPQ1(2)=OPQ1(1)-(RAYLQ1(3)*COEFF(3)+RAYLQ1(4)*COEFF(4))
      OPI2(2)=OPI2(1)-(RAYLI2(3)*COEFF(3)+RAYLI2(4)*COEFF(4))
      OPQ2(2)=OPQ2(1)-(RAYLQ2(3)*COEFF(3)+RAYLQ2(4)*COEFF(4))
      X1(1)=OPI1(2)-RAYLI1(5)*COEFF(5)
      Y1(1)=OPQ1(2)-RAYLQ1(5)*COEFF(5)
      X2(1)=OPI2(2)-RAYLI2(5)*COEFF(5)
      Y2(1)=OPQ2(2)-RAYLQ2(5)*COEFF(5)
      RAYLI1(5)=X1(1)
      RAYLQ1(5)=Y1(1)
      RAYLI2(5)=X2(1)
      RAYLQ2(5)=Y2(1)
      X1(1)=X1(1)*DCGAIN
      Y1(1)=Y1(1)*DCGAIN
      X2(1)=X2(1)*DCGAIN
      Y2(1)=Y2(1)*DCGAIN
      RAYLI1(4)=RAYLI1(3)
      RAYLI1(3)=OPI1(2)
      RAYLI1(2)=RAYLI1(1)
      RAYLI1(1)=OPI1(1)
      RAYLQ1(4)=RAYLQ1(3)
      RAYLQ1(3)=OPQ1(2)
      RAYLQ1(2)=RAYLQ1(1)
      RAYLQ1(1)=OPQ1(1)
      RAYLI2(4)=RAYLI2(3)
      RAYLI2(3)=OPI2(2)
      RAYLI2(2)=RAYLI2(1)
      RAYLI2(1)=OPI2(1)
      RAYLQ2(4)=RAYLQ2(3)
      RAYLQ2(3)=OPQ2(2)
      RAYLQ2(2)=RAYLQ2(1)
      RAYLQ2(1)=OPQ2(1)
      RAY1(K)=X1(1)
      RAY2(K)=Y1(1)
      RAY3(K)=X2(1)
   45 RAY4(K)=Y2(1)
C
C
      DO 64 J=1,IMP1
      DO 64 I=1,4
      R(I,J)=0.0
   64 Q(I,J)=0.0
      IQ=50
      CALL G05CBF(IQ)
      DO 798 I=2,60
      NSYM=INT(G05DAF(1.0,16.9999999999))
      SSR(I)=XSR(NSYM)*SCALE
  798 SSQ(I)=XSQ(NSYM)*SCALE
      DO 797 I=1,30
      ANOIR(I)=G05DDF(AMEAN,SIGMA)
  797 ANOIQ(I)=G05DDF(AMEAN,SIGMA)
```

```
      DO  400  IRUN=1,ILOP
      X1(1)=RAY1(IRUN)
      Y1(1)=RAY2(IRUN)
      X2(1)=RAY3(IRUN)
      Y2(1)=RAY4(IRUN)
      CONST1=(X1(1)-X1(2))*STIP
      CONST2=(Y1(1)-Y1(2))*STIP
      CONST3=(X2(1)-X2(2))*STIP
      CONST4=(Y2(1)-Y2(2))*STIP
C
C
   68 DO  200  ISYM=1,ISTEP
      DO  305 I=1,IMP1
      R(1,I)=0.0
  305 Q(1,I)=0.0
      K=ISYM-1
      AINCR=K*CONST1
      BINCR=K*CONST2
      DO  310  I=1,IMPL
      R(1,I)=CI(I)*(X1(2)+AINCR-Y1(2)-BINCR)-CQ(I)*(Y1(2)+BINCR+X1(2)+AI
     1NCR)
  310 Q(1,I)=CI(I)*(X1(2)+AINCR+Y1(2)+BINCR)+CQ(I)*(X1(2)+AINCR-Y1(2)-BI
     1NCR)
      AINCR=K*CONST3
      BINCR=K*CONST4
      DO  330  I=1,IMPL
      R(1,I+IDEL)=R(1,I+IDEL)+CID(I)*(X2(2)+AINCR-Y2(2)-BINCR)-CQD(I)*(Y
     12(2)+BINCR+X2(2)+AINCR)
  330 Q(1,I+IDEL)=Q(1,I+IDEL)+CID(I)*(Y2(2)+BINCR+X2(2)+AINCR)+CQD(I)*(X
     12(2)+AINCR-Y2(2)-BINCR)
      DO  596  I=1,IMP1
      DO  596  J=1,IM1
      TI(I,IMP1+1-J)=TI(I,IMP1-J)
  596 TQ(I,IMP1+1-J)=TQ(I,IMP1-J)
  590 DO  600  I=1,IMP1
      TI(I,1)=(Q(1,I)+R(1,I))*0.5
  600 TQ(I,1)=(Q(1,I)-R(1,I))*0.5
      POS=-POS
      IF(POS.LT.0.0)GO TO  200
      DO  597  I=1,IMPR
      DO  597  J=1,49
      HIT(I,51-J)=HIT(I,50-J)
  597 HQT(I,51-J)=HQT(I,50-J)
      IO=0
      DO  2010  I=1,IMP1,2
      IO=IO+1
      HIT(IO,1)=0.0
      HQT(IO,1)=0.0
      DO  2000  J=1,I
      HIT(IO,1)=HIT(IO,1)+TI(J,I+1-J)*CRI(I+1-J)-TQ(J,I+1-J)*CRQ(I+1-J)
 2000 HQT(IO,1)=HQT(IO,1)+TQ(J,I+1-J)*CRI(I+1-J)+TI(J,I+1-J)*CRQ(I+1-J)
      HIT(IO,1)=HIT(IO,1)*2.0 8333333E-4
 2010 HQT(IO,1)=HQT(IO,1)*2.0 8333333E-4
      DO  2030  I=1,IM1,2
      IO=IO+1
      HIT(IO,1)=0.0
      HQT(IO,1)=0.0
      K=1+I
```

```
      DO 2020 J=K,IMP1
      HIT(IO,1)=HIT(IO,1)+TI(J,IMP1+1+I-J)*CRI(IMP1+1+I-J)-TQ(J,IMP1+1+I
     1-J)*CRQ(IMP1+1+I-J)
2020  HQT(IO,1)=HQT(IO,1)+TQ(J,IMP1+1+I-J)*CRI(IMP1+1+I-J)+TI(J,IMP1+1+I
     1-J)*CRQ(IMP1+1+I-J)
      HIT(IO,1)=HIT(IO,1)*2.08333333E-4
2030  HQT(IO,1)=HQT(IO,1)*2.08333333E-4
      IF(IRUN.LT.MM2)GO TO 200
      IC=IC+1
      IF(IC-LB)200,805,807
 805  CONTINUE
      DO 799 I=1,IMPR
      CER(I)=HIT(I,1)
      CEQ(I)=HQT(I,1)
      XXOR(I)=HIT(I,1)
      XXOQ(I)=HQT(I,1)
 799  CONTINUE
      GO TO 200
 807  CONTINUE
      IF(IC-ITDEL)806,806,816
C
C     SETTING THE DELAY
C     DELAY = SDEL
C     ------------
 806  CONTINUE
      NSYM=INT(G05DAF(1.0,16.9999999999))
      SSR(1)=XSR(NSYM)*SCALE
      SSQ(1)=XSQ(NSYM)*SCALE
      RRR(1)=0.0
      RRQ(1)=0.0
      DO 808 I=1,IMPR
      RRR(1)=RRR(1)+SSR(I)*HIT(I,1)-SSQ(I)*HQT(I,1)
808   RRQ(1)=RRQ(1)+SSQ(I)*HIT(I,1)+SSR(I)*HQT(I,1)
      DO 810 I=1,IMPR
      ANOIR(IMPP-I)=ANOIR(IMPRP-I)
810   ANOIQ(IMPP-I)=ANOIQ(IMPRP-I)
      ANOIR(1)=G05DDF(AMEAN,SIGMA)
      ANOIQ(1)=G05DDF(AMEAN,SIGMA)
      CORNR=0.0
      CORNQ=0.0
      DO 812 I=1,IMPR
      CORNR=CORNR+ANOIR(I)*WSI(I)-ANOIQ(I)*WSQ(I)
812   CORNQ=CORNQ+ANOIQ(I)*WSI(I)+ANOIR(I)*WSQ(I)
      RRR(1)=RRR(1)+CORNR
      RRQ(1)=RRQ(1)+CORNQ
      SSIN=SSR(1)**2+SSQ(1)**2
      RROT=RRR(1)**2+RRQ(1)**2
      SIN=SIN+SSIN
      ROT=ROT+RROT
      DO 814 I=1,59
      SSR(61-I)=SSR(60-I)
      SSQ(61-I)=SSQ(60-I)
      RRR(61-I)=RRR(60-I)
814   RRQ(61-I)=RRQ(60-I)
      GO TO 200
```

```
C
C       KALMAN FILTER ESTIMATOR
C       -----------------------
  816 CONTINUE
      IS=IS+1
      NSYM=INT(G05DAF(1.0,16.9999999999))
      SSR(1)=XSR(NSYM)*SCALE
      SSQ(1)=XSQ(NSYM)*SCALE
      RRR(1)=0.0
      RRQ(1)=0.0
      DO 818 I=1,IMPR
      RRR(1)=RRR(1)+SSR(I)*HIT(I,1)-SSQ(I)*HQT(I,1)
  818 RRQ(1)=RRQ(1)+SSQ(I)*HIT(I,1)+SSR(I)*HQT(I,1)
      DO 820 I=1,IMPR
      ANOIR(IMPP-I)=ANOIR(IMPRP-I)
  820 ANOIQ(IMPP-I)=ANOIQ(IMPRP-I)
      ANOIR(1)=G05DDF(AMEAN,SIGMA)
      ANOIQ(1)=G05DDF(AMEAN,SIGMA)
      CORNR=0.0
      CORNQ=0.0
      DO 822 I=1,IMPR
      CORNR=CORNR+ANOIR(I)*WSI(I)-ANOIQ(I)*WSQ(I)
  822 CORNQ=CORNQ+ANOIQ(I)*WSI(I)+ANOIR(I)*WSQ(I)
      RRR(1)=RRR(1)+CORNR
      RRQ(1)=RRQ(1)+CORNQ
      SSIN=SSR(1)**2+SSQ(1)**2
      RROT=RRR(1)**2+RRQ(1)**2
      SIN=SIN+SSIN
      ROT=ROT+RROT
      DO 824 I=1,IMPR
      SER(I)=SSR(I+SDEL)
  824 SEQ(I)=SSQ(I+SDEL)
      ZR=RRR(1+SDEL)
      ZQ=RRQ(1+SDEL)
      ZER=0.0
      ZEQ=0.0
      DO 300 I=1,IMPR
      ZER=ZER+SER(I)*XXOR(I)-SEQ(I)*XXOQ(I)
  300 ZEQ=ZEQ+SEQ(I)*XXOR(I)+SER(I)*XXOQ(I)
      ANUR=ZR-ZER
      ANUQ=ZQ-ZEQ
      DO 9000 I=1,IMPR
      DO 9000 J=1,IMPR
      QVR(I,J)=C*PR(I,J)
      QVQ(I,J)=C*PQ(I,J)
 9000 CONTINUE
      DO 302 I=1,IMPR
      DO 302 J=I,IMPR
      IF(I.NE.J)GO TO 301
      PPR(I,J)=PR(I,J)+QVR(I,J)
      PPQ(I,J)=0.0
      GO TO 302
  301 PPR(I,J)=PR(I,J)+QVR(I,J)
      PPQ(I,J)=PQ(I,J)+QVQ(I,J)
      PPR(J,I)=PPR(I,J)
      PPQ(J,I)=-PPQ(I,J)
  302 CONTINUE
```

```
      DO 306 J=1,IMPR
      SP1=0.0
      SP2=0.0
      DO 304 I=1,IMPR
      SP1=SP1+SER(I)*PPR(I,J)-SEQ(I)*PPQ(I,J)
  304 SP2=SP2+SER(I)*PPQ(I,J)+SEQ(I)*PPR(I,J)
      SPR(J)=SP1
  306 SPQ(J)=SP2
      SPSR=0.0
      SPSQ=0.0
      DO 308 I=1,IMPR
      SPSR=SPSR+SPR(I)*SER(I)+SPQ(I)*SEQ(I)
      SPSQ=SPSQ+SPQ(I)*SER(I)-SPR(I)*SEQ(I)
  308 CONTINUE
      SPSSR=SPSR+SIGMA**2
      DO 362 I=1,IMPR
      PSR(I)=0.0
      PSQ(I)=0.0
      DO 362 J=1,IMPR
      PSR(I)=PSR(I)+PPR(I,J)*SER(J)+PPQ(I,J)*SEQ(J)
  362 PSQ(I)=PSQ(I)+PPQ(I,J)*SER(J)-PPR(I,J)*SEQ(J)
      DO 314 I=1,IMPR
      GR(I)=PSR(I)/SPSSR
  314 GQ(I)=PSQ(I)/SPSSR
      DO 326 I=1,IMPR
      DO 326 J=1,IMPR
      GSR(I,J)=GR(I)*SER(J)-GQ(I)*SEQ(J)
  326 GSQ(I,J)=GR(I)*SEQ(J)+GQ(I)*SER(J)
      DO 327 I=1,IMPR
      DO 327 J=I,IMPR
      IF(I.NE.J)GO TO 329
      GSPQ(I,J)=0.0
      GSPR(I,J)=0.0
      DO 328 K=1,IMPR
  328 GSPR(I,J)=GSPR(I,J)+GSR(I,K)*PPR(K,J)-GSQ(I,K)*PPQ(K,J)
      GO TO 327
  329 GSPR(I,J)=0.0
      GSPQ(I,J)=0.0
      DO 331 K=1,IMPR
      GSPR(I,J)=GSPR(I,J)+GSR(I,K)*PPR(K,J)-GSQ(I,K)*PPQ(K,J)
  331 GSPQ(I,J)=GSPQ(I,J)+GSR(I,K)*PPQ(K,J)+GSQ(I,K)*PPR(K,J)
      GSPR(J,I)=GSPR(I,J)
      GSPQ(J,I)=-GSPQ(I,J)
  327 CONTINUE
      DO 364 I=1,IMPR
      DO 364 J=I,IMPR
      IF(I.NE.J)GO TO 365
      PR(I,J)=PPR(I,J)-GSPR(I,J)
      PQ(I,J)=0.0
      GO TO 364
  365 PR(I,J)=PPR(I,J)-GSPR(I,J)
      PQ(I,J)=PPQ(I,J)-GSPQ(I,J)
      PR(J,I)=PR(I,J)
      PQ(J,I)=-PQ(I,J)
  364 CONTINUE
      DO 332 I=1,IMPR
      CER(I)=XXOR(I)+GR(I)*ANUR-GQ(I)*ANUQ
  332 CEQ(I)=XXOQ(I)+GQ(I)*ANUR+GR(I)*ANUQ
      DO 371 I=1,IMPR
      EPR(I)=CER(I)-XXOR(I)
  371 EPQ(I)=CEQ(I)-XXOQ(I)
      DO 373 I=1,IMPR
      XX1R(I)=XX1R(I)+THETA1*EPR(I)
  373 XX1Q(I)=XX1Q(I)+THETA1*EPQ(I)
```

```
      DO 375 I=1,IMPR
      XXOR(I)=XXOR(I)+XX1R(I)+THETA2*EPR(I)
  375 XXOQ(I)=XXOQ(I)+XX1Q(I)+THETA2*EPQ(I)
      DO 377 I=1,IMPR
      XXNR(I)=XXOR(I)+SDEL1*XX1R(I)
  377 XXNQ(I)=XXOQ(I)+SDEL1*XX1Q(I)
      SQE=0.0
      SQE1=0.0
      SQEN=0.0
      DO 334 I=1,IMPR
      SQE1=SQE1+(HIT(I,SDEL)-XXOR(I))**2+(HQT(I,SDEL)-XXOQ(I))**2
      SQEN=SQEN+(HIT(I,1)-XXNR(I))**2+(HQT(I,1)-XXNQ(I))**2
  334 SQE=SQE+(HIT(I,1+SDEL)-CER(I))**2+(HQT(I,1+SDEL)-CEQ(I))**2
      SQ1=10.0*ALOG10(SQE)
      SQ11=10.0*ALOG10(SQE1)
      SQN1=10.0*ALOG10(SQEN)
 1000 CONTINUE
      IF(IRUN.LE.100)GO TO 346
  345 TSQERR=TSQERR+SQE
      TSQ1=TSQ1+SQE1
      TSQN=TSQN+SQEN
  346 CONTINUE
      DO 338 I=1,59
      SSR(61-I)=SSR(60-I)
      SSQ(61-I)=SSQ(60-I)
      RRR(61-I)=RRR(60-I)
  338 RRQ(61-I)=RRQ(60-I)
  200 CONTINUE
C
C
      X1(2)=X1(1)
      Y1(2)=Y1(1)
      X2(2)=X2(1)
      Y2(2)=Y2(1)
  400 CONTINUE
C
C
      AVMSQE=TSQERR/FLOAT((ISTEP*ILOOPS)/2)
      AVTS1=TSQ1/FLOAT((ISTEP*ILOOPS)/2)
      AVTSN=TSQN/FLOAT((ISTEP*ILOOPS)/2)
      AVMSQE=10.0*ALOG10(AVMSQE)
      AVTS1=10.0*ALOG10(AVTS1)
      AVTSN=10.0*ALOG10(AVTSN)
      WRITE(2,341)AVMSQE
      WRITE(2,3200)AVTS1
      WRITE(2,3202)AVTSN
      WRITE(2,342) C
      WRITE(2,3204) THETA
      SIN=SIN/FLOAT(21137)
      ROT=ROT/FLOAT(21137)
      WRITE(2,7000) SIN
      WRITE(2,7002) ROT
C
C
      DCGAIN=1.0/DCGAIN
      WRITE(2,3000) (CI(I),I=1,16)
      WRITE(2,3001) (CQ(I),I=1,16)
      WRITE(2,3002) (CID(I),I=1,16)
      WRITE(2,3003) (CQD(I),I=1,16)
      WRITE(2,3004) IXX,IQ
      WRITE(2,3005) DEL
      WRITE(2,3006) (COEFF(I),I=1,5)
      WRITE(2,3007)DCGAIN
```

```
C
C
 2060 FORMAT(1H1,'KALMAN FILTER ESTIMATOR APPLIED TO 2-SKYWAVE H.F LINK'
     1,/,' INPUT SIGNAL : 16-POINT QAM',/,
     2' AVERAGE TRANSMITTED ENERGY PER BIT IS UNITY',/,
     3' BIT RATE IS 9600 BITS/SEC',/,
     4' CHANNEL VECTOR IS NOT NORMALISED',/)
 2070 FORMAT(1H ,'CHANNEL : 2 ; 1 HZ AND 2 MILLISECS',//,
     1' PREDICTION : LEAST-SQUARES FADING-MEMORY, DEGREE 1',/,
     2' INITIAL VALUES ARE :',/,
     3'                    S(0,0) = I',/,
     4'           Q(I)=C*S(I-1,I-1)',/,
     5'               X(1,0) = Y(0)',/,
     7' I TAKEN FROM 4801 TO 24000',//)
 7000  FORMAT(1H ,'INPUT SIGNAL ENERGY  = ',F15.8)
 7002  FORMAT(1H ,'OUTPUT SIGNAL ENERGY = ',F15.8)
 3000  FORMAT(1H ,'CI',/,2(10F8.4/))
 3001  FORMAT(1H ,'CQ',/,2(10F8.4/))
 3002  FORMAT(1H ,'CID',/,2(10F8.4/))
 3003  FORMAT(1H ,'CQD',/,2(10F8.4/))
 3004  FORMAT(1H ,'IXX = ',I4,',  IQ = ',I4)
 3005  FORMAT(1H ,'DEL = ',F4.1)
 3006  FORMAT(1H ,'COEFF = ',5F13.7)
  3007 FORMAT(1H ,'DCGAIN = ',F15.4)
   347 FORMAT(1H ,'ESTIMATE ERROR (INITIAL) = ',F20.10)
   341 FORMAT(1H ,'ESTIMATE ERROR (S. STATE) = ',F30.15)
 342   FORMAT(1H ,'C = ',F20.15)
  3200 FORMAT(1H ,'LAMBDA (1-STEP) = ',F30.15)
  3202 FORMAT(1H ,'LAMBDA (N-STEP) = ',F30.15)
  3204 FORMAT(1H ,'THETA = ',F6.3)
C
C
       STOP
       END
```

APPENDIX A4

AN EXAMPLE OF THE SIMULATION OF THE FEEDFORWARD TRANSVERSAL-FILTER ESTIMATOR

```
      PROGRAM R0002(INPUT,OUTPUT,TAPE1=INPUT,TAPE2=OUTPUT)
C
C
C     LINEAR FEEDFORWARD ESTIMATOR WITH PREDICTION
C           APPLIED TO 2-SKYWAVE H.F LINK
C     PREDICTION : LEAST-SQUARES FADING-MEMORY USING POLYNOMIAL OF
C                  DEGREE 1
C     DELAY IN ESTIMATION = 17 SAMPLING INTERVALS
C     INPUT SIGNAL : 16-POINT QAM
C     AVERAGE TRANSMITTED ENERGY PER BIT IS UNITY
C     BIT RATE IS 9600 BITS/SEC
C     CHANNEL VECTOR IS NOT NORMALISED
C     CHANNEL SIMULATED - CH. 2 -- 1 HZ AND 2 MILLISECS
C     ------------------------------------------------
C
C
      DIMENSION RAYLI1(5),RAYLQ1(5),RAYLI2(5),RAYLQ2(5),COEFF(5),
     1X1(2),Y1(2),X2(2),Y2(2),R(4,50),Q(4,50)
      DIMENSION OPI1(4),OPQ1(4),OPI2(4),OPQ2(4)
      DIMENSION RAY1(1100),RAY2(1100),RAY3(1100),RAY4(1100)
      DIMENSION CI(16),CQ(16),CID(16),CQD(16)
      DIMENSION WSI(30),WSQ(30)
      DIMENSION ANOIR(30),ANOIQ(30)
      DIMENSION TI(30,30),TQ(30,30)
      DIMENSION HIT(50,50),HQT(50,50),CRI(30),CRQ(30)
      DIMENSION SER(25),SEQ(25),CER(25),CEQ(25)
      DIMENSION XX1R(25),XX1Q(25),XXOR(25),XXOQ(25),XXNR(25),XXNQ(25),
     1EPR(25),EPQ(25)
      DIMENSION XSR(16),XSQ(16)
      DIMENSION SSR(60),SSQ(60),RRR(60),RRQ(60)
      INTEGER SDEL,SDEL1
      INTEGER VECL,VECLM,VECLP
      DATA WSI/-0.0059,-0.003,0.0032,0.0205,0.1662,0.4893,0.6759,
     1 0.406,-0.0371,-0.179,-0.038,0.0623,0.0289,-0.0174,-0.0109,
     2-0.0068,0.,0.,0.,0.,0.,0.,0.,0.,0.,0.,0.,0.,0./
      DATA WSQ/0.0042,0.0095,0.0293,0.0494,0.0266,-0.0748,-0.1652,
     1 -0.0739,0.1092,0.1174,-0.013,-0.0432,0.0126,0.0162,-0.0098,
     2 -0.0046,0.,0.,0.,0.,0.,0.,0.,0.,0.,0.,0.,0.,0./
      DATA CRI/-0.4107,-0.205,0.2219,1.4222,11.5059,33.8749,46.7973,
     1 28.1107,-2.5666,-12.3912,-2.6308,4.3105,2.0033,-1.205,
     2 -0.7537,0.4731,0.,0.,0.,0.,0.,0.,0.,0.,0.,0.,0.,0./
      DATA CRQ/0.2882,0.6548,2.0303,3.4222,1.8432,-5.1777,-11.4399,
     1 -5.1152,7.5627,8.128,-0.8993,-2.9923,0.873,1.1213,-0.6766,
     2 -0.3189,0.,0.,0.,0.,0.,0.,0.,0.,0.,0.,0.,0.,0./
```

```
      DATA CI/-0.0382,0.2457,0.0557,4.3052,22.3184,44.8006,42.0069,
     119.6632,-13.7143,-7.1940,4.7637,2.6054,-1.9526,-0.2429,0.7289,
     2-0.4394/
      DATA CQ/0.5007,1.3823,2.3229,1.6233,-2.3123,-7.0695,-5.2753,
     112.7801,5.0775,0.3151,-0.6568,1.3191,-0.0767,-1.0017,0.5064,
     220.3751/
      DATA CID/-0.1703,0.2024,0.0702,1.4971,13.8791,37.6942,47.5134,
     1123.1819,-8.4805,-12.2511,1.6847,4.7107,-1.0031,-1.2512,0.8066,
     2-0.06/
      DATA CQD/0.3445,0.9827,2.0572,2.2102,-0.4665,-5.6382,-7.0769,
     1-0.245,5.4433,2.2094,-1.0544,0.8176,0.778,-1.0643,-0.0624,0.7109/
      DATA XSR/1.,3.,3.,1.,-1.,-3.,-3.,-1.,1.,3.,3.,1.,-1.,-3.,-3.,-1./
      DATA XSQ/1.,1.,3.,3.,1.,1.,3.,3.,-1.,-1.,-3.,-3.,-1.,-1.,-3.,-3./
      CALL DARRAY(1000,10,10,1)
C
C
      WRITE(2,2060)
      WRITE(2,2070)
      READ(1,*)IXX
      READ(1,*)ILOOPS
      READ(1,*)(COEFF(I),I=1,5),DEL,DCGAIN
      READ(1,*) IMPL,SR
      READ(1,*)SDEL
      READ(1,*)C
      READ(1,*)AMEAN,SIGMA
      READ(1,*)THETA
      DCGAIN=1.0/DCGAIN
      DO 700 IPROG=1,1
      IF(IPROG.EQ.1)C=0.002
      IF(IPROG.EQ.2)C=0.004
      IF(IPROG.EQ.3)C=0.005
      IF(IPROG.EQ.4)C=0.006
      CALL G05CBF(IXX)
      DO 3 I=1,50
      DO 3 J=1,50
      HIT(I,J)=0.0
3     HQT(I,J)=0.0
      IDEL=INT(DEL*2*SR)
      IMP1=IMPL+IDEL
      IM1=IMP1-1
      IMPR=(2*IMPL+IDEL-1)/2
      IMPES=IMPR
      SCALE=2.0/SQRT(10.0)
      IS=0
      IC=0
      LB=31
      LB1=LB+1
      ITDEL=LB+SDEL
      SDEL1=SDEL-1
      MM=50
      MM1=MM+1
      MM2=MM+10
      SIN=0.0
      ROT=0.0
      TSQERR=0.0
      TSQ1=0.0
      TSQN=0.0
      THETA1=(1.0-THETA)**2
      THETA2=1.0-THETA**2
      DO 790 I=1,IMPR
      XX1R(I)=0.0
790   XX1Q(I)=0.0
      POS=-1.0
```

```
      DO  8 I=1,IMP1
      DO  8 J=1,IMP1
      TI(I,J)=0.0
    8 TQ(I,J)=0.0
      IMPP=IMPR+2
      IMPRP=IMPR+1
      VECL=2*IMPR
      VECLP=VECL+2
      VECLM=VECL+1
      ISTEP=20*2*SR
      STIP=1.0/ISTEP
      DO 10 I=1,5
      RAYLI1(I)=0.0
      RAYLQ1(I)=0.0
      RAYLI2(I)=0.0
   10 RAYLQ2(I)=0.0
C
C
      DO  40 J=1,50
      OPI1(1)=G05DDF(0.0,1.0)-(RAYLI1(1)*COEFF(1)+RAYLI1(2)*COEFF(2))
      OPQ1(1)=G05DDF(0.0,1.0)-(RAYLQ1(1)*COEFF(1)+RAYLQ1(2)*COEFF(2))
      OPI2(1)=G05DDF(0.0,1.0)-(RAYLI2(1)*COEFF(1)+RAYLI2(2)*COEFF(2))
      OPQ2(1)=G05DDF(0.0,1.0)-(RAYLQ2(1)*COEFF(1)+RAYLQ2(2)*COEFF(2))
      OPI1(2)=OPI1(1)-(RAYLI1(3)*COEFF(3)+RAYLI1(4)*COEFF(4))
      OPQ1(2)=OPQ1(1)-(RAYLQ1(3)*COEFF(3)+RAYLQ1(4)*COEFF(4))
      OPI2(2)=OPI2(1)-(RAYLI2(3)*COEFF(3)+RAYLI2(4)*COEFF(4))
      OPQ2(2)=OPQ2(1)-(RAYLQ2(3)*COEFF(3)+RAYLQ2(4)*COEFF(4))
      X1(2)=OPI1(2)-RAYLI1(5)*COEFF(5)
      Y1(2)=OPQ1(2)-RAYLQ1(5)*COEFF(5)
      X2(2)=OPI2(2)-RAYLI2(5)*COEFF(5)
      Y2(2)=OPQ2(2)-RAYLQ2(5)*COEFF(5)
      RAYLI1(5)=X1(2)
      RAYLQ1(5)=Y1(2)
      RAYLI2(5)=X2(2)
      RAYLQ2(5)=Y2(2)
      X1(2)=X1(2)*DCGAIN
      Y1(2)=Y1(2)*DCGAIN
      X2(2)=X2(2)*DCGAIN
      Y2(2)=Y2(2)*DCGAIN
      RAYLI1(4)=RAYLI1(3)
      RAYLI1(3)=OPI1(2)
      RAYLI1(2)=RAYLI1(1)
      RAYLI1(1)=OPI1(1)
      RAYLQ1(4)=RAYLQ1(3)
      RAYLQ1(3)=OPQ1(2)
      RAYLQ1(2)=RAYLQ1(1)
      RAYLQ1(1)=OPQ1(1)
      RAYLI2(4)=RAYLI2(3)
      RAYLI2(3)=OPI2(2)
      RAYLI2(2)=RAYLI2(1)
      RAYLI2(1)=OPI2(1)
      RAYLQ2(4)=RAYLQ2(3)
      RAYLQ2(3)=OPQ2(2)
      RAYLQ2(2)=RAYLQ2(1)
   40 RAYLQ2(1)=OPQ2(1)
C
C
      ILOP=100+ILOOPS
C
C
```

```
      DO  45 K=1,ILOP
      OPI1(1)=G05DDF(0.0,1.0)-(RAYLI1(1)*COEFF(1)+RAYLI1(2)*COEFF(2))
      OPQ1(1)=G05DDF(0.0,1.0)-(RAYLQ1(1)*COEFF(1)+RAYLQ1(2)*COEFF(2))
      OPI2(1)=G05DDF(0.0,1.0)-(RAYLI2(1)*COEFF(1)+RAYLI2(2)*COEFF(2))
      OPQ2(1)=G05DDF(0.0,1.0)-(RAYLQ2(1)*COEFF(1)+RAYLQ2(2)*COEFF(2))
      OPI1(2)=OPI1(1)-(RAYLI1(3)*COEFF(3)+RAYLI1(4)*COEFF(4))
      OPQ1(2)=OPQ1(1)-(RAYLQ1(3)*COEFF(3)+RAYLQ1(4)*COEFF(4))
      OPI2(2)=OPI2(1)-(RAYLI2(3)*COEFF(3)+RAYLI2(4)*COEFF(4))
      OPQ2(2)=OPQ2(1)-(RAYLQ2(3)*COEFF(3)+RAYLQ2(4)*COEFF(4))
      X1(1)=OPI1(2)-RAYLI1(5)*COEFF(5)
      Y1(1)=OPQ1(2)-RAYLQ1(5)*COEFF(5)
      X2(1)=OPI2(2)-RAYLI2(5)*COEFF(5)
      Y2(1)=OPQ2(2)-RAYLQ2(5)*COEFF(5)
      RAYLI1(5)=X1(1)
      RAYLQ1(5)=Y1(1)
      RAYLI2(5)=X2(1)
      RAYLQ2(5)=Y2(1)
      X1(1)=X1(1)*DCGAIN
      Y1(1)=Y1(1)*DCGAIN
      X2(1)=X2(1)*DCGAIN
      Y2(1)=Y2(1)*DCGAIN
      RAYLI1(4)=RAYLI1(3)
      RAYLI1(3)=OPI1(2)
      RAYLI1(2)=RAYLI1(1)
      RAYLI1(1)=OPI1(1)
      RAYLQ1(4)=RAYLQ1(3)
      RAYLQ1(3)=OPQ1(2)
      RAYLQ1(2)=RAYLQ1(1)
      RAYLQ1(1)=OPQ1(1)
      RAYLI2(4)=RAYLI2(3)
      RAYLI2(3)=OPI2(2)
      RAYLI2(2)=RAYLI2(1)
      RAYLI2(1)=OPI2(1)
      RAYLQ2(4)=RAYLQ2(3)
      RAYLQ2(3)=OPQ2(2)
      RAYLQ2(2)=RAYLQ2(1)
      RAYLQ2(1)=OPQ2(1)
      RAY1(K)=X1(1)
      RAY2(K)=Y1(1)
      RAY3(K)=X2(1)
   45 RAY4(K)=Y2(1)
C
C
      DO 64 J=1,IMP1
      DO 64 I=1,4
      R(I,J)=0.0
   64 Q(I,J)=0.0
      IQ=50
      CALL G05CBF(IQ)
      DO 798 I=2,60
      NSYM=INT(G05DAF(1.0,16.9999999999))
      SSR(I)=XSR(NSYM)*SCALE
  798 SSQ(I)=XSQ(NSYM)*SCALE
      DO 797 I=1,30
      ANOIR(I)=G05DDF(AMEAN,SIGMA)
  797 ANOIQ(I)=G05DDF(AMEAN,SIGMA)
      DO 400 IRUN=1,ILOP
      X1(1)=RAY1(IRUN)
      Y1(1)=RAY2(IRUN)
      X2(1)=RAY3(IRUN)
      Y2(1)=RAY4(IRUN)
      CONST1=(X1(1)-X1(2))*STIP
      CONST2=(Y1(1)-Y1(2))*STIP
      CONST3=(X2(1)-X2(2))*STIP
      CONST4=(Y2(1)-Y2(2))*STIP
```

```
C
C
   68 DO 200 ISYM=1,ISTEP
      DO 305 I=1,IMP1
      R(1,I)=0.0
  305 Q(1,I)=0.0
      K=ISYM-1
      AINCR=K*CONST1
      BINCR=K*CONST2
      DO 310 I=1,IMPL
      R(1,I)=CI(I)*(X1(2)+AINCR-Y1(2)-BINCR)-CQ(I)*(Y1(2)+BINCR+X1(2)+AI
     1NCR)
  310 Q(1,I)=CI(I)*(X1(2)+AINCR+Y1(2)+BINCR)+CQ(I)*(X1(2)+AINCR-Y1(2)-BI
     1NCR)
      AINCR=K*CONST3
      BINCR=K*CONST4
      DO 330 I=1,IMPL
      R(1,I+IDEL)=R(1,I+IDEL)+CID(I)*(X2(2)+AINCR-Y2(2)-BINCR)-CQD(I)*(Y
     12(2)+BINCR+X2(2)+AINCR)
  330 Q(1,I+IDEL)=Q(1,I+IDEL)+CID(I)*(Y2(2)+BINCR+X2(2)+AINCR)+CQD(I)*(X
     12(2)+AINCR-Y2(2)-BINCR)
      DO 596 I=1,IMP1
      DO 596 J=1,IM1
      TI(I,IMP1+1-J)=TI(I,IMP1-J)
  596 TQ(I,IMP1+1-J)=TQ(I,IMP1-J)
  590 DO 600 I=1,IMP1
      TI(I,1)=(Q(1,I)+R(1,I))*0.5
  600 TQ(I,1)=(Q(1,I)-R(1,I))*0.5
      POS=-POS
      IF(POS.LT.0.0)GO TO 200
      DO 597 I=1,IMPR
      DO 597 J=1,49
      HIT(I,51-J)=HIT(I,50-J)
  597 HQT(I,51-J)=HQT(I,50-J)
      IO=0
      DO 2010 I=1,IMP1,2
      IO=IO+1
      HIT(IO,1)=0.0
      HQT(IO,1)=0.0
      DO 2000 J=1,I
      HIT(IO,1)=HIT(IO,1)+TI(J,I+1-J)*CRI(I+1-J)-TQ(J,I+1-J)*CRQ(I+1-J)
 2000 HQT(IO,1)=HQT(IO,1)+TQ(J,I+1-J)*CRI(I+1-J)+TI(J,I+1-J)*CRQ(I+1-J)
      HIT(IO,1)=HIT(IO,1)*2.08333333E-4
 2010 HQT(IO,1)=HQT(IO,1)*2.08333333E-4
      DO 2030 I=1,IM1,2
      IO=IO+1
      HIT(IO,1)=0.0
      HQT(IO,1)=0.0
      K=1+I
      DO 2020 J=K,IMP1
      HIT(IO,1)=HIT(IO,1)+TI(J,IMP1+1+I-J)*CRI(IMP1+1+I-J)-TQ(J,IMP1+1+I
     1-J)*CRQ(IMP1+1+I-J)
 2020 HQT(IO,1)=HQT(IO,1)+TQ(J,IMP1+1+I-J)*CRI(IMP1+1+I-J)+TI(J,IMP1+1+I
     1-J)*CRQ(IMP1+1+I-J)
      HIT(IO,1)=HIT(IO,1)*2.08333333E-4
 2030 HQT(IO,1)=HQT(IO,1)*2.08333333E-4
      IF(IRUN.LT.MM2)GO TO 200
      IC=IC+1
      IF(IC-LB) 200,805,807
  805 CONTINUE
```

```
      DO 799 I=1,IMPR
      CER(I)=HIT(I,1)
      CEQ(I)=HQT(I,1)
      XXOR(I)=HIT(I,1)
      XXOQ(I)=HQT(I,1)
  799 CONTINUE
      GO TO 200
  807 CONTINUE
      IF(IC-ITDEL) 806,806,816
C
CC    SETTING THE DELAY
CC    DELAY = SDEL
C     ------------
  806 CONTINUE
      NSYM=INT(G05DAF(1.0,16.9999999999))
      SSR(1)=XSR(NSYM)*SCALE
      SSQ(1)=XSQ(NSYM)*SCALE
      RRR(1)=0.0
      RRQ(1)=0.0
      DO 808 I=1,IMPR
      RRR(1)=RRR(1)+SSR(I)*HIT(I,1)-SSQ(I)*HQT(I,1)
  808 RRQ(1)=RRQ(1)+SSQ(I)*HIT(I,1)+SSR(I)*HQT(I,1)
      DO 810 I=1,IMPR
      ANOIR(IMPP-I)=ANOIR(IMPRP-I)
  810 ANOIQ(IMPP-I)=ANOIQ(IMPRP-I)
      ANOIR(1)=G05DDF(AMEAN,SIGMA)
      ANOIQ(1)=G05DDF(AMEAN,SIGMA)
      CORNR=0.0
      CORNQ=0.0
      DO 812 I=1,IMPR
      CORNR=CORNR+ANOIR(I)*WSI(I)-ANOIQ(I)*WSQ(I)
  812 CORNQ=CORNQ+ANOIQ(I)*WSI(I)+ANOIR(I)*WSQ(I)
      RRR(1)=RRR(1)+CORNR
      RRQ(1)=RRQ(1)+CORNQ
      SSIN=SSR(1)**2+SSQ(1)**2
      RROT=RRR(1)**2+RRQ(1)**2
      SIN=SIN+SSIN
      ROT=ROT+RROT
      DO 814 I=1,59
      SSR(61-I)=SSR(60-I)
      SSQ(61-I)=SSQ(60-I)
      RRR(61-I)=RRR(60-I)
  814 RRQ(61-I)=RRQ(60-I)
      GO TO 200
C
CCC   LINEAR FEEDFORWARD ESTIMATOR
CCC   WITH DEGREE 1 LEAST-SQUARES
CCC   FADING-MEMORY PREDICTION
C     ------------------------------
  816 CONTINUE
      IS=IS+1
      NSYM=INT(G05DAF(1.0,16.9999999999))
      SSR(1)=XSR(NSYM)*SCALE
      SSQ(1)=XSQ(NSYM)*SCALE
      RRR(1)=0.0
      RRQ(1)=0.0
      DO 818 I=1,IMPR
      RRR(1)=RRR(1)+SSR(I)*HIT(I,1)-SSQ(I)*HQT(I,1)
  818 RRQ(1)=RRQ(1)+SSQ(I)*HIT(I,1)+SSR(I)*HQT(I,1)
      DO 820 I=1,IMPR
      ANOIR(IMPP-I)=ANOIR(IMPRP-I)
  820 ANOIQ(IMPP-I)=ANOIQ(IMPRP-I)
      ANOIR(1)=G05DDF(AMEAN,SIGMA)
      ANOIQ(1)=G05DDF(AMEAN,SIGMA)
```

```
      CORNR=0.0
      CORNQ=0.0
      DO  822 I=1,IMPR
      CORNR=CORNR+ANOIR(I)*WSI(I)-ANOIQ(I)*WSQ(I)
  822 CORNQ=CORNQ+ANOIQ(I)*WSI(I)+ANOIR(I)*WSQ(I)
      RRR(1)=RRR(1)+CORNR
      RRQ(1)=RRQ(1)+CORNQ
      SSIN=SSR(1)**2+SSQ(1)**2
      RROT=RRR(1)**2+RRQ(1)**2
      SIN=SIN+SSIN
      ROT=ROT+RROT
      DO  824 I=1,IMPR
      SER(I)=SSR(I+SDEL)
  824 SEQ(I)=SSQ(I+SDEL)
      ZR=RRR(1+SDEL)
      ZQ=RRQ(1+SDEL)
      ZER=0.0
      ZEQ=0.0
      DO  300 I=1,IMPR
      ZER=ZER+SER(I)*XXOR(I)-SEQ(I)*XXOQ(I)
  300 ZEQ=ZEQ+SER(I)*XXOQ(I)+SEQ(I)*XXOR(I)
      ANUR=ZR-ZER
      ANUQ=ZQ-ZEQ
      CANUR=C*ANUR
      CANUQ=C*ANUQ
      DO  332 I=1,IMPR
      CER(I)=XXOR(I)+CANUR*SER(I)+CANUQ*SEQ(I)
  332 CEQ(I)=XXOQ(I)+CANUQ*SER(I)-CANUR*SEQ(I)
      DO  371 I=1,IMPR
      EPR(I)=CER(I)-XXOR(I)
  371 EPQ(I)=CEQ(I)-XXOQ(I)
      DO  373 I=1,IMPR
      XX1R(I)=XX1R(I)+THETA1*EPR(I)
  373 XX1Q(I)=XX1Q(I)+THETA1*EPQ(I)
      DO  375 I=1,IMPR
      XXOR(I)=XXOR(I)+XX1R(I)+THETA2*EPR(I)
  375 XXOQ(I)=XXOQ(I)+XX1Q(I)+THETA2*EPQ(I)
      DO  377 I=1,IMPR
      XXNR(I)=XXOR(I)+SDEL1*XX1R(I)
  377 XXNQ(I)=XXOQ(I)+SDEL1*XX1Q(I)
      SQE=0.0
      SQE1=0.0
      SQEN=0.0
      DO  334 I=1,IMPR
      SQE1=SQE1+(HIT(I,SDEL)-XXOR(I))**2+(HQT(I,SDEL)-XXOQ(I))**2
      SQEN=SQEN+(HIT(I,1)-XXNR(I))**2+(HQT(I,1)-XXNQ(I))**2
  334 SQE=SQE+(HIT(I,1+SDEL)-CER(I))**2+(HQT(I,1+SDEL)-CEQ(I))**2
      SQ1=10.0*ALOG10(SQE)
      SQ11=10.0*ALOG10(SQE1)
      SQN1=10.0*ALOG10(SQEN)
      IF(IS.EQ.200.OR.IS.EQ.201)WRITE(2,1097)IS,SQ1,SQ11,SQN1
 1097 FORMAT(1H ,'IS = ',I6,' SQ1 = ',F15.10,' SQ11 = ',F15.10,
     1' SQN1 = ',F15.10)
 1000 CONTINUE
      IF(IRUN.LE.100)GO TO 346
      TSQ1=TSQ1+SQE1
      TSQN=TSQN+SQEN
  345 TSQERR=TSQERR+SQE
  346 CONTINUE
      DO  338 I=1,59
      SSR(61-I)=SSR(60-I)
      SSQ(61-I)=SSQ(60-I)
      RRR(61-I)=RRR(60-I)
  338 RRQ(61-I)=RRQ(60-I)
  200 CONTINUE
```

```
C
C
      X1(2)=X1(1)
      Y1(2)=Y1(1)
      X2(2)=X2(1)
      Y2(2)=Y2(1)
  400 CONTINUE
C
C
      AVMSQE=TSQERR/FLOAT((ISTEP*ILOOPS)/2)
      AVTS1=TSQ1/FLOAT((ISTEP*ILOOPS)/2)
      AVTSN=TSQN/FLOAT((ISTEP*ILOOPS)/2)
      AVMSQE=10.0*ALOG10(AVMSQE)
      AVTS1=10.0*ALOG10(AVTS1)
      AVTSN=10.0*ALOG10(AVTSN)
      SIN=SIN/FLOAT(21137)
      ROT=ROT/FLOAT(21137)
      WRITE(2,7000) SIN
      WRITE(2,7002) ROT
      WRITE(2,341)AVMSQE
      WRITE(2,3200)AVTS1
      WRITE(2,3202)AVTSN
      WRITE(2,342)C
      WRITE(2,3204)THETA
      WRITE(2,3206)SDEL
      SNR=10.0*ALOG10(1.0/(SIGMA**2))
      WRITE(2,3210) SNR
 3210 FORMAT(1H ,'SNR = ',F10.5,' DB')
  700 CONTINUE
C
C
      DCGAIN=1.0/DCGAIN
      WRITE(2,3000) (CI(I),I=1,16)
      WRITE(2,3001) (CQ(I),I=1,16)
      WRITE(2,3002) (CID(I),I=1,16)
      WRITE(2,3003) (CQD(I),I=1,16)
      WRITE(2,3004) IXX,IQ
      WRITE(2,3005) DEL
      WRITE(2,3006) (COEFF(I),I=1,5)
      WRITE(2,3007)DCGAIN
C
C
 2060 FORMAT(1H1,'LINEAR FEEDFORWARD ESTIMATOR WITH PREDICTION',/,
     5'          APPLIED TO 2-SKYWAVE H.F LINK'
     1,/,' INPUT SIGNAL : 16-POINT QAM',/,
     2' AVERAGE TRANSMITTED ENERGY PER BIT IS UNITY',/,
     3' BIT RATE IS 9600 BITS/SEC',/,
     4' CHANNEL VECTOR IS NOT NORMALISED',/)
 2070 FORMAT(1H ,'CHANNEL : 2 ; 1 HZ AND 2 MILLISECS',//,
     1' HERE X0(1,0) = Y(0)',/,
     2' AND  X1(1,0) = 0',/,
     3' SNR = 5 DB',/,
     4' FIX THETA = 0.98, VARY C',//)
```

```
 3206 FORMAT(1H ,'DELAY IN ESTIMATION = ',I5)
3000  FORMAT(1H ,'CI',/,2(10F8.4/))
3001  FORMAT(1H ,'CQ',/,2(10F8.4/))
3002  FORMAT(1H ,'CID',/,2(10F8.4/))
3003  FORMAT(1H ,'CQD',/,2(10F8.4/))
3004  FORMAT(1H ,'IXX = ',I4,',  IQ = ',I4)
3005  FORMAT(1H ,'DEL = ',F4.1)
3006  FORMAT(1H ,'COEFF = ',5F13.7)
 3007 FORMAT(1H ,'DCGAIN = ',F15.4)
 3200 FORMAT(1H ,'LAMBDA (1-STEP) = ',F30.15)
 3202 FORMAT(1H ,'LAMBDA (N-STEP) = ',F30.15)
  341 FORMAT(1H ,'ESTIMATE ERROR (S. STATE) = ',F30.15)
  342 FORMAT(1H ,'C = ',F10.5)
 3204 FORMAT(1H ,'THETA = ',F6.3)
7000  FORMAT(1H ,'INPUT SIGNAL ENERGY  = ',F15.8)
7002  FORMAT(1H ,'OUTPUT SIGNAL ENERGY = ',F15.8)
C
C
      STOP
      END
```

APPENDIX A5

AN EXAMPLE OF THE SIMULATION OF THE IMPROVED CHANNEL ESTIMATOR

```
      PROGRAM R0003(INPUT,OUTPUT,TAPE1=INPUT,TAPE2=OUTPUT)
C
CC*****************************************************************
CC
CC    IMPROVED CHANNEL ESTIMATOR FOR AN H.F. RADIOLINK
CC    NUMBER OF SKYWAVE = 3
CC    RELATIVE DELAY BETWEEN FIRST AND SECOND, AND
CC    FIRST AND THIRD SKYWAVES ARE 2/3 & 3 MILLISECS RESPECTIVELY
CC    CORRECT STARTING AND PLANE HELD FIXED
CC    STARTING ESTIMATES ARE Y(-2K),Y(-K),Y(-L),Y(0)
CC    INPUT SIGNAL : 16-POINT QAM
CC    AVERAGE TRANSMITTED ENERGY PER BIT IS UNITY
CC    BIT RATE IS 9600 BITS/SEC
CC    DELAY IN ESTIMATION = 17 SAMPLING INTERVALS
CC    TRANSMITTER & RECEIVER FILTERS ARE MINIMUM PHASE FILTERS
CC
CC*****************************************************************
C
      DIMENSION RAYLI1(5),RAYLQ1(5),RAYLI2(5),RAYLQ2(5),COEFF(5),
     1X1(2),Y1(2),X2(2),Y2(2),R(4,50),Q(4,50)
      DIMENSION OPI1(4),OPQ1(4),OPI2(4),OPQ2(4)
      DIMENSION RAY1(1100),RAY2(1100),RAY3(1100),RAY4(1100)
      DIMENSION CI(16),CQ(16),CID1(16),CQD1(16),CID2(16),CQD2(16)
      DIMENSION YMLR(30),YMLQ(30)
      DIMENSION WSI(30),WSQ(30)
      DIMENSION TI(30,30),TQ(30,30)
      DIMENSION HIT(50,50),HQT(50,50),CRI(30),CRQ(30)
      DIMENSION RAYLI3(5),RAYLQ3(5),X3(2),Y3(2)
      DIMENSION OPI3(4),OPQ3(4)
      DIMENSION RAY5(1100),RAY6(1100)
      DIMENSION YM2KR(30),YM2KQ(30),YM1KR(30),YM1KQ(30),
     *          YNOTR(30),YNOTQ(30)
      DIMENSION AR(30),AQ(30),BR(30),BQ(30),CCR(30),CCQ(30)
      DIMENSION FR(30),FQ(30),ERRR(30),ERRQ(30),YYR(30),YYQ(30),
     *          YYPR(30),YYPQ(30)
      DIMENSION XSR(16),XSQ(16)
      DIMENSION SSR(60),SSQ(60),RRR(60),RRQ(60)
      DIMENSION ANOIR(30),ANOIQ(30)
      DIMENSION SER(30),SEQ(30)
      INTEGER SDEL,SDEL1
      DATA CI/-0.1795896,-3.0773455,-9.9409021,-11.7869473,
     1 -3.4618271,4.4438154,3.0642536,-1.3596576,-1.4973528,
     2 0.2925598,0.5180829,-0.1842786,-0.3167778,0.0021899,
     3 -0.0443806,0.0515533/
      DATA CQ/2.3539405,20.7590237,45.5584592,41.4909978,
     1 8.7045826,-11.7869820,-5.5819054,3.1582131,1.7365460,
     2 -0.7776891,-0.1292556,0.2880296,-0.2324818,-0.2107548,
     3 0.0392056,0.0098505/
```

```
      DATA CID1/-0.0622160,-2.0820312,-8.5764574,-12.3102829,
     1   -5.5766967,3.5478141,3.9398962,-0.7258700,
     2   -1.7957047,0.0207712,0.6018517,-0.0464514,
     3   -0.3680978,-0.0182370,-0.0471151,0.0789564/
      DATA CQD1/0.9639589,15.5920086,41.8806123,45.4936549,
     1   15.6491184,-10.1779415,-7.9404850,2.2650217,
     2   2.4780490,-0.5908297,-0.3459233,0.3143350,
     3   -0.1350979,-0.2790169,0.0231422,0.0071662/
      DATA CID2/-0.0105240,-1.3136537,-7.1104051,-12.3469721,
     1  -7.5848703,2.2353854,4.5938614,0.0931639,
     2  -1.9704176,-0.3233694,0.6313238,0.1035718,
     3  -0.3865939,-0.0734526,-0.0386471,0.0608046/
      DATA CQD2/0.1932385,11.0688962,37.2136597,47.9575159,
     1  22.8262482,-7.2498590,-10.0026703,0.8695437,
     2  3.1072800,-0.2261096,-0.5552906,0.2882096,
     3  -0.0156703,-0.3215770,-0.0107706,0.0140909/
      DATA CRI/-1.9417691,-15.9797864,-35.1417733,-34.4788717,
     1  -11.2301982,7.8155160,7.5124057,-0.5057505,-3.3707125,
     2  -0.6759166,1.0482656,0.3621876,-0.3105902,0.0438410,
     3  0.0738947,-0.0646936,0.,0.,0.,0.,0.,0.,0.,0.,0.,0.,0.,
     4  0.,0./
      DATA CRQ/1.3625952,11.5941040,27.3342937,28.0870086,
     1  7.2714615,-9.2602472,-5.0954462,3.2326498,1.8975352,
     2  -1.2813604,-0.4830313,0.7614804,0.1979014,-0.1532672,
     3  0.0940330,-0.0312132,0.,0.,0.,0.,0.,0.,0.,0.,0.,0.,0.,
     4  0.,0./
      DATA WSI/-0.0280463,-0.2308071,-0.5075768,-0.4980021,
     1  -0.1622055,0.1128849,0.1085069,-0.0073049,
     2  -0.0486855,-0.0097627,0.0151408,0.0052313,
     3  -0.0044861,0.0006332,0.0010673,-0.0009344,
     4  0.0000000,0.0000000,0.0000000,0.0000000,
     5  0.0000000,0.0000000,0.0000000,0.0000000,
     6  0.0000000,0.0000000,0.0000000,0.0000000,
     7  0.0000000,0.0000000/
      DATA WSQ/0.0196809,0.1674616,0.3948080,0.4056800,
     1  0.1050267,-0.1337521,-0.0735970,0.0466914,
     2  0.0274074,-0.0185076,-0.0069768,0.0109986,
     3  0.0028584,-0.0022137,0.0013582,-0.0004508,
     4  0.0000000,0.0000000,0.0000000,0.0000000,
     5  0.0000000,0.0000000,0.0000000,0.0000000,
     6  0.0000000,0.0000000,0.0000000,0.0000000,
     7  0.0000000,0.0000000/
      DATA XSR/1.,3.,3.,1.,-1.,-3.,-3.,-1.,1.,3.,3.,1.,-1.,-3.,-3.,-1./
      DATA XSQ/1.,1.,3.,3.,1.,1.,3.,3.,-1.,-1.,-3.,-3.,-1.,-1.,-3.,-3./
      CALL DARRAY(1000,10,10,1)
C
C
      WRITE(2,2060)
      WRITE(2,2070)
      READ(1,*)IXX
      READ(1,*)ILOOPS
      READ(1,*)(COEFF(I),I=1,5),DEL,DCGAIN
      READ(1,*)DEL1
      READ(1,*)IMPL,SR
      READ(1,*) SDEL
      READ(1,*) K2,K1,KM1,K0,K01
      READ(1,*) NTIME,XL
      READ(1,*) AMEAN,SIGMA
      READ(1,*) C
      READ(1,*) THETA
      READ(1,*) ETA
      DCGAIN=1.0/DCGAIN
```

```
      DO 700 IPROG=1,NTIME
      CALL G05CBF(IXX)
      DO 3 I=1,50
      DO 3 J=1,50
      HIT(I,J)=0.0
3     HQT(I,J)=0.0
      IDEL=INT(DEL*2*SR)
      IDEL1=INT(DEL1*2*SR)
      IMP1=IMPL+IDEL
      IM1=IMP1-1
      IMPR=(2*IMPL+IDEL-1)/2
      IMPES=IMPR
      POS=-1.0
      DO 8 I=1,IMP1
      DO 8 J=1,IMP1
      TI(I,J)=0.0
8     TQ(I,J)=0.0
      IMPP=IMPR+2
      IMPRP=IMPR+1
      ISTEP=20*2*SR
      STIP=1.0/ISTEP
      THETA1=(1.0-THETA)**2
      THETA2=1.0-THETA**2
      SCALE=2.0/SQRT(10.0)
      SDEL1=SDEL*2-1
      TSQE1=0.0
      TSQEN=0.0
      TSQI1=0.0
      TSQIN=0.0
      TSQ=0.0
      TSQI=0.0
      RIN=0.0
      SIN=0.0
      ROT=0.0
      XXAPR=0.0
      XXAPQ=0.0
      XXBPR=0.0
      XXBPQ=0.0
      XXGPR=0.0
      XXGPQ=0.0
      IS=0
      DO 10 I=1,5
      RAYLI1(I)=0.0
      RAYLQ1(I)=0.0
      RAYLI2(I)=0.0
      RAYLQ2(I)=0.0
      RAYLI3(I)=0.0
10    RAYLQ3(I)=0.0
C
C     DO 40 J=1,50
      OPI1(1)=G05DDF(0.0,1.0)-(RAYLI1(1)*COEFF(1)+RAYLI1(2)*COEFF(2))
      OPQ1(1)=G05DDF(0.0,1.0)-(RAYLQ1(1)*COEFF(1)+RAYLQ1(2)*COEFF(2))
      OPI2(1)=G05DDF(0.0,1.0)-(RAYLI2(1)*COEFF(1)+RAYLI2(2)*COEFF(2))
      OPQ2(1)=G05DDF(0.0,1.0)-(RAYLQ2(1)*COEFF(1)+RAYLQ2(2)*COEFF(2))
      OPI3(1)=G05DDF(0.0,1.0)-(RAYLI3(1)*COEFF(1)+RAYLI3(2)*COEFF(2))
      OPQ3(1)=G05DDF(0.0,1.0)-(RAYLQ3(1)*COEFF(1)+RAYLQ3(2)*COEFF(2))
      OPI1(2)=OPI1(1)-(RAYLI1(3)*COEFF(3)+RAYLI1(4)*COEFF(4))
      OPQ1(2)=OPQ1(1)-(RAYLQ1(3)*COEFF(3)+RAYLQ1(4)*COEFF(4))
      OPI2(2)=OPI2(1)-(RAYLI2(3)*COEFF(3)+RAYLI2(4)*COEFF(4))
      OPQ2(2)=OPQ2(1)-(RAYLQ2(3)*COEFF(3)+RAYLQ2(4)*COEFF(4))
      OPI3(2)=OPI3(1)-(RAYLI3(3)*COEFF(3)+RAYLI3(4)*COEFF(4))
      OPQ3(2)=OPQ3(1)-(RAYLQ3(3)*COEFF(3)+RAYLQ3(4)*COEFF(4))
```

```
      X1(2)=OPI1(2)-RAYLI1(5)*COEFF(5)
      Y1(2)=OPQ1(2)-RAYLQ1(5)*COEFF(5)
      X2(2)=OPI2(2)-RAYLI2(5)*COEFF(5)
      Y2(2)=OPQ2(2)-RAYLQ2(5)*COEFF(5)
      X3(2)=OPI3(2)-RAYLI3(5)*COEFF(5)
      Y3(2)=OPQ3(2)-RAYLQ3(5)*COEFF(5)
      RAYLI1(5)=X1(2)
      RAYLQ1(5)=Y1(2)
      RAYLI2(5)=X2(2)
      RAYLQ2(5)=Y2(2)
      RAYLI3(5)=X3(2)
      RAYLQ3(5)=Y3(2)
      X1(2)=X1(2)*DCGAIN
      Y1(2)=Y1(2)*DCGAIN
      X2(2)=X2(2)*DCGAIN
      Y2(2)=Y2(2)*DCGAIN
      X3(2)=X3(2)*DCGAIN
      Y3(2)=Y3(2)*DCGAIN
      RAYLI1(4)=RAYLI1(3)
      RAYLI1(3)=OPI1(2)
      RAYLI1(2)=RAYLI1(1)
      RAYLI1(1)=OPI1(1)
      RAYLQ1(4)=RAYLQ1(3)
      RAYLQ1(3)=OPQ1(2)
      RAYLQ1(2)=RAYLQ1(1)
      RAYLQ1(1)=OPQ1(1)
      RAYLI2(4)=RAYLI2(3)
      RAYLI2(3)=OPI2(2)
      RAYLI2(2)=RAYLI2(1)
      RAYLI2(1)=OPI2(1)
      RAYLQ2(4)=RAYLQ2(3)
      RAYLQ2(3)=OPQ2(2)
      RAYLQ2(2)=RAYLQ2(1)
      RAYLQ2(1)=OPQ2(1)
      RAYLI3(4)=RAYLI3(3)
      RAYLI3(3)=OPI3(2)
      RAYLI3(2)=RAYLI3(1)
      RAYLI3(1)=OPI3(1)
      RAYLQ3(4)=RAYLQ3(3)
      RAYLQ3(3)=OPQ3(2)
      RAYLQ3(2)=RAYLQ3(1)
      RAYLQ3(1)=OPQ3(1)
40
C
C
      ILOP=100+ILOOPS
C
C
      DO 45 K=1,ILOP
      OPI1(1)=G05DDF(0.0,1.0)-(RAYLI1(1)*COEFF(1)+RAYLI1(2)*COEFF(2))
      OPQ1(1)=G05DDF(0.0,1.0)-(RAYLQ1(1)*COEFF(1)+RAYLQ1(2)*COEFF(2))
      OPI2(1)=G05DDF(0.0,1.0)-(RAYLI2(1)*COEFF(1)+RAYLI2(2)*COEFF(2))
      OPQ2(1)=G05DDF(0.0,1.0)-(RAYLQ2(1)*COEFF(1)+RAYLQ2(2)*COEFF(2))
      OPI3(1)=G05DDF(0.0,1.0)-(RAYLI3(1)*COEFF(1)+RAYLI3(2)*COEFF(2))
      OPQ3(1)=G05DDF(0.0,1.0)-(RAYLQ3(1)*COEFF(1)+RAYLQ3(2)*COEFF(2))
      OPI1(2)=OPI1(1)-(RAYLI1(3)*COEFF(3)+RAYLI1(4)*COEFF(4))
      OPQ1(2)=OPQ1(1)-(RAYLQ1(3)*COEFF(3)+RAYLQ1(4)*COEFF(4))
      OPI2(2)=OPI2(1)-(RAYLI2(3)*COEFF(3)+RAYLI2(4)*COEFF(4))
      OPQ2(2)=OPQ2(1)-(RAYLQ2(3)*COEFF(3)+RAYLQ2(4)*COEFF(4))
      OPI3(2)=OPI3(1)-(RAYLI3(3)*COEFF(3)+RAYLI3(4)*COEFF(4))
      OPQ3(2)=OPQ3(1)-(RAYLQ3(3)*COEFF(3)+RAYLQ3(4)*COEFF(4))
```

```
      X1(1)=OPI1(2)-RAYLI1(5)*COEFF(5)
      Y1(1)=OPQ1(2)-RAYLQ1(5)*COEFF(5)
      X2(1)=OPI2(2)-RAYLI2(5)*COEFF(5)
      Y2(1)=OPQ2(2)-RAYLQ2(5)*COEFF(5)
      X3(1)=OPI3(2)-RAYLI3(5)*COEFF(5)
      Y3(1)=OPQ3(2)-RAYLQ3(5)*COEFF(5)
      RAYLI1(5)=X1(1)
      RAYLQ1(5)=Y1(1)
      RAYLI2(5)=X2(1)
      RAYLQ2(5)=Y2(1)
      RAYLI3(5)=X3(1)
      RAYLQ3(5)=Y3(1)
      X1(1)=X1(1)*DCGAIN
      Y1(1)=Y1(1)*DCGAIN
      X2(1)=X2(1)*DCGAIN
      Y2(1)=Y2(1)*DCGAIN
      X3(1)=X3(1)*DCGAIN
      Y3(1)=Y3(1)*DCGAIN
      RAYLI1(4)=RAYLI1(3)
      RAYLI1(3)=OPI1(2)
      RAYLI1(2)=RAYLI1(1)
      RAYLI1(1)=OPI1(1)
      RAYLQ1(4)=RAYLQ1(3)
      RAYLQ1(3)=OPQ1(2)
      RAYLQ1(2)=RAYLQ1(1)
      RAYLQ1(1)=OPQ1(1)
      RAYLI2(4)=RAYLI2(3)
      RAYLI2(3)=OPI2(2)
      RAYLI2(2)=RAYLI2(1)
      RAYLI2(1)=OPI2(1)
      RAYLQ2(4)=RAYLQ2(3)
      RAYLQ2(3)=OPQ2(2)
      RAYLQ2(2)=RAYLQ2(1)
      RAYLQ2(1)=OPQ2(1)
      RAYLI3(4)=RAYLI3(3)
      RAYLI3(3)=OPI3(2)
      RAYLI3(2)=RAYLI3(1)
      RAYLI3(1)=OPI3(1)
      RAYLQ3(4)=RAYLQ3(3)
      RAYLQ3(3)=OPQ3(2)
      RAYLQ3(2)=RAYLQ3(1)
      RAYLQ3(1)=OPQ3(1)
      RAY1(K)=X1(1)
      RAY2(K)=Y1(1)
      RAY3(K)=X2(1)
      RAY4(K)=Y2(1)
      RAY5(K)=X3(1)
   45 RAY6(K)=Y3(1)
C
C
      DO 64 J=1,IMP1
      DO 64 I=1,4
      R(I,J)=0.0
   64 Q(I,J)=0.0
      IQ=50
      CALL G05CBF(IQ)
      DO 480 I=2,60
      NSYM=INT(G05DAF(1.0,16.9999999999999))
      SSR(I)=XSR(NSYM)*SCALE
  480 SSQ(I)=XSQ(NSYM)*SCALE
      DO 482 I=1,30
      ANOIR(I)=G05DDF(AMEAN,SIGMA)
  482 ANOIQ(I)=G05DDF(AMEAN,SIGMA)
```

```
      DO  400  IRUN=1,ILOP
      X1(1)=RAY1(IRUN)
      Y1(1)=RAY2(IRUN)
      X2(1)=RAY3(IRUN)
      Y2(1)=RAY4(IRUN)
      X3(1)=RAY5(IRUN)
      Y3(1)=RAY6(IRUN)
      CONST1=(X1(1)-X1(2))*STIP
      CONST2=(Y1(1)-Y1(2))*STIP
      CONST3=(X2(1)-X2(2))*STIP
      CONST4=(Y2(1)-Y2(2))*STIP
      CONST5=(X3(1)-X3(2))*STIP
      CONST6=(Y3(1)-Y3(2))*STIP
C
C
   68 DO  200  ISYM=1,ISTEP
      DO  305  I=1,IMP1
      R(1,I)=0.0
  305 Q(1,I)=0.0
      K=ISYM-1
      AINCR=K*CONST1
      BINCR=K*CONST2
      DO  310  I=1,IMPL
      R(1,I)=CI(I)*(X1(2)+AINCR-Y1(2)-BINCR)-CQ(I)*(Y1(2)+BINCR+X1(2)+AI
     1NCR)
  310 Q(1,I)=CI(I)*(X1(2)+AINCR+Y1(2)+BINCR)+CQ(I)*(X1(2)+AINCR-Y1(2)-BI
     1NCR)
      AINCR=K*CONST5
      BINCR=K*CONST6
      DO  345  I=1,IMPL
      R(1,I+IDEL1)=R(1,I+IDEL1)+CID1(I)*(X3(2)+AINCR-Y3(2)-
     1 BINCR)-CQD1(I)*(Y3(2)+BINCR+X3(2)+AINCR)
  345  Q(1,I+IDEL1)=Q(1,I+IDEL1)+CID1(I)*(Y3(2)+BINCR+X3(2)+
     1 AINCR)+CQD1(I)*(X3(2)+AINCR-Y3(2)-BINCR)
      AINCR=K*CONST3
      BINCR=K*CONST4
      DO  330  I=1,IMPL
      R(1,I+IDEL)=R(1,I+IDEL)+CID2(I)*(X2(2)+AINCR-Y2(2)-BINCR)-
     1 CQD2(I)*(Y2(2)+BINCR+X2(2)+AINCR)
  330  Q(1,I+IDEL)=Q(1,I+IDEL)+CID2(I)*(Y2(2)+BINCR+X2(2)+AINCR)+
     1 CQD2(I)*(X2(2)+AINCR-Y2(2)-BINCR)
      DO  596  I=1,IMP1
      DO  596  J=1,IM1
      TI(I,IMP1+1-J)=TI(I,IMP1-J)
  596  TQ(I,IMP1+1-J)=TQ(I,IMP1-J)
  590  DO  600  I=1,IMP1
      TI(I,1)=(Q(1,I)+R(1,I))*0.5
  600  TQ(I,1)=(Q(1,I)-R(1,I))*0.5
      DO  406  I=1,IMPR
      ANOIR(IMPP-I)=ANOIR(IMPRP-I)
  406  ANOIQ(IMPP-I)=ANOIQ(IMPRP-I)
      ANOIR(1)=G05DDF(AMEAN,SIGMA)
      ANOIQ(1)=G05DDF(AMEAN,SIGMA)
      CORNR=0.0
      CORNQ=0.0
      DO  408  I=1,IMPR
      CORNR=CORNR+ANOIR(I)*WSI(I)-ANOIQ(I)*WSQ(I)
  408  CORNQ=CORNQ+ANOIQ(I)*WSI(I)+ANOIR(I)*WSQ(I)
      POS=-POS
      IF(POS.LT.0.0)GO TO 200
```

```
      DO 597 I=1,IMPR
      DO 597 J=1,49
      HIT(I,51-J)=HIT(I,50-J)
597   HQT(I,51-J)=HQT(I,50-J)
      IO=0
      DO 2010 I=1,IMP1,2
      IO=IO+1
      HIT(IO,1)=0.0
      HQT(IO,1)=0.0
      DO 2000 J=1,I
      HIT(IO,1)=HIT(IO,1)+TI(J,I+1-J)*CRI(I+1-J)-TQ(J,I+1-J)*CRQ(I+1-J)
2000  HQT(IO,1)=HQT(IO,1)+TQ(J,I+1-J)*CRI(I+1-J)+TI(J,I+1-J)*CRQ(I+1-J)
      HIT(IO,1)=HIT(IO,1)*2.0 8333333E-4
2010  HQT(IO,1)=HQT(IO,1)*2.0 8333333E-4
      DO 2030 I=1,IM1,2
      IO=IO+1
      HIT(IO,1)=0.0
      HQT(IO,1)=0.0
      K=1+I
      DO 2020 J=K,IMP1
      HIT(IO,1)=HIT(IO,1)+TI(J,IMP1+1+I-J)*CRI(IMP1+1+I-J)-TQ(J,IMP1+1+I
     1-J)*CRQ(IMP1+1+I-J)
2020  HQT(IO,1)=HQT(IO,1)+TQ(J,IMP1+1+I-J)*CRI(IMP1+1+I-J)+TI(J,IMP1+1+I
     1-J)*CRQ(IMP1+1+I-J)
      HIT(IO,1)=HIT(IO,1)*2.0 8333333E-4
2030  HQT(IO,1)=HQT(IO,1)*2.0 8333333E-4
      IF(IRUN.EQ.K2.AND.ISYM.LT.95) GO TO 200
      IF(IRUN.EQ.K2.AND.ISYM.EQ.95) GO TO 202
      IF(IRUN.LT.K1) GO TO 200
      IF(IRUN.EQ.K1.AND.ISYM.LT.95) GO TO 200
      IF(IRUN.EQ.K1.AND.ISYM.EQ.95) GO TO 206
      IF(IRUN.EQ.KM1.AND.ISYM.EQ.63)GO TO 750
      IF(IRUN.LT.K0) GO TO 200
      IF(IRUN.EQ.K0.AND.ISYM.LT.95) GO TO 200
      IF(IRUN.EQ.K0.AND.ISYM.EQ.95) GO TO 210
      IF(IRUN.EQ.K01.AND.ISYM.LE.SDEL1) GO TO 402
      IF(IRUN.GE.K01) GO TO 412
C
CC*****************************************************************************
C
C     STARTING-UP PROCEDURE
C
CC*****************************************************************************
C
C
202   DO 204 I=1,IMPR
      YM2KR(I)=HIT(I,1)
204   YM2KQ(I)=HQT(I,1)
      WRITE(2,203) (YM2KR(I),I=1,IMPR)
      WRITE(2,205) (YM2KQ(I),I=1,IMPR)
      GO TO 200
C
C
206   DO 208 I=1,IMPR
      YM1KR(I)=HIT(I,1)
208   YM1KQ(I)=HQT(I,1)
      WRITE(2,207) (YM1KR(I),I=1,IMPR)
      WRITE(2,209) (YM1KQ(I),I=1,IMPR)
      GO TO 200
C
```

```
C
750     DO 752 I=1,IMPR
        YMLR(I)=HIT(I,1)
752     YMLQ(I)=HQT(I,1)
        WRITE(2,754) (YMLR(I),I=1,IMPR)
        WRITE(2,755) (YMLQ(I),I=1,IMPR)
        GO TO 200
C
C
210     DO 212 I=1,IMPR
        YNOTR(I)=HIT(I,1)
212     YNOTQ(I)=HQT(I,1)
        WRITE(2,211) (YNOTR(I),I=1,IMPR)
        WRITE(2,213) (YNOTQ(I),I=1,IMPR)
C
C
        ANM1R=0.0
        ANM1Q=0.0
        ANM2R=0.0
        ANM2Q=0.0
        ANM3R=0.0
        ANM3Q=0.0
        DO 214 I=1,IMPR
        ANM1R=ANM1R+YM2KR(I)*YNOTR(I)+YM2KQ(I)*YNOTQ(I)
        ANM1Q=ANM1Q+YM2KQ(I)*YNOTR(I)-YM2KR(I)*YNOTQ(I)
        ANM2R=ANM2R+YM1KR(I)*YNOTR(I)+YM1KQ(I)*YNOTQ(I)
        ANM2Q=ANM2Q+YM1KQ(I)*YNOTR(I)-YM1KR(I)*YNOTQ(I)
        ANM3R=ANM3R+YM2KR(I)*YM1KR(I)+YM2KQ(I)*YM1KQ(I)
214     ANM3Q=ANM3Q+YM2KQ(I)*YM1KR(I)-YM2KR(I)*YM1KQ(I)
        DEN11=0.0
        DEN12=0.0
        DEN21=0.0
        DO 216 I=1,IMPR
        DEN11=DEN11+YM2KR(I)**2+YM2KQ(I)**2
        DEN12=DEN12+YNOTR(I)**2+YNOTQ(I)**2
216     DEN21=DEN21+YM1KR(I)**2+YM1KQ(I)**2
        ANGL1=((ANM1R**2+ANM1Q**2)/(DEN11*DEN12))**0.5
        ANGL2=((ANM2R**2+ANM2Q**2)/(DEN21*DEN12))**0.5
        ANGL3=((ANM3R**2+ANM3Q**2)/(DEN11*DEN21))**0.5
        ANGL1=(180.0*7.0*ACOS(ANGL1))/22.0
        ANGL2=(180.0*7.0*ACOS(ANGL2))/22.0
        ANGL3=(180.0*7.0*ACOS(ANGL3))/22.0
        WRITE(2,218) ANGL1,ANGL2,ANGL3
        IF(DEN11) 220,222,220
222     Y2KM=0.0
        GO TO 224
220     Y2KM=1.0/DEN11**0.5
224     DO 226 I=1,IMPR
        AR(I)=Y2KM*YM2KR(I)
226     AQ(I)=Y2KM*YM2KQ(I)
        WRITE(2,225) (AR(I),I=1,IMPR)
        WRITE(2,227) (AQ(I),I=1,IMPR)
        YKR=0.0
        YKQ=0.0
        DO 228 I=1,IMPR
        YKR=YKR+YM1KR(I)*AR(I)+YM1KQ(I)*AQ(I)
228     YKQ=YKQ+YM1KQ(I)*AR(I)-YM1KR(I)*AQ(I)
        DO 230 I=1,IMPR
        BR(I)=YM1KR(I)-(YKR*AR(I)-YKQ*AQ(I))
230     BQ(I)=YM1KQ(I)-(YKQ*AR(I)+YKR*AQ(I))
```

```
      BMAG=0.0
      DO  232 I=1,IMPR
232   BMAG=BMAG+BR(I)**2+BQ(I)**2
      BMAG=SQRT(BMAG)
      IF(BMAG) 234,236,234
236   BMAG=0.0
      GO TO 238
234   BMAG=1.0/BMAG
238   DO  240 I=1,IMPR
      BR(I)=BMAG*BR(I)
240   BQ(I)=BMAG*BQ(I)
      WRITE(2,241)  (BR(I),I=1,IMPR)
      WRITE(2,243)  (BQ(I),I=1,IMPR)
      YNBR=0.0
      YNBQ=0.0
      YNAR=0.0
      YNAQ=0.0
      DO  242 I=1,IMPR
      YNBR=YNBR+YNOTR(I)*BR(I)+YNOTQ(I)*BQ(I)
      YNBQ=YNBQ+YNOTQ(I)*BR(I)-YNOTR(I)*BQ(I)
      YNAR=YNAR+YNOTR(I)*AR(I)+YNOTQ(I)*AQ(I)
242   YNAQ=YNAQ+YNOTQ(I)*AR(I)-YNOTR(I)*AQ(I)
      DO  244 I=1,IMPR
      CCR(I)=YNOTR(I)-(YNBR*BR(I)-YNBQ*BQ(I))-(YNAR*AR(I)-YNAQ*AQ(I))
244   CCQ(I)=YNOTQ(I)-(YNBQ*BR(I)+YNBR*BQ(I))-(YNAQ*AR(I)+YNAR*AQ(I))
      CMAG=0.0
      DO  246 I=1,IMPR
246   CMAG=CMAG+CCR(I)**2+CCQ(I)**2
      CMAG=SQRT(CMAG)
      IF(CMAG) 247,248,247
248   CMAG=0.0
      GO TO 250
247   CMAG=1.0/CMAG
250   DO  252 I=1,IMPR
      CCR(I)=CMAG*CCR(I)
252   CCQ(I)=CMAG*CCQ(I)
      WRITE(2,251)  (CCR(I),I=1,IMPR)
      WRITE(2,253)  (CCQ(I),I=1,IMPR)
      AMAG=0.0
      BMAG=0.0
      CMAG=0.0
      DO  254 I=1,IMPR
      AMAG=AMAG+AR(I)**2+AQ(I)**2
      BMAG=BMAG+BR(I)**2+BQ(I)**2
254   CMAG=CMAG+CCR(I)**2+CCQ(I)**2
      AMAG=SQRT(AMAG)
      BMAG=SQRT(BMAG)
      CMAG=SQRT(CMAG)
      WRITE(2,255)  AMAG,BMAG,CMAG
      XBAR=0.0
      XBAQ=0.0
      XCAR=0.0
      XCAQ=0.0
      XBCR=0.0
      XBCQ=0.0
      DO  484 I=1,IMPR
      XBAR=XBAR+BR(I)*AR(I)+BQ(I)*AQ(I)
      XBAQ=XBAQ+BQ(I)*AR(I)-BR(I)*AQ(I)
      XCAR=XCAR+CCR(I)*AR(I)+CCQ(I)*AQ(I)
      XCAQ=XCAQ+CCQ(I)*AR(I)-CCR(I)*AQ(I)
      XBCR=XBCR+BR(I)*CCR(I)+BQ(I)*CCQ(I)
484   XBCQ=XBCQ+BQ(I)*CCR(I)-BR(I)*CCQ(I)
      WRITE(2,486)  XBAR,XBAQ,XCAR,XCAQ,XBCR,XBCQ
```

```
      YNCR=0.0
      YNCQ=0.0
      DO 256 I=1,IMPR
      YNCR=YNCR+YNOTR(I)*CCR(I)+YNOTQ(I)*CCQ(I)
  256 YNCQ=YNCQ+YNOTQ(I)*CCR(I)-YNOTR(I)*CCQ(I)
      ALR=YNAR
      ALQ=YNAQ
      BBER=YNBR
      BBEQ=YNBQ
      GAMR=YNCR
      GAMQ=YNCQ
      ALMLR=0.0
      ALMLQ=0.0
      BBMLR=0.0
      BBMLQ=0.0
      GAMLR=0.0
      GAMLQ=0.0
      DO 760 I=1,IMPR
      ALMLR=ALMLR+YMLR(I)*AR(I)+YMLQ(I)*AQ(I)
      ALMLQ=ALMLQ+YMLQ(I)*AR(I)-YMLR(I)*AQ(I)
      BBMLR=BBMLR+YMLR(I)*BR(I)+YMLQ(I)*BQ(I)
      BBMLQ=BBMLQ+YMLQ(I)*BR(I)-YMLR(I)*BQ(I)
      GAMLR=GAMLR+YMLR(I)*CCR(I)+YMLQ(I)*CCQ(I)
  760 GAMLQ=GAMLQ+YMLQ(I)*CCR(I)-YMLR(I)*CCQ(I)
      XXAPR=(ALR-ALMLR)/XL
      XXAPQ=(ALQ-ALMLQ)/XL
      XXBPR=(BBER-BBMLR)/XL
      XXBPQ=(BBEQ-BBMLQ)/XL
      XXGPR=(GAMR-GAMLR)/XL
      XXGPQ=(GAMQ-GAMLQ)/XL
      PALR=YNAR+XXAPR
      PALQ=YNAQ+XXAPQ
      PBBER=YNBR+XXBPR
      PBBEQ=YNBQ+XXBPQ
      PGAMR=YNCR+XXGPR
      PGAMQ=YNCQ+XXGPQ
      DO 258 I=1,IMPR
      FR(I)=(ALR*AR(I)-ALQ*AQ(I))+(BBER*BR(I)-BBEQ*BQ(I))
     *                            +(GAMR*CCR(I)-GAMQ*CCQ(I))
  258 FQ(I)=(ALQ*AR(I)+ALR*AQ(I))+(BBEQ*BR(I)+BBER*BQ(I))
     *                            +(GAMQ*CCR(I)+GAMR*CCQ(I))
      DO 260 I=1,IMPR
      ERRR(I)=YNOTR(I)-FR(I)
  260 ERRQ(I)=YNOTQ(I)-FQ(I)
      DO 262 I=1,IMPR
      AR(I)=AR(I)+ETA*(ALR*ERRR(I)+ALQ*ERRQ(I))
      AQ(I)=AQ(I)+ETA*(ALR*ERRQ(I)-ALQ*ERRR(I))
      BR(I)=BR(I)+ETA*(BBER*ERRR(I)+BBEQ*ERRQ(I))
      BQ(I)=BQ(I)+ETA*(BBER*ERRQ(I)-BBEQ*ERRR(I))
      CCR(I)=CCR(I)+ETA*(GAMR*ERRR(I)+GAMQ*ERRQ(I))
  262 CCQ(I)=CCQ(I)+ETA*(GAMR*ERRQ(I)-GAMQ*ERRR(I))
      AMAG=0.0
      DO 264 I=1,IMPR
  264 AMAG=AMAG+AR(I)**2+AQ(I)**2
      AMAG=SQRT(AMAG)
      IF(AMAG) 265,266,265
  266 AMAG=0.0
      GO TO 268
  265 AMAG=1.0/AMAG
  268 DO 270 I=1,IMPR
      AR(I)=AMAG*AR(I)
  270 AQ(I)=AMAG*AQ(I)
```

```
      BAR=0.0
      BAQ=0.0
      DO 272 I=1,IMPR
      BAR=BAR+BR(I)*AR(I)+BQ(I)*AQ(I)
272   BAQ=BAQ+BQ(I)*AR(I)-BR(I)*AQ(I)
      DO 274 I=1,IMPR
      BR(I)=BR(I)-(BAR*AR(I)-BAQ*AQ(I))
274   BQ(I)=BQ(I)-(BAQ*AR(I)+BAR*AQ(I))
      BMAG=0.0
      DO 273 I=1,IMPR
273   BMAG=BMAG+BR(I)**2+BQ(I)**2
      IF(BMAG) 277,275,277
275   BMAG=0.0
      GO TO 276
277   BMAG=1.0/BMAG
276   DO 278 I=1,IMPR
      BR(I)=BMAG*BR(I)
278   BQ(I)=BMAG*BQ(I)
      CBR=0.0
      CBQ=0.0
      CAR=0.0
      CAQ=0.0
      DO 280 I=1,IMPR
      CBR=CBR+CCR(I)*BR(I)+CCQ(I)*BQ(I)
      CBQ=CBQ+CCQ(I)*BR(I)-CCR(I)*BQ(I)
      CAR=CAR+CCR(I)*AR(I)+CCQ(I)*AQ(I)
280   CAQ=CAQ+CCQ(I)*AR(I)-CCR(I)*AQ(I)
      DO 282 I=1,IMPR
      CCR(I)=CCR(I)-(CBR*BR(I)-CBQ*BQ(I))-(CAR*AR(I)-CAQ*AQ(I))
282   CCQ(I)=CCQ(I)-(CBQ*BR(I)+CBR*BQ(I))-(CAQ*AR(I)+CAR*AQ(I))
      CMAG=0.0
      DO 283 I=1,IMPR
283   CMAG=CMAG+CCR(I)**2+CCQ(I)**2
      CMAG=SQRT(CMAG)
      IF(CMAG) 284,285,284
285   CMAG=0.0
      GO TO 286
284   CMAG=1.0/CMAG
286   DO 288 I=1,IMPR
      CCR(I)=CMAG*CCR(I)
288   CCQ(I)=CMAG*CCQ(I)
      DO 290 I=1,IMPR
      YYR(I)=(PALR*AR(I)-PALQ*AQ(I))+(PBBER*BR(I)-PBBEQ*BQ(I))
     *                               +(GAMR*CCR(I)-GAMQ*CCQ(I))
290   YYQ(I)=(PALQ*AR(I)+PALR*AQ(I))+(PBBEQ*BR(I)+PBBER*BQ(I))
     *                               +(GAMQ*CCR(I)+GAMR*CCQ(I))
      WRITE(2,291) (YYR(I),I=1,IMPR)
      WRITE(2,292) (YYQ(I),I=1,IMPR)
      GO TO 200
C
CC
C
C*************************************************************************
C
C     SETTING-UP THE DELAY
C     DELAY = SDEL
C
C*************************************************************************
C
CC
C
```

```
 402    CONTINUE
        NSYM=INT(G05DAF(1.0,16.9999999999999))
        SSR(1)=XSR(NSYM)*SCALE
        SSQ(1)=XSQ(NSYM)*SCALE
        RRR(1)=0.0
        RRQ(1)=0.0
        DO  404 I=1,IMPR
        RRR(1)=RRR(1)+SSR(I)*HIT(I,1)-SSQ(I)*HQT(I,1)
 404    RRQ(1)=RRQ(1)+SSQ(I)*HIT(I,1)+SSR(I)*HQT(I,1)
        RRIN=RRR(1)**2+RRQ(1)**2
        RIN=RIN+RRIN
        RRR(1)=RRR(1)+CORNR
        RRQ(1)=RRQ(1)+CORNQ
        SSIN=SSR(1)**2+SSQ(1)**2
        RROT=RRR(1)**2+RRQ(1)**2
        SIN=SIN+SSIN
        ROT=ROT+RROT
        DO  410 I=1,59
        SSR(61-I)=SSR(60-I)
        SSQ(61-I)=SSQ(60-I)
        RRR(61-I)=RRR(60-I)
 410    RRQ(61-I)=RRQ(60-I)
        GO TO 200
C
C
C*****************************************************************
C
C       IMPROVED CHANNEL ESTIMATOR
C       NO. OF SKYWAVE = 3
C
C*****************************************************************
C
C
 412    CONTINUE
        IS=IS+1
        NSYM=INT(G05DAF(1.0,16.9999999999999))
        SSR(1)=XSR(NSYM)*SCALE
        SSQ(1)=XSQ(NSYM)*SCALE
        RRR(1)=0.0
        RRQ(1)=0.0
        DO  414 I=1,IMPR
        RRR(1)=RRR(1)+SSR(I)*HIT(I,1)-SSQ(I)*HQT(I,1)
 414    RRQ(1)=RRQ(1)+SSQ(I)*HIT(I,1)+SSR(I)*HQT(I,1)
        RRIN=RRR(1)**2+RRQ(1)**2
        RIN=RIN+RRIN
        RRR(1)=RRR(1)+CORNR
        RRQ(1)=RRQ(1)+CORNQ
        SSIN=SSR(1)**2+SSQ(1)**2
        RROT=RRR(1)**2+RRQ(1)**2
        SIN=SIN+SSIN
        ROT=ROT+RROT
        DO  420 I=1,IMPR
        SER(I)=SSR(I+SDEL)
 420    SEQ(I)=SSQ(I+SDEL)
        ZR=RRR(1+SDEL)
        ZQ=RRQ(1+SDEL)
        ZER=0.0
        ZEQ=0.0
        DO  422 I=1,IMPR
        ZER=ZER+SER(I)*YYR(I)-SEQ(I)*YYQ(I)
 422    ZEQ=ZEQ+SEQ(I)*YYR(I)+SER(I)*YYQ(I)
        ER=ZR-ZER
        EQ=ZQ-ZEQ
```

```
      DO  424 I=1,IMPR
      YYR(I)=YYR(I)+C*(ER*SER(I)+EQ*SEQ(I))
424   YYQ(I)=YYQ(I)+C*(EQ*SER(I)-ER*SEQ(I))
      SQ=0.0
      DO  25 I=1,IMPR
25    SQ=SQ+(HIT(I,1+SDEL)-YYR(I))**2+(HQT(I,1+SDEL)-YYQ(I))**2
      ALR=0.0
      ALQ=0.0
      BBER=0.0
      BBEQ=0.0
      GAMR=0.0
      GAMQ=0.0
      DO  426 I=1,IMPR
      ALR=ALR+YYR(I)*AR(I)+YYQ(I)*AQ(I)
      ALQ=ALQ+YYQ(I)*AR(I)-YYR(I)*AQ(I)
      BBER=BBER+YYR(I)*BR(I)+YYQ(I)*BQ(I)
      BBEQ=BBEQ+YYQ(I)*BR(I)-YYR(I)*BQ(I)
      GAMR=GAMR+YYR(I)*CCR(I)+YYQ(I)*CCQ(I)
426   GAMQ=GAMQ+YYQ(I)*CCR(I)-YYR(I)*CCQ(I)
      DO  428 I=1,IMPR
      FR(I)=(ALR*AR(I)-ALQ*AQ(I))+(BBER*BR(I)-BBEQ*BQ(I))
     *                            +(GAMR*CCR(I)-GAMQ*CCQ(I))
428   FQ(I)=(ALQ*AR(I)+ALR*AQ(I))+(BBEQ*BR(I)+BBER*BQ(I))
     *                            +(GAMQ*CCR(I)+GAMR*CCQ(I))
      DO  430 I=1,IMPR
      ERRR(I)=YYR(I)-FR(I)
430   ERRQ(I)=YYQ(I)-FQ(I)
      DO  432 I=1,IMPR
      AR(I)=AR(I)+ETA*(ALR*ERRR(I)+ALQ*ERRQ(I))
      AQ(I)=AQ(I)+ETA*(ALR*ERRQ(I)-ALQ*ERRR(I))
      BR(I)=BR(I)+ETA*(BBER*ERRR(I)+BBEQ*ERRQ(I))
      BQ(I)=BQ(I)+ETA*(BBER*ERRQ(I)-BBEQ*ERRR(I))
      CCR(I)=CCR(I)+ETA*(GAMR*ERRR(I)+GAMQ*ERRQ(I))
432   CCQ(I)=CCQ(I)+ETA*(GAMR*ERRQ(I)-GAMQ*ERRR(I))
      AMAG=0.0
      DO  434 I=1,IMPR
434   AMAG=AMAG+AR(I)**2+AQ(I)**2
      AMAG=SQRT(AMAG)
      IF(AMAG) 433,435,433
435   AMAG=0.0
      GO TO  436
433   AMAG=1.0/AMAG
436   DO  438 I=1,IMPR
      AR(I)=AMAG*AR(I)
438   AQ(I)=AMAG*AQ(I)
      BAR=0.0
      BAQ=0.0
      DO  440 I=1,IMPR
      BAR=BAR+BR(I)*AR(I)+BQ(I)*AQ(I)
440   BAQ=BAQ+BQ(I)*AR(I)-BR(I)*AQ(I)
      DO  442 I=1,IMPR
      BR(I)=BR(I)-(BAR*AR(I)-BAQ*AQ(I))
442   BQ(I)=BQ(I)-(BAQ*AR(I)+BAR*AQ(I))
      BMAG=0.0
      DO  444 I=1,IMPR
444   BMAG=BMAG+BR(I)**2+BQ(I)**2
      IF(BMAG) 443,445,443
445   BMAG=0.0
      GO TO  446
443   BMAG=1.0/BMAG
446   DO  448 I=1,IMPR
      BR(I)=BMAG*BR(I)
448   BQ(I)=BMAG*BQ(I)
```

```
      CBR=0.0
      CBQ=0.0
      CAR=0.0
      CAQ=0.0
      DO 450 I=1,IMPR
      CBR=CBR+CCR(I)*BR(I)+CCQ(I)*BQ(I)
      CBQ=CBQ+CCQ(I)*BR(I)-CCR(I)*BQ(I)
      CAR=CAR+CCR(I)*AR(I)+CCQ(I)*AQ(I)
450   CAQ=CAQ+CCQ(I)*AR(I)-CCR(I)*AQ(I)
      DO 452 I=1,IMPR
      CCR(I)=CCR(I)-(CBR*BR(I)-CBQ*BQ(I))-(CAR*AR(I)-CAQ*AQ(I))
452   CCQ(I)=CCQ(I)-(CBQ*BR(I)+CBR*BQ(I))-(CAQ*AR(I)+CAR*AQ(I))
      CMAG=0.0
      DO 454 I=1,IMPR
454   CMAG=CMAG+CCR(I)**2+CCQ(I)**2
      CMAG=SQRT(CMAG)
      IF(CMAG) 453,455,453
455   CMAG=0.0
      GO TO 456
453   CMAG=1.0/CMAG
456   DO 458 I=1,IMPR
      CCR(I)=CMAG*CCR(I)
458   CCQ(I)=CMAG*CCQ(I)
      ERRAR=ALR-PALR
      ERRAQ=ALQ-PALQ
      ERRBR=BBER-PBBER
      ERRBQ=BBEQ-PBBEQ
      ERRGR=GAMR-PGAMR
      ERRGQ=GAMQ-PGAMQ
      XXAPR=XXAPR+THETA1*ERRAR
      XXAPQ=XXAPQ+THETA1*ERRAQ
      XXBPR=XXBPR+THETA1*ERRBR
      XXBPQ=XXBPQ+THETA1*ERRBQ
      XXGPR=XXGPR+THETA1*ERRGR
      XXGPQ=XXGPQ+THETA1*ERRGQ
      PALR=PALR+XXAPR+THETA2*ERRAR
      PALQ=PALQ+XXAPQ+THETA2*ERRAQ
      PBBER=PBBER+XXBPR+THETA2*ERRBR
      PBBEQ=PBBEQ+XXBPQ+THETA2*ERRBQ
      PGAMR=PGAMR+XXGPR+THETA2*ERRGR
      PGAMQ=PGAMQ+XXGPQ+THETA2*ERRGQ
      DO 460 I=1,IMPR
      YYR(I)=(PALR*AR(I)-PALQ*AQ(I))+(PBBER*BR(I)-PBBEQ*BQ(I))
     *                               +(PGAMR*CCR(I)-PGAMQ*CCQ(I))
460   YYQ(I)=(PALQ*AR(I)+PALR*AQ(I))+(PBBEQ*BR(I)+PBBER*BQ(I))
     *                               +(PGAMQ*CCR(I)+PGAMR*CCQ(I))
      PALNR=PALR+(SDEL-1.0)*XXAPR
      PALNQ=PALQ+(SDEL-1.0)*XXAPQ
      PBENR=PBBER+(SDEL-1.0)*XXBPR
      PBENQ=PBBEQ+(SDEL-1.0)*XXBPQ
      PGANR=PGAMR+(SDEL-1.0)*XXGPR
      PGANQ=PGAMQ+(SDEL-1.0)*XXGPQ
      DO 462 I=1,IMPR
      YYPR(I)=(PALNR*AR(I)-PALNQ*AQ(I))+(PBENR*BR(I)-PBENQ*BQ(I))
     *                                  +(PGANR*CCR(I)-PGANQ*CCQ(I))
462   YYPQ(I)=(PALNQ*AR(I)+PALNR*AQ(I))+(PBENQ*BR(I)+PBENR*BQ(I))
     *                                  +(PGANQ*CCR(I)+PGANR*CCQ(I))
```

```
      SQE1=0.0
      SQEN=0.0
      DO  464 I=1,IMPR
      SQE1=SQE1+(HIT(I,SDEL)-YYR(I))**2+(HQT(I,SDEL)-YYQ(I))**2
 464  SQEN=SQEN+(HIT(I,1)-YYPR(I))**2+(HQT(I,1)-YYPQ(I))**2
      SQEL1=10.0*ALOG10(SQE1)
      SQELN=10.0*ALOG10(SQEN)
      IF(IRUN-100)774,774,775
 774  TSQI1=TSQI1+SQE1
      TSQIN=TSQIN+SQEN
      TSQI=TSQI+SQ
      GO TO 776
 775  TSQE1=TSQE1+SQE1
      TSQEN=TSQEN+SQEN
      TSQ=TSQ+SQ
 776  CONTINUE
 466  DO  468 I=1,59
      SSR(61-I)=SSR(60-I)
      SSQ(61-I)=SSQ(60-I)
      RRR(61-I)=RRR(60-I)
 468  RRQ(61-I)=RRQ(60-I)
  200 CONTINUE
C
C
      X1(2)=X1(1)
      Y1(2)=Y1(1)
      X2(2)=X2(1)
      Y2(2)=Y2(1)
      X3(2)=X3(1)
      Y3(2)=Y3(1)
  400 CONTINUE
C
C
      AVM1=TSQE1/FLOAT((ISTEP*ILOOPS)/2)
      AVMN=TSQEN/FLOAT((ISTEP*ILOOPS)/2)
      AV=TSQ/FLOAT((ISTEP*ILOOPS)/2)
      AVIN1=TSQI1/FLOAT((ISTEP*(100-K0))/2)
      AVINN=TSQIN/FLOAT((ISTEP*(100-K0))/2)
      AVI=TSQI/FLOAT((ISTEP*(100-K0))/2)
      AVL=10.0*ALOG10(AV)
      AVIL=10.0*ALOG10(AVI)
      AVI1L=10.0*ALOG10(AVIN1)
      AVINL=10.0*ALOG10(AVINN)
      AVM1L=10.0*ALOG10(AVM1)
      AVMNL=10.0*ALOG10(AVMN)
      SIN=SIN/FLOAT((ISTEP*(ILOOPS+(100-K0)))/2)
      ROT=ROT/FLOAT((ISTEP*(ILOOPS+(100-K0)))/2)
      RIN=RIN/FLOAT((ISTEP*(ILOOPS+(100-K0)))/2)
      WRITE(2,26) AVL
      WRITE(2,27)AVIL
      WRITE(2,779) AVI1L
      WRITE(2,780) AVINL
      WRITE(2,470) AVM1L
      WRITE(2,471) AVMNL
      WRITE(2,472) SIN
      WRITE(2,772) RIN
      WRITE(2,473) ROT
      WRITE(2,474) C
      WRITE(2,475) THETA
      WRITE(2,476) ETA
      WRITE(2,477) SDEL
 700  CONTINUE
```

```
      WRITE(2,3000) (CI(I),I=1,16)
      WRITE(2,3001) (CQ(I),I=1,16)
      WRITE(2,3002)(CID1(I),I=1,16)
      WRITE(2,3003)(CQD1(I),I=1,16)
      WRITE(2,3020)(CID2(I),I=1,16)
      WRITE(2,3021)(CQD2(I),I=1,16)
      WRITE(2,3022)(CRI(I),I=1,30)
      WRITE(2,3023)(CRQ(I),I=1,30)
      WRITE(2,3024)(WSI(I),I=1,30)
      WRITE(2,3025)(WSQ(I),I=1,30)
      WRITE(2,3004) IXX,IQ
      WRITE(2,3005)DEL1,DEL
      WRITE(2,3006) (COEFF(I),I=1,5)
      DCGAIN=1.0/DCGAIN
      WRITE(2,3008) DCGAIN
      WRITE(2,3010) K2,K1,KM1,K0,K01,XL
      WRITE(2,3012) ILOOPS
      IF(SIGMA.EQ.0.0) GO TO 770
      SNR=10.0*ALOG10(1.0/(SIGMA**2))
      WRITE(2,791) SNR
  770 CONTINUE
C
C
 2060 FORMAT(///,1H ,'IMPROVED CHANNEL ESTIMATOR')
 2070 FORMAT(1H ,'3-SKYWAVE MODEL - CHANNEL 3',///)
 3000 FORMAT(1H ,'CI',/,2(10F12.7/))
 3001 FORMAT(1H ,'CQ',/,2(10F12.7/))
 3002 FORMAT(1H ,'CID1',/,2(10F12.7/))
 3003 FORMAT(1H ,'CQD1',/,2(10F12.7/))
 3020 FORMAT(1H ,'CID2',/,2(10F12.7/))
 3021 FORMAT(1H ,'CQD2',/,2(10F12.7/))
 3022 FORMAT(1H ,'CRI',/,3(10F12.7/))
 3023 FORMAT(1H ,'CRQ',/,3(10F12.7/))
 3024 FORMAT(1H ,'WSI',/,3(10F12.7/))
 3025 FORMAT(1H ,'WSQ',/,3(10F12.7/))
 3004 FORMAT(1H ,'IXX = ',I4,',  IQ = ',I4)
 3005 FORMAT(1H ,'DEL1 = ',F15.10,'   DEL = ',F15.10)
 3006 FORMAT(1H ,'COEFF = ',5F13.7)
  203 FORMAT(1H ,'REAL PART OF Y(-2K)',/,3(10F10.6/))
  205 FORMAT(1H ,'IMAGINARY PART OF Y(-2K)',/,3(10F10.6/))
  207 FORMAT(1H ,'REAL PART OF Y(-K)',/,3(10F10.6/))
  209 FORMAT(1H ,'IMAGINARY PART OF Y(-K)',/,3(10F10.6/))
  754 FORMAT(1H ,'REAL PART OF Y(-L)',/,3(10F10.6/))
  755 FORMAT(1H ,'IMAGINARY PART OF Y(-L)',/,3(10F10.6/))
  211 FORMAT(1H ,'REAL PART OF Y(0)',/,3(10F10.6/))
  213 FORMAT(1H ,'IMAGINARY PART OF Y(0)',/,3(10F10.6/))
  218 FORMAT(1H ,'ANGLE BETWEEN Y(-2K) & Y(0)   = ',F7.3,' DEGREES',/,
     *           ' ANGLE BETWEEN Y(-K) & Y(0)    = ',F7.3,' DEGREES',/,
     &           ' ANGLE BETWEEN Y(-2K) & Y(-K) = ',F7.3,' DEGREES')
  225 FORMAT(1H ,'REAL PART OF A(0)',/,3(10F10.6/))
  227 FORMAT(1H ,'IMAGINARY PART OF A(0)',/,3(10F10.6/))
  241 FORMAT(1H ,'REAL PART OF B(0)',/,3(10F10.6/))
  243 FORMAT(1H ,'IMAGINARY PART OF B(0)',/,3(10F10.6/))
  251 FORMAT(1H ,'REAL PART OF C(0)',/,3(10F10.6/))
  253 FORMAT(1H ,'IMAGINARY PART OF C(0)',/,3(10F10.6/))
  255 FORMAT(1H ,'AMAG = ',F10.5,' BMAG = ',F10.5,' CMAG =',F10.5)
  291 FORMAT(1H ,'REAL PART OF Y(1,0)',/,3(10F10.6/))
  292 FORMAT(1H ,'IMAGINARY PART OF Y(1,0)',/,3(10F10.6/))
  467 FORMAT(1H ,'IS = ',I6,'  L-1STEP = ',F15.8,'  L-NSTEP = ',F15.8)
   27 FORMAT(1H ,'AVERAGE LAMBDA (TRAINING PERIOD) = ',F15.8)
  779 FORMAT(1H ,'AVERAGE L-1STEP (TRAINING PERIOD) = ',F15.8)
  780 FORMAT(1H ,'AVERAGE L-NSTEP (TRAINING PERIOD) = ',F15.8)
```

```
 26     FORMAT(1H ,'AVERAGE LAMBDA = ',F15.8)
470     FORMAT(1H ,'AVERAGE L-1STEP = ',F15.8)
471     FORMAT(1H ,'AVERAGE L-NSTEP = ',F15.8)
472     FORMAT(1H ,'INPUT SIGNAL ENERGY = ',F20.10)
772     FORMAT(1H ,'REC. SIG. ENERGY BEFORE NOISE ADDED = ',F20.10)
473     FORMAT(1H ,'OUTPUT SIGNAL ENERGY = ',F20.10)
474     FORMAT(1H ,'STEP SIZE FOR FEEDFORWARD ESTIMATOR, C = ',F10.5)
475     FORMAT(1H ,'PREDICTION CONSTANT, THETA = ',F10.5)
476     FORMAT(1H ,'PLANE UPDATE CONSTANT, ETA = ',F10.5)
477     FORMAT(1H ,'DELAY IN ESTIMATION = ',I4)
486     FORMAT(1H ,'B.A = ',F10.7,' +J',F10.7,
     *           '  C.A = ',F10.7,' +J',F10.7,
     $           '  B.C = ',F10.7,' +J',F10.7)
3008    FORMAT(1H ,'DCGAIN = ',F20.10)
3010    FORMAT(1H ,'-2K = ',I3,',  -K = ',I3,',  -L = ',I3,
     1 ',  0 = ',I3,',  01 = ',I3,',  L = ',F4.1)
791     FORMAT(1H ,'SNR = ',F20.10)
3012    FORMAT(1H ,'ILOOPS = ',I5)
C
C
        STOP
        END
```

REFERENCES

1. Clark, A.P.: 'Principles of digital data transmission', (Pentech Press, 1977).

2. Clark, A.P.: 'Advanced data-transmission systems', (Pentech Press, 1976).

3. Clark, A.P.: 'Adaptive detection of distorted digital signals', Radio and Electron. Eng., 1970, 40, pp. 107-119.

4. Clark, A.P.: 'A synchronous serial data-transmission system using orthogonal groups of binary signal-elements', IEEE Trans., 1971, COM-19, pp. 1101-1110.

5. Lucky, R.W., Salz, J., and Weldon, E.J.: 'Principles of data communication', (McGraw-Hill, 1968).

6. Bennett, W.R., and Davey, J.R.: 'Data transmission', (McGraw-Hill, 1965).

7. Sklar, B.: 'A structured overview of digital communications - a tutorial review - part 1', IEEE Communications Magazine, 1983, 21, pp. 4-17.

8. Qureshi, S.: 'Adaptive equalization', IEEE Communications Magazine, 1982, 20, pp. 9-16.

9. Clark, A.P., and Fairfield, M.J.: 'Detection processes for a 9600 bit/s modem', Radio & Electron. Eng., 1981, 51, pp. 455-465.

10. Clark, A.P., and Asghar, S.M.: 'Detection of digital signals transmitted over a known time-varying channel', IEE Proc. F, Commun. Radar & Signal Process., 1981, 128, pp. 167-174.

11. Mohammed, H.D.: 'Carrier phase predictors for high-speed data transmission systems', IEE Proc. F, Commun. Radar & Signal Process., 1983, 130, pp. 173-184.

12. Clark, A.P., and Harvey, J.D.: 'Detection of distorted QAM signals', Electronic Circuits and Systems, 1977, 1, pp. 103-109.

13. Akashi, F., Tatsui, N., Sato, Y., Koike, S., and Marumo, Y.: 'A high performance digital QAM 9600 bit/s modem', NEC Research & Develop., 1977, 45, pp. 38-48.

14. Hirosaki, B.: 'An analysis of automatic equalizers for orthogonally multiplexed QAM systems', IEEE Trans., 1980, COM-28, pp. 73-83.

15. Prabhu, V.K.: 'The detection efficiency of 16-ary QAM', Bell Syst. Tech. J., 1984, 59, pp. 639-656.

16. Najdi, H.Y.: 'Digital data transmission over voice channels', PhD Thesis, Dept. of Electronic & Electrical Eng., Loughborough Univ. of Technology, 1982.

17. Harvey, J.D.: 'Adaptive detection of digital suppressed-carrier A.M. signals', PhD Thesis, Dept. of Electronic & Electrical Eng., Loughborough Univ. of Technology, 1978.

18. Abend, K., Harley, T.J., Fritchman, B.D., and Gumacos, C.: 'On optimum receivers for channels having memory', IEEE Trans., 1968, IT-14, pp. 819-820.

19. Forney, G.D.: 'Maximum-likelihood sequence estimation of digital sequences in the presence of intersymbol interference', IEEE Trans., 1972, IT-18, pp. 363-378.

20. Forney, G.D.: 'The Viterbi algorithm', Proc. IEEE, 1973, 61, pp. 268-278.

21. Proakis, J.G.: 'Advances in equalization for intersymbol interference', in 'Advances in communication systems theory and applications', A.J. Viterbi (ed), 1975, 4, pp.123-198.

22. Clark, A.P., Harvey, J.D., and Driscoll, J.P.: 'Improved detection processes for distorted digital signals', IERE Conf. Proc. No. 37, 1977, pp. 125-136.

23. Clark, A.P., Harvey, J.D., and Driscoll, J.P.: 'Near-maximum likelihood detection processes for distorted digital signals', Radio & Electron. Eng., 1978, 48, pp. 301-309.

24. Foschini, G.J.: 'A reduced state variant of maximum likelihood sequence detection attaining optimum performance for high signal-to-noise ratios', IEEE Trans., 1977, IT-23, pp. 605-609.

25. Linder, J.: 'Identification of dispersive nonlinear systems with noisy outputs', in 'Signal processing: theories and applications', M. Kunt and F. de Coulon (eds), North-Holland, 1980, pp. 91-95.

26. Clark, A.P., Kwong, C.P., and McVerry, F.: 'Estimation of the sampled impulse-response of a channel', Signal Process., 1980, 2, pp. 39-53.

27. Magee, F.R., and Proakis, J.G.: 'Adaptive maximum-likelihood sequence estimation for digital signalling in the presence of intersymbol interference', IEEE Trans., 1973, IT-19, pp. 120-124.

28. Schwartz, M., and Shaw, L.: 'Signal processing - discrete spectral analysis, detection and estimation',(McGraw-Hill, 1975).

29. Kalman, R.E.: 'A new approach to linear and prediction problems', Trans. ASME J. Basic Eng., 1960, 82-D, pp. 34-45.

30. Kalman, R.E., and Bucy, R.S.: 'New results in linear filtering and prediction theory', Trans. ASME J. Basic Eng., 1961, 83-D, pp. 95-108.

31. Godard, D.: 'Channel equalization using a Kalman filter for fast data transmission', IBM J. Res. Develop., 1974, 18, pp. 267-273.

32. Young, P.C.: 'Recursive approaches to time series analysis', Bull. Inst. Math. Appl., 1974, 10, pp. 209-223.

33. Nicholson, G., and Norton, J.P.: 'Kalman filter equalization for a time-varying communication channel', Aust. Telecom. Research, 1973, 13, pp. 3-11.

34. Bozic, S.M.: 'Digital and Kalman filtering', (Edward Arnold, 1979).

35. Young, P.C.: 'Applying parameter estimation to dynamic systems - Part I', Control Eng., 1969, 16, pp. 119-125.

36. Young, P.C.: 'Applying parameter estimation to dynamic systems - Part II', Control Eng., 1969, 16, pp. 118-124.

37. Shicor, E.: 'Fast recursive estimation using the lattice structure', Bell.Syst. Tech J., 1982, 61, pp. 97-115.

38. Sorenson, H.W.: 'Least-squares estimation: from Gauss to Kalman', IEEE Spectrum, 1970, 7, pp. 63-68.

39. Sorenson, H.W.: 'Kalman filtering techniques', in 'Advances in control systems', C.T. Leondes (ed), 1966, 3, pp. 219-292.

40. Seber, G.A.F.: 'Linear regression analysis', (Wiley, 1977).

41. Priestley, M.B.: 'Spectral analysis and time series, Vol. 1: Univariate series', (Academic, 1981).

42. Wilks, S.S.: 'Mathematical statistics', (Wiley, 1962).

43. Quigley, A.L.C.: 'An approach to the control of divergence in Kalman filter algorithm', Int. J. Control., 1973, 17, pp.741-746.

44. Morrison, N.: 'Introduction to sequential smoothing and prediction', (McGraw-Hill, 1968).

45. Falconer, D.D., and Ljung, L.: 'Application of fast Kalman estimation to adaptive equalization', IEEE Trans., 1978, COM-26, pp. 1439-1446.

46. Gitlin, R.D., and Magee, F.R.: 'Self-orthogonalizing adaptive equalization algorithms', IEEE Trans., 1977, COM-25, pp. 666-672.

47. Schmidt, S.F.: 'Estimation of state with acceptable accuracy constraints', Report No. 67-4, Analytical Mechanics Associates, Inc., New York, 1967.

48. Luvison, A., and Pirani, G.: 'A state-variable approach to the equalization of multilevel digital signals', CSELT Rapporti tecnici, No. 3, 1974.

49. Jazwinski, A.H.: 'Adaptive filtering', Automatica, 1969, 5, pp. 475-485.

50. Richards, G.A.: 'Implementation of Kalman filters for process identification', GEC J. of Res., 1983, 1, pp. 100-107.

51. Anderson, B.D.O., and Moore, J.B.: 'Optimal filtering', (Prentice-Hall, 1979).

52. Luvison, A., Sacchi, L., and Tamburelli, G.: 'Theory and implementation of adaptive equalizers', Proc. Int. Conf. Commun., Boston, Mass., USA, 1979, pp. 45.6.1-6.

53. Luvison, A., and Mosca, E.: 'Development of recursive deconvolution algorithms via innovations analysis with application to identification by PRBS's', in 'Identification and system parameter estimation', Rajbman (ed), North-Holland, 1978, pp. 2061-2071.

54. Beumert, L.D.: 'Construction of PN sequences' in 'Digital communications with space applications', S.W. Golomb (ed), Prentice Hall, 1964, pp.165-172.

55. Justesen, J.: 'Fast calculation of impulse responses without multiplications', Electron. Lett., 1981, 17, pp. 700-701.

56. Fukuhashi, Y., and Nakamura, K.: 'Parameter estimation of discrete-time systems using short-periodic pseudo-random sequences', Int. J. Control, 1974, 19, pp. 1101-1110.

57. Butcher, W.E., and Cook, G.E.: 'Identification of linear sampled data systems by transform techniques', IEEE Trans., 1969, AC-14, pp. 582-584.

58. Desai, R.C.: 'Identification of impulse response from normal operating data using the delay line synthesizer principle', IEEE Trans., 1969, AC-14, pp. 580-582.

59. Brigham, E.O.: 'The fast Fourier transform', (Prentice-Hall, 1974).

60. De Visme, G.H.: 'Binary sequences', (English Univ. Press, 1971).

61. Golomb, S.W. (ed): 'Digital communications with space applications',(Prentice-Hall, 1964).

62. Levin, M.J.: 'Optimum estimation of impulse response in the presence of noise', IRE Trans., 1960, CT-7, pp. 50-56.

63. Davies, K.: 'Ionospheric Radio Propagation', US Dept. of Commerce, Nat. Bureau of Standards Monograph 80, 1965.

64. Rush, C.M.: 'HF propagation: what we know and what we need to know', Proc. IEE Conf. on Antennas and Propagation, York, England, 1981, pp. 229-236.

65. Maslin, N.M.: 'High data rate transmissions over HF links', Radio & Electron. Eng., 1982, 52, pp. 75-87.

66. Goldberg, B.: '300 kHz - 30 MHz MF/HF', IEEE Trans., 1966, COM-14, pp. 767-784.

67. The Radio Society of Great Britain: 'The radio communication handbook', 1968.

68. Picquenard, A.: 'Radio wave propagation', (Macmillan, 1974).

69. Bain, W.C., and Rishbeth, H.: 'Developments in ionospheric physics since 1957', Radio & Electron. Eng., 1975, 45, pp. 3-10.

70. Budden, K.G.: 'Radio waves in the ionosphere', (Cambridge Univ. Press, 1961).

71. David, P., and Voge, J.: "Propagation of waves',(Pergamon, 1969).

72. Schwartz, M., Bennett, W.R., and Stein, S.: 'Communication systems and techniques',(McGraw-Hill, 1966).

73. Freeman, R.L.: 'Telecommunication transmission handbook', (Wiley, 1981).

74. CCIR: 'Fading of radio signals received via the ionosphere', CCIR XIIIth Plenary Assembly, Vol. VI, Report No. 266-3, Geneva, 1974.

75. CCIR: 'Multipath propagation on HF radio circuits', CCIR XIIIth Plenary Assembly, VOL. III, Report No. 203, Geneva, 1974.

76. Watterson, C.C., Juroshek, J.R., and Bensema, W.D.: 'Experimental confirmation of an HF channel model', IEEE Trans., 1970, COM-18, pp. 792-803.

77. CCIR: 'HF ionospheric channel simulators', CCIR XIIIth Plenary Assembly, Vol. III, Report No. 549, Geneva, 1974.

78. Ralph, J.D., and Sladen, F.M.E.: 'An HF channel simulator using a new Rayleigh fading method', Radio & Electron. Eng., 1976, 46, pp. 579-587.

79. Matley, W., and Bywater, R.E.H.: 'A digital high-frequency multipath propagation simulator', Radio & Electron. Eng., 1977, 47, pp. 305-314.

80. Ehrman, L., Bates, L.B., Eschle, J.F., and Kates, J.M.: 'Real-time software simulation of the HF radio channel', IEEE Trans., 1982, COM-30, pp. 1809-1817.

81. Ream, N.: 'Simulation of Rayleigh fading by digital generation of amplitude and phase', Radio & Electron. Eng., 1978, pp. 567-572.

82. Packer, R.J., and Fox, J.A.S.: 'A simulator of ionospheric propagation of amplitude modulated signals', BBC (UK) Res. Dept. Report 1969/24, 1969, pp. 1-8.

83. Beck, D., and Betts, J.A.: 'Fading machine for the simulation of the ionosphere', Electron. Eng., 1965, 37, pp. 74-79.

84. Shaver, H.N., Tupper, B.C. and Lomax, J.B.: 'Evaluation of a Gaussian HF channel model', IEEE Trans., 1967, COM-15, pp. 79-88.

85. Di Toro, M.J., Hanulec, J., and Goldberg, B.: 'Design and performance of a new adaptive serial data modem on a simulated time-variable multipath HF link', IEEE 1st Annual Communications Convention (Conference Record), Boulder, Colorado, 1965, pp. 769-773.

86. Walker, W.F.: 'A simple baseband fading multipath channel simulator', Radio Science, 1966, 1, pp. 763-767.

87. O'Reilly, E.P.: 'A real-time HF channel simulator', Proc. IEE Int. Conf. on HF Commun. Systems & Techniques, London, 1982, pp. 41-45.

88. Jewett, W., and Cole, R.: 'Narrowband HF communication systems for digital voice', AGARD Conf. Proc. No. 173 on Radio Systems and the Ionosphere, Athens, 1975, pp. 20.1-13.

89. Clark, A.P., and McVerry, F.: 'Channel estimation for an HF radio link', IEE Proc. F, 1981, 128, pp. 33-42.

90. Kuo, F.F.: 'Network analysis and synthesis', (Wiley, 1966).

91. Zverev, A.I.: 'Handbook of filter synthesis', (Wiley, 1967).

92. Rabiner, L.K., and Gold, B.: 'Theory and application of digital signal processing', (Prentice-Hall, 1975).

93. Oppenheim, A.V., and Schafer, R.W.: 'Digital signal processing', (Prentice-Hall, 1975).

94. Subroutine GØ5DDF, Numerical Algorithms Group.

95. Clark, A.P., and McVerry, F.: 'Improved channel estimator for an HF radio link', Signal. Process., 1983, 5, pp. 241-255.

96. Clark, A.P., and McVerry, F.: 'Performance of 2400 bit/s serial and parallel modems over an HF channel simulator', IERE Conf. Proc. No. 49, Loughborough, England, 1981, pp. 167-179.

97. McVerry, F.: 'High speed data transmission over HF radio links', PhD Thesis, Dept. of Electronic & Electrical Eng., Loughborough Univ. of Technology, 1982.

98. Ayes, F.: 'Matrices', (McGraw-Hill, 1962).

99. Frederick, D.K., and Carlson, A.B.: 'Linear systems in communication and control', (Wiley, 1971).

100. Betts, J.A.: 'Signal processing, modulation and noise', (Hodder and Stoughton, 1970).

101. Couch, L.W.: 'Digital and analog communication systems', (Macmillan, 1983).

102. Gockler, H.: 'A general approach to the design of sampled-data FIR filters with optimum magnitude and minimum phase', in 'Signal process: theories and applications', M. Kunt and F. de Coulon (eds), North-Holland, 1980, pp. 679-685.

103. Kamp, Y., and Wellekens, C.J.: 'Optimal design of minimum phase FIR filters', Proc. IEEE Int. Conf. on Acoustic, Speech and Signal Process., Paris, 1982, pp. 1817-1820.

104. Subroutine CØ2ADF, Numerical Algorithms Group.

105. Shearman, E.D.R.: 'The ionosphere as a propagation medium - an engineer's view', Proc. IEE Int. Conf. on Antennas and Propagation, London, 1978, pp. 41-46.

106. Monsen, P.: 'Fading channel communications', IEEE Communications Magazine, 1980, 18, pp. 16-25.

107. Darnell, M.: 'Future HF system architecture', Proc. IEE Conf. on HF Communication Systems and Techniques, London, 1982, pp. 13-17.

108. Darnell, M.: 'The characteristics of HF propagation paths and their implications in digital communication system design', Proc. IEE Int. Conf. on Antennas and Propagation, York, 1981, pp. 254-257.

109. Darnell, M.: 'New HF data transmission techniques', in 'Communication systems and random process theory', J.K. Skwirzynski (ed), Sijthoff and Noordhoff, Holland, 1978, pp. 891-932.

110. Pennington, J.: 'Comparative measurements of parallel and serial 2.4 kbps modems', Proc. IEE Conf. on HF Communication Systems and Techniques, London, 1982, pp. 141-144.

111. Darnell, M.: 'Medium-speed digital data transmission over HF channels', Proc. IERE Conf. on Digital Processing of Signals in Communications, Loughborough, 1977, pp. 393-402.

112. Gold, B., and Rader, C.M.: 'Digital processing of signals', (McGraw-Hill, 1969).

113. Doelz, M.L., Heald, E.T., and Martin, D.L.: 'Binary data transmission techniques for linear systems', Proc. IRE, 1957, 45, pp. 656-661.

114. Sage, A.P., and Melsa, J.L.: 'Estimation theory with applications to communications and control', (McGraw-Hill, 1971).

115. Deutch, R.: 'Estimation theory', (Prentice-Hall, 1965).

116. Proakis, J.G.: 'Digital communications', (McGraw-Hill, 1983).

117. Sari, H.: 'Performance evaluation of three adaptive equalization algorithms', Proc. IEEE Int. Conf. on Acoustic, Speech and Signal Process., Paris, 1982, pp. 1385-1389.

118. Farhang-Boroujeny, B., and Turner, L.F.: 'Fast converging stochastic gradient algorithm', IEE Proc. F, 1981, 128, pp. 271-274.

119. Widrow, B., and McCool, J.M.: 'A comparison of adaptive algorithms based on the methods of steepest descent and random search', IEEE Trans., 1976, AP-24, pp. 615-637.

120. Widrow, B.: 'Adaptive filters', in 'Aspects of network and system theory', R.E. Kalman and N. De Claris (eds), Holt, Rinehart & Winston, 1970, pp. 563-567.

121. Widrow, B., McCool, J.M., Larimore, M.G., and Johnson, C.R.: 'Stationary and nonstationary learning characteristics of the LMS adaptive filter', Proc. IEEE, 1976, 64, pp. 1151-1162.

122. Rhodes, I.B.: 'A tutorial introduction to estimation and filtering', IEEE Trans., 1971, AC-16, pp. 688-706.

123. Hodgkiss, W., and Turner, L.F.: 'Practical equalization and synchronization strategies for use in serial data transmission over HF channels', Radio & Electron. Eng., 1983, 53, pp. 141-146.

124. Ungerboeck, G.: 'Theory and the speed of convergence in adaptive equalizers for digital communications', IBM J. Res. & Develop., 1972, pp. 546-555.

125. Proakis, J.G., and Miller, J.H.: 'An adaptive receiver for digital signalling through channels with intersymbol interference', IEEE Trans., 1969, IT-15, pp. 484-497.

126. Hsu, F.M.: 'Square root Kalman filtering for high-speed data received over fading dispersive HF channels', IEEE Trans., 1982, IT-28, pp. 753-763.

127. de Pedro, H., Hsu, F.M., Giordano, A., and Proakis, J.G.: 'Signal design for high-speed serial transmission on fading dispersive channels', Proc. Nat. Telecommun. Conf., Birmingham, AL, 1978, pp.27.4.1-27.4.4.

128. Falconer, D.D., and Ljung, L.: 'Application of fast Kalman estimation to adaptive equalization', IEEE Trans., 1978, COM-26, pp. 1439-1446.

129. Lawrence, R.E., and Kaufman, H.: 'The Kalman filter for the equalization of a digital communications channel', IEEE Trans., 1971, COM-19, pp. 1137-1141.

130. Leondes, C.T., and Pearson, J.O.: 'Kalman filtering of systems with parameter uncertainties - a survey', Int. J. Control, 1973, 17, pp. 785-801.

131. Doan, H.B., and Cantoni, A.: 'Fast adaptation of equalizer and desired response for digital data receivers', Electronic Circuits and Systems, 1978, 2, pp. 159-166.

132. Dalle Mese, E., and Giuli, D.: 'Generalised decision feedback equalization of digital communication channels', Electronics Circuits & Systems, 1979, 3, pp. 145-152.